Contrôle chromatinien et transcriptionnel de l'expression des gènes codant des effecteurs chez Leptosphaeria maculans, champignon pathogène du colza

Colin Clairet

NNT : 2019SACLS433

Contrôle chromatinien et transcriptionnel de l'expression des gènes codant des effecteurs chez *Leptosphaeria maculans*, champignon pathogène du colza

Thèse de doctorat de l'Université Paris-Saclay
Préparée à Université Paris-Sud

École doctorale n°567 : sciences du végétal : du gène à l'écosystème (SDV) Spécialité de doctorat : Biologie

Thèse présentée et soutenue à Thiverval-Grignon, le 25/11/19, par

Colin Clairet

Composition du Jury :

Fabienne Malagnac Professeure, Université Paris-Sud	Présidente
Philippe Silar Professeur, Université Paris-Diderot	Rapporteur
Claire Veneault-Fourrey Directrice de recherche, INRA Nancy	Rapportrice
Nicolas Nègre Chercheur, Université Montpellier	Examinateur
Isabelle Fudal Chercheuse, INRA Thiverval-Grignon	Directrice de thèse
Jessica L. Soyer Chercheuse, INRA Thiverval-Grignon	Co-Directrice de thèse

Thèse de doctorat

La réalisation de cette thèse au sein de l'équipe EPLM (INRA-BIOGER) dirigée par Mylène a été pour moi une aventure extrêmement formatrice. Merci à Thierry et Mylène de m'avoir accueilli à BIOGER, soutenu pendant la thèse et pour les moments passés à rigoler (ou réfléchir) au café le matin. Un remerciement spécial à Mylène qui m'a appris l'art subtil de l'entremise des champignons. Et un pour Thierry qui aura été le parfait guide de visite d'Asilomar (et de ses environs).

Merci à Isabelle et Jessica de m'avoir encadré dans la découverte du monde époustouflant de l'épigénétique fongique. Merci également de m'avoir supporté et soutenu tout au long de mon travail, d'avoir toujours été présentes et réactives, de m'avoir fait confiance et de m'avoir donnée une grande liberté dans mon travail.

Merci à Philippe Silar et Claire Veneault-Fourrey d'avoir accepté d'évaluer mon manuscrit ainsi qu'a Fabienne Malagnac et Nicolas Negre d'avoir accepté de participer à mon jury de thèse. Merci aux membres de mon comité de thèse, Muriel Viaud, Nicolas Lapalu, Thomas Guillemette, Pierre Grognet et Fredy Barnèche pour leurs conseils avisés et leur support tout au long de mon travail.

Merci à Moussa Benhamed, Cécile Raynaud, David Latrasse et Nadia Ponts pour les collaborations fructueuses ainsi que pour leur expertise en épigénétique.

Un très grand merci à la cellule bio-informatique, Nicolas Lapalu et Adeline Simon, qui m'ont beaucoup apporté, notamment les bases de la bio-informatique ainsi que du soutien sans faille lors de nos travaux inter-équipe, mon travail n'aurait pas été le même sans vous.

Un remerciement spécial au LIED (de l'époque), Philippe, Fabienne, Hervé, Sylvain, Gwenaëlle et Florence sans qui je n'aurai pas découvert le monde merveilleux des champignons (et l'art de la brasserie), et sans qui, sans doute, je n'en serai pas là. Merci pour votre encadrement depuis le début de mes études (et aussi pour les pots partagés au LIED ou ailleurs). Sylvain, ce fût un plaisir de collaborer pour notre première publi premier auteur !

Marc-Henri Lebrun et Richard Laugé pour toutes les discussions intéressantes (et parfois perchées) du matin autour du café. Merci à Marc-Henri d'avoir co-voituré avec moi pendant les grèves SNCF et pour les discussions scientifiques que nous avons pu avoir à ces occasions.

Je tiens aussi à remercier tous mes camarades thésards pour leur soutien et les échanges enrichissant que nous avons pu avoir : Maëllys Kevin, Alex Mercier, Elise Gay, Guillaume Fouché, Arthur Jallet, Morgane Grand, Yohann Petit, Jafar Kilani, Antoine Porquier, Julie Gervais, Audren Jiquel, Nacera Talbi et tous les futurs thésards du labo. Avec une mention spéciale pour Maëllys, Elise et Alex avec qui nous avons parcouru le grand Ouest Américain toujours dans la bonne humeur (et parfois un peu en mode aventure il faut bien le dire). Alex pour t'être accroché, avec moi, (depuis un moment déjà) comme deux pauvres bulots, à leur rocher qu'est la science. Et Maëllys pour avoir traversé l'océan de la thèse avec moi.

Merci à mon premier encadrant de stage, Sylvain Merlot et à toute l'équipe de Sebastien Thomine, qui m'ont fait découvrir le monde de la recherche et grâce à qui j'ai moi-même voulu en faire partie.

Université Paris-Saclay
Espace Technologique / Immeuble Discovery
Route de l'Orme aux Merisiers RD 128 / 91190 Saint-Aubin, France

Merci à tous ceux qui m'ont aidé dans la réalisation des manips, Bérengère pour la microscopie, Bertrand, Martin et Yannick pour s'être occupés de mes pauvres plantes cobayes, Françoise pour les WB et autres manips au début de mon stage, Bénédicte pour son expertise inégalable en transformation et en tant d'autres choses !

Merci à Michel Meyer pour ses blagues, sa bonne humeur, les échanges de matériel ou d'astuces et les discussions parfois capilotractées mais toujours enrichissantes.

Merci à Laurent Coudard pour toutes les étiquettes que je t'ai fait imprimer, tous les primers commandés et pour ta gestion de la collection de souches.

Merci à tous les membres de l'unité BIOGER, Romain, Guillaume, Bérangère, Anaïs, Clémentine et tous les autres avec qui j'ai pu rire, partager, jouer au baby-foot ou même juste me bâfrer de fromage en gloussant.

Merci à mes vieux amis, Arthur, Manon, Alexandre, Xavier, Laura pour leur amitié et leur soutien indéfectible depuis un moment déjà (le collège et le lycée ça date).

Merci à notre crew, les célèbres BassHeads (Alex, Vince, Juline, Cedric, Yanis, Erjan, Jeseune, Dylann, Julie, Lalita, Arthur, Nico, Keyhan, Adam, Dylan, Eloy, Marine (Qu'on croise partout…. même en hollande) et bien d'autres pour m'avoir soutenu et surtout permis de décompresser (fort) durant ma thèse. Je n'aurai surement pas survécu sans vous et ça a été un plaisir de tous vous rencontrer.

Et enfin merci à mes parents de m'avoir toujours poussé à apprendre et d'avoir toléré mes diverses expériences et élevages depuis longtemps déjà. Et enfin merci à mes frères et sœurs, Natacha, Hugo, Alexandre et Kevin pour tous ces moments partagés …. On a une sacrée famille quand même.

Université Paris-Saclay
Espace Technologique / Immeuble Discovery
Route de l'Orme aux Merisiers RD 128 / 91190 Saint-Aubin,
France

LISTE DES ABREVIATIONS

5mC : méthylation en position 5 de la cytosine (méthylation d'ADN)

Ac : groupement acétyle

ADN : acide désoxyribonucléique

ARN : acide ribonucléique

ARNi : ARN interférence

ARNm : ARN messager

ARNg : ARN guide

ARN Pol : ARN Polymérase

ChIP : immunoprécipitation de la chromatine

CT : Territoire chromosomique

DBD : DNA binding domain (domaine de liaison à l'ADN)

DIM-2 : defective in DNA methylation-2

DIM-5 (KMT1) : defective in DNA methylation-5

ET : Élément Transposable

FT : Facteur de Transcription

FTF : Fusarium transcription factors

GTF : General Transcription Factor (Facteur de transcription général)

H3 : Histone 3

H4 : Histone 4

H3K4me2 : di-méthylation de l'histone H3 au niveau du résidu lysine 4

H3K9me3 : tri-méthylation de l'histone H3 au niveau du résidu lysine 9

H3K9ac : acétylation de l'histone H3 au niveau du résidu lysine 9

H3K27me3 : tri-méthylation de l'histone H3 au niveau du résidu lysine 27

HMEs : enzyme modificatrice d'histone

HP1 : Heterochromatin Protein 1

IC : Compartiment inter-chromosomique

Jpi (ou DPI an anglais) : jours post infection (days post-infection)

NRPS : peptide synthétase non-ribosomale (Non-Ribosomal Peptide synthase)

PKS : polycétide synthase (PolyKetide Synthase)

PPS (SSP en anglais) : Petite Protéine Sécrétée (Small Secreted Protein)

RIP : Repeat-Induced Point mutation

SIX : Secreted in Xylem (Sécrétée dans le xylème)

"Silencing" : extinction de l'expression des gènes à l'aide d'ARNi

TAD : Topologically-Associated Domain (Domaine d'Association Topologique)

Université Paris-Saclay
Espace Technologique / Immeuble Discovery
Route de l'Orme aux Merisiers RD 128 / 91190 Saint-Aubin,
France

LISTE DES FIGURES

INTRODUCTION

Figure 1 : Mode d'infection en fonction du type de nutrition des champignons phytopathogènes

Figure 2 : Exemple de symptômes causés par différents champignons phytopathogènes

Figure 3 : Répertoire de gènes codant des protéines sécrétées en fonction du mode de nutrition de l'espèce fongique

Figure 4 : Schéma représentant les différents niveaux de compaction de la molécule d'ADN dans un noyau Eucaryote

Figure 5 : Régulation allostérique des deux modifications répressives d'histone les plus étudiées (H3K9me3 et H3K27me3)

Figure 6 : Organisation du noyau de mammifère

Figure 7 : Interactions physiques successives de plusieurs régions chromosomiques avec la fraction active de la chromatine

Figure 8 : Schéma explicatif de la technique de séquençage Hi-C

Figure 9 : Schéma représentant l'action d'un facteur de transcription général (GTF)

Figure 10 : Figure comparant des zones régulatrices chez un Eucaryotes unicellulaire par rapport à un Eucaryote complexe

Figure 11 : Nombre de facteurs de transcription par règne et par espèce en fonction du type de FT

Figure 12 : Cycle de vie de *Leptosphaeria maculans* en Europe

Figure 13 : Modèle de contrôle de l'expression des gènes codant des effecteurs 'précoces' chez *Leptosphaeria maculans*

Figure 14 : Méthode de mutagénèse dirigée CRISPR-Cas9

Université Paris-Saclay
Espace Technologique / Immeuble Discovery
Route de l'Orme aux Merisiers RD 128 / 91190 Saint-Aubin, France

CHAPITRE I: Etude genome-wide du paysage chromatinien et nucleosomal

CHAPITRE I – ARTICLE I: Nucleosome patterns in four plant pathogenic fungi with different genome structures

Figure 1: Nucleosome phasing in the four fungi studied

Figure 2: Nucleosome density profiles in F. graminearum

Figure 3: Nucleosome density profiles in *L. maculans* 'brassicae'

Figure 4: Repeated di-nucleotide patterns in nucleosomal DNA

Figure 5: Nucleosome organization of fungal gene units

Figure 6: Nucleosome organization of fungal near-universal single copy orthologous gene units (BUSCO3)

Figure 7: Nucleosome organization at start codons/TSS *vs.* gene expression

Figure S1: Nucleosome density profiles in *B. cinereal*

Figure S2: Nucleosome *vs*. SNP density profiles in individual biological replicates of *F. graminearum*

Figure S3: Nucleosome density profiles *vs*. AT-rich regions in individual biological replicates of *L. maculans* 'brassicae'

Figure S4: Nucleosome density profiles *vs*. AT content in individual biological replicates of *L. maculans* 'lepidii'

Figure S5: Pearson autocorrelation coefficients of di-nucleotides frequencies (average of three biological replicates) for *L. maculans* 'brassicae'

Figure S6: Repeated di-nucleotide patterns in nucleosomal DNA located in AT and GC isochores of *L. maculans* 'brassicae'

Figure S7: Nucleosome organization at stop codons/TTS *vs.* gene expression

Université Paris-Saclay
Espace Technologique / Immeuble Discovery
Route de l'Orme aux Merisiers RD 128 / 91190 Saint-Aubin, France

CHAPITRE I – ARTICLE II: A comparative analysis of the genome-wide histone modification maps in two subspecies of Leptosphaeria maculans showing contrasted genomic organization and different host specialization

Figure 1: Coverage of genes, transposable elements, H3K4me2-, H3K9me3

Figure 2: Genome of L. maculans 'brassicae' harbors large TE-rich, H3K9me3-domains compared to L. maculans 'lepidii'

Figure 3: Size of the H3K4me2-, H3K9me3-, H3K27me3-domains in the genomes of Leptosphaeria maculans 'brassicae' (Lmb) and L. maculans 'lepidii' (Lml)

Figure 4: Number of genes associated with H3K4me2, H3K9me3 or H3K27me3 during axenic growth in A. Leptosphaeria maculans 'brassicae' (Lmb) and B. L. maculans 'lepidii'.

Figure 5: Genes associated with heterochromatin are less expressed than genes associated with euchromatin in the genomes of L. maculans 'brassicae' and L. maculans 'lepidii'

Figure S1 : Correlation analysis of the genes, transposable elements and domains enriched for H3K4me2, H3K9me3 and H3K27me3 in the genomes of A: *Leptosphaeria maculans* 'brassicae'; B: *Leptosphaeria maculans* 'lepidii'.

Université Paris-Saclay
Espace Technologique / Immeuble Discovery
Route de l'Orme aux Merisiers RD 128 / 91190 Saint-Aubin, France

CHAPITRE II: Protéines modificatrices d'histone

CHAPITRE II – ARTICLE III: Histone methyltransferases KMT1 and KMT6 regulate effector gene expression and pathogenicity in the plant-pathogenic fungus Leptosphaeria maculans

Figure 1: Identification of *KMT6* in *Leptosphaeria maculans*

Figure 2: Effect of *Δkmt1* and *Δkmt6* inactivations on pathogenicity mutants of *L. maculans* inoculated on a susceptible cultivar of oilseed rape

Figure 3: Effect *Δkmt1* and *Δkmt6* on *L. maculans* pathogenicity on a susceptible cultivar of oilseed rape (Bristol) at 28 DPI

Figure 4: Effect of KMT1, KMT6 and KMT1-KMT6 deletion on *AvrLm4-7* profile of expression during early cotyledons colonization

Figure 5: Effect of KMT1, KMT6 and KMT1-KMT6 deletion on *AvrLm6* profile of expression during early cotyledons colonization

Figure 6: Effect of KMT1, KMT6 and KMT1-KMT6 deletion on *Lmb_jn3_11364* profile of expression during early cotyledons colonization

Figure 7: Effect of KMT1, KMT6 and KMT1-KMT6 deletion on *Lmb_jn3_00284* profile of expression during early cotyledons colonization

Figure 8: Effect of *Δkmt1* on 'early' effector genes expression in susceptible oilseed rape stems (Bristol) at 14DPI

Figure S1: Effect *Δkmt6* mutations on KMT6 protein structure and impact of kmt1 complementation on KMT1 activity

Figure S2: Trimethylation of lysine 27 of histone H3 (H3K27me3) is abolished in *Δkmt6* and *Δkmt1_Δkmt6* backgrounds and recovered in complemented 2, 7, 9 and 10 transformants

CHAPITRE II – RESULTATS COMPLEMENTAIRES

Figure 1: Expression profile of *Leptosphaeria maculans* avirulence genes and *Kdm8* during axenic growth and infection of oilseed rape cotyledons

Figure 2: Effect of the *Kdm8* mutations on Kdm8 protein structure

Figure 3: Effect of *kdm8* inactivation on mycelial growth and pathogenicity of *Leptosphaeria maculans*

Figure 4: Influence of *Kdm8* inactivation on expression of several *L. maculans* 'early' and 'late' effector genes *in vitro*

Figure 5: Influence of *Kdm8* inactivation on the expression of six *L. maculans* avirulence genes during infection of oilseed rape

Université Paris-Saclay
Espace Technologique / Immeuble Discovery
Route de l'Orme aux Merisiers RD 128 / 91190 Saint-Aubin,
France

CHAPITRE III: Régulation transcriptionnelle

CHAPITRE III – ARTICLE IV: Regulation of effector gene expression as concerted waves in Leptosphaeria maculans: a two-players game

Figure 1: Identification of the Pf2 orthologue in *Leptosphaeria maculans*

Figure 2: Expression profile of *Leptosphaeria maculans* avirulence genes, *LmPf2* transcription factor and *Kmt1* during axenic growth and infection of oilseed rape cotyledons

Figure 3: Effect of the LmPf2 mutations on LmPf2 protein structure

Figure 4: Effect of the *Δkmt1* mutation on the KMT1 protein structure and function

Figure 5: Effect of *LmPf2* and *LmKmt1* inactivations on pathogenicity of *L. maculans*

Figure 6: Influence of *LmPf2* overexpression and *KMT1* inactivation on the expression of two *L. maculans* avirulence genes during axenic growth

Figure 7: Hierarchical clustering of the pairwise Pearson correlation between the 18 conditions

Figure 8: Differential control of effector genes concerted expression

Figure 9: Inverted regulation of *KMT1* and *LmPf2* during *Leptosphaeria maculans* life cycle

Figure 10: Key players of effector genes regulation as concerted waves during Leptosphaeria maculans colonization of oilseed rape

Figure S1: Morphological characterization of *LmPf2* mutants and over-expression transformants

Figure S2: Immunoblot analysis showing presence of H3K9me3

Figure S3: Level of *LmPf2* expression in the *L. maculans* transformants during axenic growth

Figure S4: Pathogenicity assays of WT*, Δkmt1* and *ΔLmPf2* mutants after crossing with JN2-GFP

Figure S5: Influence of *LmPf2* overexpression and *KMT1* inactivation on the expression of two *L. maculans* avirulence genes during axenic growth

Figure S6: Reproducibility of RNA-Seq replicates

Université Paris-Saclay
Espace Technologique / Immeuble Discovery
Route de l'Orme aux Merisiers RD 128 / 91190 Saint-Aubin, France

CHAPITRE III – RESULTATS COMPLEMENTAIRES

Figure 1: Expression profile of cloned effector genes and three specific transcription factors during infection and axenic growth obtained by RNA-seq

Figure 2: Effect of the *Lmb_jn3_09123* mutations on Lmb_jn3_09123 protein structure

Figure 3: Effect of *Lmb_jn3_09123* inactivation on mycelial growth and pathogenicity of *Leptosphaeria maculans*

Figure 4 : Effect of the *Lmb_jn3_02170* mutations on Lmb_jn3_02170 protein structure

Figure 5: Effect of *Lmb_jn3_02170* inactivation on mycelial growth and pathogenicity of *Leptosphaeria maculans*

DISCUSSION

Figure 1: Key players of effector genes regulation as concerted waves during Leptosphaeria maculans colonization of oilseed rape

Université Paris-Saclay
Espace Technologique / Immeuble Discovery
Route de l'Orme aux Merisiers RD 128 / 91190 Saint-Aubin, France

LISTE DES TABLEAUX

INTRODUCTION

Table 1 : Protéines modificatrices d'histone, domaines actifs, fonction et effecteur allostérique associé

CHAPITRE I : Etude genome-wide du paysage chromatinien et nucleosomal

CHAPITRE I – ARTICLE I : Nucleosome patterns in four plant pathogenic fungi with different genome structures

Table 1: Characteristics of reference genomes for the four fungal species studied

Table S1: Summary of sequencing and mapping metrics

Table S2: Nucleosome landscapes as a function of gene expression defining metrics

CHAPITRE I – ARTICLE II: A comparative analysis of the genome-wide histone modification maps in two subspecies of Leptosphaeria maculans showing contrasted genomic organization and different host specialization

Table 1: Number of effector genes located in different compartments in L. maculans 'brassicae' and L. maculans 'lepidii'

Table S1: Statistics of ChIP-seq and RNA-seq datasets and alignments

Table S2: Correlation analysis between the different ChIP experiments generated with antibodies targeting histone modifications H3K4me2, H3K9me3 and H3K27me3 in the L. maculans 'lepidii', during in vitro growth

Table S3: Correlation analysis between the different ChIP experiments generated with antibodies targeting histone modifications H3K4me2, H3K9me3 and H3K27me3 in the L. maculans 'brassicae', during in vitro growth

Table S4: Coverage of histone modifications H3K4me2, H3K9me3 and H3K27me3 in the genome of Leptosphaeria maculans 'brassicae'

Table S5: Coverage of histone modifications H3K4me2, H3K9me3 and H3K27me3 in the genome of L. maculans 'lepidii'

Table S6: Correlation analysis between the coverage of transposable elements (TE) and coding sequences (CDS) location, H3K4me2-, H3K9me3- and H3K27me3-domains in the L. maculans 'brassicae' genome

Table S7: Correlation analysis between the coverage of transposable elements (TE) and coding sequences (CDS) location, H3K4me2-, H3K9me3- and H3K27me3-domains in the L. maculans 'lepidii' genome

Table S8: GO categories enriched in genes associated with H3K27me3 during axenic culture of L. maculans 'brassicae'.

Table S9: GO categories enriched in genes associated with H3K4me2 during axenic culture of *L. maculans* 'brassicae'

Table S10: GO categories enriched in genes associated with H3K4me2 during axenic culture of L. maculans 'lepidii'.

Table S11: GO categories enriched in genes associated with H3K27me3 during axenic culture of L. maculans 'lepidii'

Université Paris-Saclay
Espace Technologique / Immeuble Discovery
Route de l'Orme aux Merisiers RD 128 / 91190 Saint-Aubin, France

CHAPITRE II: Protéines modificatrices d'histone

CHAPITRE II – ARTICLE III: Histone methyltransferases KMT1 and KMT6 regulate effector gene expression and pathogenicity in the plant-pathogenic fungus Leptosphaeria maculans

Table 1: Effect of *Lmkmt1* inactivation and *LmPf2* inactivation or over-expression on in vitro growth, conidia production, pathogenicity and effector gene expression

Table S1: Primers used for genetic constructions.

Table S2: Strains used for mutants purification

Table S3: qPCR primers used for genetic constructions

Université Paris-Saclay
Espace Technologique / Immeuble Discovery
Route de l'Orme aux Merisiers RD 128 / 91190 Saint-Aubin, France

CHAPITRE III: Régulation transcriptionnelle

CHAPITRE III – ARTICLE IV: Regulation of effector gene expression as concerted waves in Leptosphaeria maculans: a two-players game

Table 1: Effect of *kmt1* and *LmPf2* inactivations and of *LmPf2* over-expression on mycelial growth, conidia production, pathogenicity and effector gene expression of *Leptosphaeria maculans*

Table 2: Effect of *LmPf2* and *KMT1* inactivation on avirulence gene expression during primary oilseed rape infection

Table S1: Primers used in the study

Table S2: Crosses performed for mutant purification

Table S3: qPCR primers used in the study

Table S4: RNA-Seq reads informations

Table S5: Differentially expressed genes in all transformants

Table S6: Differentially expressed transcription factor coding genes in LmPf2 over-expressor harbouring different chromatinian context

Université Paris-Saclay
Espace Technologique / Immeuble Discovery
Route de l'Orme aux Merisiers RD 128 / 91190 Saint-Aubin, France

LISTE DES ABREVIATIONS 4

LISTE DES FIGURES 5

LISTE DES TABLEAUX 11

INTRODUCTION 17

RESULTATS 46

CHAPITRE I 46

ETUDE GENOME-WIDE DU PAYSAGE CHROMATINIEN ET NUCLEOSOMAL 46

INTRODUCTION 47

RESULTATS 48

ARTICLE 1 **48**

Nucleosome patterns in four plant pathogenic fungi with different genome structures **48**

ARTICLE 2 **82**

A comparative analysis of the genome-wide histone modification maps in two subspecies of Leptosphaeria maculans showing contrasted genomic organization and different host specialization **82**

CHAPITRE II 118

PROTEINES MODIFICATRICES D'HISTONE 118

INTRODUCTION 119

RESULTATS 120

ARTICLE 3 **120**

Histone methyltransferases KMT1 and KMT6 regulate effector gene expression and pathogenicity in the plant-pathogenic fungus Leptosphaeria maculans **120**

RESULTATS COMPLEMENTAIRES **141**

CHAPITRE III 146

REGULATION TRANSCRIPTIONNELLE 146

INTRODUCTION 147

Université Paris-Saclay
Espace Technologique / Immeuble Discovery
Route de l'Orme aux Merisiers RD 128 / 91190 Saint-Aubin,
France

RESULTATS 148

ARTICLE IV 148

Regulation of effector gene expression as concerted waves in Leptosphaeria maculans: a two-players game 148

RESULTATS COMPLEMENTAIRES 187

Analyse fonctionnelle de facteurs de transcription putatifs pour leur implication dans la régulation de l'expression des gènes codant des effecteurs de *Leptosphaeria maculans* 187

DISCUSSION 193

Contrôle chromatinien de l'expression des gènes codant des effecteurs 194

Contrôle transcriptionnel de l'expression des gènes codant des effecteurs 195

Double contrôle, chromatinien et transcriptionel, de l'expression des gènes codant des effecteurs précoces 196

PERSPECTIVES 198

Conformation 3D des génomes et contrôle de l'expression des gènes codant des effecteurs chez *L. maculans* 198

Différents répertoires d'effecteurs pour différentes phases d'infection 199

Applications liées à la compréhension des mécanismes épigénétiques et transcriptionnels 199

Valorisation du matériel produit pendant la thèse 200

CONCLUSION 201

BIBLIOGRAPHIE 201

INTRODUCTION

Les champignons des organismes plastiques et très adaptables

Les Mycètes, organismes filamenteux (ou levures), se nourrissent par absorption de sources carbonées, possèdent une paroi chitineuse et sont présents dans la plupart des milieux terrestre. Du fait de leur hétérotrophie pour le carbone, les champignons ont dû dès leur apparition interagir avec les autres organismes terrestres (Taylor et Osborn, 1994). Ils sont dits thallophytes et cryptogames, possédant un appareil végétatif non différencié et se reproduisant par la production de spores (Silar et Malagnac, 2013). Les champignons produisent une grande variété de métabolites primaires et secondaires permettant une meilleure adaptation à leur milieu de vie et ces métabolites sont exploités par les hommes pour diverses activités (chimie, médecine, industrie ; Lindequist *et al.,* 2005 ; Gerke et Braus, 2014 ; Carhart-Harris *et al.,* 2017). Ils peuvent adopter plusieurs styles de vie afin d'assurer leur survie (**Figure1**). Les champignons saprophytes se nourrissent de la matière organique en décomposition et participent ainsi notamment au renouvellement du sol des forêts (Kubartová *et al.,* 2009) (**Figure 1A**). Les champignons peuvent également interagir de façon symbiotique avec d'autres organismes. Ainsi on distingue deux grands types de symbioses : (i) les lichens qui sont des organismes composés par un mycobionte représentant 90 % des cellules totales et un phytobionte ou organisme photosynthétique (algue ou cyanobactérie) représentant les 10 % de cellules restantes (Muggia et Grube, 2018) et (ii) les mycorhizes qui sont formées de champignons entrant en contact avec les racines des plantes ; 80 % des plantes sont mycorhizées. La plante apporte une source de carbone au champignon tandis que ce dernier apporte une source minérale telle que le phosphore et l'azote (Harrison, 2012). Enfin les champignons peuvent être pathogènes de plantes ou d'autres types d'organismes. La plupart des champignons pathogènes identifiés se trouvent êtres pathogènes de plantes, résultat de leur longue histoire co-évolutive avec les végétaux (Brundrett, 2002). Depuis 10 000 ans, les hommes utilisent les plantes à des fins multiples, que ce soit pour l'alimentation humaine et animale ou bien plus récemment pour l'industrie (Wolter *et al.,* 2019). L'avènement de l'ère industrielle et de la monoculture a rendu les parcelles cultivées de plus en plus vulnérables face aux menaces environnementales. Cette vulnérabilité accrue est le fruit de la faible diversité génétique de la plupart des surfaces cultivées alourdissant la pression de sélection pesant sur les agents pathogènes (Stukenbrock et McDonald, 2007). A cette faible diversité génétique des plantes cultivées s'ajoute la pression de sélection représentée par la forte dose d'intrants utilisés en agriculture (engrais et produits phytosanitaires). La plus grande des menaces rencontrées au champ est constituée des champignons phytopathogènes (Fisher *et al.,* 2012).

1. Différents styles de vie et déterminants de la pathogénie chez les champignons phytopathogènes

1.1 Stratégies infectieuses développées par les champignons phytopathogènes

Les champignons phytopathogènes établissent l'infection de leur plante hôte en suivant des étapes communes : adhésion d'une spore (sexuée ou asexuée) à la surface de la plante, germination de cette spore et pénétration dans les tissus végétaux, parfois à l'aide de structures spécialisées appelées appressoria (Deising *et al.,*

Université Paris-Saclay
Espace Technologique / Immeuble Discovery
Route de l'Orme aux Merisiers RD 128 / 91190 Saint-Aubin,
France

2000). Ces champignons développent ensuite différentes stratégies pour poursuivre leur cycle infectieux et sont distingués selon leur capacité à se développer sur des tissus végétaux vivants ou morts. En effet, certains champignons pénètrent la cuticule de leur plante hôte en échappant à sa reconnaissance alors que d'autres vont provoquer des nécroses directement après l'adhésion à la surface de la plante. On distingue donc plusieurs types de Mycètes en fonction de leur stratégie infectieuse.

1.2 Les champignons biotrophes

Les champignons biotrophes vivent en association avec leur plante hôte sans causer de symptômes jusqu'à la phase finale de leur cycle infectieux où a lieu la production de spores sexuées ou asexuées (**Figure 1B** ; **Figure 2F** ; Wipf *et al.,* 2019). On trouve des traces de leur présence sur terre au Dévonien (-400 millions d'années). Ils seraient potentiellement apparus au moment de la colonisation terrestre par les plantes (Remy *et al.*, 1994) et leur capacité à s'associer à d'autres espèces est apparue chez différents taxa : *Ascomycota, Basidiomycota, Zygomycota, Chytridiomycota, Plasmodiophoromycota* (O'Connell et Panstruga, 2006). Après adhésion à la surface de la plante, germination et pénétration dans la plante, les champignons phytopathogènes biotrophes forment généralement des structures spécialisées permettant leur nutrition (haustoria, arbuscules ; Zuccaro *et al.,* 2014). Ces structures spécialisées d'échange entre l'hôte et l'agent pathogène peuvent prendre différentes formes et localisations mais ne sont pas forcément néfastes pour l'hôte et ne mènent donc pas forcément à sa mort (cf. *Ustilago maydis ; Blumeria graminis f. sp hordei* ; **Figure 2B** ; Horbach *et al.,* 2011 ; Hassing *et al.,* 2019).

1.3 Les champignons nécrotrophes

Les champignons nécrotrophes, après avoir pénétré dans leur plante hôte, sécrètent un arsenal de molécules permettant la lyse cellulaire. Ils sont ensuite capables de se nourrir des cellules mortes de leur hôte (**Figure 1C** ; **Figure 2C** ; van Kan, 2006). Bien que n'ayant pas de phase asymptomatique sur plante identifiée à ce jour, les champignons nécrotrophes possèdent tout de même un arsenal de gènes codant des molécules de pathogénie très diversifié (**Figure 3** ; Lo Presti *et al.,* 2015).

1.4 Les champignons hémibiotrophes

Les champignons hémibiotrophes ont un cycle de vie complexe, alternant plusieurs modes de nutrition durant ce cycle (**Figure 1D** ; **Figure 2A, B et D** ; O'Connell *et al.,* 2012). Ils initient souvent la colonisation de leur hôte de façon biotrophe puis basculent vers un mode de vie nécrotrophe, causant l'apparition de symptômes sur leur hôte, pouvant mener à la mort de ce dernier (Jupe *et al.,* 2013). Cette capacité des agents hémibiotrophes à changer drastiquement de mode de vie durant leur cycle infectieux est en partie due à une capacité de régulation génique très fine. Ces champignons expriment spécifiquement des gènes permettant d'échapper à la reconnaissance par leur hôte et de s'établir dans les tissus végétaux durant leur phase biotrophe. Ils vont par la suite exprimer un set de gènes codant des protéases, des protéines permettant la production de ROS (espèces activées d'oxygène), et d'autres protéines impliquées dans la dégradation de la biomasse ligno-cellulosique menant à la lyse cellulaire de la plante (Rohe *et al.,* 1995 ; De Wit *et al.,* 2009). Le champignon peut ensuite se nourrir de façon saprophyte sur la matière végétale morte.

Université Paris-Saclay
Espace Technologique / Immeuble Discovery
Route de l'Orme aux Merisiers RD 128 / 91190 Saint-Aubin,
France

Le mode de vie hémibiotrophe est sans doute le plus complexe parmi les modes d'infection possibles car il nécessite un répertoire de gènes codant des effecteurs plus large que les deux autres types (Lo Presti *et al.,* 2015). Il est également très efficace car il permet au champignon de se développer au sein de son hôte sans causer de symptôme ce qui lui permet d'atteindre de nombreuses parties de la plante avant de passer à un mode de vie nécrotrophe qui endommagera grandement voire tuera la plante hôte (Fitt *et al.*, 2006).

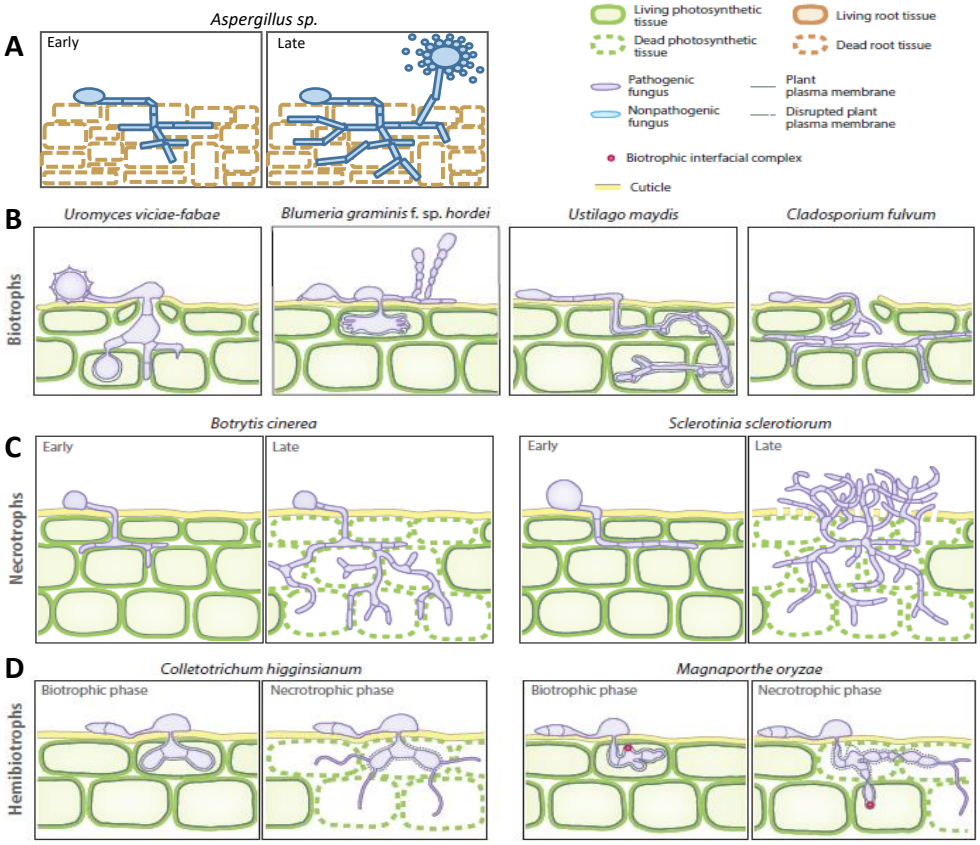

Figure 1 : Mode d'infection en fonction du type de nutrition des champignons phytopathogènes. A : Les saprophytes avec à gauche la colonisation du milieu et à droite la sporulation (ex. d'*Aspergillus sp*.). **B :** les champignons biotrophes, avec de gauche à droite *Uromyces vicia-fabae*, *Blumeria graminis* f. sp. *hordei*, *Ustilago maydis* et *Cladosporium fulvum*. **C :** les champignons nécrotrophes avec à gauche *Botrytis cinerea* et à droite *Sclerotinia sclerotiorum* aux stades précoces et tardifs d'infection. **D :** les champignons hémibiotrophes, à gauche *Colletotrichum higginsianum* et à droite *Magnaporthe oryzae.* D'après Lo presti *et al.,* 2015.

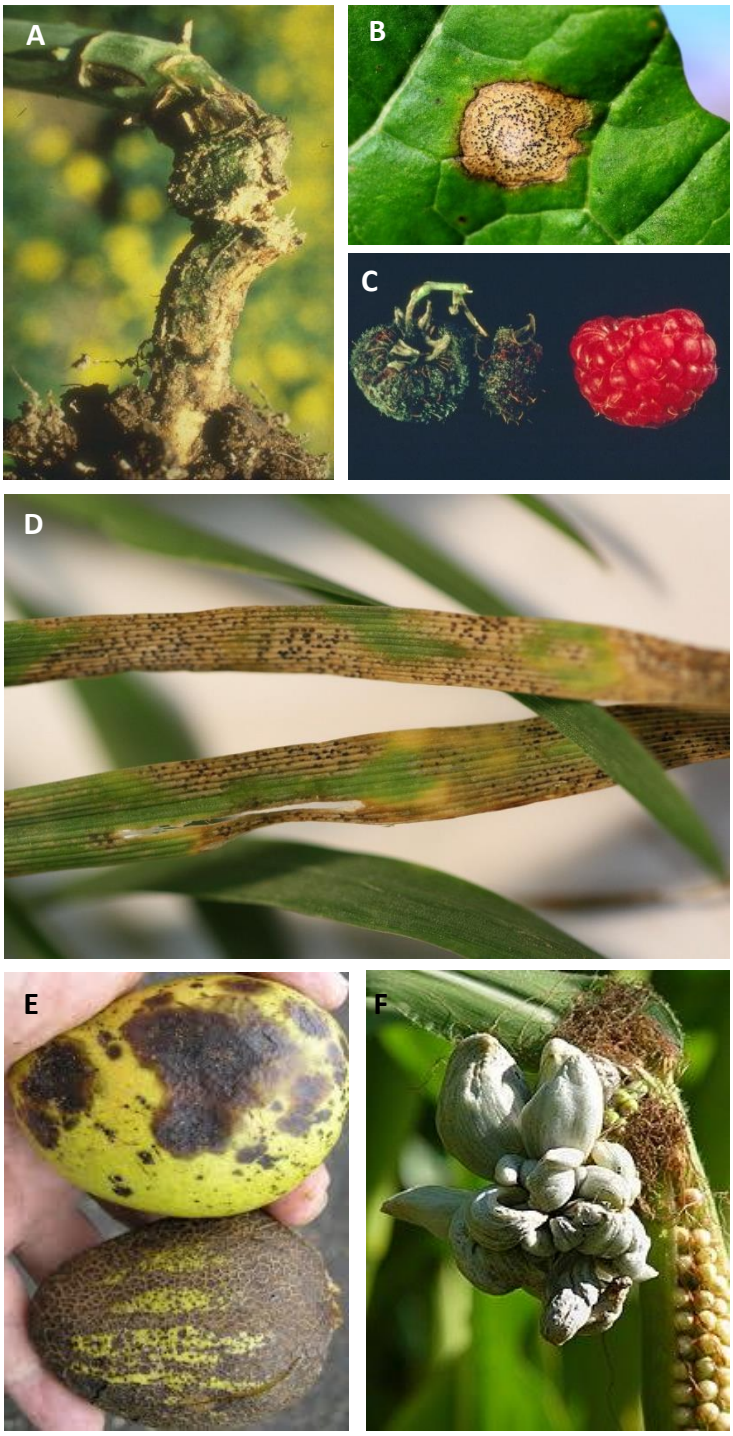

Figure 2 : Exemple de symptômes causés par différents champignons phytopathogènes. A : Symptômes de *Leptosphaeria maculans* sur tige de colza. **B :** Symptômes causés par *L. maculans* sur feuille de colza (macule). **C :** Symptômes causés par *Botrytis cinerea* sur framboise, à gauche une framboise infectée et à droite une framboise saine. **D :** Symptômes causés par *Zymoseptoria tritici* sur feuille de blé tendre. **E :** Symptômes causés par *Colletotrichum gloeosporioides* sur mangue (antrachnose). **F :** Symptômes causés par *Ustilago maydis* sur épi de maïs. Photos issues de la banque d'images de l'INRA.

Université Paris-Saclay
Espace Technologique / Immeuble Discovery
Route de l'Orme aux Merisiers RD 128 / 91190 Saint-Aubin, France

2. Déterminants de la pathogénie

Les champignons phytopathogènes ont, à l'exception des champignons biotrophes strictes, tous une partie saprophyte dans leur cycle de vie. Cette conservation du mode de vie saprophyte au sein du règne fongique indique un mode de vie ancestral de ce règne. Le dogme est qu'à l'origine les champignons étaient tous saprophytes mais certains ont acquis peu à peu un répertoire de gènes leur permettant de se nourrir de végétaux vivants (Cooke et Whipps, 1980).

2.1 Effecteurs fongiques et pathogénie

Pour infecter un hôte vivant, l'agent pathogène produit des effecteurs, définis comme l'ensemble des molécules sécrétées au moment de l'infection modulant l'immunité végétale et favorisant l'infection (Sánchez-Vallet *et al.,* 2018). Ces effecteurs correspondent principalement à des protéines sécrétées, mais peuvent également être des métabolites secondaires (Collemare et Seidl, 2019) ou des petits ARNs (siRNA) qui permettent à l'agent pathogène de moduler l'immunité végétale (Wang *et al.,* 2015). Chez les champignons nécrotrophes, on retrouve essentiellement des répertoires de gènes codant des cellulases et autres enzymes lytiques ainsi que des gènes impliqués dans la biosynthèse de métabolites secondaires alors que, chez les champignons biotrophes stricts, on retrouve essentiellement des gènes codant des protéines sécrétées de fonction inconnue. Enfin chez les champignons hémibiotrophes, on retrouve à la fois des gènes codant des enzymes lytiques, des gènes codant des protéines sécrétées sans fonction connue et des gènes impliqués dans la biosynthèse de métabolites secondaires (**Figure 3** ; Lo Presti *et al.,* 2015). Les effecteurs les plus étudiés chez les champignons phytopathogènes sont les petites protéines sécrétées (PPS). Celles-ci sont de petite taille (moins de 300 AA), souvent riches en cystéines permettant la formation de ponts disulfure qui améliorent la stabilité de la protéine dans l'apoplasme, et n'ont souvent pas de fonction prédite (Lo Presti et Kahmann, 2017).

2.2 Localisation des gènes codant des effecteurs dans les génomes fongiques

Le séquençage des génomes de champignons a révélé que les espèces associées aux plantes présentent souvent des régions génomiques contrastées : des régions évoluant rapidement comportant une grande proportion d'éléments transposables (ET) et des régions riches en gènes plus conservées. Cette observation a mené à la notion de génomes « à deux vitesses » dans lesquels la partie « plastique » des génomes contient des gènes impliqués dans l'adaptation à de nouvelles plantes hôtes ou de nouveaux génotypes. La partie moins plastique du génome étant composée des régions riches en gènes. Cette partie de génome est très conservée du fait de l'importance des gènes qui s'y trouvent. Les régions malléables permettent d'une part, une évolution plus rapide et spécifique des gènes dans ces régions et d'autre part une régulation spécifique de ces gènes (Raffaele et Kamoun, 2012). Les génomes des champignons phytopathogènes peuvent présenter une proportion globalement importante d'ET (45 à 75 % du génome, par ex. chez *Blumeria graminis* ou *Melampsora larici-populina* ; Spanu *et al.,* 2010 ; Duplessis *et al.,* 2011) et une distribution uniforme des ET dans l'ensemble du génome. Ils peuvent présenter une plus faible proportion d'ET regroupés dans des régions génomiques spécifiques telles que de longs blocs de séquences répétées (par ex. dans les génomes de *Leptosphaeria maculans* ou *Epichloe festucae* ; Rouxel *et al.*, 2011 ; Schardl *et al*., 2013). On peut

Université Paris-Saclay
Espace Technologique / Immeuble Discovery
Route de l'Orme aux Merisiers RD 128 / 91190 Saint-Aubin,
France

retrouver ces régions dans des chromosomes accessoires ou dispensables comme chez *Fusarium oxysporum* ou *Nectria haematococca*, où ces chromosomes peuvent être gagnés ou perdus facilement ce qui permet à leur porteur d'acquérir un nouveau spectre d'hôte ou une capacité accrue à infecter l'hôte (Coleman *et al.,* 2009 ; Ma *et al.,* 2010 ; pour revue voire Soyer *et al.,* 2015,A) ou à des extrémités chromosomiques, appelées régions sub-télomériques. Les gènes codant des effecteurs putatifs sont sur-représentés dans ces régions dynamiques, enrichies en ET. Par exemple, chez *L. maculans*, les gènes codant des effecteurs exprimés au moment de l'infection des feuilles de colza sont

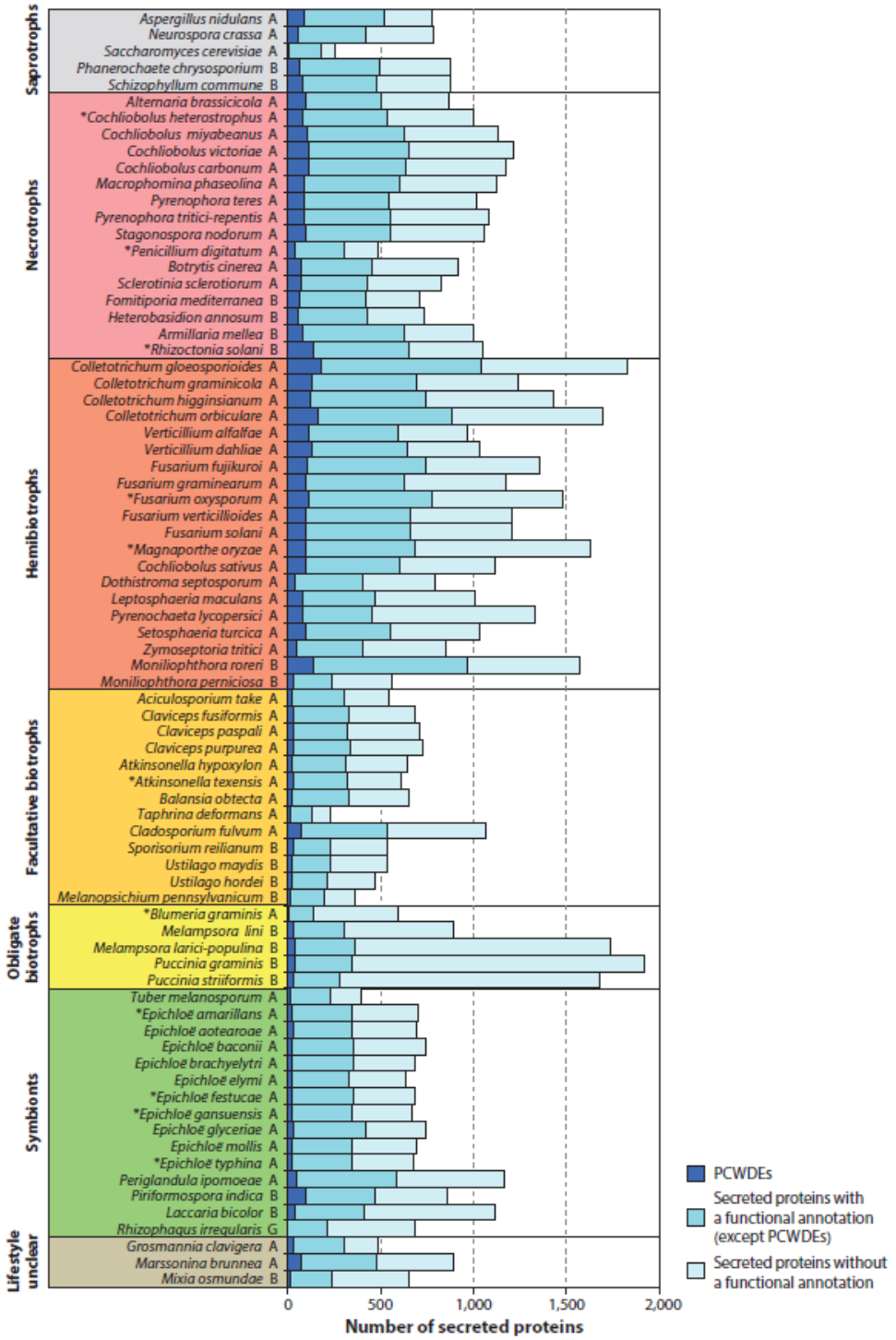

Figure 3 : Répertoire de gènes codant des protéines sécrétées en fonction du mode de nutrition de l'espèce fongique. En bleu foncé, les protéines ayant une fonction enzymatique de dégradation de la paroi végétale, en bleu plus clair, les protéines ayant une autre fonction prédite et en bleu pâle les protéines n'ayant pas de fonction prédite. D'après Lo Presti e*t al.,* 2015.

Université Paris-Saclay
Espace Technologique / Immeuble Discovery
Route de l'Orme aux Merisiers RD 128 / 91190 Saint-Aubin,
France

majoritairement localisés dans des régions riches en ET et chez *F. oxysporum*, presque tous les gènes codant des effecteurs sont localisés dans les chromosomes accessoires (Ma *et al.,* 2010 ; Rouxel *et al*., 2011). Les gènes impliqués dans la biosynthèse de métabolites secondaires sont, eux, souvent localisés à proximité de régions riches en ET, notamment dans les régions sub-télomériques des génomes (Ohm *et al.,* 2012). Ces régions riches en ET sont parfois inactivées via un mécanisme pré-méiotique spécifique des ascomycètes appelé RIP (Repeat-Induced Point mutation) qui induit la mutation des cytosines en thymines et entraine l'apparition de codons Stop (Galagan et Selker, 2004).

2.3 Régulation de l'expression des gènes codant des effecteurs

Les gènes codant des effecteurs protéiques sont souvent peu exprimés en culture axénique et spécifiquement exprimés pendant l'infection de la plante hôte par vagues successives à des étapes stratégiques du cycle infectieux (e.g. pendant la phase de colonisation asymptomatique des feuilles, tiges ou racines ou lors du passage à un mode de vie nécrotrophe). Ceci suggère qu'une régulation fine de l'expression des effecteurs est un élément crucial du succès de l'infection / de la colonisation. Néanmoins, peu de choses sont connues concernant les bases de la régulation de l'expression des effecteurs. L'expression des gènes codant des effecteurs protéiques, tout comme celle des gènes impliqués dans la biosynthèse des métabolites secondaires, est régulée par des facteurs de transcription (TFs) spécifiques et / ou généraux (Cho *et al.,* 2013 ; Rybak *et al.,* 2017 ; Tan et Oliver, 2017). Des études récentes mettent également en évidence l'implication de facteurs physiques tels que l'encombrement stérique de la chromatine, que ce soit pour la régulation de l'expression de clusters de métabolisme secondaire ou des effecteurs protéiques (Strauss et Reyes-Dominguez, 2011 ; Connolly *et al.,* 2013 ; Soyer *et al*., 2014 ; Chujo et Scott, 2014 ; Gacek-Matthews *et al.,* 2016 ; Soyer *et al.,* 2019). Enfin il a récemment été montré, notamment chez les mammifères et la drosophile, que l'organisation des chromosomes au sein des noyaux intervient également dans cette régulation génique et que certaines régions chromosomiques interagissent physiquement via des complexes protéiques permettant l'expression simultanée de ces régions (Cremer et Cremer, 2001 ; Hou *et al.,* 2012 ; Winter *et al*., 2018). Il convient d'explorer l'implication de ces différents niveaux de régulation de l'expression des gènes codant des effecteurs dans la mise en place de l'infection et le déroulement du cycle infectieux.

3. Régulation chromatinienne et expression génique

Au sein des cellules Eucaryotes, l'ADN présente différents niveaux de compaction et l'un des premiers niveaux est la chromatine, qui est l'association entre la molécule d'ADN, des ARN et des protéines, notamment les histones (**Figure 4**). L'état de compaction de cette chromatine n'est pas figé et il peut varier pour une même région génomique pendant le cycle cellulaire. Au-delà de son importance dans la compaction de l'information génétique, c'est aussi à ce niveau que sont régulés les processus cellulaires fondamentaux tels que la réplication, la réparation de l'ADN et elle constitue le premier niveau de régulation de l'expression des gènes. La chromatine peut être dans un état dit « ouvert » qui va favoriser l'expression génique ou au contraire « fermé » qui va réprimer l'expression génique. Ces états de condensation sont contrôlés par la modification chimique de la molécule d'ADN directement ou par des protéines qui constituent la chromatine (Jenuwein et Allis, 2001 ; Bird, 2002).

Université Paris-Saclay
Espace Technologique / Immeuble Discovery
Route de l'Orme aux Merisiers RD 128 / 91190 Saint-Aubin,
France

3.1. Composants fondamentaux de la chromatine

La chromatine se compose du double brin d'ADN associé à des protéines, les histones, constituant le composant principal du « collier de perle », le nucléosome (**Figure 4**). Environ 150 paires de bases d'ADN sont enroulées autour du nucléosome cœur constitué d'un octamère d'histones (dimère d'histones H3-H4 et H2A-H2B ; Smith, 1991 ; Luger *et al.,* 1997). Chaque nucléosome est relié par la région inter-nucléosomale formée de l'ADN de liaison qui interagit avec l'histone H1. Il existe plusieurs types de protéines histone. Ainsi, on retrouve les histones H1, H2A, H2B, H3, H4 et H5. Les gènes codant les core-histones sont co-régulés avec un pic d'expression durant la phase S du cycle cellulaire (phase durant laquelle l'organisme va doubler son matériel génétique afin de réaliser une mitose ; Marino-Ramirez *et al.,* 2011). Chaque core-histone est composé de deux structures protéiques distinctes, une partie flexible représentant 20 à 30 % de la protéine appelée « queue » et pouvant être modifiée chimiquement, et une partie globulaire autour de laquelle se structure l'ADN (**Figure 4**).

3.2. Etats de la chromatine : euchromatine et hétérochromatine

La chromatine peut se trouver dans deux états de condensation : on nommera euchromatine la chromatine ayant une structure décondensée et, au contraire, hétérochromatine la chromatine présentant un état de condensation élevé. Ces domaines, présentant des caractéristiques fonctionnelles et biochimiques distinctes (Grewal et Jia, 2007), avaient été identifiés initialement sur la base de critères cytologiques (Heitz, 1928). Fonctionnellement, l'hétérochromatine reste hautement condensée tout au long du cycle cellulaire, se réplique plus tardivement dans la phase S, est pauvre en gènes, comporte une grande proportion de séquences répétées et présente un faible taux de recombinaison (Richards et Elgin, 2002 ; Huisinga *et al*., 2006, Grewal et Jia, 2007). En assurant un niveau de compaction élevé, l'hétérochromatine est garante de l'intégrité des génomes, soit structuralement, puisqu'on la retrouve au niveau des centromères et télomères, soit parce qu'elle contribue à empêcher la propagation anarchique des éléments répétés (Papamichos-Chronakis et Peterson, 2013). L'hétérochromatine, parce qu'elle est très condensée, participe également aux mécanismes d'inhibition de l'expression des gènes. Au contraire, l'euchromatine,

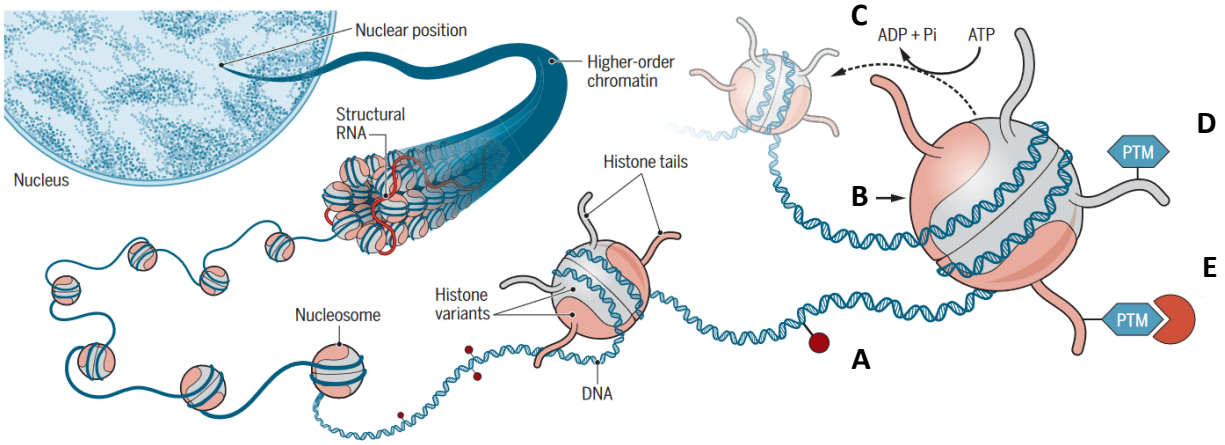

Figure 4 : Schéma représentant les différents niveaux de compaction de la molécule d'ADN dans un noyau Eucaryote. A : Modification de la molécule d'ADN (e.g méthylation des cytosines). **B :** Protéine chaperonne d'histone. **C :** Facteur de remodelage. **D :** Protéine modificatrice d'histone. **E :** Protéine 'histone reader', capable de reconnaitre les modifications de queue d'histone. Issu de Yadav *et al.,* 2018.

Université Paris-Saclay
Espace Technologique / Immeuble Discovery
Route de l'Orme aux Merisiers RD 128 / 91190 Saint-Aubin, France

décondensée, est plutôt « permissive » pour l'expression des gènes. Ces deux territoires sont aussi caractérisés par des modifications biochimiques de l'ADN et / ou des histones, discutées ci-après. On distingue hétérochromatine constitutive, la forme stable et très condensée de la chromatine, que l'on retrouve le plus souvent dans les régions inactives transcriptionnellement des génomes (e.g. ETs, télomères et centromères ; Saksouk *et al.,* 2015) de l'hétérochromatine facultative que l'on retrouve dans les régions plutôt actives transcriptionnellement et qui sont régulées finement (e.g. clusters de métabolisme secondaire ; Trojer et Reinberg, 2007).

3.3 Régulation nucléosomique

La position des nucléosomes dans la séquence génique peut également influencer l'expression des gènes en modifiant l'accessibilité des promoteurs ou des séquences régulatrices aux facteurs de transcription (FTs) ou aux protéines modificatrices d'histone (HMEs ; Radman-Livaja et Rando, 2010 ; Struhl et Segal, 2013). Leur positionnement est défini par la séquence génique. Des cartes nucléosomiques ont été réalisées chez des levures et chez le champignon saprophyte *Aspergillus fumigatus* (Tsankov *et al.,* 2010 ; Nishida *et al.*, 2009). Ces résultats ont montré que les nucléosomes sont généralement déplétés dans les promoteurs, enhancers et terminateurs des gènes actifs transcriptionnellement ce qui indique un contrôle nucléosomique de l'expression des gènes. Cependant, aucune étude de positionnement des nucléosomes n'a été réalisée chez des champignons phytopathogènes et donc aucune relation entre positionnement des nucléosomes et régulation de l'expression des gènes et de la pathogenèse n'a pu être mise en évidence. Seules des études menées chez *Plasmodium falciparum,* agent pathogène de l'homme, ont permis d'identifier une régulation via la localisation des nucléosomes de gène de pathogénie (Ponts *et al*., 2010 ; Bunnik *et al.,* 2014).

3.4 Modifications chimiques de l'ADN

Chez les champignons filamenteux, le génome est globalement peu méthylé (environ 1,5 % chez *N. crassa* ; Selker *et al.,* 1993). De plus, contrairement aux mammifères (Li *et al.,* 1993), la méthylation de l'ADN est dispensable à la vie des champignons (Foss *et al.,* 1993 ; Kouzminova et Selker, 2001). C'est l'ADN méthyltransférase DIM-2 (defective in DNA methylation-2) qui catalyse la méthylation de l'ADN (Kouzminova et Selker, 2001), presque exclusivement au niveau des régions riches en transposons affectés par le mécanisme de RIP (Selker, 2002 ; Selker *et al.,* 2003). La méthylation de l'ADN au sein du règne des Mycètes n'a été mise en évidence que chez très peu d'organismes (i.e. *N. crassa* ; Selker et Stevens, 1985 ; Foss *et al.,* 1993) ; *Mycosphaerella fijiensis* (Dhillon *et al.,* 2010) ; *Ascobolus immersus* (Goyon *et al.,* 1996) ; *Coprinus cinereus* (Zolan et Pukkila, 1985) ; *M. oryzae* (Jeon *et al.,* 2015) ; *Aspergillus flavus* (Gowher *et al.,* 2001) et il a été au contraire mis en évidence chez d'autres filamenteux que l'ADN n'était pas méthylé (i.e. *Z. tritici* (Dhillon *et al.,* 2010), *S. pombe* (Antequera *et al.,* 1984), ou encore *L. maculans* (Bewick *et al.,* 2019). Une étude récente de la méthylation de l'ADN chez de nombreux Mycètes a mis en évidence que chez ce règne le mécanisme canonique de méthylation dans le corps des gènes est absent ce qui les distinguent de certains insectes et des plantes. Mais il arrive que certains champignons possèdent des clusters de méthylation d'ADN mis en place par des mécanismes indépendants de ceux précédemment décrits, mécanismes communs aux autres espèces de champignon (Bewick *et al.,* 2019).

Université Paris-Saclay
Espace Technologique / Immeuble Discovery
Route de l'Orme aux Merisiers RD 128 / 91190 Saint-Aubin,
France

3.5 Modifications chimiques des queues d'histones et protéines impliquées dans ces modifications

Chaque core-histone est composée de deux structures protéiques distinctes : une partie flexible représentant 20 à 30 % de la protéine appelée « queue » et pouvant être modifiée chimiquement et une partie globulaire autour de laquelle se structure l'ADN. Les queues d'histones peuvent subir une large variété de modifications chimiques (acétylations, méthylation, sumoylation, ubiquitination etc…), qui, en fonction de l'acide aminé modifié, changera le niveau de compaction de la chromatine et ainsi l'accessibilité de l'ADN et, du même coup, son niveau de transcription (Luger et Richmond, 1998 ; Bannister et Kouzarides, 2005). Ainsi, chez de nombreux champignons, on retrouve dans les régions hétérochromatiniennes des modifications de type tri-méthylation de la lysine 9 de la queue de l'histone H3 (H3K9me3) et tri-méthylation de la lysine 27 de la queue de l'histone H3 (H3K27me3 ; Freitag, 2017). Chez les plantes et les animaux on retrouve souvent des méthylations des cytosines ou des adénines associées aux histones portant des marques répressives (Jackson *et al.,* 2002 ; Law et Jacobsen, 2010). Au contraire les régions euchromatiniennes sont plutôt marquées par des modifications de type di- ou trimethylation de la lysine 4 de l'histone H3 (H3K4me2/3) ou acétylation de la lysine 9 de l'histone H3 (H3K9ac ; **Figure 5** ; Kouzarides, 2007). De nombreuses protéines sont capables de reconnaître, d'ajouter ou de retirer des groupements chimiques aux queues d'histones, ou aux nucléotides directement, modifiant ainsi l'accessibilité de l'ADN de la région génomique concernée (Kim *et al.,* 2019). On appelle ces protéines des « histones modifying proteins (HMEs) ». Beaucoup de ces protéines possèdent des domaines de lecture des modifications de l'ADN ou des histones et permettent ainsi le recrutement d'une machinerie complexe (Kim *et al.,* 2019). Il est même souvent question d'une lecture des modifications chimiques par plusieurs protéines ce qui renforce encore la spécificité et l'efficacité de ce mécanisme (Ruthenburg *et al.,* 2007 ; Savitsky *et al.,* 2016). Des études récentes ont prouvé que les HMEs sont affectées par des composants particuliers des histones comme les modifications d'ADN/d'histone ou la longueur du linker (brin d'ADN reliant deux nucléosomes). Ces observations pourraient indiquer que ces protéines agissent comme des senseurs allostériques (**Tableau 1** ; Motlagh *et al.,* 2014). Il a par exemple été montré chez *N. crassa* que la méthylation d'ADN est induite par deux HMEs : la première, KMT1 (DIM-5), capable de déposer la marque H3K9me3 sur les queues d'histones et la deuxième, DIM-2, capable de reconnaître ces méthylations et de méthyler les cytosines associées (**Figure 5** ; Tamaru et Selker, 2001). Une autre méthyltransférase d'histone très étudiée, KMT6, responsable de la méthylation H3K27me3, est impliquée chez *F. graminearum* et *E. festucae* dans la régulation du métabolisme secondaire (**Figure 5** ; Connolly *et al.,* 2013 ; Chujo et Scott, 2014). Les méthylations répressives déposées sur les queues d'histones peuvent ensuite être retirées par des protéines appelées déméthylases. Les marques d'histones modifiant l'accessibilité de la chromatine aux facteurs de transcription et autres protéines servant à la transcription peuvent être retirées, modifiées ou remplacées ce qui permet un contrôle très fin de l'expression des gènes dans ces régions (Jamieson *et al.*, 2013). Au même titre que les méthylations déposées et retirées par les méthylases et déméthylases, on retrouve des acétylases et déacétylases, des phosphorylases et phosphatases (etc..) qui équilibrent les acétylations, les phosphorylations d'histones (etc.. ; Eberharter, 2002 ; Rossetto *et al.,* 2012). C'est cet équilibre très fin entre les différents acteurs réalisant les modifications chimiques qui permet une régulation dynamique et complexe de l'expression des gènes (Cedar et Bergman, 2009 ; Kim *et al.,* 2019). Il a également été montré chez l'homme que certaines histones peuvent porter

Université Paris-Saclay
Espace Technologique / Immeuble Discovery
Route de l'Orme aux Merisiers RD 128 / 91190 Saint-Aubin,
France

plusieurs types de modifications (une activatrice et une répressive) permettant de contrôler encore plus finement l'expression des gènes dans ces régions (Mauser *et al.,* 2017).

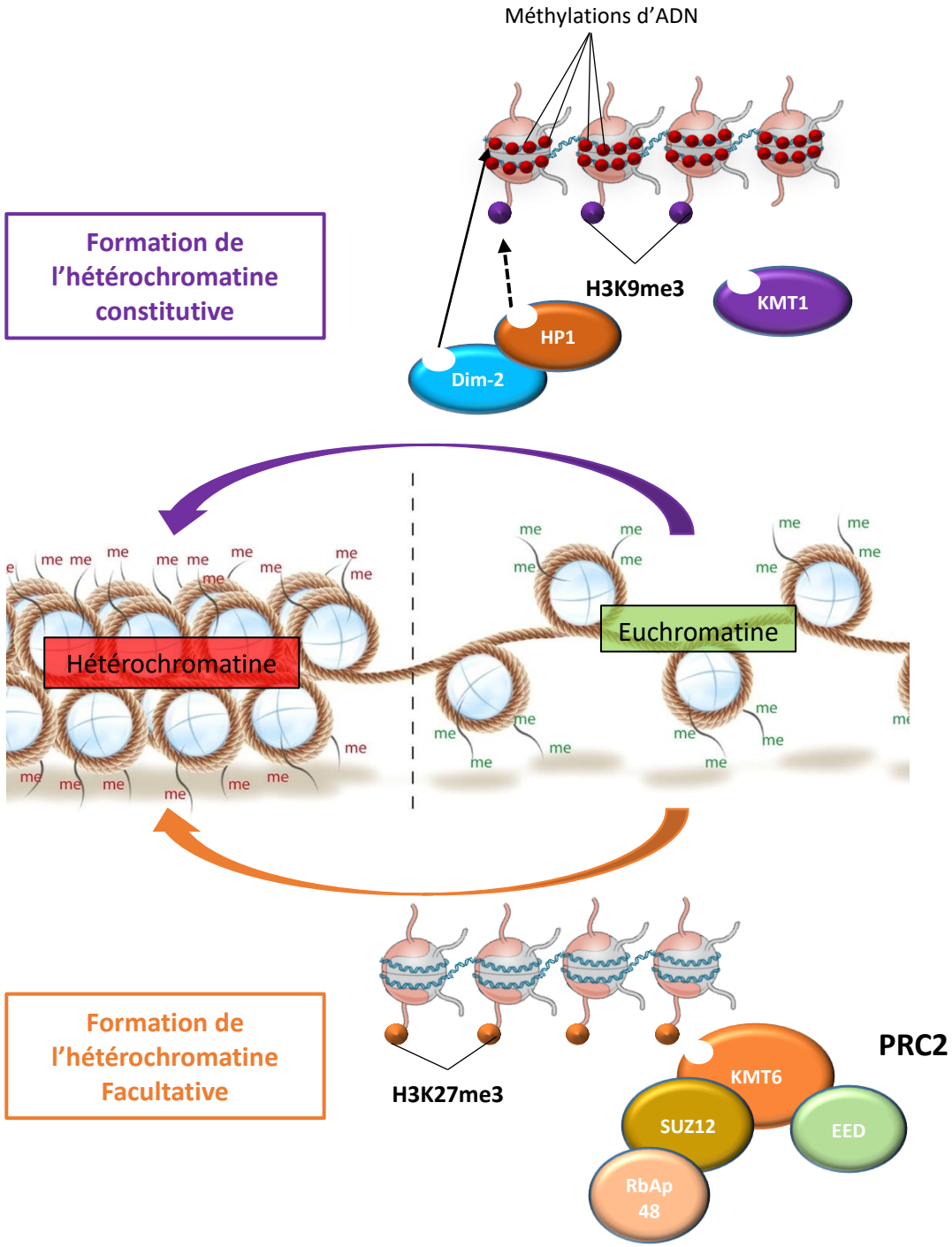

Figure 5 : Régulation allostérique des deux modifications répressives d'histone les plus étudiées (H3K9me3 et H3K27me3). A : Le complexe KMT1/Dim-2 responsable de la méthylation de type H3K9me3 et de la méthylation d'ADN associée. KMT1 est responsable du dépôt de H3K9me3 puis HP1 est capable de reconnaitre ces modifications et de recruter Dim-2 qui va méthyler les cytosine associées (issu de Honda *et al.,* 2010). **B :** Le complexe PRC2 responsable de la méthylation H3K27me3, KMT6 étant responsable du dépôt des modifications chimiques (issu de Kim *et al.,* 2019). Image de nucléosome issu de Yadav *et al.,* 2018.

Université Paris-Saclay
Espace Technologique / Immeuble Discovery
Route de l'Orme aux Merisiers RD 128 / 91190 Saint-Aubin, France

3.6 Contrôle chromatinien de l'expression génique chez les champignons

Du fait de leur possible modification chimique, les histones ainsi que la molécule d'ADN elle-même peuvent être utilisées à des fins de régulation génique (Kouzminova et Selker, 2001 ; Jamieson *et al.*, 2013). Ces modifications vont entrainer des changements d'encombrements stériques, modifiant l'accessibilité de la molécule d'ADN aux facteurs pouvant réguler l'expression des gènes. Chez certains champignons tels que *M. oryzae*, la méthylation de la molécule d'ADN est capable de réguler de nombreux processus tels que la reproduction sexuée ou la pathogénie (Jeon *et al.,* 2015). Chez d'autres champignons tels que *L. maculans*, la méthylation de la molécule d'ADN n'est pas un processus conservé et actif (Bewick *et al.,* 2019), le champignon ne peut donc utiliser que les modifications d'histone et la régulation tridimensionnelle du génome (influencée par les modifications d'histone) pour réguler l'accessibilité de ses gènes. Les marques activatrices d'histone les plus étudiées chez les champignons filamenteux sont H3K4me2, H3K36me3 et H3K9ac (di-méthylation de la lysine 4 de l'histone H3, tri-méthylation de la lysine 36 de l'histone H3 et acétylation de la lysine 9 de l'histone H3 ; Gacek et Strauss, 2012 ; Smith *et al.,* 2012 ; Janevska *et al.,* 2018). Au contraire les marques chromatiniennes répressives les plus étudiées chez les Mycètes sont H3K9me3 et H3K27me3 respectivement marqueurs de la chromatine constitutive et facultative. Chez *N. crassa*, on retrouve les marques H3K9me3 dans les régions très peu exprimées tels que les centromères ou les télomères mais ces marques ne participent pas à la conformation 3D du génome (Klocko *et al.,* 2016). Chez *Fusarium graminearum* au contraire on retrouve des modifications de type H3K27me3 dans les centromères et télomères (Connolly *et al*., 2013). Chez *Z. tritici,* qui possède plusieurs chromosomes dispensables fortement enrichis en ETs, on retrouve la marques H3K27me3 dans ces régions fortement réprimées ainsi que dans les télomères alors que la marque H3K9me3 est spécifiquement retrouvée sur les ETs (Schotanus *et al*., 2015). Des études récentes tendent à prouver que les modifications d'histones sont capables de réguler de nombreux processus chez les champignons ayant des styles de vie bien différents. On peut

Tableau 1 : Protéines modificatrices d'histones, domaines actifs, fonction et effecteur allostérique associé.

Allosteric Effectors		Chromatin Modifiers	Effector Sensing Domains/Subunits	Functions
Activators	H3K4me0	DNMT3A	ADD domain of DNMT3A	DNA methylation
		KDM5A	PHD1 domain of KDM5A	H3K4 demethylation
	H3K27me3	PRC2	EED	H3K27 methylation
	H3K36me3	Rpd3S	Eaf3	Histone deacetylation
	Length of linker DNA	Rpd3S	Not determined	Histone deacetylation
		ISWI	HSS and NegC domains of ISWI	Nucleosome spacing
		ACF	ACF1	Nucleosome spacing
	N-terminal tail of H4	ISWI	AutoN domain of ISWI	Nucleosome spacing
		ACF	ACF1	Nucleosome spacing
		Chd1	Chromodomains of Chd1	Nucleosome remodeling
	Nucleosome density	PRC2	SUZ12	H3K27 methylation
Inhibitors	H3K4me3	PRC2	RbAp48	H3K27 methylation
	H3K36me2/3	PRC2	RbAp48	H3K27 methylation

Ces protéines sont retrouvées chez la plupart des organismes. Un effecteur allostérique est une molécule se fixant à un site particulier d'une enzyme (appelé site allostérique et impactant positivement ou négativement l'activité de l'enzyme. Issu de Kim *et al*., 2019.

Université Paris-Saclay
Espace Technologique / Immeuble Discovery
Route de l'Orme aux Merisiers RD 128 / 91190 Saint-Aubin,
France

ici prendre l'exemple de *N. crassa* pour lequel la modification H3K36me3 contrôle la tolérance au stress thermique et au pH (Kronholm *et al.,* 2016). Il a également été montré que les deux marques répressives H3K9me3 et H3K27me3 sont capables de contrôler la biosynthèse d'alcaloïdes et l'expression de gènes du métabolisme secondaire chez *E. festucae, A. nidulans* et *F. graminearum* (Gacek et Strauss, 2012 ; Connolly *et al.,* 2013 ; Chujo et Scott, 2014). De plus l'inactivation d'un des acteurs responsables du dépôt de H3K9me3, *KMT1*, peut mener à des relocalisations de H3K27me3 chez *N. crassa* ce qui induit un stress génotoxique, un défaut de croissance ainsi qu'une instabilité chromosomique (Basenko *et al.,* 2015) .Chez *Z. tritici,* l'inactivation de *KMT1* induit une instabilité chromosomique résultant de la perte de H3K9me3 et de la relocalisation des marques H3K27me3 à l'endroit de ces dernières et du même coup de la déplétion de celles si sur les chromosomes accessoires. Au contraire l'inactivation de *KMT6* chez *Z. tritici* induit une plus grande stabilité chromosomique (Möller *et al.,* 2019). Enfin les déméthylases peuvent également agir sur les queues d'histones et ainsi jouer un rôle de répression ou d'activation de l'expression. Chez *A. nidulans*, deux déméthylases d'histones, KdmA et KdmB sont responsables de l'enlèvement respectif de la marque répressive H3K9me3 et de la marque activatrice H3K4me3 et ainsi de la régulation du métabolisme primaire et secondaire (Gacek-Matthews *et al.,* 2015 ; Gacek-Matthews *et al.,* 2016). Il a également récemment été montré que les effecteurs protéiques pouvaient être régulés par la structure de la chromatine. Ainsi, lors d'une précédente thèse dans notre équipe, un contrôle de l'expression des effecteurs de *L. maculans* via la marque répressive H3K9me3 mise en place par KMT1 avait été mis en évidence (Soyer *et al.,* 2014) ; nous reviendrons sur ces travaux dans la partie Objectifs de la thèse.

4. Conformation tridimensionnelle de la chromatine et co-régulation génique

Le génome nucléaire des Eucaryotes est l'élément central de la cellule. C'est là qu'est gardée et condensée toute l'information nécessaire à la vie de l'organisme. Afin que la régulation génique soit correctement réalisée et permette à l'organisme de vivre, il faut organiser l'immense quantité d'information que représentent les chromosomes. De nombreuses protéines nucléaires sont utilisées par les organismes pour structurer les génomes au sein des noyaux (e.g. condensines, cohésines, nucleoporines etc…; Casolari *et al.,* 2004 ; Skibbens, 2019). Les modifications chimiques de l'ADN, des queues d'histones et les séquences répétées servent également de base à la structuration tridimensionnelle (3D) du génome (Bonev et Cavalli, 2016).

4.1 Interaction physique des régions chromosomiques

Pour permettre l'expression correcte des gènes à tous les moments de la vie de la cellule, le génome des Eucaryotes est organisé spatialement en domaines 3D appelés Territoires Chromosomiques (CTs) ainsi qu'en compartiments interchromatiniens (ICs) qui contiennent des complexes macromoléculaires nécessaires à la réplication, la transcription, l'épissage et à la réparation de l'ADN (**Figure 9** ; Cremer et Cremer, 2001). Les domaines chromosomiques interagissant physiquement sont appelés TADs pour 'Topologically Associated Domains'. Chez la levure, pendant la mitose, de larges domaines de 300 kb à 1 Mb sont formés grâce aux condensines. Ces domaines disparaissent ensuite peu à peu jusqu'à la prochaine mitose. Au contraire, de petits domaines de 30 à 40 kb formés

Université Paris-Saclay
Espace Technologique / Immeuble Discovery
Route de l'Orme aux Merisiers RD 128 / 91190 Saint-Aubin, France

par les cohésines sont très stables tout au long du cycle cellulaire. Ces deux types de domaines sont régulés de façon inverse au cours du cycle cellulaire et sont mis en place indépendamment (**Figure 6** ; Tanizawa *et al.,* 2017).

4.2 Organisation 3D des génomes

Chez la drosophile il a été montré que les chromosomes sont organisés en domaines où la transcription est active et où on retrouve de nombreux gènes, des FTs et des protéines 'insulatrices' (protéines servant à protéger un promoteur ou une région régulatrice de l'action d'une protéine régulatrice agissant sur la région régulatrice voisine) et en domaines où la transcription est faible et où on ne retrouve pas de machinerie d'expression. Ces domaines diffèrent par leurs modifications épigénétiques et la présence de protéines spécifiques. La chromatine inactive est plutôt retrouvée dans les bordures alors que la chromatine active est plutôt retrouvée au milieu du noyau chez les mammifères à l'inverse des levures et des insectes (Lanctôt *et al.,* 2007). Des réarrangements chromosomiques peuvent avoir lieu durant le cycle cellulaire, mais ces derniers sont rares car la chromatine est très contrainte physiquement et ces réarrangements n'ont lieux que pendant de très courtes périodes de temps durant la phase G1. Une fois cette fenêtre temporelle passée, les mouvements chromatiniens sont réduits à des petits domaines subnucléaires (Lanctôt *et al.,* 2007). Chez la levure, les pores nucléaires sont d'importantes zones de transcription et

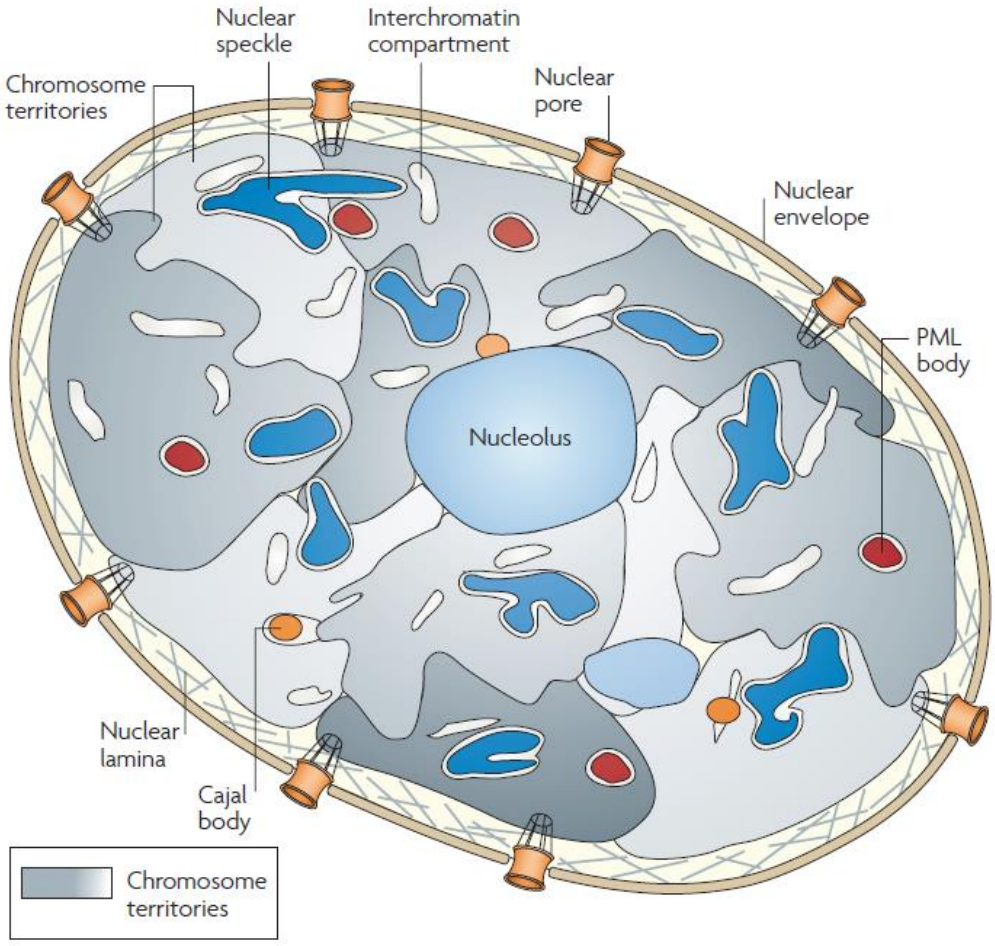

Figure 6 : Organisation du noyau de mammifère. Il se caractérise par une compartimentation des composants fonctionnels. L'enveloppe nucléaire qui contient des pores et repose sur un réseau de filaments intermédiaires appelés lamina nucléaire, les territoires chromosomiques et les compartiments interchromatiniens (CT-IT). La chromatine est organisée en différents CTs aussi appelés 'nuclear speckles'. (Issu de Lanctôt *et al.,* 2007).

Université Paris-Saclay
Espace Technologique / Immeuble Discovery
Route de l'Orme aux Merisiers RD 128 / 91190 Saint-Aubin, France

des protéines appelées 'nuclear-pore-associated proteins' intéragissent spécifiquement avec les gènes actifs. Les mammifères, au contraire, du fait de la grande taille de leur génome, empèchent la liaison des gènes actifs aux pores nucléaires par contrainte physique. Mais ces observations sont nuancées par l'existence chez la levure (*Saccharomyces cerevisiae*) de régions nucléaires périphériques transcriptionnellement inactives (Andrulis *et al.,* 1998). Les cellules de mammifères sont, elles, suspectées de subir d'autres formes de contraintes structurales du fait de la très grande quantité d'hétérochromatine qui les constituent (Casolari *et al.,* 2004; Schmid *et al.,* 2006; Lanctôt *et al*., 2007).

4.3 Co-régulation des régions chromosomiques

Le cas le plus frappant de co-régulation de régions chromosomiques différentes est constitués des 'kissing-genes'. Il a été observé chez la Drosophile que deux versions du même gène étaient capables d'interagir physiquement notamment pour maintenir le silencing de certains gènes après la division cellulaire (Francis et Kingston, 2001). Chez *Drosophila melanogaster*, il a été montré que l'intégration ectopique de la même version d'un gène suffit à entrainer l'interaction physique entre les deux copies (Bantignies *et al.*, 2003). De plus il est connu que certains gènes interagissent avec des éléments régulateurs parfois situés très loin et même sur d'autres chromosomes (Lomvardas *et al.,* 2006). Il a été montré récemment que les gènes nécessitent d'être associés à des 'transcription factories', complexes protéiques enrichis en PolII, pour être exprimés. De plus le nombres de ces 'factories' étant limités, les gènes sont parfois contraints de partager ces complexes (**Figure 7** ; Osborne *et al.,* 2004). Chez les champignons filamenteux, ces mécanismes ne sont pas encore très documentés. Le developpement de nouvelles techniques permettant d'analyser les régions interagissant physiquement permette d'accroitre la compréhension de l'organisation des chromosomes au sein des noyaux et de leur impact sur l'expression des gènes. On peut ici prendre l'exemple du Hi-C sequencing, technique qui se base sur le crosslinking du génome puis sur une étape de ligation, de

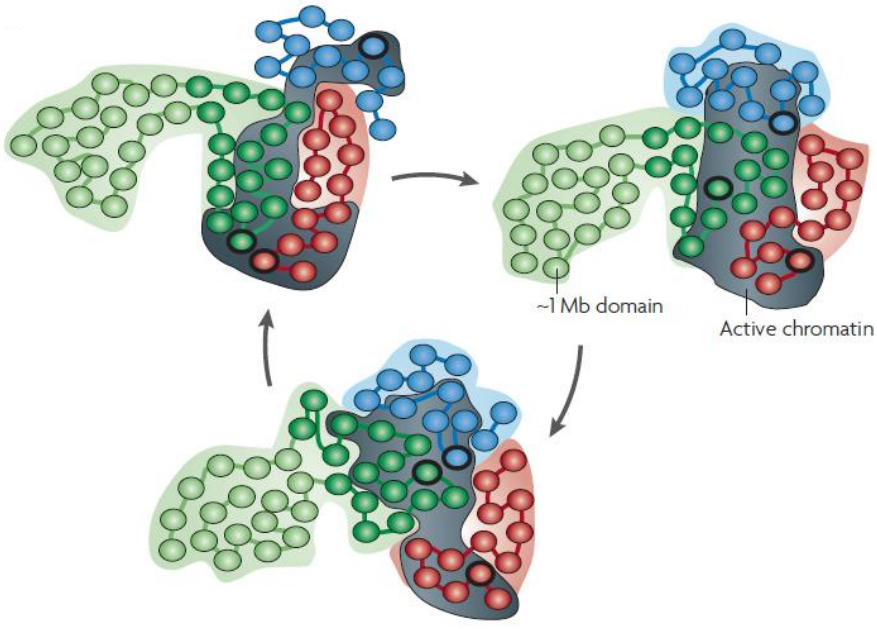

Figure 7 : Interactions physiques successives de plusieurs régions chromosomiques avec la fraction active de la chromatine. En vert, rouge et bleu, trois chromosomes différents. En gris est représentée la fraction active de la chromatine. On voit ici que la fraction active de la chromatine a une taille réduite et que pour pouvoir être exprimés correctement, les régions chromosomiques doivent interagir tour à tour avec la fraction active de la chromatine (Issu de Lanctôt *et al.,* 2007).

Université Paris-Saclay
Espace Technologique / Immeuble Discovery
Route de l'Orme aux Merisiers RD 128 / 91190 Saint-Aubin, France

dé-crosslinking puis d'amplification et de séquençage. Mais alors que le 3C sequencing permet d'identifier des séquences cibles, le Hi-C permet de réaliser la carte des interactions à l'échelle du génome (**Figure 8** ; Lieberman-Aiden *et al.,* 2009). Chez *N.crassa*, il a été montré que les régions hétérochromatiniennes (surtout les régions d'hétérochromatine constitutive enrichies en H3K9me3) développent des liaisons physiques entres elles mais que l'inactivation de *KMT1* n'entraine pas de modification de l'organisation 3D du noyau. Au contraire, les régions d'hétérochromatine facultative, enrichies en H3K27me3, sont essentielles au maintient de l'organisation 3D des génomes car elles se lient à la membrane nucléaire (Klocko *et al.,* 2016). Chez *N. crassa*, l'inactivation de *KMT1* et la perte des marques H3K9me3 entraine une relocalisation des marques H3K27me3, qui, une fois relocalisées à l'emplacement des marques H3K9me3, ne participent pas à l'organisation 3D du génome. Ces résultats indiquent une robustesse de la structure 3D des génomes qui n'est pas mise à mal par l'inactivation de facteurs clefs impliqués dans l'établissement de la structure chromatinienne (Basenko *et al.,* 2015; Galazka *et al.,* 2016; Klocko *et al.,* 2016). L'organisation 3D du génome d'*E. festucae*, un champignon endophyte ayant une structure genomique en isochores, a été décrite récemment (Winter *et al.,* 2018). Les ETs ayant envahi le génome d'*E. festucae* ont été dégénérés par le RIP conduisant à la formation de régions riches en ETs enrichies en bases A et T (isochores AT) et de régions riches en gènes et enrichies en bases G et C (isochores GC ; Winter *et al.,* 2018). Winter *et al*. (2018) ont mis en évidence des contacts physiques entre les isochores AT et entre les isochores GC mais très peu d'interactions entre les deux types de domaines. De plus, les contacts entre régions AT sont très majoritaires (50 % de tous les contacts interchromosomiques), ce qui indique une structuration par les isochores AT dans ce type de génome. De façon intéressante, les isochores AT contiennent la plupart du temps un unique TAD alors que les isochores GC en contiennent plusieurs, ces TADs étant connus pour permettre une co-régulation génique (Ulianov *et al.,* 2016). Les isochores AT sont très enrichis en gènes fortement exprimés *in planta* et peu en condition de culture axénique, ce qui pourrait suggérer une régulation via les TADs des gènes impliqués dans la mise en place de l'infection (Winter *et al.,* 2018).

5. Facteurs de transcription et expression génique

Les facteurs de transcription (FTs) sont des protéines capables de se lier à l'ADN pour effectuer de nombreuses fonctions de régulation telles que le contrôle de l'expression génique, la réplication ou encore la réparation de l'ADN (Latchman, 1997). Les FTs, par ces mécanismes de liaison à l'ADN, permettent d'effectuer des fonctions essentielles à la vie de la cellule, régulant le développement, la croissance et la différentiation cellulaire (Pabo et Sauer, 1992). Les facteurs de transcription possèdent souvent plusieurs domaines dont un permettant la fixation à l'ADN et d'autres permettant de se lier à d'autres protéines ou cofacteurs. Les domaines de fixation à l'ADN (DNA-Binding Domain, DBD) sont des domaines conservés qui permettent de classer les FTs en différentes familles (Pabo et Sauer, 1992). Les facteurs de transcription agissent en amont des gènes. Ils peuvent avoir une fonction activatrice ou répressive sur le niveau de transcription du gène associé. Les FTs agissent en se fixant sur les sites de régulation de la transcription dans les promoteurs et recrutent ou empêchent la fixation des protéines de la machinerie de la transcription (**Figure 9** ; Thomas et Chiang, 2006).

Université Paris-Saclay
Espace Technologique / Immeuble Discovery
Route de l'Orme aux Merisiers RD 128 / 91190 Saint-Aubin, France

5.1 Transcription et facteurs de transcription chez les Eucaryotes

Chez les Eucaryotes, il existe un grand nombre de polymérases capables de transcrire l'ADN en ARN. Le nombre de polymérases par génome est variable en fonction des organismes. On retrouve par exemple huit polymérases chez *Escherichia coli*, douze chez *Arabidopsis thaliana* et quinze chez l'homme (Garcia-Diaz et Bebenek, 2007). Toutes les fonctions des polymérases ne sont pas connues. Il y a trois polymérases majoritairement étudiées dont les fonctions sont bien décryptées, la Pol I, la Pol II et la Pol III. La Pol I est surtout impliquée dans la réparation de l'ADN et la production de ribosomes (Khatter *et al.,* 2017). La Pol II est responsable de la transcription des ARNm et de certains sRNA. La Pol III est responsable de la production de petits ARN comme le ribosome 5S ou les ARN de transferts (Garcia-Diaz et Bebenek, 2007). Les ARN polymérases ne sont pas capables d'initier la transcription seule. Elles ont besoin de cofacteurs, de co-activateurs et de FTs pour reconnaître le site d'initiation de la transcription, s'y fixer et initier la transcription (Patikoglou et Burley, 1997). Les Eucaryotes unicellulaires tels que les levures possèdent des régions régulatrices très courtes (quelques paires de bases à quelques centaines de paires de bases) positionnées juste à côté du promoteur (**Figure 10** ; Levine et Tjian, 2003). Chez les animaux, on retrouve des régions régulatrices plus complexes avec des éléments régulateurs en amont, en aval et dans les introns, et parfois même très éloignés de la séquence codante (jusqu'à 100 kb). Les gènes d'animaux possèdent la plupart du temps plusieurs enhancers avec un enhancer classique mesurant environ 500 pb. Ces régions régulatrices nécessitent l'action simultanée de complexes protéiques contenant de nombreux type de protéiques (facteurs de transcription, ARN polymérases, protéines de remodellage de la chromatine etc… ; Levine et Tjian, 2003). Chez les Eucaryotes, les FTs reconnaissent de courtes séquences dégénérées contrairement aux FTs des prokaryotes qui reconnaissent de larges motifs conservés (Wunderlich et Mirny, 2009). La reconnaissance de la région régulatrice par les FTs se fait via leur DBD. Il existe de nombreuses familles de FTs chez les Eucaryotes, une partie étant conservée entre les espèces, d'autres étant spécifiques de certains règnes (Shelest, 2008). Les gènes codant des FTs représentent 0.5 à 8 % du génome des Eucaryotes selon la complexité de

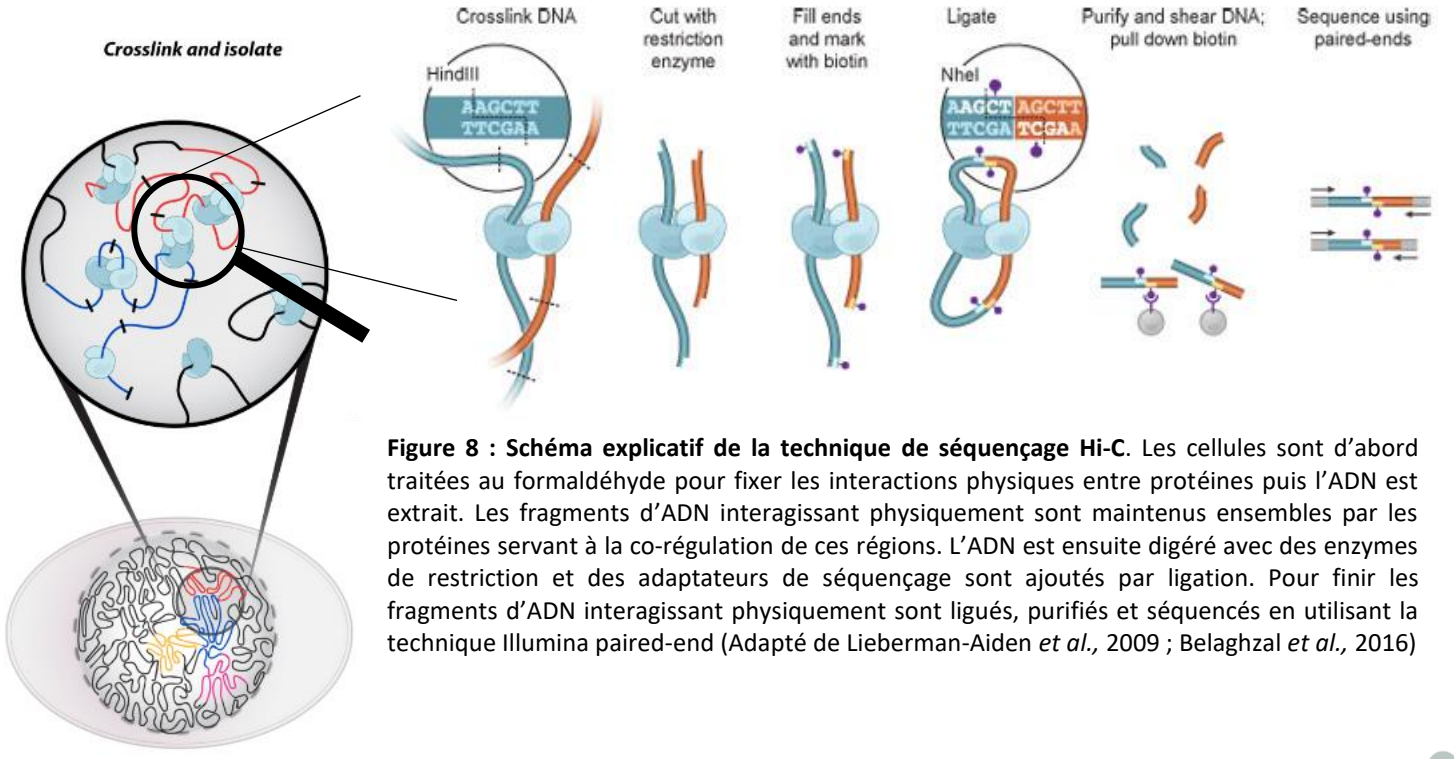

Figure 8 : Schéma explicatif de la technique de séquençage Hi-C. Les cellules sont d'abord traitées au formaldéhyde pour fixer les interactions physiques entre protéines puis l'ADN est extrait. Les fragments d'ADN interagissant physiquement sont maintenus ensembles par les protéines servant à la co-régulation de ces régions. L'ADN est ensuite digéré avec des enzymes de restriction et des adaptateurs de séquençage sont ajoutés par ligation. Pour finir les fragments d'ADN interagissant physiquement sont ligués, purifiés et séquencés en utilisant la technique Illumina paired-end (Adapté de Lieberman-Aiden *et al.,* 2009 ; Belaghzal *et al.,* 2016)

Université Paris-Saclay
Espace Technologique / Immeuble Discovery
Route de l'Orme aux Merisiers RD 128 / 91190 Saint-Aubin, France

l'organisme observé. Les familles les plus retrouvées chez les Eucaryotes sont les FTs à doigt de Zinc et les Zinc cluster (C2H2 et C4 zinc fingers ; ZnCys6/C6 zinc cluster), les helice-tour-helice (HTH), les basic leucine zipper (bZip) et les basic helice-tour-helice (bHLH ; Wunderlich et Mirny, 2009). Chez les plantes, on retrouve également les familles AP2, MADS box, WRKY et B3 (**Figure 10** ; Weirauch et Hughes, 2011).

5.2 Les facteurs de transcription spécifiques du règne des Fungi

Les Fungi comme les autres Eucaryotes possèdent un arsenal de FTs permettant la régulation de l'expression génique. Park *et al*. (2008) ont ainsi identifié 31 832 FTs putatifs à partir de 62 espèces de champignons. Chez les champignons, on retrouve 37 superfamilles de domaines de liaison à l'ADN et parmi celles-ci 12 sont spécifiques des champignons (**Figure 11** ; Shelest, 2008). On y retrouve des FTs à poing de cuivre 'copper fist domains' stabilisés par de multiples ions Cuivre et des FTs APSES qui pourraient avoir été acquis par transfert horizontal d'un KilA-N-like précurseur viral au début de l'évolution du règne des Fungi (Weirauch et Hughes, 2011). Chez *N. crassa*, un projet visant à inactiver les 10 000 gènes de son génome avait été initié : parmi les 312 gènes codant des FTs identifiés chez ce champignon, 242 ont été inactivés et 43 % des mutants obtenus avait un phénotype défectif pour au moins une fonction développementale (défauts de croissance mycélienne et/ou de conidiation), la majorité d'entre eux étant affectés dans plusieurs processus développementaux (morphologie, développement asexué, croissance, et développement sexué ; Colot *et al.,* 2006 ; Dunlap *et al.,* 2007 ; Carrillo *et al.,* 2017). On retrouve chez *N. crassa* 130 gènes codant des 'C6 binuclear cluster' qui constituent la plus grande famille de FTs chez ce champignon. La deuxième famille la plus représentée est constituée des C2H2 à doigt de Zinc avec 54 gènes. Ensuite, les familles les plus présentes chez *N. crassa* sont les bZIP (23 gènes), les MYB (16 gènes) et les bHLH (13 gènes). Une étude récente montre que chez six espèces pathogènes de l'homme seuls deux facteurs de réponse au stress oxydatif sont conservés, Yap1

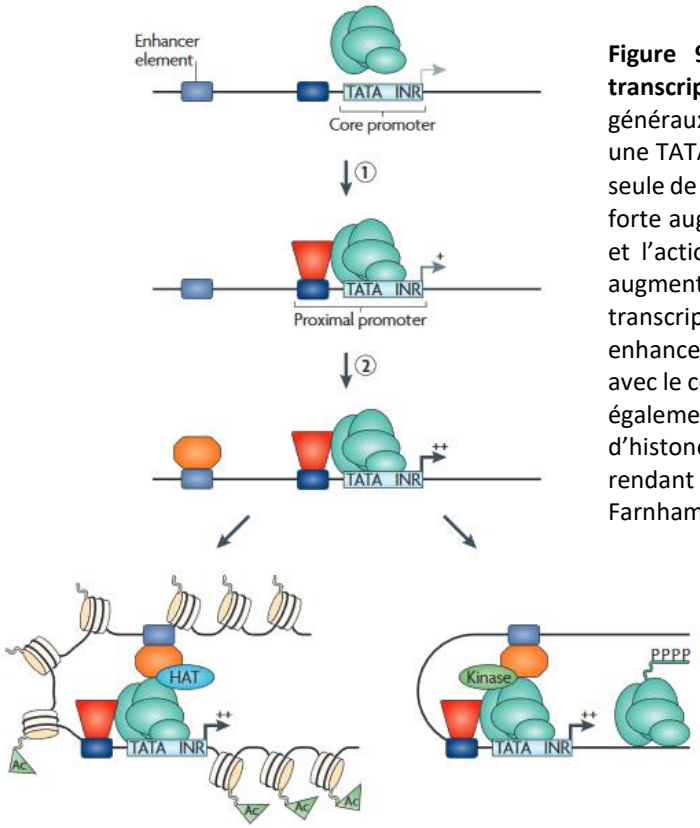

Figure 9 : Schéma représentant l'action d'un facteur de transcription général (GTF). Les facteurs de transcription généraux (ovales verts) se fixent au site de régulation du gène, une TATA box ou un initiateur (INR) par exemple. Mais la fixation seule de ce type de facteur de transcription n'induit pas une très forte augmentation de la transcription. Il permet le recrutement et l'action de FTs spécifiques (trapèze rouge ; étape 1) ce qui augmente fortement le niveau de transcription (+). La transcription peut être encore améliorée en recrutant un enhancer (octogone orange ; étape 2) qui stabilisera l'interaction avec le complexe d'initiation de la transcription. Enfin le GFT peut également permettre le recrutement de protéines modificatrices d'histones qui modifieront la structure de la chromatine la rendant plus accessible à la machinerie de transcription. (D'après Farnham, 2009).

Université Paris-Saclay
Espace Technologique / Immeuble Discovery
Route de l'Orme aux Merisiers RD 128 / 91190 Saint-Aubin, France

et Skn7. Il semble donc que les FTs soient très espèces spécifiques en ce qui concerne le contrôle des facteurs de virulence fongiques (Pais *et al.,* 2016).

5.3 Contrôle transcriptionnel et pathogénie chez les champignons filamenteux

Les FTs fongiques peuvent avoir de multiples fonctions. Certains ont des rôles pléiotropes alors que d'autres ont des fonctions très ciblées et uniques. Ainsi chez *N. crassa* ou encore la levure (*S. cerevisiae*), le facteur de transcription StuA, FT général de la famille des APSES, est capable de réguler la reproduction ou encore le dimorphisme (ici, passage d'un état levure à un état filamenteux ; Gimeno et Fink, 1994 ; Aramayo *et al.,* 1996). Chez *Parastagonospora nodorum*, un champignon pathogène du blé de la famille des Dothidéomycètes, *SnStuA* a été identifié comme régulateur du métabolisme carboné et de la production de toxines. Ce facteur de transcription de la famille des APSES a été l'objet d'un transfert horizontal d'un virus vers le règne des champignons au début de leur histoire évolutive (Weirauch et Hughes, 2011 ; IpCho *et al.,* 2010). Le gène orthologue codant ce FT a été inactivé chez plusieurs autres ascomycètes (*Fusarium oxysporum, Glomerella cingulata, A. fumigatus*), entrainant une altération de la conidiation, de la croissance et même de la pathogénie (Ohara et Tsuge, 2004 ; Tong *et al.,* 2007 ; Sheppard *et al.,* 2005). Si certains facteurs de transcription comme StuA régulent de nombreuses étapes du développement fongique, d'autres tels que Ros1, un facteur de transcription de la famille des WOPR, régulent spécifiquement l'expression de gènes codant des effecteurs. Cette famille de FTs spécifique du règne des Fungi a été découverte chez *Fusarium oxysporum f. sp. lycopersici*, où ce FT avait été nommé Sge1. L'inactivation de Sge1 chez ce champignon mène à un défaut de pathogénie. Les spores du mutant Sge1 sont toujours capable de germer et de permettre la pénétration dans la tomate mais un défaut d'expression des gènes codant des effecteurs a été observé (Michielse *et al.,* 2009). Chez le basidiomycète *U. maydis*, Ros1 régule la conidiation et l'expression des effecteurs tardifs (Tollot *et al.,* 2016). Deux autres FTs regroupés au sein de la famille FTF (*Fusarium* Transcription Factors) ont été décrits chez *F. oxysporum* : FTF2 qui est présent chez tous les ascomycètes filamenteux et FTF1 qui est spécifiquement retrouvé, en plusieurs

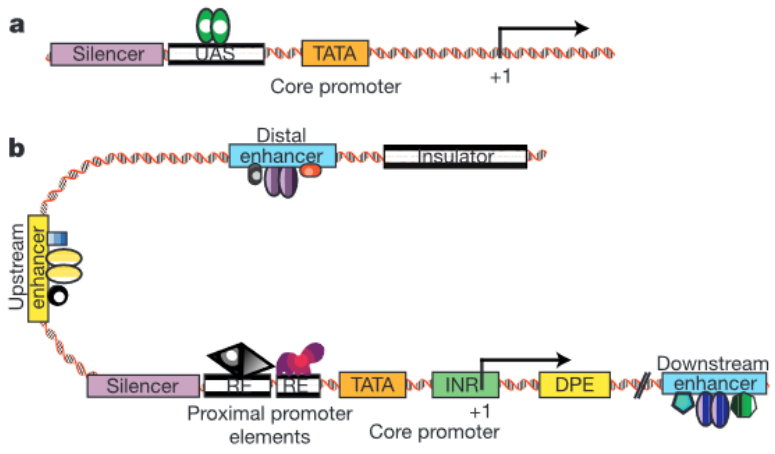

Figure 10 : Figure comparant des zones régulatrices chez un Eucaryotes unicellulaire par rapport à un Eucaryote complexe. A : unité transcriptionnelle chez un Eucaryote simple. Un core promoteur simple (TATA), un activateur amont (UAS), une séquence initiatrice (INR), un élément promoteur aval (DPE), des éléments promoteurs amonts (RE) et un silenceur, le tout entre 100 et 200 pb de la TATA box. **B** : Unité transcriptionnelle chez un Eucaryote complexe. Arrangement complexe de plusieurs enhancers clusterisés avec des silenceurs et insulateurs qui peuvent être situés en amont ou en aval à des distances allant de 10 kb à 50 kb de la TATA box (Issu de Levine et Tjian, 2003).

Université Paris-Saclay
Espace Technologique / Immeuble Discovery
Route de l'Orme aux Merisiers RD 128 / 91190 Saint-Aubin, France

copies, chez *F. oxysporum.* L'inactivation de ces gènes induit un défaut de pathogénie ainsi qu'une diminution du niveau d'expression de gènes codant des effecteurs (effecteurs SIX, Secreted In Xylem) et de *SGE1* qui régule lui-même l'expression des gènes *SIX* (Niño-Sánchez *et al.,* 2016). Une étude récente confirme ce résultat chez *F. oxysporum*. En effet ce champignon possède un chromosome accessoire de pathogénie sur lequel sont localisés 13 FTs ainsi que de nombreux gènes codant des effecteurs. L'expression constitutive de *FTF1* ou *FTF2* induit l'expression de presque tous les gènes codant des effecteurs portés par le chromosome accessoire indiquant l'autonomie transcriptionnelle de ce chromosome qui peut être transféré horizontalement (van der Does *et al.,* 2016). Enfin un autre FT de la famille des Zn2Cys6 binuclear cluster, AbPf2, a été décrit comme impliqué dans le contrôle de l'expression de gènes codant des

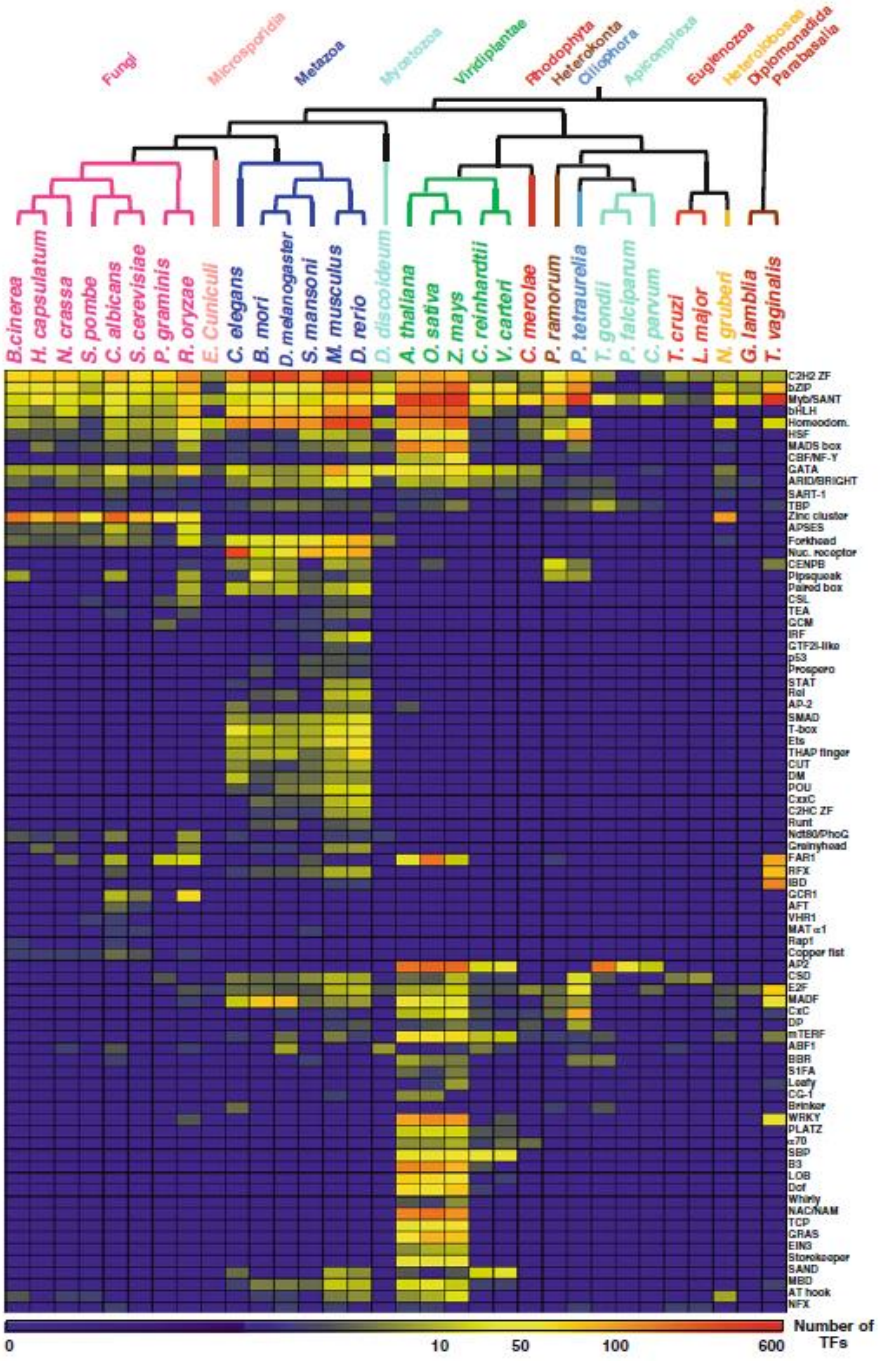

Figure 11 : Nombre de facteurs de transcription par règne et par espèce en fonction du type de FT. Heatmap réalisée à partir des domaines protéiques issus de Pfam. (D'après Weirauch et Hughes, 2011).

Université Paris-Saclay
Espace Technologique / Immeuble Discovery
Route de l'Orme aux Merisiers RD 128 / 91190 Saint-Aubin, France

effecteurs chez *Alternaria brassicicola*. AbPf2 serait impliqué dans le contrôle de l'expression de 106 gènes dont 33 codent des SSPs (Cho *et al.,* 2013). Ce FT possède des homologues chez les Dothideomycetes et son inactivation chez deux espèces de Pleosporales pathogènes du blé (*P. nodorum* et *Pyrenophora tritici-repentis*) induit une diminution d'expression de gènes codant des toxines hôte-spécifique (SnToxA et PtrToxA) présentes chez les deux espèces et ayant été acquis par transfert horizontal de *P. nodorum* vers *P. tritici-repentis* (Rybak *et al.,* 2017). Cette inactivation n'entraine ni défaut de croissance ni défaut de conidiation chez *A. brassicicola* et quelques défaut développementaux chez *P. nodorum* et *P. tritici-repentis* mais abolie totalement la capacité à infecter son hôte chez les trois espèces, ce qui indique la capacité de certains FTs à réguler uniquement la pathogénèse chez les ascomycètes phytopathogènes (Cho *et al.,* 2013 ; Rybak *et al.,* 2017).

6. *Leptosphaeria maculans*, champignon pathogène du colza : un bon modèle pour étudier les mécanismes contrôlant l'expression des gènes codant des effecteurs

6.1 Le colza, une brassicacée très cultivée mais ciblée par des agents pathogènes

Le colza, *Brassica napus*, appartient à la famille des Brassicaceae et est issu d'un croisement inter-spécifique entre deux espèces diploïdes : le chou, *Brassica oleracea* (2n = CC), et la navette, *Brassica rapa* (2n = AA), ayant eu lieu il y a 7 000 à 12 500 ans (Chalhoub *et al*., 2014). Le colza est donc un allotétraploïde (AACC). La culture du colza remonte à l'Antiquité, notamment en Chine. Elle aurait été introduite en Europe vers le XIIIème siècle (Hebinger, 2013). Son huile servait à la fois à l'alimentation et à d'autres usages comme l'éclairage ou la savonnerie. On utilise actuellement non seulement le colza pour son huile mais également pour la production de tourteaux, galettes protéinées co-produits de l'extraction d'huile utilisés pour l'alimentation animale. Des programmes de sélection variétale ont permis au colza de perdre ses fortes teneurs en acide érucique et en glucosinolates qui provoquaient des baisses d'appétence, particulièrement chez les bovins, et induisaient des troubles thyroïdiens chez les animaux monogastriques (Bonneuil et Thomas, 2012). Suite à ce programme d'amélioration du colza, la culture du colza a connu un fort essor dès 1980. On cultive aujourd'hui en France 1,48 MHa de colza d'hiver (http://agreste.agriculture.gouv.fr). Le colza d'hiver est une plante annuelle. Semé de la mi-août à la fin septembre en Europe de l'Ouest, le colza connait d'abord une première phase de levée puis reste végétatif jusqu'à fin novembre/décembre où il rentre dans une phase vernalisante. La croissance reprend à la sortie de l'hiver (février à mars), quand les températures augmentent. La tige s'allonge rapidement et de nouvelles feuilles se mettent en place ainsi que de nouvelles racines. La maturation des graines se termine en juillet (Hebinger, 2013). Les pertes de rendement dues à des bioagresseurs sont généralement causées par des champignons et des insectes ravageurs. Parmi les principaux agents pathogènes fongiques, on retrouve *Sclerotinia sclerotiorum* et *L. maculans* (agent causal de la nécrose du collet, ou phoma). D'autres champignons comme *Cylindrosporium concentricum* (agent responsable de la cylindrosporiose), *Erysiphe cruciferarum* (agent responsable de l'oïdium), *Plasmodiophora brassicae* (responsable de la hernie des crucifères) ou *Alternaria brassicae* (responsable de l'alternatiose) causent également des symptômes sur colza mais avec une incidence moindre ou une répartition locale (Source : www.terresinovia.fr/colza/cultiver-du-colza/maladies). Le sclérotinia est une maladie relativement

Université Paris-Saclay
Espace Technologique / Immeuble Discovery
Route de l'Orme aux Merisiers RD 128 / 91190 Saint-Aubin,
France

bien contrôlée par les fongicides à l'inverse de la nécrose du collet qui nécessite l'utilisation de variétés génétiquement résistantes pour éviter des pertes pouvant aller jusqu'à 20% de la récolte (Fitt *et al*., 2006).

6.2 Le champignon pathogène responsable de la nécrose du collet (ou «blackleg disease»)

Leptosphaeria maculans 'brassicae' (*L. maculans* dans la suite de l'introduction) est un champignon Ascomycète, appartenant à la classe des Dothidéomycètes et à l'ordre des Pléosporales. Ce champignon est responsable de la nécrose du collet du colza et d'autres crucifères, pouvant occasionner des pertes de rendement allant jusqu'à 20 % de la récolte (Fitt *et al.,* 2006). En Europe, *L. maculans* effectue sa reproduction sexuée à l'automne sur les résidus de culture de l'année précédente puis les ascospores, dispersées par le vent, peuvent coloniser les premières feuilles au champ. Après germination des ascospores, l'hyphe mycélien pénètre dans les feuilles via les stomates ou des blessures. Après une phase de développement asymptomatique, des nécroses foliaires apparaissent. Ces macules foliaires, caractérisées par la présence de conidies (inoculum secondaire), produits de la reproduction asexuée, vont permettre de propager l'agent pathogène à courte distance. A partir de ces nécroses, le mycélium colonise de façon systémique et endophyte les espaces intercellulaires des tissus des feuilles, du pétiole et de la tige, sans provoquer de symptômes. Après cette phase endophyte de plusieurs mois, *L. maculans* devient nécrotrophe et provoque alors une nécrose de la base de la tige, qui peut conduire à la verse parasitaire des plantes (**Figure 12** ; Williams et Fitt, 1999 ; West *et al.,* 2002 ; Rouxel *et al.,* 2004). *L. maculans* possède un génome riche en ETs (33 % du génome) qui se caractérise par la présence de deux types de compartiments : des isochores GC représentant deux tiers du génome pauvres en ETs et riches en gènes (contenant 95 % des gènes) et des isochores AT, représentant un tiers du génome, pauvres en gènes et riches en ETs (Rouxel *et al*., 2011). Une première prédiction du répertoire d'effecteurs de *L. maculans* (correspondant à des PPS de moins de 300 aa) avait permis d'identifier 651 effecteurs putatifs : 122 codés par des gènes localisés en isochores AT et 529 par des gènes localisés en isochores GC. Les gènes codant des effecteurs situés en isochores AT représentent donc 20 % des gènes prédits dans ces régions contre seulement 4 % dans le cas des isochores GC, suggérant que les isochores AT sont enrichis en gènes codant des effecteurs (Rouxel *et al.*, 2011). Plus récemment, un nouvel assemblage, une nouvelle annotation du génome de *L. maculans* et une nouvelle prédiction du répertoire de gènes codant des effecteurs ont été réalisés et utilisés pour une partie des analyses réalisées au cours de la thèse (Dutreux *et al.,* 2018 ; EJ. Gay thèse en cours).

Université Paris-Saclay
Espace Technologique / Immeuble Discovery
Route de l'Orme aux Merisiers RD 128 / 91190 Saint-Aubin, France

6.3 Expression synchronisée des effecteurs chez *L. maculans*

Une première vague d'expression d'effecteurs (incluant les gènes d'avirulence clonés chez *L.* maculans) a été identifiée durant les étapes précoces de l'infection (effecteurs 'précoces' ; Rouxel *et al*., 2011 ; Gervais *et al*., 2017). Les gènes codant des effecteurs situés en isochores AT présentent une faible expression pendant la croissance mycélienne et une forte induction de leur expression pendant la phase de colonisation asymptomatique des cotylédons et des feuilles de colza, avec un pic d'expression 7 jours post infection (jpi). Les gènes codant pour des effecteurs précoces sont majoritairement localisés dans les isochores AT puisqu'à 7 jpi, 73 % des gènes codant des effecteurs en isochore AT sont sur-exprimés contre 19 % des mêmes gènes en isochore GC (Rouxel *et al.,* 2011). Par ailleurs, 8 % des gènes codant des effecteurs localisés en isochore AT sont exprimés *in vitro* contre 55 % de ceux localisés en isochore GC. Une deuxième vague d'effecteurs spécifiquement exprimés pendant les phases de colonisation systémique et de nécrose de la tige (effecteurs 'tardifs') a récemment été identifiée grâce à des analyses RNA-Seq. Les gènes codant ces effecteurs sont, eux, localisés majoritairement dans les isochores GC. 307 gènes (ont été identifiés comme spécifiquement sur-exprimés en condition tardive d'infection (Gervais et *al.,* 2017). Enfin, une

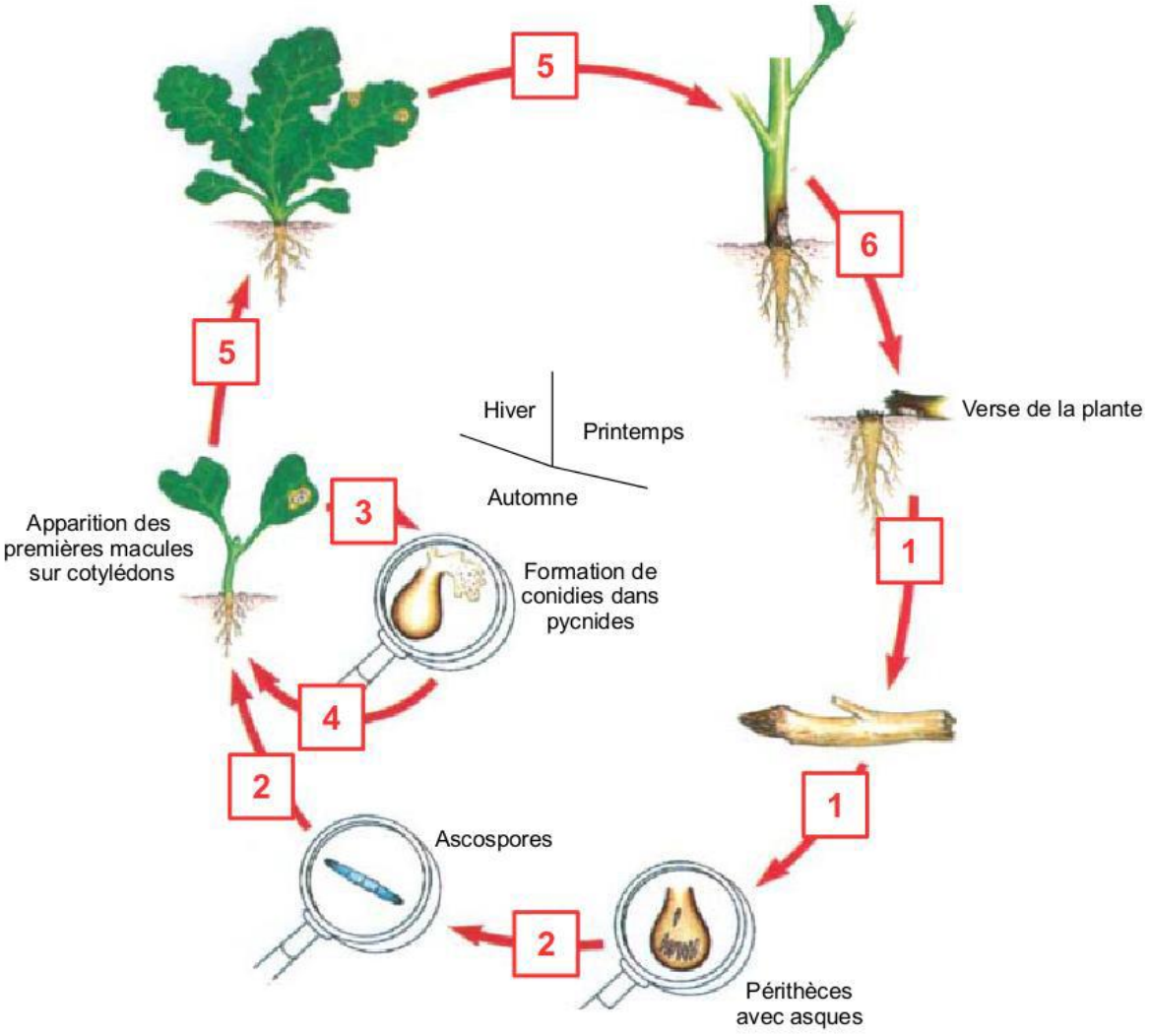

Figure 12 : Cycle de vie de *Leptosphaeria maculans* en Europe. 1 : phase saprophyte sur résidus de culture ; **2 :** reproduction sexuée produisant des ascoscpores constituant l'inoculum primaire ; **3, 4 :** courte phase nécrotrophe suivant l'infection primaire caractérisée par l'apparition de macules foliaires et multiplication asexuée produisant des conidies ; **5 :** longue phase endophyte avec colonisation systémique de la tige et du collet ; **6 :** phase nécrotrophe à l'origine de la verse de la plante. Adapté de CETIOM (1996).

Université Paris-Saclay
Espace Technologique / Immeuble Discovery
Route de l'Orme aux Merisiers RD 128 / 91190 Saint-Aubin,
France

analyse RNA-Seq est actuellement menée sur l'ensemble du cycle de vie de *L. maculans* (incluant infection en conditions contrôlées et infection au champ ; EJ. Gay, thèse en cours) et permet d'identifier de nouveaux profils d'expression de gènes codant des effecteurs. La localisation distincte des gènes codant des effecteurs 'précoces' ou 'tardif' au sein du génome de *L. maculans* 'brassicae' a des conséquences sur leur évolution dans les populations de *L. maculans* (les gènes codant des effecteurs 'tardifs' étant mieux conservés dans les populations de *L. maculans* que ceux codant des effecteurs précoces ; Rouxel *et al.,* 2011 ; Gervais *et al.,* 2017) et sur le contrôle de leur expression (cf. **partie 6.5**).

6.4 Le complexe d'espèces *L. maculans* / *L. biglobosa*

L. maculans fait partie d'un complexe comprenant au moins deux groupes génétiquement distincts initialement décrits comme respectivement « virulent » et « avirulent » (McGee et Petrie, 1978). Grâce à l'avènement des outils moléculaires, ces deux groupes ont été reconnus comme étant deux espèces différentes : *L. maculans* et *Leptosphaeria biglobosa* (Shoemaker et Brun, 2001). Sur colza, ces deux espèces se développent sur les mêmes hôtes et peuvent être retrouvées simultanément sur la même plante. Elles sont toutes les deux capables de provoquer des lésions nécrotiques et de coloniser les tissus des plantes hôtes mais leur impact sur les cultures ne sont pas similaires : seule *L. maculans* est susceptible de provoquer la verse parasitaire et donc d'être dommageable pour les cultures (Williams et Fitt, 1999 ; West *et al.,* 2002 ; Rouxel *et al.,* 2004), Contrairement à *L. maculans*, *L. biglobosa* cause des lésions de la tige ne conduisant qu'à des dégâts mineurs. Chez *L. maculans*, de nombreuses interactions spécifiques (interactions gène-pour-gène) ont été montrées avec ses différents hôtes alors que pour le moment aucune interaction de ce type n'a été décrite chez *L. biglobosa* (Dilmaghani *et al.,* 2009). Des relations phylogénétiques entre les membres du complexe d'espèces ont été établies sur la base d'analyses de plusieurs séquences nucléiques (*ITS*, *actine*, *β-tubuline*), révélant un niveau de complexité inattendu en comparaison à la simple séparation en deux espèces (Mendes-Pereira *et al.,* 2003 ; Voigt *et al.,* 2005 ; Vincenot *et al*., 2008). En effet, ces résultats montrent que *L. maculans* est une espèce très monomorphe avec uniquement une séparation en deux sous-clades dont l'un, *L. maculans* 'lepidii' (Lml), est très rare et représenté seulement par quelques individus isolés sur *Lepidium sp*., une crucifère adventice. *L. biglobosa* est une espèce très polymorphe avec une séparation en six sous-clades correspondant à différentes spécificités d'hôtes ou origines géographiques : *L. biglobosa* 'brassicae' présent sur plusieurs espèces de Brassicaceae en Eurasie et aux Etats-Unis, *L. biglobosa* 'canadensis' retrouvé principalement sur les cultures de colza en Amérique et en Australie, *L. biglobosa* 'occiaustralensis' présent sur colza et chou en Australie et au Mexique, *L. biglobosa* 'australensis' présent sur colza en Australie, *L. biglobosa* 'thlaspii' isolé sur *Thlaspii arvense* au Canada et le très rare *L. biglobosa* 'erysimii' isolé sur *Erysimum spp*. au Canada (Mendes-Pereira *et al.,* 2003 ; Voigt *et al.,* 2005 ; Vincenot *et al.,* 2008 ; Van de Wouw *et al.,* 2009 ; Dilmaghani *et al.,* 2009, 2012). Etonnamment les autres espèces du complexe possèdent des répertoires d'effecteurs de tailles similaire à celui de Lmb malgré leur taille de génome plus réduite avec 875 gènes codant des effecteurs prédits chez *L. biglobosa* dont 75 d'entre eux localisés dans les isochores AT de son génome (Dutreux *et al.,* 2018). Les génomes de *L. biglobosa* 'thlaspii', *L. biglobosa* 'brassicae', *L. biglobosa* 'canadensis' et *L. maculans* 'lepidii', contiennent respectivement, 4 %, 3,2 %, 2,9 % et 2,7 % d'ETs (Grandaubert *et al*., 2014). Mais une étude récente a permis d'identifier que le génome de *L. biglobosa* 'brassicae' pouvait contenir jusqu'à

Université Paris-Saclay
Espace Technologique / Immeuble Discovery
Route de l'Orme aux Merisiers RD 128 / 91190 Saint-Aubin,
France

15 % d'ETs (Dutreux *et al.,* 2018). De façon surprenante, *L. maculans* 'lepidii' possède un génome quasi identique à celui de *L. maculans* 'brassicae' avec une structuration en isochores moins marquée que celle de *L. maculans* 'brassicae' mais un répertoire d'effecteurs similaire en nombre. En revanche, malgré le nombre similaire d'effecteurs, 41 % des gènes codant des effecteurs localisés en isochore AT chez *L. maculans* 'brassicae' lui sont spécifiques, ce qui pourrait indiquer que l'invasion du génome de *L. maculans* 'brassicae' par des ETs est un mécanisme permettant de diversifier le répertoire d'effecteurs. *L. maculans* 'lepidii' possède, lui aussi, un répertoire d'effecteurs spécifique par rapport aux autres espèces du complexe (Grandaubert *et al.,* 2014).

6.5 Contrôle chromatinien de l'expression des gènes codant des effecteurs chez *L. maculans*

Il y a une dizaine d'années, un projet visant à déterminer l'impact de la structure de la chromatine sur la régulation de l'expression des gènes, en particulier des gènes impliqués dans la pathogénie, chez *L. maculans* a été initié. Il était alors établi que i) *L. maculans* possédait une structuration complexe de son génome, avec une alternance de régions riches en ETs et de régions riches en gènes ; ii) que les régions riches en ETs, bien que pauvres en gènes, étaient enrichies en gènes codant des protéines d'avirulence et d'autres effecteurs putatifs, et iii) que ces gènes étaient spécifiquement exprimés *in planta*. Dans ce contexte, l'hypothèse établie était que les isochores AT pouvaient correspondre à des régions hétérochromatiniennes et que la condensation de la chromatine de ces régions pouvait être à la base d'un processus efficace de régulation de l'expression de gènes codant des effecteurs permettant leur expression concertée *in planta*, et leur répression *in vitro*. Pendant la thèse de J. Soyer, une caractérisation fonctionnelle de deux protéines, HP1 et KMT1, a été menée. Ces deux protéines sont indispensables à la formation de l'hétérochromatine via la tri-méthylation H3K9me3. Le silencing par ARNi de *HP1* et *KMT1* a conduit à une augmentation d'expression *in vitro* de 41 % des gènes codant des effecteurs localisés en isochores AT, ce qui suggère que la structure de la chromatine dans ces régions contribue à une répression de l'expression de ces gènes lors des phases de croissance végétative. Cette augmentation d'expression s'accompagne pour au moins deux gènes codant des effecteurs (*AvrLm4-7* et *AvrLm1*) d'une diminution de la marque H3K9me3. Cependant, l'augmentation d'expression n'atteint pas le niveau d'expression observé lors de l'infection primaire du colza par une souche sauvage (Soyer *et al.,* 2014). L'ensemble de ces résultats suggère que la structuration de la chromatine et la régulation dynamique de cette structure ne serait pas le seul acteur impliqué dans la régulation de l'expression des gènes codant des effecteurs et qu'un, ou plusieurs, FT(s) spécifique(s) seraient également impliqués dans le contrôle de l'expression des effecteurs. Suite à cette étude, le modèle suivant a été proposé (**Figure 13**) : pendant la croissance axénique, les régions génomiques contenant les gènes codant des effecteurs situés en isochores AT sont condensées, ce qui induit une répression de l'expression génique. Au moment de l'infection, le changement de mode de vie et le shift vers la pathogenèse se traduirait par une décondensation de la chromatine (via l'élimination des marques H3K9me3), dont le déterminisme est inconnu, rendant les promoteurs géniques accessibles aux FTs. Une action de FTs spécifiques permettrait ensuite d'exprimer de façon concertée les gènes codant des effecteurs. Ce mécanisme permettrait une adaptation rapide aux nouvelles conditions d'infection en permettant une régulation similaire de l'expression de nombreux gènes, ayant pour fonction de faciliter d'infection, et localisés dans un environnement génomique similaire (Soyer *et al*., 2015. A).

Université Paris-Saclay
Espace Technologique / Immeuble Discovery
Route de l'Orme aux Merisiers RD 128 / 91190 Saint-Aubin,
France

6.6 Contrôle transcriptionnel de l'expression des gènes codant des effecteurs chez *L. maculans*

L'étude du contrôle transcriptionnel de l'expression des gènes codant des effecteurs chez *L. maculans* a également été initiée lors de la thèse de J. Soyer. Afin d'identifier un ou des FTs contrôlant l'expression des gènes codant des effecteurs de *L. maculans*, deux approches avaient été choisies : (i) une approche avec *a priori* consistant à identifier les gènes orthologues de FTs décrits chez les champignons comme impliqués dans le contrôle de l'expression des effecteurs (e.g. *Sge1*, *StuA*, cf. **partie 5.3**) et (ii) une approche sans *a priori* consistant à prédire le répertoire de FTs de *L. maculans* et à rechercher les FTs surexprimés pendant l'infection ou spécifiques de *L. maculans*. En recherchant des domaines caractéristiques des FTs comme décrit par Park *et al.* (2008), J. Soyer a pu identifier un répertoire de 682 FTs putatifs. Après avoir éliminé les FTs ayant un domaine de fixation à l'ADN mais sans prédiction d'initiation de transcription, une liste de 355 TFs putatifs a été obtenue. Après comparaison des séquences de ces FTs avec les génomes du complexe d'espèces, une liste de 44 FTs spécifiques de *L. maculans* a pu être obtenue. Par ailleurs, une analyse transcriptomique à 3, 7 et 14 jpi de cotylédons de colza a permis d'identifier 38 FTs surexprimés pendant l'infection dont deux FTs surexprimés à 3 jpi, 14 à 7 jpi et 21 à 14 jpi. Le silencing des 14 gènes codant des FTs exprimés spécifiquement à 7 jpi et de *StuA et Sge1* a été entrepris mais, en dehors de *StuA* et de deux FTs surexprimés pendant l'infection (gènes ID : *Lema_P013470.1* et *Lema_P074920.1*), le silencing n'avait pas été efficace (pas de diminution d'expression génique). L'inactivation de *LmStuA* entraînait des défauts de sporulation, de croissance et de pathogénie et une diminution d'expression d'au moins deux gènes codant des effecteurs 'précoces' (Soyer *et al.,* 2015. B).

6.7 Objectifs de la thèse

Actuellement, la façon dont l'expression concertée des gènes codant des effecteurs fongiques est régulée est mal comprise. *L. maculans* est un bon modèle pour l'étude du contrôle de l'expression des effecteurs : (i) il possède un cycle de vie complexe, alternant les modes de vie et les stratégies nutritionnelles au cours de son cycle. Ces capacités d'alternance entre modes de vie indiquent un système de régulation sophistiqué de ses gènes ; (ii) le génome de *L. maculans* présente une structure en isochores, alternant régions riche en gènes et régions riches en ETs enrichies en gènes codant des effecteurs 'précoces' ; (iii) au moins deux vagues de gènes codant des effecteurs sont exprimées au cours de l'infection (effecteurs 'précoces' produits pendant l'infection primaire et effecteurs 'tardifs' produits pendant la colonisation des tiges) ; (iv) *L. maculans* 'brassicae' appartient à un complexe d'espèces dont la sous-espèce la plus proche, *L. maculans* 'lepidii', ne présente pas de structure de génome en isochores, et un contenu faible en éléments répétés, et n'est pas pathogène du colza.

Université Paris-Saclay
Espace Technologique / Immeuble Discovery
Route de l'Orme aux Merisiers RD 128 / 91190 Saint-Aubin,
France

Le travail réalisé par J. Soyer durant sa thèse a permis d'initier une étude de l'influence de la structure de la chromatine et de FTs spécifique sur le contrôle de l'expression des effecteurs chez *L. maculans* 'brassicae'. Il a été ainsi mis en évidence un rôle de KMT1 et HP1 dans la mise en place de la marque H3K9me3 et le contrôle de l'expression d'effecteurs localisés dans les régions riches en ETs. L'inactivation par ARNi de *KMT1* et *HP1* a permis d'obtenir une diminution de la modification H3K9me3 dans le promoteur d'au moins deux gènes codant des effecteurs situés dans des régions riches en ETs, accompagnée d'une augmentation de l'expression de ces gènes *in vitro*. Néanmoins, le niveau d'expression de ces gènes *in vitro* chez les transformants n'atteignant pas le niveau d'expression observée pendant l'infection, chez la souche sauvage, ceci suggère l'intervention supplémentaire de FTs spécifiques au moment de l'infection. Ces FTs se fixeraient sur les promoteurs des gènes codant des effecteurs après décondensation de la chromatine (**Figure 13**).

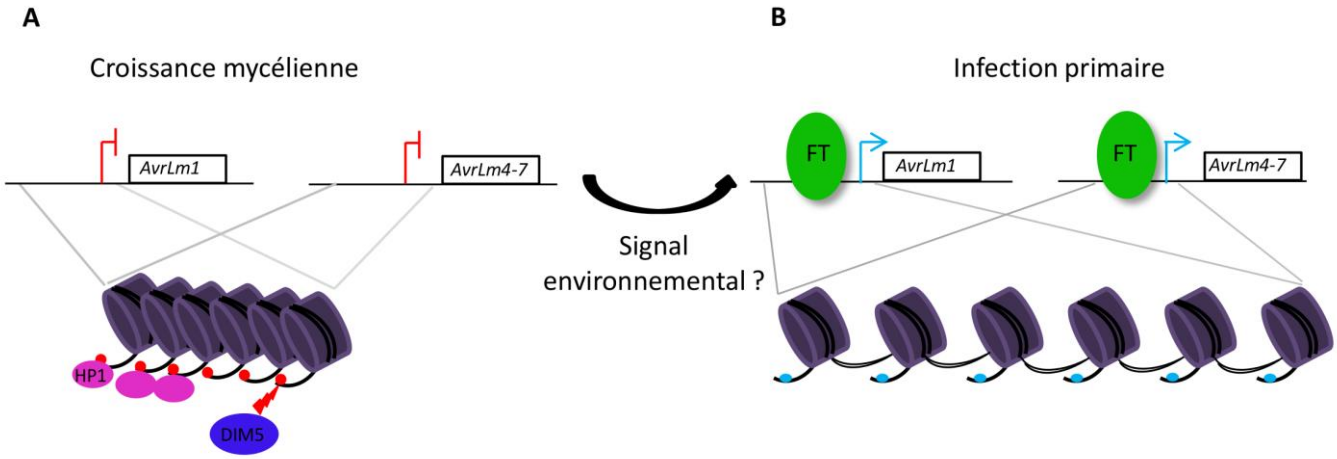

Figure 13 : Modèle de contrôle de l'expression des gènes codant des effecteurs situés en isochores AT chez *Leptosphaeria maculans*. A : Pendant la croissance mycélienne, un mécanisme épigénétique reposant sur une modification des histones associée à l'hétérochromatine, H3K9me3, *via* l'action de LmHP1 et LmDIM5 (i.e. KMT1), entraine une condensation de la chromatine dans l'environnement génomique des gènes et ainsi une répression globale de leur expression. **B :** Pendant l'infection primaire, un signal de l'environnement ou endogène, de nature inconnue, est reconnu par le champignon, permettant de lever la répression, *via* la disparition de la marque H3K9me3, et un espacement des nucléosomes, autorisant l'accès des promoteurs à un, ou plusieurs, FT(s) spécifique(s) permettant une expression concertée pendant l'infection. Boules rouges, modification des histones associée à l'hétérochromatine (ici H3K9me3) ; boules bleues, modification des histones associée à l'euchromatine.

L'objectif de ma thèse est donc de comprendre le rôle de la structure de la chromatine (à plusieurs échelles : position des nucléosomes, modification des histones et organisation intra-nucléaire des chromosomes) et de FTs dans le contrôle de l'expression concertée des gènes codant des effecteurs de Lmb, et plus globalement dans le contrôle de l'expression génique et la pathogénie. Dans ce but, deux thématiques de recherche sont développées en parallèle : (i) l'étude de l'influence de la structure de la chromatine sur la régulation de l'expression génique et de la pathogénie et (ii) la recherche de facteurs de transcription impliqués dans la régulation des effecteurs au cours de l'infection. Cet objectif nécessite la mise en place d'approches complémentaires : des analyses bio-informatiques et des analyses fonctionnelles.

Afin de réaliser des analyses fonctionnelles de FTs candidats ou de protéines impliquées dans le remodelage de la chromatine, j'ai utilisé une technique de mutagenèse permettant de s'affranchir des limites de la technique d'ARNi utilisée précédemment dans l'équipe. En effet, l'analyse fonctionnelle par ARNi nécessite le criblage d'un grand nombre de transformants car le niveau de diminution d'expression est très variable. Les transformants silencés

Université Paris-Saclay
Espace Technologique / Immeuble Discovery
Route de l'Orme aux Merisiers RD 128 / 91190 Saint-Aubin, France

générés par Soyer *et al*. (2014) permettaient encore une expression résiduelle de ~20 % de *KMT1*, ce qui ne permettait pas de déterminer les effets d'une absence totale de H3K9me3 sur la structure chromatinienne et l'expression génétique. La technologie CRISPR-Cas9 a récemment été mise au point pour *L. maculans* afin de générer des mutants knock-out (**Figure 14** ; Idnurm *et al.,* 2017). J'ai pu transférer avec succès la méthode CRISPR-Cas9 au laboratoire et inactiver plusieurs gènes codant des histones méthyltransférases, des déméthylases d'histone et des FTs.

1. Etude de l'influence de la structure de la chromatine sur la régulation de l'expression génique et de la pathogénie

Les études réalisées précédemment dans l'équipe concernant l'organisation de la structure de la chromatine étaient menées par des approches ciblées (ChIP-qPCR) et concernaient l'effet des modifications biochimiques des histones sur l'expression des gènes. Au cours de cette thèse, grâce notamment au développement de nouvelles technologies et à la diminution des coûts de séquençage, nous avons pu aller plus loin et développer des analyses «genome-wide» et, autant que possible, comparatives, de i) la position des nucléosomes chez quatre espèces de champignons phytopathogènes présentant des modes de vie distincts (en développant des approches de MAINE-Seq et RNA-Seq), (**Chapitre 1.1**) ; ii) la localisation des modifications des histones H3K4me2, H3K9me3 et H3K27me3 chez deux espèces du complexe d'espèces ayant des structures de génome différentes, Lmb et Lml (par des approches de ChiP-Seq et RNA-Seq), (**Figure 13** ; **Chapitre 1.2**). La combinaison de ces approches permet d'obtenir une vue complète du paysage épigénomique de *L. maculans* 'brassicae' et de son influence sur l'expression des gènes, en particulier des gènes codant des effecteurs. La comparaison de l'organisation épigénomique du génome de *L. maculans* 'brassicae' avec d'autres espèces a pour objectif d'identifier des particularités d'organisation de ce génome, ou, au contraire, ce qui est conservé, et de déterminer dans quelle mesure la structure du génome et de la chromatine influent sur l'adaptation et la spécialisation à l'hôte. Par ailleurs, afin de décrypter l'influence des modifications hétérochromatiniennes H3K9me3 et H3K27me3 sur l'expression génique, des analyses fonctionnelles de trois gènes responsables de modifications chimiques de queues d'histone, KMT1, KMT6 (responsable respectivement de la mise en place de la marque répressive H3K9me3 et H3K27me3) et Kdm8 (responsable de l'enlèvement de la marque H3K36me2) ont été réalisées (**Chapitre 2.1 et 2.2**). iii) l'organisation intra-nucléaire des chromosomes (par une approche de HiC-Seq). L'étude de l'organisation intranucléaire des chromosomes, par Hi-C sequencing (**Figure 8**), a été initiée. Les données relatives à cette approche seront présentées dans le **chapitre 2.1**.

2. Recherche de facteurs de transcription impliqués dans la régulation des effecteurs au cours de l'infection

L'approche d'identification de FTs sans *a priori* avait permis pendant la thèse de J. Soyer l'identification et l'annotation de 355 FTs chez Lmb, dont 38 sont sur-exprimés pendant l'infection primaire du colza et huit sont spécifiques de Lmb. Parmi ces FTs, nous avons choisi de focaliser notre analyse fonctionnelle sur des FTs sur-exprimés pendant l'infection primaire, en particulier deux FTs spécifiques de Lmb et un portant des signatures de sélection positive au sein du complexe d'espèces *L. maculans* / *L. biglobosa*. J'ai réalisé l'analyse fonctionnelle de ces trois FTs en les inactivant grâce à la technologie CRISPR-Cas9 et en les sur-exprimant sous le contrôle d'un promoteur *EF1a* : parmi les trois FTs étudiés, l'un, LmPf2, s'est avéré impliqué dans la pathogenèse et le contrôle de l'expression des effecteurs précoces. En effet, l'inactivation par CRISPR-Cas9 de *LmPf2,* qui a un profil d'expression suivant celui

Université Paris-Saclay
Espace Technologique / Immeuble Discovery
Route de l'Orme aux Merisiers RD 128 / 91190 Saint-Aubin,
France

des effecteurs précoces, déjà décrit chez trois Dothidéomycètes (*P. tritici* 'repentis', *A. brassicicola* et *P. nodorum*) comme impliqué dans la pathogénie a été réalisée ainsi qu'une sur-expression de ce même gène dans deux fonds génétiques différents (WT et *Δkmt1*). L'expression génique chez les transformants ainsi obtenus a été étudiée par RNA-Seq, ce qui m'a permis de déterminer que ce FT ainsi que de l'état de compaction de la chromatine étaient impliqués dans le contrôle de l'expression des gènes codant des effecteurs (**Chapitre 3.1**). L'inactivation de deux autres FTs présentant des patterns d'expression correspondant à celui des effecteurs 'précoces' n'a pas permis de mettre en évidence une implication dans la pathogénèse du colza (**Chapitre 3.2**).

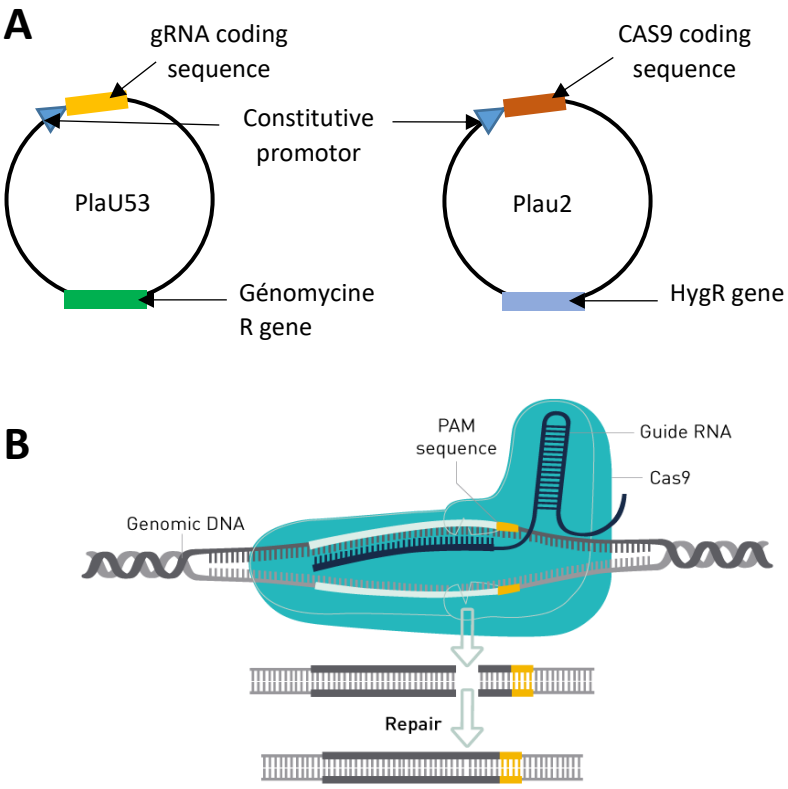

Figure 14: Méthode de mutagénèse dirigée CRISPR-Cas9. A: Constructions utilisées pour mettre en place la mutagénèse dirigée. A gauche le plasmide portant la séquence de l'ARN guide ciblant le gène d'intérêt et à gauche le vecteur contenant la séquence de la Cas9 reconnaissant l'ARN guide. **B:** Schéma de l'action combinée de l'ARN guide reconnaissant sa séquence cible et de la Cas9 reconnaissant le gRNA et coupant l'ADNg en amont de la séquence PAM. L'ADNg sera ensuite réparé ce qui mènera dans certains cas à des mutations délétères pour le gène cible.

Université Paris-Saclay
Espace Technologique / Immeuble Discovery
Route de l'Orme aux Merisiers RD 128 / 91190 Saint-Aubin, France

RESULTATS

CHAPITRE I

Etude genome-wide du paysage chromatinien et nucleosomal

Université Paris-Saclay
Espace Technologique / Immeuble Discovery
Route de l'Orme aux Merisiers RD 128 / 91190 Saint-Aubin, France

INTRODUCTION

Dans le chapitre I nous nous intéresserons au contrôle chromatinien de l'expression des gènes, en particulier des gènes codant des effecteurs.

Dans la première partie de ce chapitre, nous avons étudié, chez différentes espèces de champignons phytopathogènes, l'organisation du paysage nucléosomique ainsi que l'impact des positions des nucléosomes sur l'expression génique. La position des nucléosomes, en condition de vie axénique, a été analysée chez quatre espèces (*L. maculans* 'brassicae', *L. maculans* 'lepidii', *Fusarium graminearum* et *Botrytis cinerea*) via une expérience de MAINE-Seq consistant à digérer la chromatine ne formant pas de nucléosomes à l'aide d'une enzyme, la miccrococale nucléase. L'ADN enroulé autour des octamères d'histones est ensuite extrait, séquencé et aligné sur le génome de chacune des espèces pour identifier les portions d'ADN au niveau desquelles sont positionnés des nucléosomes. En parallèle, une analyse transcriptomique a été réalisée dans les mêmes conditions par RNA-Seq. Nous avons pu ensuite relier paysage nucléosomique et expression chez les différents champignons étudiés et comparer ceci entre les différentes espèces. A mon arrivée au laboratoire, les expériences de MAINE avaient déjà été réalisées et les données de séquençage venaient d'être obtenues. L'analyse bio-informatique des données n'avait pas été réalisée. J'ai réalisé l'analyse des données de *L. maculans* 'brassicae' et *L. maculans* 'lepidii', participé aux réflexions sur le choix et la mise en place des outils à utiliser pour l'analyse et j'ai participé à la rédaction de l'article. Il s'agit à notre connaissance de la première analyse comparative chez des champignons filamenteux.

Dans la deuxième partie de ce chapitre nous avons mené, en phase de croissance axénique, des expériences de ChIP-Seq qui consistent, après une étape de digestion de la chromatine, à immunoprécipiter les nucléosomes avec des anticorps spécifiques des modifications des histones de type H3K9me3, H3K4me2 et H3K27me3. Ces expériences ont été réalisées chez *L. maculans* 'brassicae' et *L. maculans* 'lepidii', deux espèces ayant un contenu en ETs différent ainsi qu'une différence dans leur spectre d'hôte connu. Une analyse transcriptomique par RNA-Seq a été menée dans les mêmes conditions pour relier modifications chromatiniennes et expression génique chez ces deux espèces. A mon arrivée au laboratoire, les expériences de ChIP avaient déjà été réalisées et les données de séquençage venaient d'être obtenues. J'ai participé à l'analyse des données, aux réflexions sur le choix et la mise en place des outils à utiliser pour l'analyse et j'ai participé à la rédaction de l'article.

Université Paris-Saclay
Espace Technologique / Immeuble Discovery
Route de l'Orme aux Merisiers RD 128 / 91190 Saint-Aubin, France

RESULTATS

ARTICLE 1

Nucleosome patterns in four plant pathogenic fungi with different genome structures

Nucleosome patterns in four plant pathogenic fungi with different genome structures

C. Clairet[1,2], N. Lapalu[1], A. Simon[1], J. L. Soyer[1,3], M. Viaud[1], E. Zehraoui[4], B. Dalmais[1], I. Fudal[1,*] and N. Ponts[4,*]

[1]UMR BIOGER, INRA, AgroParisTech, Université Paris-Saclay, Avenue Lucien Brétignières, BP 01, F-78850 Thiverval-Grignon, France

[2]Université Paris-Sud, 91405, Orsay, France

[3]Max Planck Institute for Evolutionary Biology, August-Thienemann-Str. 2, 24306 Plön, and Christian-Albrechts University of Kiel, Am Botanischen Garten 1-9, 24118 Kiel, Germany

[4]UR1264-MycSA, INRA, Villenave d'Ornon, 33140, France

* To whom correspondence should be addressed.

Nadia Ponts Tel: +33557122482; Email: nadia.ponts@inra.fr;

Isabelle Fudal Tel: +33130814590; Email: Isabelle.Fudal@inra.fr;

INTRODUCTION

Fungi account for a huge part of the Earth biodiversity; they rank second in terms of species number, behind the insects, with a current estimate of 2.2 to 3.8 million species (Hawksworth and Lücking, 2018). Fungi are organisms of major environmental importance as they develop beneficial symbiotic associations with plants and are able to decay dead organic matter (Taylor and Osborn, 1994). Unfortunately, fungi are also very efficient pathogens causing important damages in agriculture, human health, and environment (Fisher *et al.,* 2012). Control of fungal diseases on crops necessitates a global understanding of fungal pathogenicity determinants. Among these pathogenicity determinants, fungi secrete an arsenal of molecules known as effectors, key elements of pathogenesis which modulate innate immunity of the plant and facilitate infection, corresponding to small proteins, secondary metabolites and small RNAs (Fox and Howlett., 2008; Möbius and Hertweck, 2009; Weiberg *et al.,* 2013; Lo Presti *et al.,* 2015; Wang *et al.,* 2016). Upon plant infection, fungi undergo a tightly controlled transcriptional reprogramming, and different sets of effectors are expressed at specific stages of pathogen development and host colonization. It follows that fine-tuned regulation of effector-encoding genes is important for the successful outcome of plant infection. However, so far, very little is known about the regulation of effector gene expression. Effector gene expression can be regulated by several mechanisms including specific transcription factors (reviewed in Tan and Oliver, 2017) and the structure of the genomic regions in which effector genes are located. Plant-associated fungi generally show contrasted genomic landscapes including 'plastic' regions with a high prevalence of transposable elements (TEs). These genomes either show an overall large proportion of TEs evenly distributed throughout the genome, or TEs clustered in specific regions such as long repeat-rich blocks, accessory chromosomes or subtelomeric areas (Soyer *et al.,* 2015,b). Effector-encoding genes are overrepresented in these TE-rich regions. TE-rich compartments have heterochromatin properties contrary to TE-poor regions which have euchromatin properties. The location of effector genes in regions enriched in repeats has been shown to provide a tight control of effector gene expression through chromatin remodeling. Indeed, several

recent studies pointed out the potential role of chromatin remodeling in the regulation of pathogenicity and the control of secondary metabolism (reviewed in Strauss and Reyes-Dominguez, 2011; and in Soyer *et al.,* 2015,b).

Eukaryotic chromatin is packaged into nucleosomes, each composed of DNA wrapped around a histone octamer associated with various other proteins, and separated by linker DNA (Richmond and Davey, 2003). These histone proteins are composed of histone core where the DNA is wrapped and histone tails which can be chemically modified by specific enzymes changing the chromatin 3D structure and DNA accessibility to polymerases and transcription factors (TFs). Positioning of nucleosomes throughout the genome and post-translational modifications of histones have a significant regulatory function by modifying availability of binding sites to transcription factors (TFs) and to polymerases, affecting DNA-dependent processes such as transcription, DNA repair, replication and recombination (Radman-Livaja and Rando, 2010; Struhl and Segal, 2013). Nucleosome positioning and occupancy are determined by a combination of DNA sequence features, TFs, chromatin remodelers and histones modifiers. Genome-wide maps of nucleosome occupancy and positioning are still sparse in fungi and have only been developed in Hemiascomycota (Saccharomyces cerevisiae (Yuan *et al.,* 2005) and other Hemiascomycota yeast species (Tsankov *et al.,* 2010), in the ascomycete *Aspergillus fumigatus* (Nishida *et al.,* 2009) and the basidiomycete *Mixia osmundae* (Nishida *et al.,* 2012). The studies revealed that nucleosomes are depleted at promoter, enhancer and terminator regions, allowing access to TFs, and that the nucleosomal DNA length distribution was similar in *M. osmundae* and *A. fumigatus* but differed from that of hemiascomycetous yeasts. In contrast, no comparative genome-wide analyses of nucleosome positioning have been performed in ascomycetes and notably not in plant pathogenic fungi.

In the present study, we investigated genome-wide nucleosome localization and its impact on gene expression, particularly on (putative) effector gene expression, in four different plant pathogenic fungi showing different host ranges, lifestyles and genomic organizations: i) *Leptosphaeria maculans* 'brassicae' (Lmb), a hemibiotrophic pathogen of oilseed rape; ii) the most closely related species of Lmb, *Leptosphaeria maculans* 'lepidii' (Lml), a pathogen of *Lepidium* spp.; iii) *Fusarium graminearum*, a hemibiotrophic pathogen of cereals and iv) *Botrytis cinerea*, a polyphagous necrotrophic pathogen causing grey mould on more than 1400 plant species. The genome of Lmb has been invaded by TEs (which represent more than 39% of its genome) and is composed of alternating compartments: gene-rich GC-isochores and TE-rich AT-isochores (Rouxel *et al.,* 2011; Dutreux *et al.,* 2018). On the contrary, genomes of Lml, *F. graminearum* and *B. cinerea* have a low TE-content with TE-rich regions mainly restricted to sub-telomeric domains (Grandaubert *et al.,* 2014; Amselem *et al.,* 2011; Cuomo *et al.* 2007; King *et al* 2015). The genome of the reference strain of *B. cinerea* B05.10 contains 4% of TE which are localized essentially in the telomeric and centromeric regions of the core chromosomes, or on the two dispensable chromosomes (Porquier *et al.,* 2016). The genome of *F. graminearum* contains very little repeated sequences and TE, 1% and 0.3 % respectively (King *et al.,* 2018).

The aim of this study is to describe nucleosome repartition patterns on whole genome depending on the lifestyle of the fungus. To gain insight into the role of nucleosome positioning and occupancy in regulating fungal pathogen transcription, we applied micrococcal nuclease digestion of mono-nucleosomes (MNase-assisted isolation

Université Paris-Saclay
Espace Technologique / Immeuble Discovery
Route de l'Orme aux Merisiers RD 128 / 91190 Saint-Aubin, France

of nucleosomes or MAINE) with regards to mRNA abundance to concomitantly map nucleosome-rich regions and transcriptionally active regions during fungal growth in contrasted media.

MATERIAL AND METHODS

Strains and culture conditions

Leptosphaeria maculans 'brassicae' v23.1.3 and *Leptosphaeria maculans* 'lepidii' IBCN84 mycelia were inoculated into 100 mL of Fries liquid medium (1 g/L NH_4NO_3, 5 g/L $C_4H_{12}N_2O_6$, 1 g/L KH_2PO_4, 0.5 mg/L $MgSO_4$ $7H_2O$, 130 mg/L $CaCl_2$, 100 mg/L NaCl, 30 g/L $C_{12}H_{22}O_{11}$ and 5 g/L Yeast extract). Tissues were harvested after growing for seven days in the dark at 27°C. *Botrytis cinerea* strain B05.10 (10^6 spores/mL) was grown for two days on two different solid media: Malt Medium (MM, 20 g/L malt extract, 5 g/L yeast extract and 15 g/L agar), and Grape Juice (GJ, pH adjusted to 4; 15 g/L agar) media, both covered with a cellophane layer (Simon *et al.,* 2013; Kelloniemi *et al.,* 2015). The plates were incubated in a growth chamber (Sanyo MLR-350H) at 23°C with an alternation of 14 h of white light and 10 h of darkness. After two days of culture, mycelia were ground in liquid nitrogen and stored to -80°C until further processing. *Fusarium graminearum* strain CBS185.32 (Centraal Bureau voor Schimmelcultures, Utrecht, the Netherlands) was grown for three days in modified liquid MS (glucose was substituted with sucrose) as previously described (Boutigny *et al.,* 2009). All cultures were done in three biological replicates.

Preparation of nucleosomal DNA

Fungal material was harvested and immediately treated with micrococcal nuclease (MNase, cat. #MS0247S, New England BioLabs). For *L. maculans* 'brassicae' and 'lepidii', 100 mg of mycelium were digested with 5 µL of MNase for 10 min at 37 °C, directly followed by DNA purification (Soyer *et al.,* 2015a). For *F. graminearum*, mycelia were harvested by filtering and immediately ground for 1 min at 30 Hz using a TissueLyzer (Qiagen). Then, 100 mg of ground mycelium was digested for 10 min at 37°C with 15 µL of MNase in 600 µL of digestion buffer (0.6% v/v IGEPAL, 50 mM NaCl, 2 mM Pefabloc, 50 mM Tris-HCl pH8, 10 mM $CaCl_2$). The reactions were stopped with EDTA and the samples treated with RNAse followed by proteinase K prior DNA purification with phenol/chloroform and ethanol precipitation. For *B. cinerea*, we digested 100-200 mg of mycelium per sample with 1 µL MNase at 37°C (Soyer *et al.,* 2015,a), for 10 min (MM cultures) or 30 min (GJ cultures). The reactions were stopped with EDTA and samples treated with RNAse A followed by proteinase K. DNA purification was realized with the "Nucleospin Gel and PCR clean up kit" (Macherey Nagel, cat #740609.250). For all samples, nucleic acid quantification was performed by UV spectrometry using a Nanodrop-ND 1000 apparatus, and digestion profiles were checked by 2% agarose gel electrophoresis. Nucleosomal DNA for stored at -20°C waiting for DNA library preparation.

Extraction of total RNA

For *L. maculans* 'brassicae' and *L. maculans* 'lepidii', total RNA was extracted from mycelium grown for one week in Fries liquid medium as previously described (Fudal *et al.,* 2007). For *F. graminearum*, mycelia were harvested by filtering, rinsed twice with sterile deionized water, and flash frozen in liquid nitrogen. One milliliter of TRIzol™ Reagent (Thermo Fischer Scientific) was added to 200 mg of mycelium before grinding for 1.5 min at 30 Hz using

Université Paris-Saclay
Espace Technologique / Immeuble Discovery
Route de l'Orme aux Merisiers RD 128 / 91190 Saint-Aubin,
France

a TissueLyzer (Qiagen). Total RNA was then extracted using a previously published protocol (Hallen *et al.,* 2007). For *B. cinerea*, total RNA was extracted from frozen ground mycelium using a previously published protocol (Kelloniemi *et al.,* 2015). All total RNA samples were stored at -80°C until sequencing RNA library preparation.

Preparation of sequencing libraries, high-throughput sequencing, and read pre-processing

MNase-seq libraries were prepared from purified nucleosomal DNA using the kit NEBNext Ultra DNA Library Prep Kit for Illumina (cat. # E7370L New England BioLabs) following the manufacturer's instructions. The NEBNext Ultra Directional RNA Library Prep Kit for Illumina (cat. # E7420L New England BioLabs) was used to prepare all RNA-seq libraries, following the manufacturer's instructions. Sequencing was performed by the GenomEast platform, a member of the 'France Génomique' consortium (ANR-10-INBS-0009). Samples were run in 9-plex on an Illumina HiSeq 4000 in paired mode, 2x50 bp. Initial read quality check was performed using FastQC (https://www.bioinformatics.babraham.ac.uk/projects/fastqc/). Raw reads were then pre-processed with Trimmomatic v0.32 (Bolger *et al.,* 2014) to clip out any remaining sequencing adapter sequence and crop low quality nucleotides (minimum accepted Phred score of 30). Reads in pairs of 40 bp or more in length were used in the present analysis.

Transcriptome analyses

RNA-seq reads were mapped against their respective reference genomes (see **Table 1**) using STAR v2.5.1 (Dobin *et al.,* 2013). For *F. graminearum*, genome sequence and annotation files were downloaded from FungiDB v44 (Stajich *et al.*, 2012; Basenko *et al*., 2018). TPM counts (Transcripts Per Million reads; Li *et al.,* 2010) were computed using the count TPM tool provided with the MAINE-Seq Tool Suite (MSTS) (https://github.com/nlapalu/MSTS). For *B. cinerea*, differential expression analysis was performed using SARTools commands (Varet *et al.,* 2016) with DESeq2 settings (Love *et al.,* 2014).

MAINE analyses

MNase-seq paired-end reads were mapped using Bowtie2 software ran in very-sensitive mode (Langmead and Salzberg, 2012). MSTS (https://github.com/nlapalu/MSTS) was used to compute all phasograms, dinucleotide composition, as well as nucleosome density profiles of genomic compartments and/or gene lists. Lists of near-universal single copy orthologs were obtained by running BUSCO3 for Fungi (Simão *et al.,* 2015; Waterhouse *et al.,* 2017) on each reference genome studied. Graphical visualisations were computed with MSTS and Matlab R2019a (MathWorks)

Université Paris-Saclay
Espace Technologique / Immeuble Discovery
Route de l'Orme aux Merisiers RD 128 / 91190 Saint-Aubin, France

Table 1: Characteristics of reference genomes for the four fungal species studied.

Species	*Leptosphaeria maculans* 'brassicae'	*Leptosphaeria maculans* 'lepidii'	*Botrytis cinerea*	*Fusarium graminearum*
Strain	v23.1.3	IBCN84	B05.10	CBS85.32
Reference genome	v23.1.3 (Rouxel et al., 2011)	IBCN84 (Grandaubert et al., 2014)	B05.10 (Amselem et al., 2011)	PH-1 vRR5 (Cuomo *et al.* 2007; King *et al* 2015 and 2018)
Avaibility			EnsemblFungi v1	FungiDB v44
Genome size (Mb)	45.1	31.5	42	38.1
Number of protein-coding genes	12,468	11,272	11,701	14,164
GC content (%)*	44.1	50.9	42	48.2
Transposable elements content (%)	34.2	4.0	4.0	0.29

*excluding N's and mitochondrial genomes; **also excluding the largely repetitive 3' end of chromosome 4

RESULTS

Establishing nucleosome landscapes of the Pezizomycotina *L. maculans* 'brassicae', *L. maculans* 'lepidii', *B. cinerea*, and *F. graminearum*

We investigated the nucleosome landscapes of four fungal species of the Ascomycota subdivision Pezizomycotina (*L. maculans* 'brassicae', *L. maculans* 'lepidii', *B. cinerea*, and *F. graminearum*) by MAINE coupled to deep sequencing (see **Table S1** for descriptive sequencing metrics). Each sample was analysed in triplicate at more than 80-fold coverage depths and nearly 70X genome coverage by 147 bp-long nucleosome footprints (defined as the core coverage by Valouev *et al*. (2011), depths of sequence sufficient for in-depth characterization of nucleosome positioning (Valouev *et al.,* 2011).

Genome-wide nucleosome spacing

We first explored nucleosome landscapes in our four fungal genomes by measuring the average distance between nucleosomes genome-wide; we computed phasograms, i.e., frequency distributions of read coverage per base genome-wide for all four species (**Figure 1**). Phasograms obtained in nucleosome mapping resemble oscillating sine wave signals which period is the length of DNA bound to the histone octamer plus the length of the DNA stretch to the next nucleosome, averaged genome wide (Valouev *et al.,* 2011). Phasing signals were observed genome-wide over

Université Paris-Saclay
Espace Technologique / Immeuble Discovery
Route de l'Orme aux Merisiers RD 128 / 91190 Saint-Aubin, France

1,200 bp sliding windows revealing six to seven nucleosome peaks in a wave signal decaying in intensity with increasing distance and significant linear regression on peak apex positions (**Figure 1A-E**). We found that, in the fungi studied, nucleosomes are 161 to 173 bp distant from each other (centre to centre), also called nucleosome repeat length or NRL (*i.e.,* the length of DNA wrapped around the histone octamer plus linker DNA), depending on the considered species and culture condition. In *L. maculans* 'brassicae' and *L. maculans* 'lepidii' (**Figures 1A and 1B**), NRL is 163 bp and 161 bp, respectively. In *Botrytis cinerea*, NRL is 173 bp when grown in malt-based medium (MM, **Figure 1C**), and 169 bp when a nutrient-rich grape juice-based medium (GJ) is used (**Figure 1D**). In *F. graminearum*, this distance reaches 172 bp (**Figure 1E**). Considering these values and the canonical length of nucleosomal DNA (147 bp), linker DNA length can be estimated to stand, in average, between 14 to 16 bp for *L. maculans* 'lepidii' and 'brassicae', 25-26 bp for *F. graminearum* and *B. cinerea* in malt medium, and 22 bp for *B. cinerea* grown in grape juice medium. Nucleosome phasing genome-wide seems to be particularly tight in *F. graminearum*, with very little deviation in the measured phases (**Figure 1E and 1F**). Similar tight phasing can also be observed in *B. cinerea* grown in grape juice-based medium (**Figure 1C and 1F**) whereas higher deviations are observed in malt-based cultures (**Figure 1D and 1F**). Similarly, phasing in grape juice-based medium is smaller (168-169 bp) than the one measured in malt medium (173-174 bp). Examining TPM expression counts in both conditions (see Materials and Methods) for the gene coding the unique H1 histone of the fungus (BcH1), we observed a diminution from 11,183 (sd = 202) in malt medium to 8,597 (sd = 422) in grape juice medium (data not shown), consistently with previous reports of decreased contents in linker histones leading to shorter NRLs (Nucleosome repeat length) (Valouev *et al.,* 2011; Luque *et al.,* 2016).

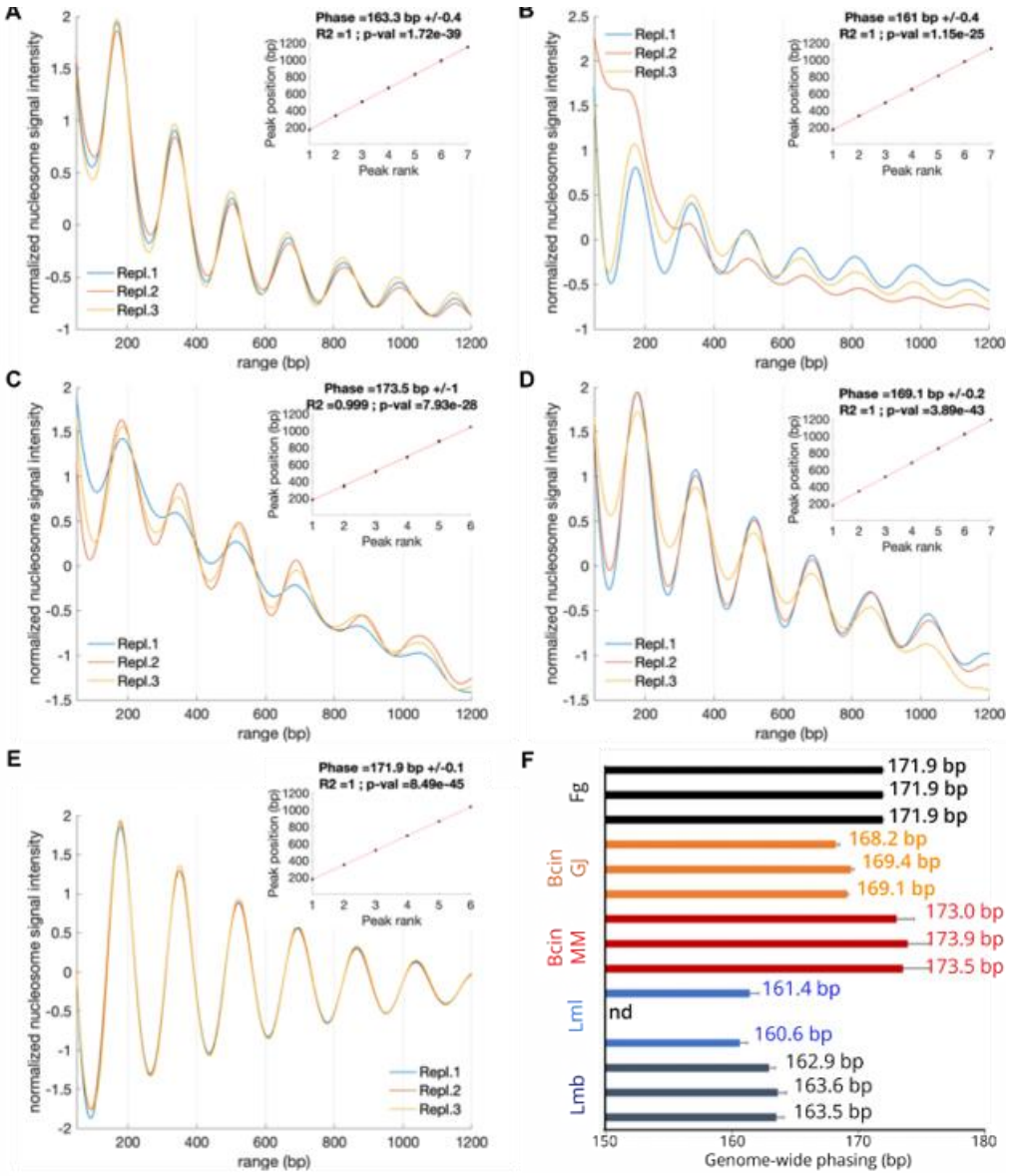

Figure 1: Nucleosome phasing in the four fungi studied. A-E: Main graphs display normalized (z-score) phase frequencies (y-axis) as a function of position (in base pair; x-axis). Graphs in inserts show peak positions (in base pairs; y-axis) as a function of peak order (x-axis). Phases +/- standard errors, R^2 (coefficient of determination), and p-values (*F*-test) are determined after linear regression fitting to peak positions in all replicates. Repl = replicate. **A:** *Leptosphaeria maculans* 'brassicae'; **B:** *Leptosphaeria maculans* 'lepidii'; here, phase value was measured excluding replicate #2 for which a peak apex was not clearly visible at the beginning of the profile; **C:** *Botrytis cinerea* grown in malt-based medium; **D.** *Botrytis cinerea* grown in grape juice-based medium; **E:** *Fusarium graminearum*; **F:** Genome-wide nucleosome phasing measured per individual replicate for each considered species/culture condition after fitting a linear regression model to the positions of six to seven successive peaks. Error bars are standard errors; nd = not determined. For each replicate: R2 > 0.99 and p-value < 10^{-6}.

Université Paris-Saclay
Espace Technologique / Immeuble Discovery
Route de l'Orme aux Merisiers RD 128 / 91190 Saint-Aubin, France

Nucleosome distribution profiles

Read density was plotted genome-wide in one kb-long sliding non-overlapping windows along chromosomes for all four fungi (**Figure 2 and 3**, and **Figures S1 and S2**). The density profiles obtained for *B. cinerea* grown in malt or grape juice media both show remarkable regularity of nucleosome density genome-wide (**Figure S1**) whereas, in *F. graminearum*, regions equally packed with nucleosomes are interspaced with area with lower density (**Figure 2A** and **Figure 2**). Strikingly, this profile mirrors the previously described SNP density profiles in *F. graminearum* (Laurent *et al.,* 2017). We investigated whether or not this profile was the result of increased spacing between nucleosomes in regions found denser in SNPs. Phasograms were plotted as described above restricting our analysis to the SNP-enriched polymorphic islands or the rest of the genome, as defined by Laurent *et al.* (2017). Wave signals similar to the ones observed genome-wide were obtained, with phases of 172.4 bp in polymorphic islands (**Figure 2B**) and 171.7 bp outside these regions (**Figure 2C**). These results indicate that nucleosomes appear well-arrayed genome-wide, with phases only slightly longer within polymorphic islands. Thus, the observed read density profile may be more the result of reduced nucleosome occupancy, *i.e.,* a measure of the stability of a nucleosome at a given position in a multiple cell sample, than a depletion in nucleosomes. This observation suggests increased frequencies of transient nucleosome positioning events in *F. graminearum* polymorphic islands and thus more relaxed chromatin structures.

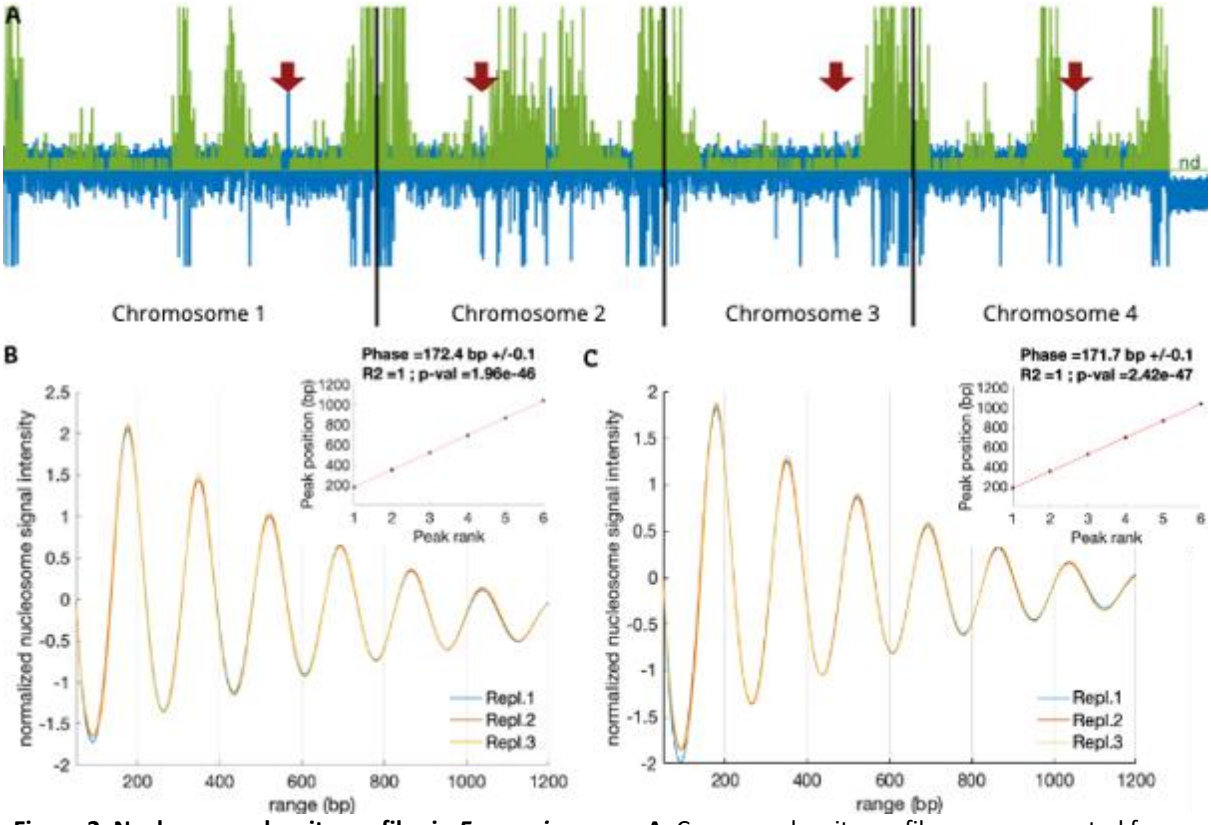

Figure 2: Nucleosome density profiles in *F. graminearum*. A: Coverage density profiles were computed for non-overlapping 1 kb-long bins along the four chromosomes of *F. graminearum*. In green are plotted SNP density profiles as previously described (15). "nd" indicates the highly variable 3' end of chromosome 4 for which SNP were not called. In blue are plotted the z-scored average nucleosome density profile (see supplementary figure 1 for individual replicate plots). The red arrows indicate centromeres (31); **B** and **C:** Nucleosome phasing in the polymorphic islands (**B**) or outside the polymorphic islands (**C**) as previously defined (15). Main graphs display phase frequencies (y-axis) as a function of position (in base pair; x-axis). Graphs in inserts show peak positions (in base pairs; y-axis) as a function of peak order (x-axis); Phases +/- standard errors, R2 (coefficient of determination), and p-values (F-test) are determined after linear regression fitting to peak positions in all replicates. Repl = replicate.

Université Paris-Saclay
Espace Technologique / Immeuble Discovery
Route de l'Orme aux Merisiers RD 128 / 91190 Saint-Aubin, France

In *L. maculans* 'brassicae', numerous "islands" of nucleosome-dense regions can be observed at various locations of the genome (**Figure 3A** and **Figure S3**). Beside few contigs displaying higher nucleosome density, such characteristics were not observed for the closely related *L. maculans* 'lepidii' (**Figure S4**). The locations of these nucleosome-dense islands in *L. maculans* 'brassicae' parallel those of AT-rich regions of the genome (**Figure 3A**), features not visible in the genome of *L. maculans* 'lepidii' (**Figure S4**), suggesting that AT-rich regions are particularly dense in nucleosomes. Considering the remarkable GC- vs. AT-isochore organization of the genome of *L. maculans* 'brassicae' (Rouxel *et al.,* 2011), absent from *L. maculans* 'lepidii', differences of nucleosome phasing and occupancy in AT-rich *vs.* GC-rich regions were investigated. A region was considered AT-rich if it contains less than 40 % of GC. As described earlier, AT isochores represent one third of the *L. maculans* 'brassicae' genome divided in 419 of 1 to 320 kb-long regions. Examination of unprocessed mapping outputs reveals that the number of fragments (read pairs) mapped in AT- and GC- regions are very similar with 23.8 million and 24.8 million fragments, respectively, which is far from the 1/3 vs. 2/3 ratio expected. In terms of depth of coverage, mean coverage is 207 *vs.* 135 fragments for AT-rich and GC-rich regions, respectively, which could suggest higher nucleosome occupancy in the former. We explored this hypothesis and compared phasograms for AT-rich *vs*. GC-rich regions (**Figure 3B** and **3C**). NRLs were found larger in AT-rich than GC-rich compartments, measured at 168.5 bp and 163.3 bp respectively, suggesting lower nucleosome frequencies in AT-rich regions. Nonetheless, coverage density is higher in AT-rich regions, as seen on **Figure 3A** and **Figure S3**, consistently with our hypothesis of stronger nucleosome occupancy in these regions and thus less accessible

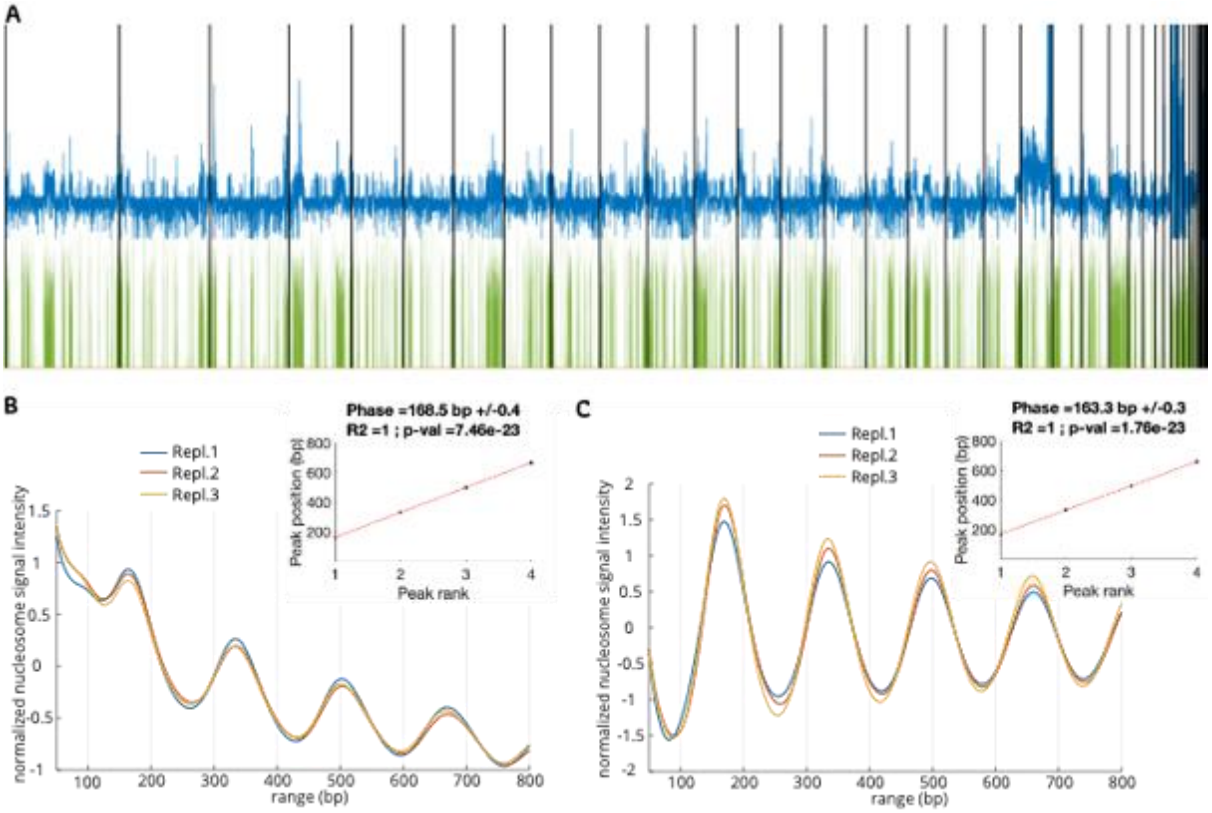

Figure 3: Nucleosome density profiles in *L. maculans* 'brassicae'. A: Coverage density profiles were computed for non-overlapping 1 kb-long bins along all supercontigs, separated by black lines. AT-rich regions are plotted in green. In blue are plotted the z-scored average nucleosome density profile (see supplementary figure 3 for individual replicate plots). **B and C:** Nucleosome phasing in AT-isochores (**B**) and GC-isochores (**C**). Main graphs display phase frequencies (y-axis) as a function of position (in base pair; x-axis). Graphs in inserts show peak positions (in base pairs; y-axis) as a function of peak order (x-axis).

Université Paris-Saclay
Espace Technologique / Immeuble Discovery
Route de l'Orme aux Merisiers RD 128 / 91190 Saint-Aubin, France

genome compartment in heterochromatic state. Finally, signal intensity in phasograms appear more stable on the long nucleotide range in GC- than in AT-rich regions, an observation in line with the well-known destabilizing effect of AT stretches on nucleosome positioning leading to fuzzier signals (Kaplan *et al.,* 2009; (Ponts *et al.,* 2010; Tillo *et al.,* 2010; Bunnik *et al.,* 2014; Russell *et al.,* 2014; Jin *et al.,* 2018). All together, these data support a heterochromatic state of *L. maculans* 'brassicae' AT-rich regions mediated by strong nucleosome occupancy.

Sequence composition and nucleosome positioning

Literature data report abundantly that distribution of bases in nucleosome core DNA is non-random and exhibits a ~10 bp AA/TT/AT/TA offset with GG/CC/GC/CG dinucleotide frequency (Satchwell *et al.,* 1986; Segal *et al.,* 2006; Segal and Widom, 2009). Here, we investigated di-nucleotide frequencies in nucleosomal DNA segments in all four fungi. Averaged di-nucleotide contents centred around all fragment (read pairs) were plotted (**Figure 4** and **Figure S5**). Normalized frequency graphs display the previously described ~10 bp periodicity of A+T dinucleotides oscillating out of phase with a ~10 bp G+C periodicity, the oscillation patterns being nonetheless very different between the four studied fungi. This periodicity is not constant along the entire nucleosomal DNA segment, shorter periodicities alternating with longer ones. In particular, the nucleosome dyad axis appears marked by longer periods flanked with short alternating AT and GC dinucleotide motifs. Specificities between the considered fungi can further be observed. In *L. maculans* 'lepidii', the average period along nucleosomal fragments is 10.1 bp for both AT and GC dinucleotide motifs. In *F. graminearum*, this period is shorter (8.8 bp), mostly due to very marked drops in period length around nucleosome dyads. Autocorrelation analyses of these dinucleotide frequency profiles highlight these 10 bp-periodicities in all fungi while revealing important differences in the absolute variations if the instant autocorrelation coefficients Rh (**Figure S5**). Signal is indeed very regular in *F. graminearum* and, to a lesser extent, *L. maculans* 'brassicae' whereas *L. maculans* 'brassicae' and *B. cinerea* (grown in Malt medium) show more irregular autocorrelation profiles. These results are consistent with our previous observation that nucleosomes are tightly phased in *F. graminearum* whereas somehow fuzzier (higher deviation) in *B. cinerea* grown in malt medium (**Figure 1C**). Di-nucleotide frequencies of *L. maculans* 'brassicae' AT- and GC-isochores were also inspected (**Figure S**6). As one would expect, the A+T periodicity is more pronounced in AT-isochores, but interestingly GC periodicity remains conserved.

Université Paris-Saclay
Espace Technologique / Immeuble Discovery
Route de l'Orme aux Merisiers RD 128 / 91190 Saint-Aubin, France

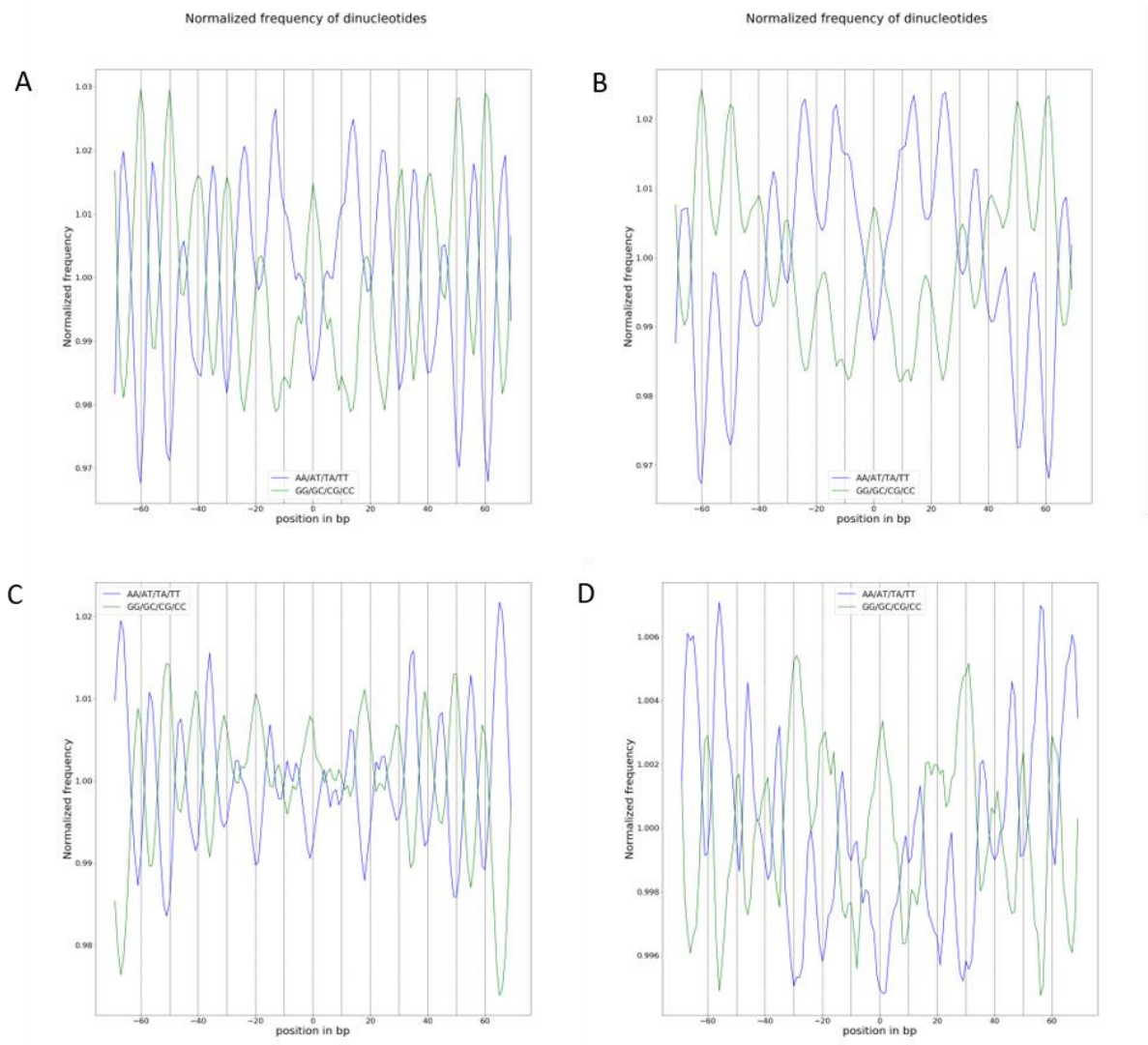

Figure 4: Repeated di-nucleotide patterns in nucleosomal DNA. Normalised di-nucleotides frequency plots (average of three biological replicates) for *L. maculans* 'brassicae' (**A**), *L. maculans* 'lepidii' (**B**), *F. graminearum* (**C**), and *B. cinerea* grown in malt medium (**D**).

Nucleosome landscapes of fungal gene units

Nucleosome occupancy profiles of gene units were investigated in all fungi (**Figure 5**). As previously reported in other eukaryotes, translation start sites (the ATG codon) are preceded by a nucleosome-depleted region (NDR) and immediately followed by a well-positioned +1 nucleosome (**Figure 5A**). Variations of the exact position of these features relative to the ATG start codon, as well as the intensity of the NDR valley, are nonetheless observed when fungal species are compared, For example, the NDR and the centre of the +1 nucleosome (or +1Nucl) are found at -155 bp and +14 bp, respectively, in *F. graminearum* whereas they are located at -99 bp and + 26 bp, respectively, in *B. cinerea* grown in malt medium. *B. cinerea* grown in malt medium shows the deepest NDR valley among all observed profiles. Differences can further be observed in *B. cinerea* grown in grape juice-based medium, with NDR and +1Nucl found at -136 bp and +31 bp, respectively. In *L. maculans* 'brassicae' and 'lepidii', NDRs are found at -129 and 144 bp from ATG, respectively, and +1Nucl at +19 bp and +55 bp. Finally, nucleosome profiles upstream of NDRs appear fuzzy for all fungi but *L. maculans* 'brassicae', with varying degrees of fuzziness. This fuzziness is no longer visible when nucleosome profiles are centred on TSS for *F. graminearum* (N_{TSS} = 6,212, **Figure 5C** and **Table S2**). The NDR is more

Université Paris-Saclay
Espace Technologique / Immeuble Discovery
Route de l'Orme aux Merisiers RD 128 / 91190 Saint-Aubin, France

defined, and located immediately upstream of the TSS, with a minimum detected at -58 bp and +1Nucl found 110 bp downstream of *F. graminearum* TSS. These values are consistent with our previous measure of the average absolute distance NDR-+1Nucl. Considering nucleosome environments at stop codons (**Figure 5B**), strongly arrayed nucleosomes are particularly found upstream the stop codon, fewer signal variations being observed downstream. Here, the stop codon is a clear boundary for nucleosome arraying and occupancy in all fungi and all conditions investigated. A nucleosome seems remarkably well positioned exactly on stop codons in *F. graminearum*. Repeating the analysis on TTS in *F. graminearum* (N_{TTS} = 5,292), strong positioning of nucleosomes -2 and -1 (-178 bp and -16 bp relative to TTS, respectively) followed by a deep 3' end NDR (+100 bp downstream of TTS) can be observed (**Figure 5D**).

For comparison purposes, nucleosome profiling was repeated restricting our analysis to genes identified as BUSCO lineage-specific single-copy evolutionary conserved orthologs in Fungi (Simao *et al.,* 2015; Waterhouse *et al.,* 2018). Overall broad patterns remain similar to those obtained while investigating whole genomes (**Figure 6**). Nonetheless, in *F. graminearum*, whilst the distance NDR-to-TSS (- 60 bp) remains very similar to the one measured earlier genome-wide (**Figure 6C**), distance NDR-to-ATG increases by 28 bp (**Figure 6A**). In *B. cinerea*, such an increase is also observed when grown in grape juice medium (+ 32 bp) but not in malt medium (+ 3 bp). Towards the 3' end of the gene unit, nucleosome signals around stop codons are similar to those obtained genome-wide for all fungi (**Figure**

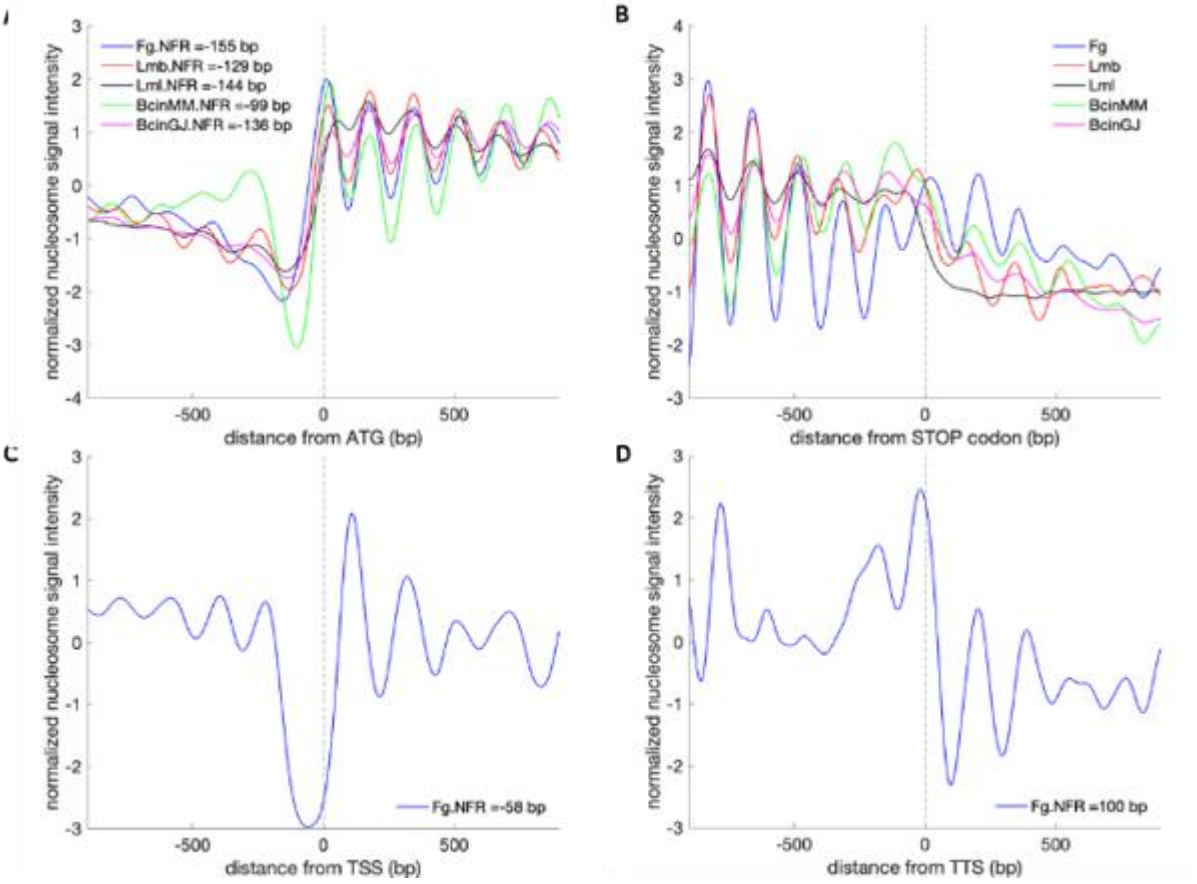

Figure 5: Nucleosome organization of fungal gene units. A-D: Normalised averages (three biological replicates for each fungus/condition) of nucleosome signals as a function of position (in base pairs) relative to the start codon ATG (**A**), the stop codon (**B**), TSS (**C**), and TTS (**D**). Fg = *F. graminearum*; Lmb = *L. maculans* 'brassicae'; Lml = *L. maculans* 'lepidii = BcinMM = *B. cinerea* grown in malt medium; BcinGJ = *B. cinerea* grown in grape juice medium; NFR = nucleosome-free region.

Université Paris-Saclay
Espace Technologique / Immeuble Discovery
Route de l'Orme aux Merisiers RD 128 / 91190 Saint-Aubin, France

6B). However, the deep NDR found downstream of TTS of *F. graminearum* genome-wide can no longer be observed at "Fungi" TTS *loci* (**Figure 6D**). Similar to genome-wide profile, strongly positioned -1Nucl and -2Nucl are still visible at -5 bp and -209 bp, respectively, the latter being more intense and defined.

Nucleosome landscapes of gene units and gene expression

Same analyses were repeated for genes categorized according to their expression levels (expressed in TPM counts, see Materials and Methods). The general variations in nucleosome profiles around translation start sites are similar for all expression categories in all considered fungi and culture conditions: ATG codons are immediately followed by a well-positioned +1 nucleosome and preceded by a dip in nucleosome density (**Figure 7**). Remarkable variations are nonetheless observed with regard to positions of +1 nucleosomes and NDRs, as well as the amplitude of the nucleosome signal difference between them (here defined as Δnucl = ($signal_{+1nucl}$ - $signal_{NDR}$), depending on gene expression. ATG-centred nucleosome profiles for genes not expressed in our conditions (TPM = 0) show remarkably reduced Δnucl when compared to those measured for genes more expressed (**Figure 7** and **Table S2**). Conversely, highly expressed genes display the deepest NDRs located at the furthest upstream the ATG. Similar trends are observed when profiles are centred on *F. graminearum* TSS (**Figure 7F**). Remarkably, in *B. cinerea* these differences are exacerbated when grown in grape juice medium (**Figure 7D**) compared to malt medium (**Figure 7C**). In summary, our results indicate that, in the four Ascomycota investigated here, genes highly expressed are characterised by high

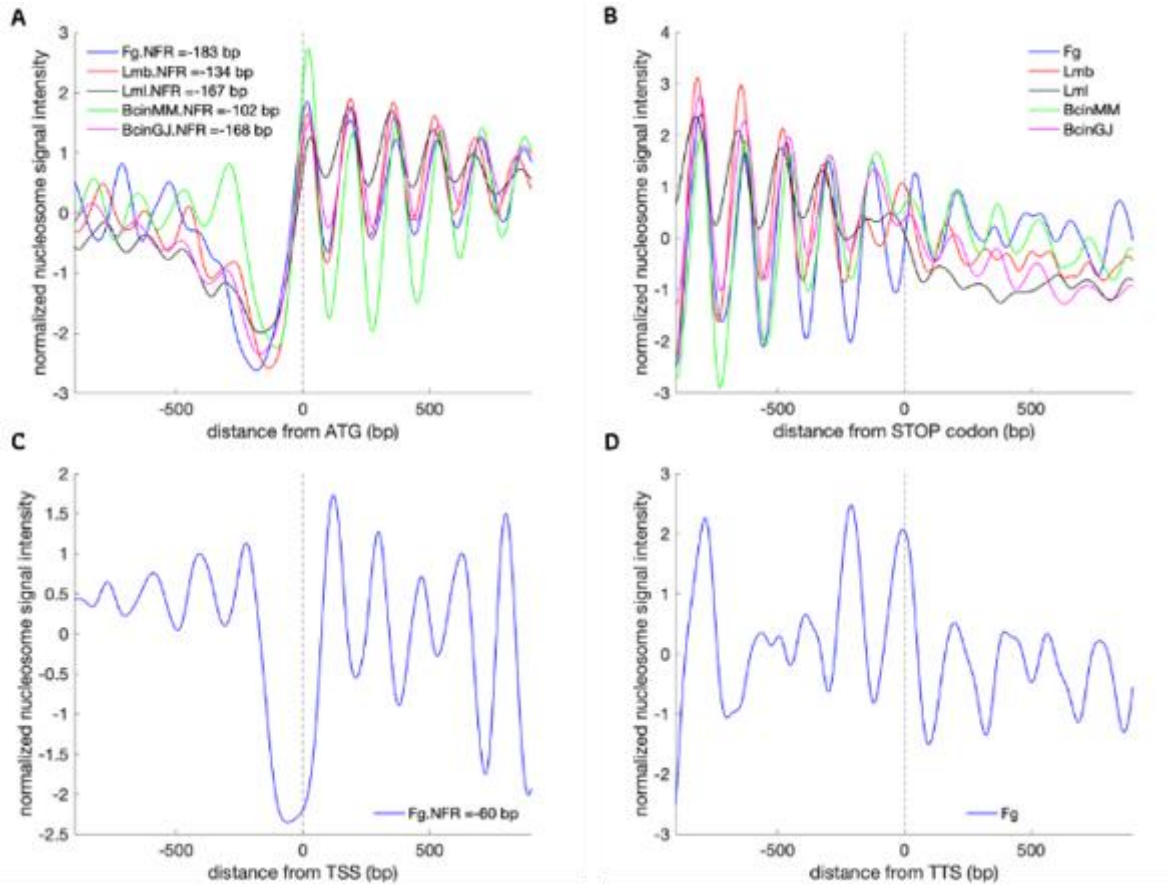

Figure 6: Nucleosome organization of fungal near-universal single copy orthologous gene units (BUSCO3). A-D. Normalised averages (three biological replicates for each fungus/condition) of nucleosome signals as a function of position (in base pairs) relative to the start codon ATG (**A**), the stop codon (**B**), TSS (**C**), and TTS (**D**). Fg = *F. graminearum*; Lmb = *L. maculans* 'brassicae'; Lml = *L. maculans* 'lepidii = BcinMM = *B. cinerea* grown in malt medium; BcinGJ = *B. cinerea* grown in grape juice medium; NFR = nucleosome-free region.

Université Paris-Saclay
Espace Technologique / Immeuble Discovery
Route de l'Orme aux Merisiers RD 128 / 91190 Saint-Aubin,
France

amplitudes of nucleosome signal between the NDR valley upstream the ATG codon and the +1 nucleosome peak. In addition, these NDRs are usually found further from the ATG site than those in genes expressed at lower levels or not expressed. Finally, the nucleosome wave signal decay phenomenon is observed at distances from the ATG codons shorter in poorly expressed genes than in highly expressed genes, although the +1 nucleosome remains fairly well conserved. At the end of gene units, wave signal decay was also observed downstream of stop codons in all studied fungi (**Figure S7**). In *F. graminearum*, signal remained nonetheless stronger in genes lowly/not expressed than in those with higher expression levels (**Figure S7E**) although with species-specific features. In *L. maculans* 'brassicae' and 'lepidii', strong nucleosome positioning can be found upstream the stop codon, immediately followed by a strong nucleosome valley in the case of *L. maculans* 'lepidii'. Finally, *F. graminearum* TTS are characterized by a fuzzy

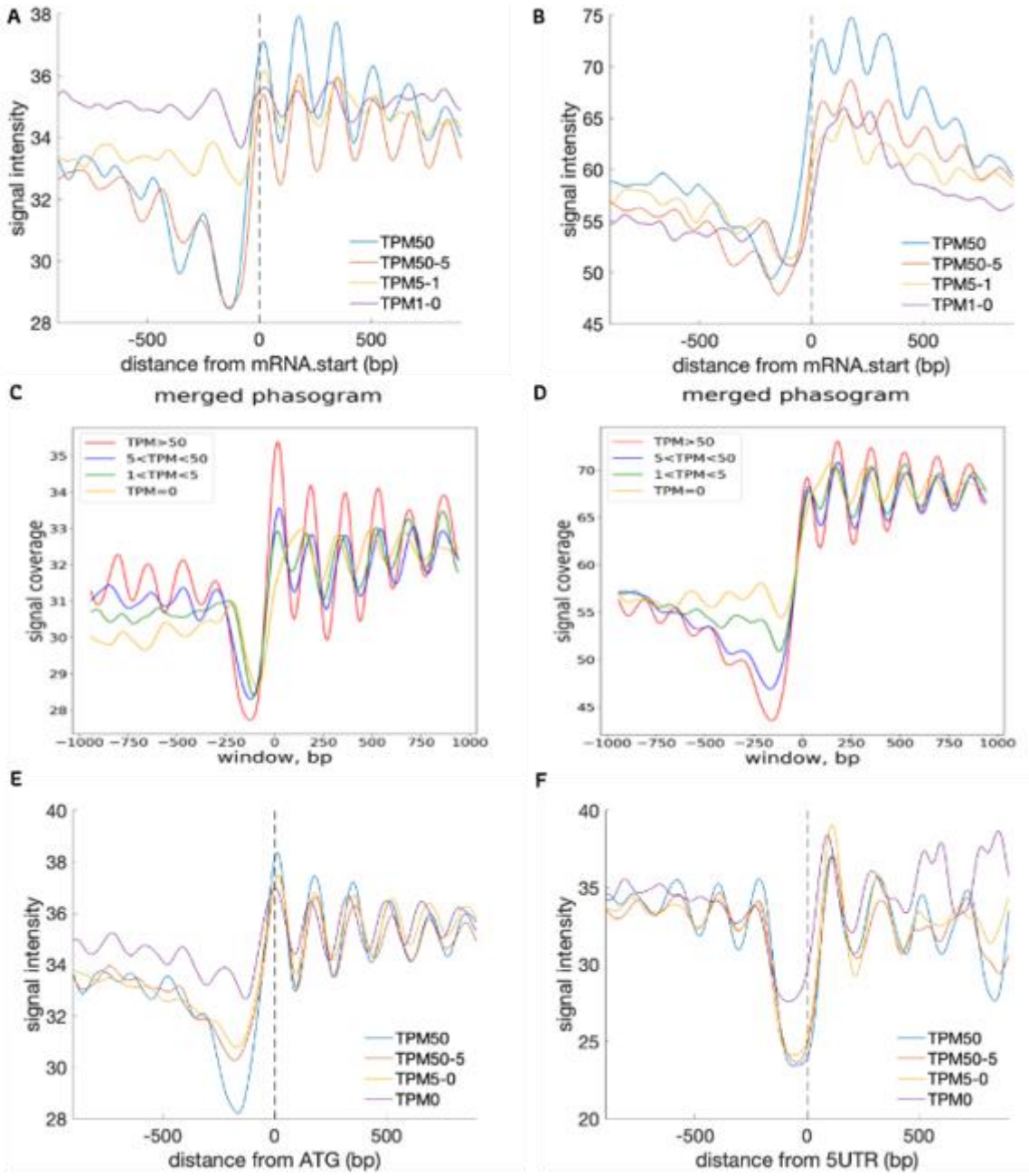

Figure 7: Nucleosome organization at start codons/TSS *vs.* gene expression. Average (three biological replicates for each fungus/condition) nucleosome signal as a function of position (in base pairs) relative to the start codon ATG (and TSS for *F. graminearum*). TPM = Transcripts Per Million. **A:** *Leptosphaeria maculans* 'brassicae'; **B:** *Leptosphaeria maculans* 'lepidii'; **C:** *Botrytis cinerea* grown in malt-based medium; **D:** *Botrytis cinerea* grown in grape juice-based medium; **E:** *Fusarium graminearum*, ATG-centred; **F:** *Fusarium graminearum*, TSS-centred.

Université Paris-Saclay
Espace Technologique / Immeuble Discovery
Route de l'Orme aux Merisiers RD 128 / 91190 Saint-Aubin,
France

nucleosome wave signal expect for genes not expressed that display well-arrayed nucleosomes (**Figure S7F**). Altogether, our results show strong association of nucleosome landscapes at gene unit boundaries with expression levels in the four studied ascomycetes.

DISCUSSION

Nucleosome landscapes are increasingly documented in a large array of organisms, tissues, and cell types in order to understand the impact of their dynamics in gene expression. The present study explores nucleosome positioning characteristics in four different filamentous fungi, *L. maculans* 'brassicae', *L. maculans* 'lepidii', *B. cinerea*, and *F. graminearum*, with the initial ambition to unravel features of a fungal meta-nucleosome landscape. Here, we found features shared by all four investigated fungal genomes, as well as more specific ones.

Nucleosome spacing influences the formation of the higher order chromatin fibre, often referred to as the 30-nm chromatin fibre (Szerlong and Hansen, 2011). Several structural models of the chromatin fibre have been proposed, all underlining nucleosome-nucleosome interactions including the length of linker DNA fragments as major driving factors (see Zhu and Li, 2016). Notably, the chromatin fibre was found to be narrower (21-nm in diameter) for a short NRL of 167 bp (Robinson *et al.,* 2006). Similarly, increasing NRLs lead to increasingly wider fibres, reaching a highly compact 30-nm solenoid structure for an NRL of 197 bp (Robinson *et al.,* 2006; Song *et al.,* 2014). Typically, NRLs are ~175-200 bp in plants and other higher eukaryotes (Valouev *et al.,* 2008; Valouev et al., 2011; Nishida *et al.,* 2012; Locke *et al.,* 2013; Zhang *et al.,* 2015), and ~165 bp and 154 bp in the yeasts *S. cerevisiae* and *S. pombe*, respectively (Yuan *et al.,* 2005; Lantermann *et al.,* 2010). In the present study, we found NRLs ranging from 161 to 173 bp in our fungal pathogens. These values are remarkably constant between biological replicates of a given fungus, a phenomenon sometimes referred to as clamping that involves ATP-dependent chromatin remodelers in purified experimental systems (Lieleg *et al.,* 2015). *F. graminearum* and *B. cinerea* show similar NRLs in the middle range (169 bp to 173 bp), possibly indicating intermediate levels of compaction of the higher order chromatin fibre. These values are similar to those obtained for *Aspergillus fumigatus*, *i.e.,* linker length ranging from 21 to 27 bp, using a MNase treatment similar to the one used in the present study (Nishida *et al.,* 2012). *L. maculans* 'brassicae' and 'lepidii' distinguish themselves with shorter NRLs of only 161-163 bp, suggesting a narrower chromatin fibre structure. In *B. cinerea*, our data reveal a shorter NRL when grown in grape juice-based medium than when grown in malt-based medium correlating with increased histone H1 transcript levels, as previously reported in other eukaryotes (Valouev *et al.,* 2011; Luque *et al.,* 2016). Roles of histone H1 in fungi are diverse and remain largely unknown (Brosch *et al.,* 2008). Here, the changes observed in *B. cinerea* grown in two different media may suggest that, beyond its structural role, H1 participates to reorganizing gene expression networks in response to environmental parameters.

Nucleosome positioning is believed to be particularly hard-wired to DNA sequence and especially the largely documented anti-nucleosome effect of Poly(dA:dT) tracts (Segal and Widom, 2009; Struhl and Segal, 2013). In the present study, whilst nucleosome phase was indeed found 5 bp longer in *L. maculans* 'brassicae' AT-isochores than GC-isochores, occupancy was nonetheless higher in the former leading to the formation of the previously suggested heterochromatic state of these regions (Rouxel *et al.,* 2011; Soyer *et al.,* 2014). These observations indicate the

Université Paris-Saclay
Espace Technologique / Immeuble Discovery
Route de l'Orme aux Merisiers RD 128 / 91190 Saint-Aubin,
France

mobilisation of trans-acting chromatin remodelling factors to maintain heterochromatin structures on such disfavouring sequences. Importantly, we found that GC periodicity at nucleosome dyads is preserved even within AT-isochores, suggesting such pattern in an AT-rich environment is sufficient to permit efficient wrapping of DNA around nucleosomes and strong occupancy. Conversely, our results reveal lower nucleosome occupancy in the previously described *F. graminearum* fast evolving polymorphic islands (Laurent *et al.,* 2017). Here, nucleosome dynamics may enable fast evolution of particular genome segments while regions defined by higher occupancies may secure sequence conservation.

The general profile of a fungal gene unit shares similarities with those previously described in various eukaryotes: the ATG codon is decorated by a well-positioned +1 nucleosome and preceded by an NDR. The NDR observed for *B. cinerea* grown in malt medium was remarkable in its intensity, deeper than all others. When we restricted our analysis to conserved orthologous fungal genes, the overall profiles and the intensities of NDRs were more homogenous between fungi and culture conditions. These observations suggest that NDRs positions and intensities are subjected to evolution. Similarly, whilst an NDR can be observed downstream of *F. graminearum* TTS, it is no longer visible when the analysis is restricted to fungal genes indicating again an evolutionary component.

From the gene expression perspective, nucleosome depletion can be the side-effect of active transcription with the binding of pre-initiation complex resulting in nucleosome eviction as previously shown in yeast (Venters and Pugh, 2009). Indeed, we evidenced valleys of nucleosome signals upstream of ATG codons found deeper in highly expressed genes. On the contrary, genes not expressed show little or no NDR, depending on the considered species or culture condition. In our conditions, the amplitude between the NDR and the +1 nucleosome seems to be an informative measure of gene expression level: the more this value is high, the more genes are expressed. Strikingly, this feature is less strict when TSS are considered raising the question of different mechanisms of transcription regulation depending on gene unit structures.

ACKNOWLEDGEMENT

We are grateful to the Genotoul bioinformatics platform Toulouse Midi-Pyrenees for providing computing resources. J. L. Soyer was founded by a “Contrat Jeune Scientifique” grant from INRA.

FUNDING

This work was supported by the Plant Health and Environment division of the French National Institute for Agricultural Research [MAINE Project AAP 2014]. Funding for open access charge: Plant Health and Environment department of the French National Institute for Agricultural Research.

CONFLICT OF INTEREST

The authors declare no conflict of interest.

AVAILABILITY

Université Paris-Saclay
Espace Technologique / Immeuble Discovery
Route de l'Orme aux Merisiers RD 128 / 91190 Saint-Aubin, France

The MSTS (MAINE-Seq Tool Suite) is an open source collection of tools developed by the BioinfoBIOGER platform by N. Lapalu and A. Simon, and available in the GitHub repository (https://github.com/nlapalu/MSTS).

ACCESSION NUMBERS

All sequenced reads have been deposited with the Short Read Archive under accession numbers XXXX.

REFERENCES

Amselem, J., Cuomo, C.A., van Kan, J.A.L., Viaud, M., Benito, E.P., Couloux, A., Coutinho, P.M., de Vries, R.P., Dyer, P.S., Fillinger, S., Fournier, E., Gout, L., Hahn, M., Kohn, L., Lapalu, N., Plummer, K.M., Pradier, J.-M., Quévillon, E., Sharon, A., Simon, A., ten Have, A., Tudzynski, B., Tudzynski, P., Wincker, P., Andrew, M., Anthouard, V., Beever, R.E., Beffa, R., Benoit, I., Bouzid, O., Brault, B., Chen, Z., Choquer, M., Collémare, J., Cotton, P., Danchin, E.G., Da Silva, C., Gautier, A., Giraud, C., Giraud, T., Gonzalez, C., Grossetete, S., Güldener, U., Henrissat, B., Howlett, B.J., Kodira, C., Kretschmer, M., Lappartient, A., Leroch, M., Levis, C., Mauceli, E., Neuvéglise, C., Oeser, B., Pearson, M., Poulain, J., Poussereau, N., Quesneville, H., Rascle, C., Schumacher, J., Ségurens, B., Sexton, A., Silva, E., Sirven, C., Soanes, D.M., Talbot, N.J., Templeton, M., Yandava, C., Yarden, O., Zeng, Q., Rollins, J.A., Lebrun, M.-H., Dickman, M., 2011. Genomic Analysis of the Necrotrophic Fungal Pathogens Sclerotinia sclerotiorum and Botrytis cinerea. PLoS Genet 7.

Basenko, E.Y., Pulman, J.A., Shanmugasundram, A., Harb, O.S., Crouch, K., Starns, D., Warrenfeltz, S., Aurrecoechea, C., Stoeckert, C.J., Kissinger, J.C., Roos, D.S., Hertz-Fowler, C., 2018. FungiDB: An Integrated Bioinformatic Resource for Fungi and Oomycetes. J Fungi (Basel) 4.

Bolger, A.M., Lohse, M., Usadel, B., 2014. Trimmomatic: a flexible trimmer for Illumina sequence data. Bioinformatics 30, 2114–2120.

Boutigny, A.-L., Barreau, C., Atanasova-Penichon, V., Verdal-Bonnin, M.-N., Pinson-Gadais, L., Richard-Forget, F., 2009. Ferulic acid, an efficient inhibitor of type B trichothecene biosynthesis and Tri gene expression in Fusarium liquid cultures. Mycol. Res. 113, 746–753.

Brosch, G., Loidl, P., Graessle, S., 2008. Histone modifications and chromatin dynamics: a focus on filamentous fungi. FEMS Microbiol Rev 32, 409–439.

Bunnik, E.M., Polishko, A., Prudhomme, J., Ponts, N., Gill, S.S., Lonardi, S., Le Roch, K.G., 2014. DNA-encoded nucleosome occupancy is associated with transcription levels in the human malaria parasite Plasmodium falciparum. BMC Genomics 15, 347.

Cuomo, C.A., Güldener, U., Xu, J.-R., Trail, F., Turgeon, B.G., Di Pietro, A., Walton, J.D., Ma, L.-J., Baker, S.E., Rep, M., Adam, G., Antoniw, J., Baldwin, T., Calvo, S., Chang, Y.-L., Decaprio, D., Gale, L.R., Gnerre, S., Goswami, R.S., Hammond-Kosack, K., Harris, L.J., Hilburn, K., Kennell, J.C., Kroken, S., Magnuson, J.K., Mannhaupt, G., Mauceli, E., Mewes, H.-W., Mitterbauer, R., Muehlbauer, G., Münsterkötter, M., Nelson, D., O'donnell, K., Ouellet, T., Qi, W., Quesneville, H., Roncero, M.I.G., Seong, K.-Y., Tetko, I.V., Urban, M., Waalwijk, C., Ward, T.J., Yao, J., Birren, B.W., Kistler, H.C., 2007. The Fusarium graminearum genome reveals a link between localized polymorphism and pathogen specialization. Science 317, 1400–1402.

Dobin, A., Davis, C.A., Schlesinger, F., Drenkow, J., Zaleski, C., Jha, S., Batut, P., Chaisson, M., Gingeras, T.R., 2013. STAR: ultrafast universal RNA-seq aligner. Bioinformatics 29, 15–21.

Dutreux, F., Da Silva, C., d'Agata, L., Couloux, A., Gay, E.J., Istace, B., Lapalu, N., Lemainque, A., Linglin, J., Noel, B., Wincker, P., Cruaud, C., Rouxel, T., Balesdent, M.-H., Aury, J.-M., 2018. De novo assembly and annotation of three Leptosphaeria genomes using Oxford Nanopore MinION sequencing. Scientific Data 5.

Fisher, M.C., Henk, D.A., Briggs, C.J., Brownstein, J.S., Madoff, L.C., McCraw, S.L., Gurr, S.J., 2012. Emerging fungal threats to animal, plant and ecosystem health. Nature 484, 186–194.

Fox, E.M., Howlett, B.J., 2008. Secondary metabolism: regulation and role in fungal biology. Current Opinion in Microbiology 11, 481–487.

Fudal, I., Ross, S., Gout, L., Blaise, F., Kuhn, M.L., Eckert, M.R., Cattolico, L., Bernard-Samain, S., Balesdent, M.H., Rouxel, T., 2007. Heterochromatin-like regions as ecological niches for avirulence genes in the Leptosphaeria maculans genome: map-based cloning of AvrLm6. Mol. Plant Microbe Interact. 20, 459–470.

Grandaubert, J., Lowe, R.G., Soyer, J.L., Schoch, C.L., Van de Wouw, A.P., Fudal, I., Robbertse, B., Lapalu, N., Links, M.G., Ollivier, B., 2014. Transposable element-assisted evolution and adaptation to host plant within the Leptosphaeria maculans-Leptosphaeria biglobosa species complex of fungal pathogens. BMC genomics 15, 891.

Hallen, H.E., Huebner, M., Shiu, S.-H., Güldener, U., Trail, F., 2007. Gene expression shifts during perithecium development in Gibberella zeae (anamorph Fusarium graminearum), with particular emphasis on ion transport proteins. Fungal Genet. Biol. 44, 1146–1156.

Hawksworth, D.L., Lücking, R., 2017. Fungal Diversity Revisited: 2.2 to 3.8 Million Species. Microbiol Spectr 5.

Jin, H., Finnegan, A.I., Song, J.S., 2018. A unified computational framework for modeling genome-wide nucleosome landscape. Phys Biol 15, 066011.

Kaplan, N., Moore, I.K., Fondufe-Mittendorf, Y., Gossett, A.J., Tillo, D., Field, Y., LeProust, E.M., Hughes, T.R., Lieb, J.D., Widom, J., Segal, E., 2009. The DNA-encoded nucleosome organization of a eukaryotic genome. Nature 458, 362–366.

Kelloniemi, J., Trouvelot, S., Héloir, M.-C., Simon, A., Dalmais, B., Frettinger, P., Cimerman, A., Fermaud, M., Roudet, J., Baulande, S., Bruel, C., Choquer, M., Couvelard, L., Duthieuw, M., Ferrarini, A., Flors, V., Le Pêcheur, P., Loisel, E., Morgant, G., Poussereau, N., Pradier, J.-M., Rascle, C., Trdá, L., Poinssot, B., Viaud, M., 2015. Analysis of the Molecular Dialogue Between Gray Mold (Botrytis cinerea) and Grapevine (Vitis vinifera) Reveals a Clear Shift in Defense Mechanisms During Berry Ripening. Mol. Plant Microbe Interact. 28, 1167–1180.

King, R., Urban, M., Hammond-Kosack, M.C.U., Hassani-Pak, K., Hammond-Kosack, K.E., 2015. The completed genome sequence of the pathogenic ascomycete fungus Fusarium graminearum. BMC Genomics 16, 544.

King, R., Urban, M., Hammond-Kosack, K.E., 2017. Annotation of Fusarium graminearum (PH-1) Version 5.0. Genome Announcements 5.

Langmead, B., Salzberg, S.L., 2012. Fast gapped-read alignment with Bowtie 2. Nat. Methods 9, 357–359.

Lantermann, A.B., Straub, T., Strålfors, A., Yuan, G.-C., Ekwall, K., Korber, P., 2010. Schizosaccharomyces pombe genome-wide nucleosome mapping reveals positioning mechanisms distinct from those of Saccharomyces cerevisiae. Nat. Struct. Mol. Biol. 17, 251–257.

Université Paris-Saclay
Espace Technologique / Immeuble Discovery
Route de l'Orme aux Merisiers RD 128 / 91190 Saint-Aubin, France

Laurent, B., Moinard, M., Spataro, C., Ponts, N., Barreau, C., Foulongne-Oriol, M., 2017. Landscape of genomic diversity and host adaptation in Fusarium graminearum. BMC Genomics 18, 203.

Li, B., Ruotti, V., Stewart, R.M., Thomson, J.A., Dewey, C.N., 2010. RNA-Seq gene expression estimation with read mapping uncertainty. Bioinformatics 26, 493–500.

Lieleg, C., Ketterer, P., Nuebler, J., Ludwigsen, J., Gerland, U., Dietz, H., Mueller-Planitz, F., Korber, P., 2015. Nucleosome spacing generated by ISWI and CHD1 remodelers is constant regardless of nucleosome density. Mol. Cell. Biol. 35, 1588–1605.

Lo Presti, L., Lanver, D., Schweizer, G., Tanaka, S., Liang, L., Tollot, M., Zuccaro, A., Reissmann, S., Kahmann, R., 2015. Fungal Effectors and Plant Susceptibility. Annual Review of Plant Biology 66, 513–545.

Locke, G., Haberman, D., Johnson, S.M., Morozov, A.V., 2013. Global remodeling of nucleosome positions in C. elegans. BMC Genomics 14, 284.

Love, M.I., Huber, W., Anders, S., 2014. Moderated estimation of fold change and dispersion for RNA-seq data with DESeq2. Genome Biol. 15, 550.

Luque, A., Ozer, G., Schlick, T., 2016. Correlation among DNA Linker Length, Linker Histone Concentration, and Histone Tails in Chromatin. Biophys. J. 110, 2309–2319.

Möbius, N., Hertweck, C., 2009. Fungal phytotoxins as mediators of virulence. Curr. Opin. Plant Biol. 12, 390–398.

Nishida, H., Kondo, S., Matsumoto, T., Suzuki, Y., Yoshikawa, H., Taylor, T.D., Sugiyama, J., 2012. Characteristics of nucleosomes and linker DNA regions on the genome of the basidiomycete Mixia osmundae revealed by mono- and dinucleosome mapping. Open Biol 2, 120043.

Nishida, H., Motoyama, T., Yamamoto, S., Aburatani, H., Osada, H., 2009. Genome-wide maps of mono- and di-nucleosomes of Aspergillus fumigatus. Bioinformatics 25, 2295–2297.

Ponts, N., Harris, E.Y., Prudhomme, J., Wick, I., Eckhardt-Ludka, C., Hicks, G.R., Hardiman, G., Lonardi, S., Le Roch, K.G., 2010. Nucleosome landscape and control of transcription in the human malaria parasite. Genome Res. 20, 228–238.

Porquier, A., Morgant, G., Moraga, J., Dalmais, B., Luyten, I., Simon, A., Pradier, J.-M., Amselem, J., Collado, I.G., Viaud, M., 2016. The botrydial biosynthetic gene cluster of Botrytis cinerea displays a bipartite genomic structure and is positively regulated by the putative Zn(II)2Cys6 transcription factor BcBot6. Fungal Genetics and Biology 96, 33–46.

Radman-Livaja, M., Rando, O.J., 2010. Nucleosome positioning: how is it established, and why does it matter? Dev. Biol. 339, 258–266.

Richmond, T.J., Davey, C.A., 2003. The structure of DNA in the nucleosome core. Nature 423, 145–150.

Robinson, P.J.J., Fairall, L., Huynh, V.A.T., Rhodes, D., 2006. EM measurements define the dimensions of the "30-nm" chromatin fiber: evidence for a compact, interdigitated structure. Proc. Natl. Acad. Sci. U.S.A. 103, 6506–6511.

Rouxel, T., Grandaubert, J., Hane, J.K., Hoede, C., van de Wouw, A.P., Couloux, A., Dominguez, V., Anthouard, V., Bally, P., Bourras, S., Cozijnsen, A.J., Ciuffetti, L.M., Degrave, A., Dilmaghani, A., Duret, L., Fudal, I., Goodwin,

Université Paris-Saclay
Espace Technologique / Immeuble Discovery
Route de l'Orme aux Merisiers RD 128 / 91190 Saint-Aubin,
France

S.B., Gout, L., Glaser, N., Linglin, J., Kema, G.H.J., Lapalu, N., Lawrence, C.B., May, K., Meyer, M., Ollivier, B., Poulain, J., Schoch, C.L., Simon, A., Spatafora, J.W., Stachowiak, A., Turgeon, B.G., Tyler, B.M., Vincent, D., Weissenbach, J., Amselem, J., Quesneville, H., Oliver, R.P., Wincker, P., Balesdent, M.-H., Howlett, B.J., 2011. Effector diversification within compartments of the Leptosphaeria maculans genome affected by Repeat-Induced Point mutations. Nat Commun 2, 202.

Russell, K., Cheng, C.-H., Bizzaro, J.W., Ponts, N., Emes, R.D., Le Roch, K., Marx, K.A., Horrocks, P., 2014. Homopolymer tract organization in the human malarial parasite Plasmodium falciparum and related Apicomplexan parasites. BMC Genomics 15.

Satchwell, S.C., Drew, H.R., Travers, A.A., 1986. Sequence periodicities in chicken nucleosome core DNA. J. Mol. Biol. 191, 659–675.

Segal, E., Fondufe-Mittendorf, Y., Chen, L., Thåström, A., Field, Y., Moore, I.K., Wang, J.-P.Z., Widom, J., 2006. A genomic code for nucleosome positioning. Nature 442, 772–778.

Segal, E., Widom, J., 2009. What controls nucleosome positions? Trends in Genetics 25, 335–343.

Simão, F.A., Waterhouse, R.M., Ioannidis, P., Kriventseva, E.V., Zdobnov, E.M., 2015. BUSCO: assessing genome assembly and annotation completeness with single-copy orthologs. Bioinformatics 31, 3210–3212.

Simon, A., Dalmais, B., Morgant, G., Viaud, M., 2013. Screening of a Botrytis cinerea one-hybrid library reveals a Cys2His2 transcription factor involved in the regulation of secondary metabolism gene clusters. Fungal Genet. Biol. 52, 9–19.

Song, F., Chen, P., Sun, D., Wang, M., Dong, L., Liang, D., Xu, R.-M., Zhu, P., Li, G., 2014. Cryo-EM study of the chromatin fiber reveals a double helix twisted by tetranucleosomal units. Science 344, 376–380.

Soyer, J.L., El Ghalid, M., Glaser, N., Ollivier, B., Linglin, J., Grandaubert, J., Balesdent, M.-H., Connolly, L.R., Freitag, M., Rouxel, T., Fudal, I., 2014. Epigenetic Control of Effector Gene Expression in the Plant Pathogenic Fungus Leptosphaeria maculans. PLoS Genetics 10, e1004227.

Soyer, Jessica L., Möller, M., Schotanus, K., Connolly, L.R., Galazka, J.M., Freitag, M., Stukenbrock, E.H., 2015. Chromatin analyses of Zymoseptoria tritici: Methods for chromatin immunoprecipitation followed by high-throughput sequencing (ChIP-seq). Fungal Genet. Biol. 79, 63–70.

Soyer, Jessica L, Rouxel, T., Fudal, I., 2015. Chromatin-based control of effector gene expression in plant-associated fungi. Current Opinion in Plant Biology 26, 51–56.

Stajich, J.E., Harris, T., Brunk, B.P., Brestelli, J., Fischer, S., Harb, O.S., Kissinger, J.C., Li, W., Nayak, V., Pinney, D.F., Stoeckert, C.J., Roos, D.S., 2012. FungiDB: an integrated functional genomics database for fungi. Nucleic Acids Res. 40, D675-681.

Strauss, J., Reyes-Dominguez, Y., 2011. Regulation of secondary metabolism by chromatin structure and epigenetic codes. Fungal Genetics and Biology 48, 62–69.

Struhl, K., Segal, E., 2013. Determinants of nucleosome positioning. Nat. Struct. Mol. Biol. 20, 267–273.

Szerlong, H.J., Hansen, J.C., 2011. Nucleosome distribution and linker DNA: connecting nuclear function to dynamic chromatin structure. Biochem. Cell Biol. 89, 24–34.

Université Paris-Saclay
Espace Technologique / Immeuble Discovery
Route de l'Orme aux Merisiers RD 128 / 91190 Saint-Aubin, France

Tan, K.-C., Oliver, R.P., 2017. Regulation of proteinaceous effector expression in phytopathogenic fungi. PLoS pathogens 13, e1006241.

Taylor, T.N., Osborn, J.M., 1996. The importance of fungi in shaping the paleoecosystem. Review of Palaeobotany and Palynology 90, 249–262.

Tillo, D., Kaplan, N., Moore, I.K., Fondufe-Mittendorf, Y., Gossett, A.J., Field, Y., Lieb, J.D., Widom, J., Segal, E., Hughes, T.R., 2010. High nucleosome occupancy is encoded at human regulatory sequences. PLoS ONE 5, e9129.

Tsankov, A.M., Thompson, D.A., Socha, A., Regev, A., Rando, O.J., 2010. The Role of Nucleosome Positioning in the Evolution of Gene Regulation. PLoS Biology 8, e1000414.

Valouev, A., Ichikawa, J., Tonthat, T., Stuart, J., Ranade, S., Peckham, H., Zeng, K., Malek, J.A., Costa, G., McKernan, K., Sidow, A., Fire, A., Johnson, S.M., 2008. A high-resolution, nucleosome position map of C. elegans reveals a lack of universal sequence-dictated positioning. Genome Res. 18, 1051–1063.

Valouev, A., Johnson, S.M., Boyd, S.D., Smith, C.L., Fire, A.Z., Sidow, A., 2011. Determinants of nucleosome organization in primary human cells. Nature 474, 516–520.

Varet, H., Brillet-Guéguen, L., Coppée, J.-Y., Dillies, M.-A., 2016. SARTools: A DESeq2- and EdgeR-Based R Pipeline for Comprehensive Differential Analysis of RNA-Seq Data. PLoS ONE 11, e0157022.

Venters, B.J., Pugh, B.F., 2009. A canonical promoter organization of the transcription machinery and its regulators in the Saccharomyces genome. Genome Res. 19, 360–371.

Wang, M., Weiberg, A., Lin, F.-M., Thomma, B.P.H.J., Huang, H.-D., Jin, H., 2016. Bidirectional cross-kingdom RNAi and fungal uptake of external RNAs confer plant protection. Nature Plants 2, 16151.

Waterhouse, R.M., Seppey, M., Simão, F.A., Manni, M., Ioannidis, P., Klioutchnikov, G., Kriventseva, E.V., Zdobnov, E.M., 2017. BUSCO applications from quality assessments to gene prediction and phylogenomics. Mol. Biol. Evol.

Weiberg, A., Wang, M., Lin, F.-M., Zhao, H., Zhang, Z., Kaloshian, I., Huang, H.-D., Jin, H., 2013. Fungal Small RNAs Suppress Plant Immunity by Hijacking Host RNA Interference Pathways. Science 342, 118–123.

Yuan, G.-C., Liu, Y.-J., Dion, M.F., Slack, M.D., Wu, L.F., Altschuler, S.J., Rando, O.J., 2005. Genome-scale identification of nucleosome positions in S. cerevisiae. Science 309, 626–630.

Zhang, T., Zhang, W., Jiang, J., 2015. Genome-Wide Nucleosome Occupancy and Positioning and Their Impact on Gene Expression and Evolution in Plants. Plant Physiology 168, 1406–1416.

Zhu, P., Li, G., 2016. Structural insights of nucleosome and the 30-nm chromatin fiber. Curr. Opin. Struct. Biol. 36, 106–115.

Université Paris-Saclay
Espace Technologique / Immeuble Discovery
Route de l'Orme aux Merisiers RD 128 / 91190 Saint-Aubin, France

528 **SUPPLEMENTARY DATA**

529 Supplementary Data are available at NAR online.

530

531

532

533

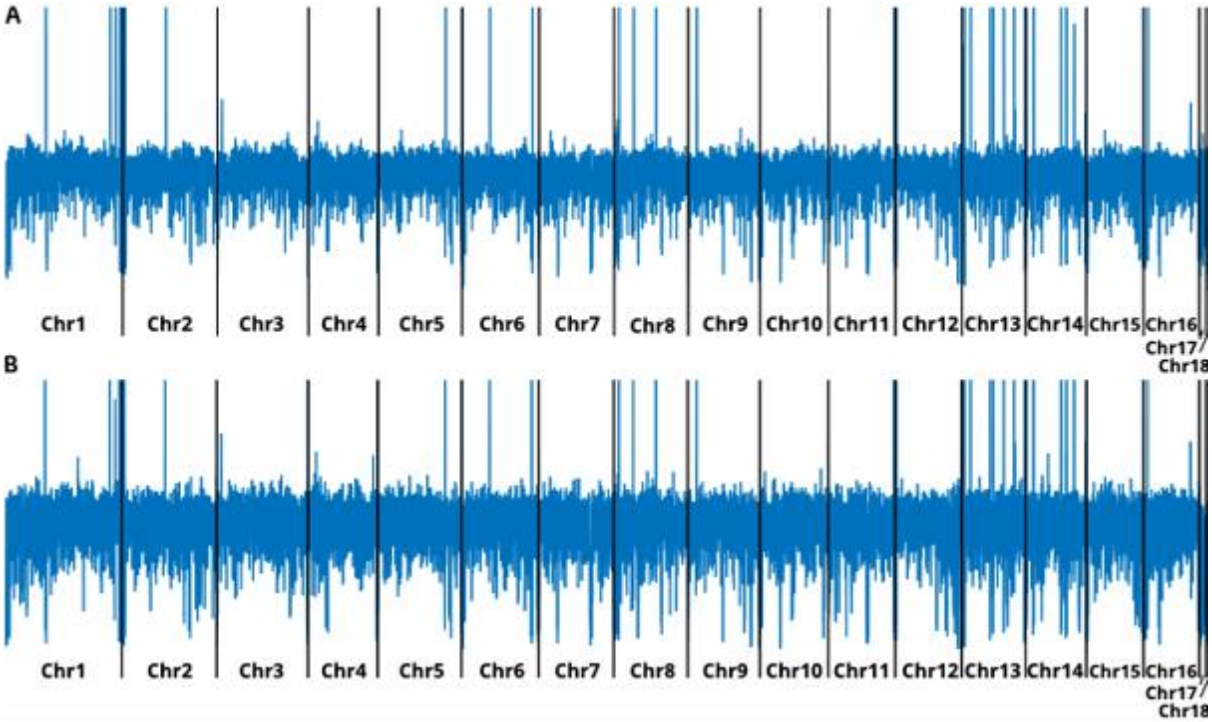

Figure S1: Nucleosome density profiles in *B. cinerea*. A. Coverage density profiles were computed for non-overlapping 1 kb-long bins along all chromosomes of *B. cinerea* grown in malt medium (A) or grape juice medium (B).

Université Paris-Saclay
Espace Technologique / Immeuble Discovery
Route de l'Orme aux Merisiers RD 128 / 91190 Saint-Aubin, France

534

535

536

537

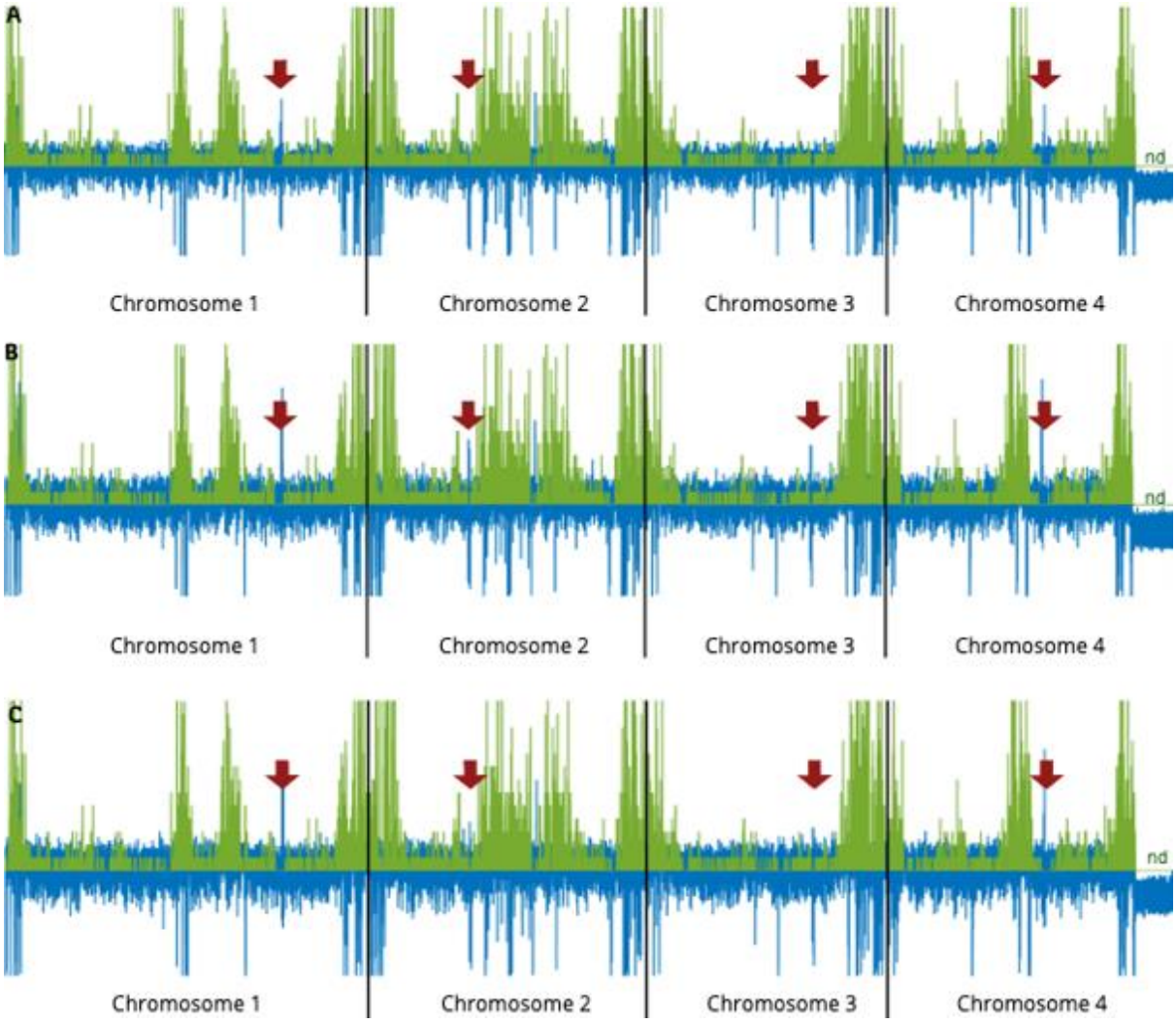

Figure S2: Nucleosome *vs*. SNP density profiles in individual biological replicates of *F. graminearum*. Coverage density profiles were computed for non-overlapping 1 kb-long bins along the four chromosomes of *F. graminearum*. In green are plotted SNP density profiles as previously described (1). "nd" indicates the highly variable 3' end of chromosome 4 for which SNP were not called. In blue are plotted the z-scored nucleosome density profiles. The red arrows indicate centromeres (2); **A:** Biological replicate #1; **B:** Biological Replicate #2; **C:** Biological replicate #3.

Université Paris-Saclay
Espace Technologique / Immeuble Discovery
Route de l'Orme aux Merisiers RD 128 / 91190 Saint-Aubin, France

538

539

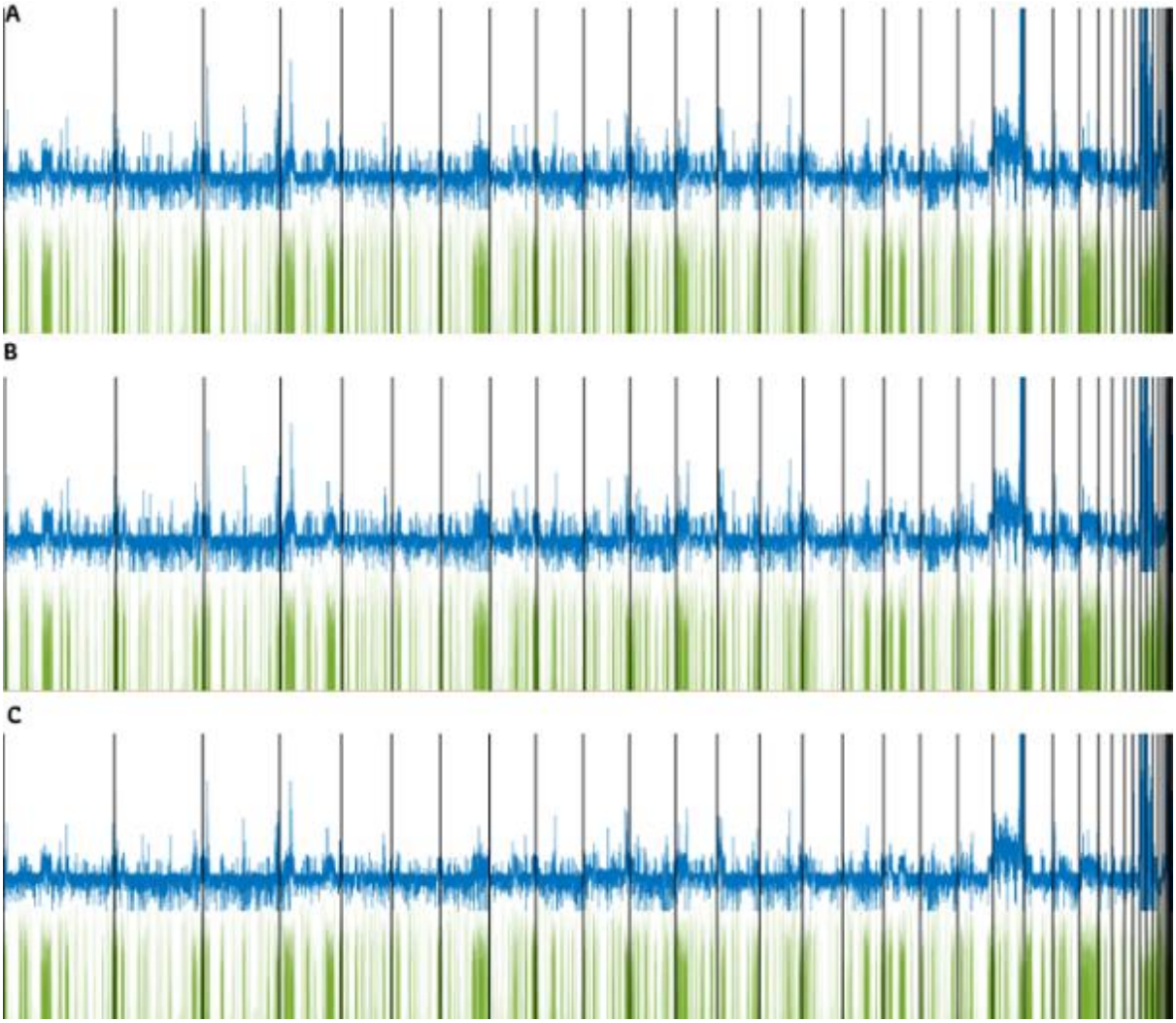

Figure S3: Nucleosome density profiles *vs*. AT-rich regions in individual biological replicates of *L. maculans* 'brassicae'. Coverage density profiles were computed for non-overlapping 1 kb-long bins along all supercontigs, separated by black lines. AT-rich 1 kb-long bins are plotted in green, isochores showing as dense regions. In blue are plotted the z-scored average nucleosome density profile **A:** Biological replicate #1; **B:** Biological Replicate #2; **C:** Biological replicate #3.

Université Paris-Saclay
Espace Technologique / Immeuble Discovery
Route de l'Orme aux Merisiers RD 128 / 91190 Saint-Aubin, France

540

541

542

543

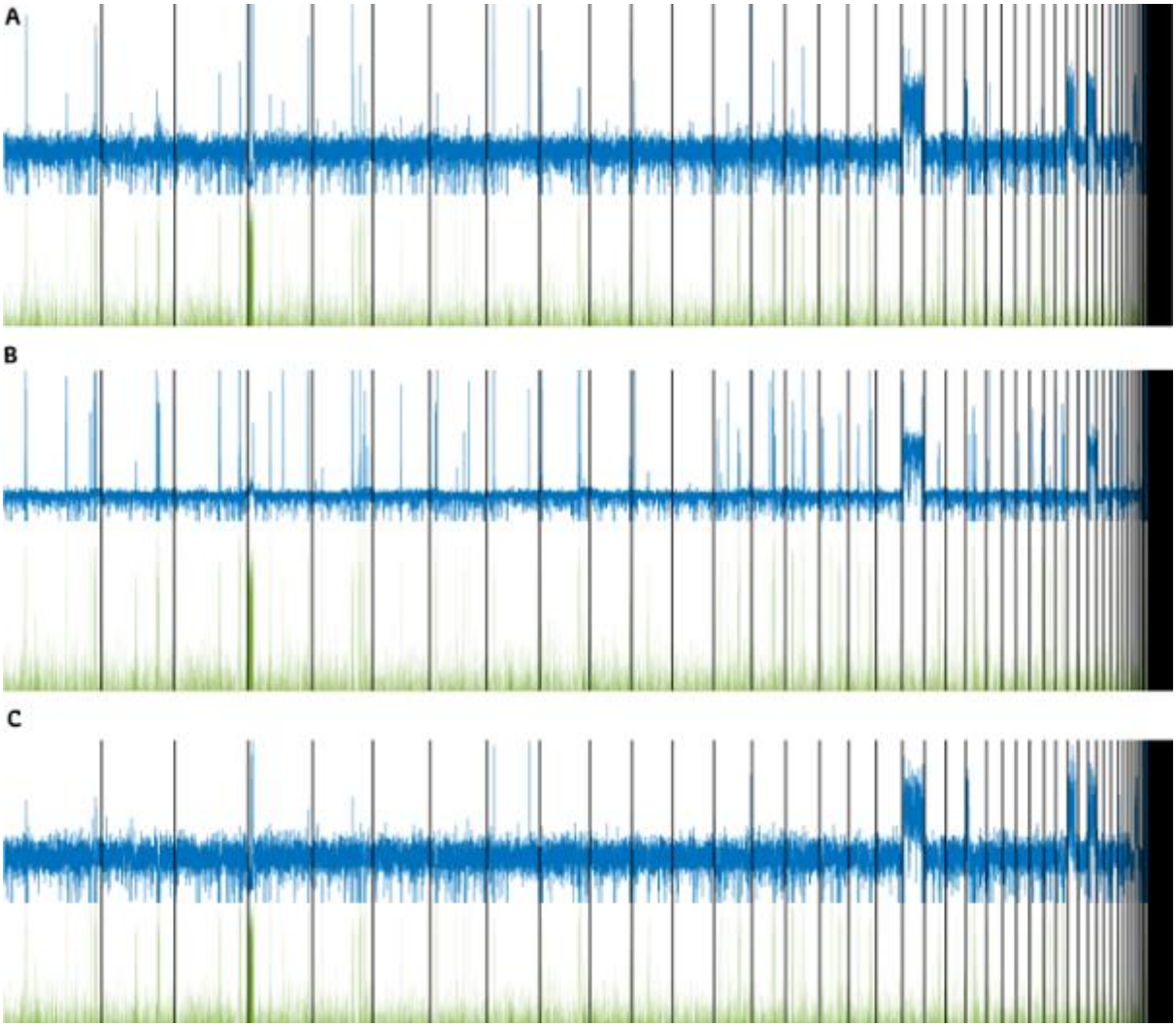

Figure S4: Nucleosome density profiles *vs.* AT content in individual biological replicates of *L. maculans* 'lepidii'. Coverage density profiles were computed for non-overlapping 1 kb-long bins along all supercontigs, separated by black lines. AT-rich 1 kb-long bins are plotted in green, with no isochore visible. In blue are plotted the z-scored average nucleosome density profile **A:** Biological replicate #1; **B:** Biological Replicate #2; **C:** Biological replicate #3.

Université Paris-Saclay
Espace Technologique / Immeuble Discovery
Route de l'Orme aux Merisiers RD 128 / 91190 Saint-Aubin, France

544

545

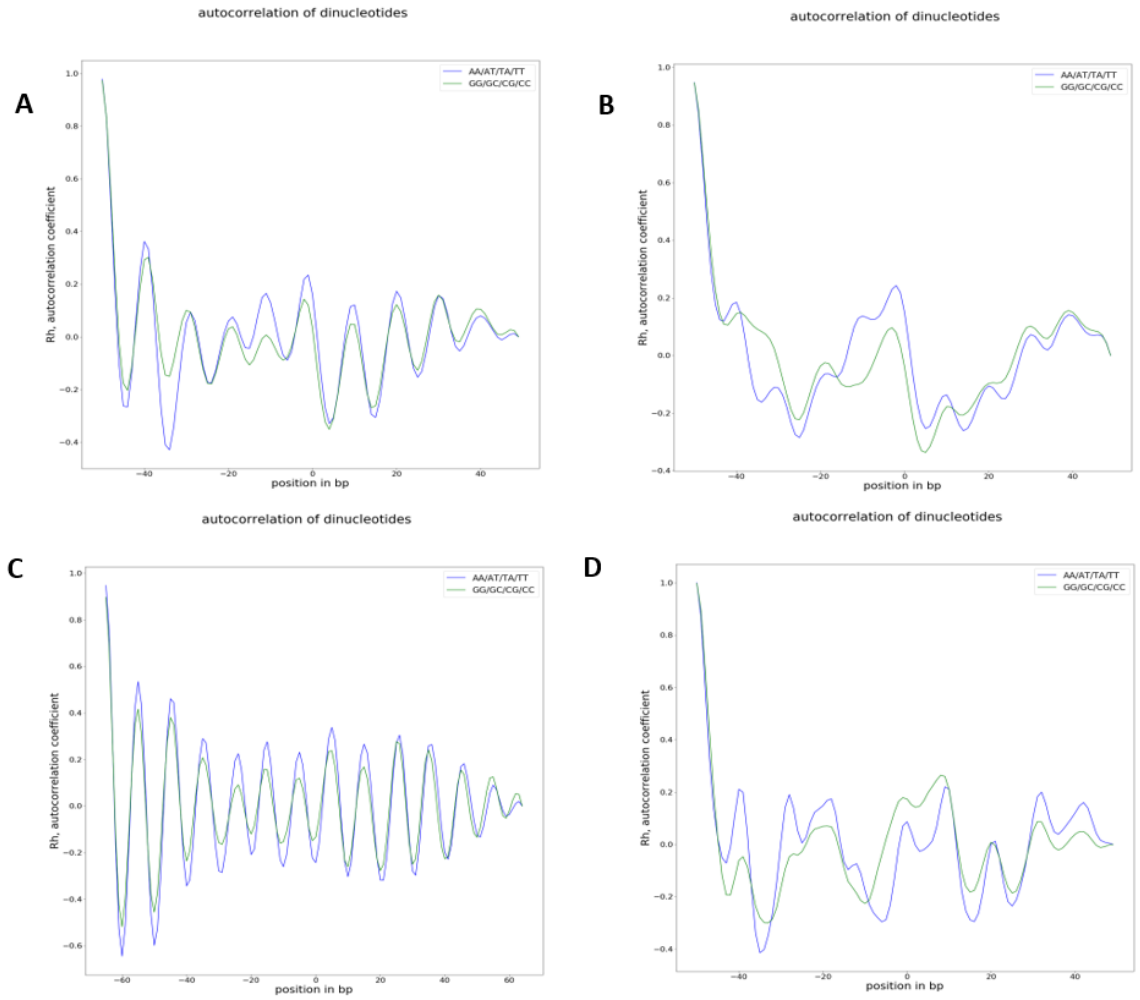

Figure S5: Pearson autocorrelation coefficients of di-nucleotides frequencies (average of three biological replicates) for *L. maculans* 'brassicae' (A), L. *maculans* 'lepidii' (B), *F. graminearum* (C), and *B. cinerea* grown in malt medium (D).

Université Paris-Saclay
Espace Technologique / Immeuble Discovery
Route de l'Orme aux Merisiers RD 128 / 91190 Saint-Aubin, France

546

547

548

549

550

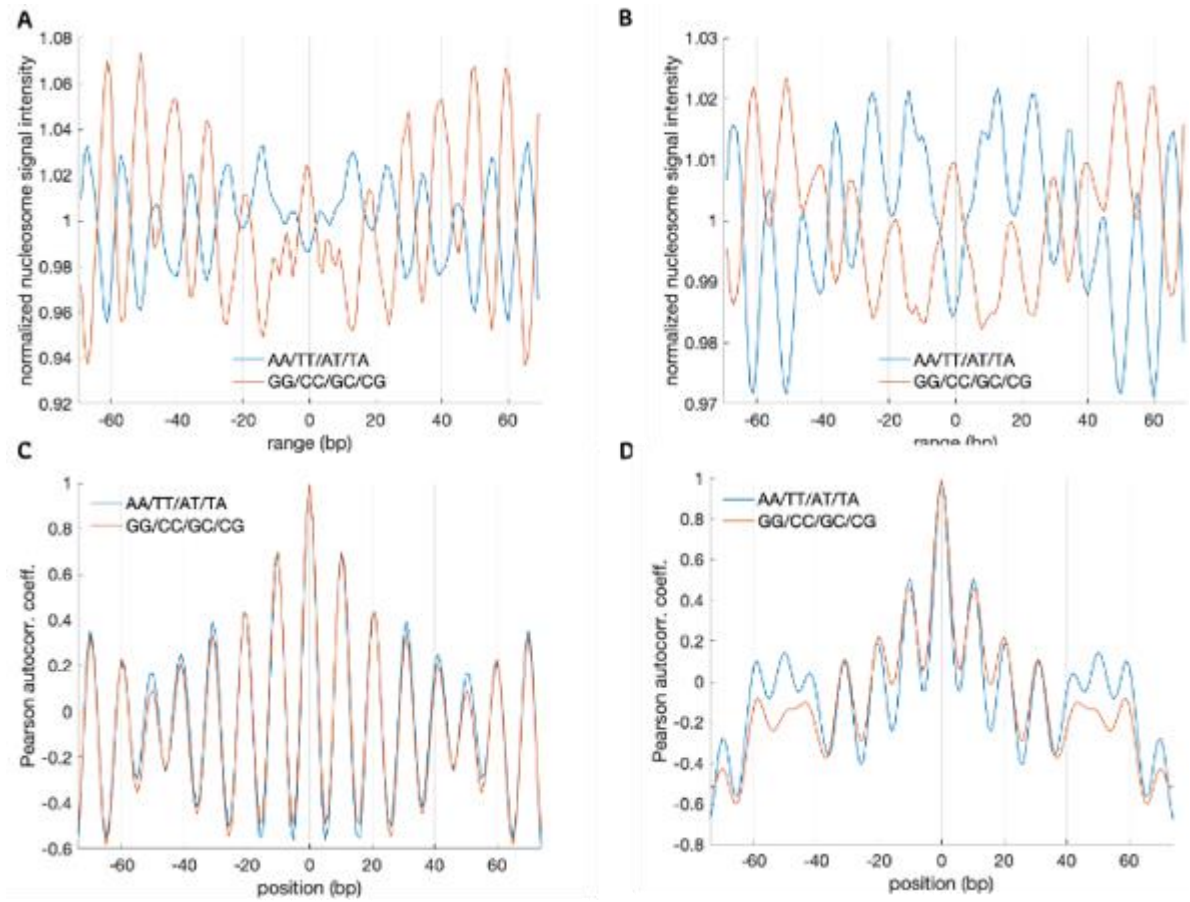

Figure S6: Repeated di-nucleotide patterns in nucleosomal DNA located in AT and GC isochores of *L. maculans* 'brassicae'. A and B: Normalized di-nucleotides frequency plots (average of three biological replicates) for nucleosomal DNA in AT-isochores (A) and GC-isochores **(B): C and D:** Pearson autocorrelation coefficients of di-nucleotides frequencies (average of three biological replicates) for nucleosomal DNA in AT-isochores (C) and GC-isochores (D).

Université Paris-Saclay
Espace Technologique / Immeuble Discovery
Route de l'Orme aux Merisiers RD 128 / 91190 Saint-Aubin, France

551

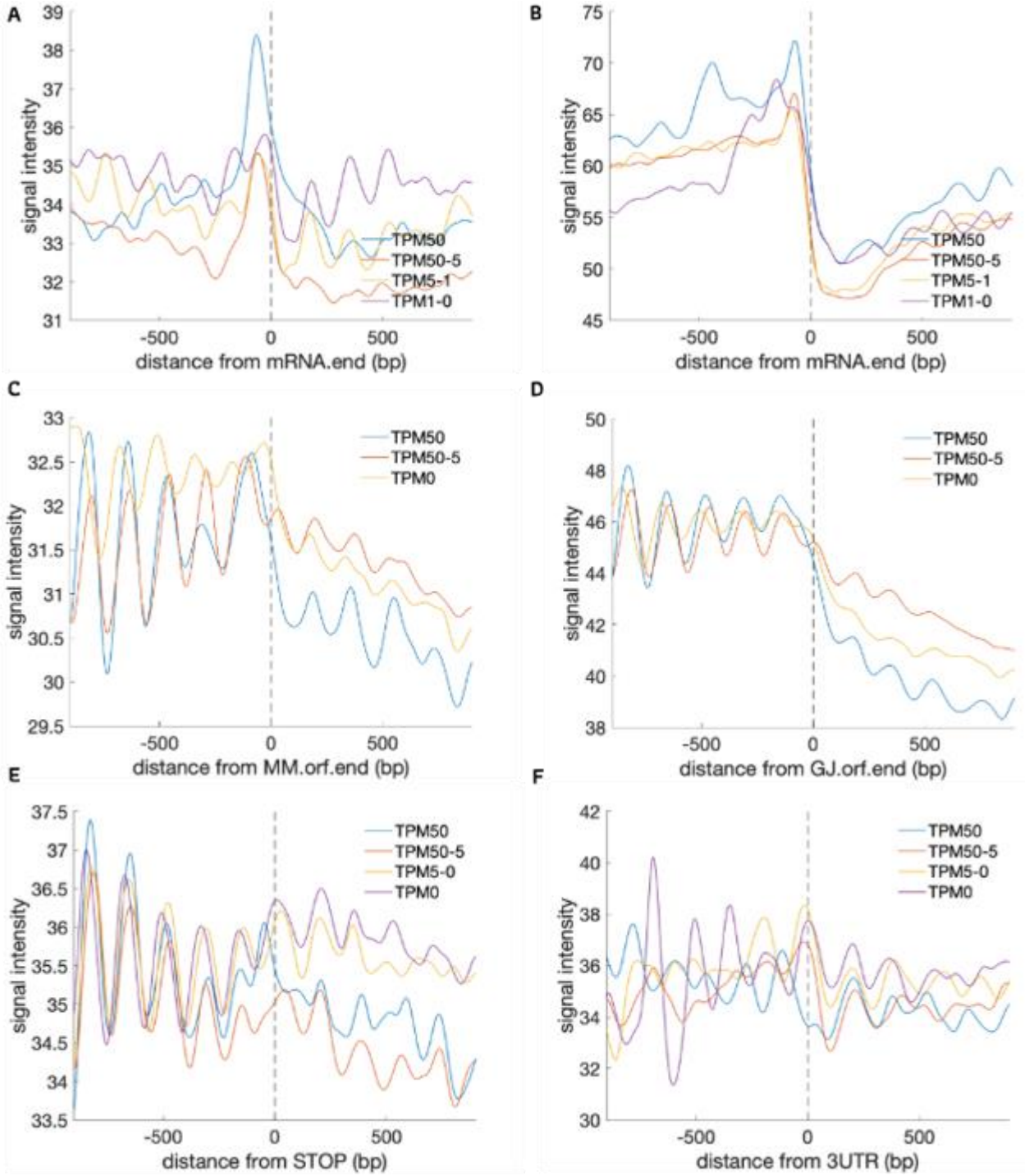

Figure S7: Nucleosome organization at stop codons/TTS *vs.* gene expression. Average (three biological replicates for each fungus/condition) nucleosome signal as a function of position (in base pairs) relative to the stop codon (and TTS for *F. graminearum*). TPM = Transcripts Per Million. **A:** *Leptosphaeria maculans* 'brassicae'; **B:** *Leptosphaeria maculans* 'lepidii'; **C:** *Botrytis cinerea* grown in malt-based medium; **D:** *Botrytis cinerea* grown in grape juice-based medium; **E:** *Fusarium graminearum*, ATG-centred; F. *Fusarium graminearum*, TSS-centred.

Université Paris-Saclay
Espace Technologique / Immeuble Discovery
Route de l'Orme aux Merisiers RD 128 / 91190 Saint-Aubin, France

552 **Table S1: Summary of sequencing and mapping metrics**

Species	Culture condition	Analysis type	Biological replicate	SRA accession number	Number of raw read pairs	Number of high-quality reads pairs*	Percentage of read pairs aligned to reference genome**
Fusarium graminearum	Liquid MS, 3 days	MNase-seq	Fg#1		38,25,6895	36,297,487	88.1
			Fg#2		38,122,290	36,271,479	86.6
			Fg#3		37,122,439	35,234,660	88.7
		mRNA-seq	Fg#1		34,215,941	31,728,079	98.3
			Fg#2		37,209,377	34,506,796	98.3
			Fg#3		34,108,125	31,674,167	92.7
***Leptosphaeria maculans* 'brassicae'**	Fries 7 days	MNase--seq	NDPS40		54,617,195	52,061,453	83.33
			NDPS41		60,172,292	57,137,679	83.80
			NDPS42		52,577,396	49,579,029	84.65
		mRNA-seq	NDPS13		47,088,366	43,637,526	95.49
			NDPS14		46,486,817	43,749,842	95.66
			NDPS15		51,131,206	48,088,521	95.75
***Leptosphaeria maculans* 'lepidii'**	Fries 7 days	MNase--seq	NDPS37		41,026,352	39,044,192	92.93
			NDPS38		54,531,542	51,203,357	90.55
			NDPS39		55,487,109	52,896,833	91.59
		mRNA-seq	NDPS10		52,095,284	43,637,526	96.58
			NDPS11		50,886,249	49,097,848	96.79
			NDPS12		50,800,169	49,014,722	96.73
		MNAse-seq	Bc#1		36,861,968	34,606,209	94.8

Université Paris-Saclay
Espace Technologique / Immeuble Discovery
Route de l'Orme aux Merisiers RD 128 / 91190 Saint-Aubin, France

Botrytis cinerea	Solid MM, 2 days	mRNA-seq	Bc#2		38,675,606	36,199,325	92.2
			Bc#3		36,684,375	34,437,003	95.0
	Solid GJ, 2 days		Bc#1		68,917,035	66,005,200	95.6
			Bc#2		38,025,909	36,154,916	96.0
			Bc#3		37,107,636	34,557,519	95.0
	Solid MM, 2 days		Bc#1		31,479,569	29,140,587	97.4
			Bc#2		38,826,778	35,931,380	97.6
			Bc#3		35,761,014	33,138,116	97.3
	Solid GJ, 2 days		Bc#1		37,895,154	35,310,616	91.0
			Bc#2		36,522,014	33,981,149	94.1
			Bc#3		37,506,128	34,587,157	94.3

*post quality trimming (see Materials and methods); **concordantly exactly one time

555 **Table S2: Nucleosome landscapes as a function of gene expression defining metrics**

Species	Gene expression category[1]	Position of +1 nucleosome (bp from ATG)	Position of NDR (bp from ATG)	Relative nucleosome signal amplitude[2]
***Leptosphaeria maculans* 'brassicae'**	Not expressed	25	-83	2.0
	Weakly expressed	21	-86	3.7
	Moderately expressed	18	-139	6.9
	Highly expressed	18	-131	8.7
***Leptosphaeria maculans* 'lepidii'**	Not expressed	75	-88	13.4
	Weakly expressed	58	-130	11.9
	Moderately expressed	53	-146	18.8
	Highly expressed	44	-183	23.3
Fusarium graminearum	Not expressed	1	-130	4.3
	Weakly expressed	18	-171	6.7
	Moderately expressed	17	-179	7.2
	Highly expressed	12	-163	10.1
***B. cinerea* grown in malt medium**	Not expressed	75	-90	3.7
	Weakly expressed	20	-99	4.0
	Moderately expressed	25	-104	4.4
	Highly expressed	18	-104	6.1
***B. cinerea* grown in grape juice medium**	Not expressed	147 (with shoulder at 67)	-108	9.6
	Weakly expressed	34	-118	9.5
	Moderately expressed	29	-159	12.3
	Highly expressed	**21**	**-153**	**15.4**
Species	**Gene expression category[1]**	**Position of +1 nucleosome (bp from ATG)**	**Position of NDR (bp from ATG)**	**Relative nucleosome signal amplitude[2]**

Université Paris-Saclay
Espace Technologique / Immeuble Discovery
Route de l'Orme aux Merisiers RD 128 / 91190 Saint-Aubin, France

***Leptosphaeria maculans* 'brassicae'**	Not expressed	25	-83	2.0
	Weakly expressed	21	-86	3.7
	Moderately expressed	18	-139	6.9
	Highly expressed	18	-131	8.7
***Leptosphaeria maculans* 'lepidii'**	Not expressed	75	-88	13.4
	Weakly expressed	58	-130	11.9
	Moderately expressed	53	-146	18.8
	Highly expressed	44	-183	23.3
Fusarium graminearum	Not expressed	1	-130	4.3
	Weakly expressed	18	-171	6.7
	Moderately expressed	17	-179	7.2
	Highly expressed	12	-163	10.1

[1]According to the average of TPM values for three biological replicates; not expressed: TPM = 0; weakly expressed: $0 < TPM \leq 5$; moderately expressed $5 < TPM \leq 50$; $50 < TPM$

[2]$\Delta nucl = |signal_{+1nucl} - signal_{NDR}$

Université Paris-Saclay
Espace Technologique / Immeuble Discovery
Route de l'Orme aux Merisiers RD 128 / 91190 Saint-Aubin, France

561

562

ARTICLE 2

A comparative analysis of the genome-wide histone modification maps in two subspecies of Leptosphaeria maculans showing contrasted genomic organization and different host specialization

Université Paris-Saclay
Espace Technologique / Immeuble Discovery
Route de l'Orme aux Merisiers RD 128 / 91190 Saint-Aubin, France

A comparative analysis of the genome-wide histone modification maps in two subspecies of *Leptosphaeria maculans* showing contrasted genomic organization and different host specialization

J.L. Soyer[1,2], C. Clairet[1,3], E.J. Gay[1,3], N. Lapalu[1], T. Rouxel[1], E.H. Stukenbrock[2,¥], I. Fudal[1,¥]

[1]UMR BIOGER, INRA, AgroParisTech, University of Paris-Saclay, 78850 Thiverval-Grignon, France

[2]Max Planck Institute for Evolutionary Biology, August-Thienemann-Str. 2, 24306 Plön, and Christian-Albrechts University of Kiel, Am Botanischen Garten 1-9, 24118 Kiel, Germany

[3]Université Paris-Sud, 91405, Orsay, France.

[¥]These authors contributed equally to this work.

Corresponding author: J.L. Soyer

E-mail: jessica.soyer@inra.fr

INTRODUCTION

Each year, hundreds of millions of tons of agricultural crops are devastated by plant pathogenic fungi or made unfit for consumption due to contamination by mycotoxins. Management strategies to control fungal infection mainly involve chemical control using fungicides or breeding for naturally resistant crop cultivars. Fungal plant pathogens have however proven capable of rapidly evolving resistance against implemented fungicides (Fisher *et al*., 2018) and to be able to overcome specific plant resistance genes within a few years (for instance in *Leptosphaeria maculans*; Rouxel & Balesdent, 2017) stimulating the need for the constant development of new control methods. Comprehending the determinants of their extreme adaptive abilities is a critical issue for the development of effective and sustainable control methods. In that respect, comparative and population genomic analyses have provided new insights into the evolutionary dynamics of fungal plant pathogens (e.g. Stukenbrock *et al.,* 2011; Grandaubert *et al.,* 2014; Sánchez-Vallet *et al.,* 2018). Notably, transposable elements (TE) have been shown to play a crucial role in organizing the genome of plant-pathogenic fungi. TEs are often found to be organized in clusters, compartmentalizing the genome into gene-rich regions and TE-rich regions (e.g. in *L. maculans* or in *Mycosphaerella fijiensis*; Rouxel *et al.,* 2011; Ohm *et al.,* 2012; Grandaubert *et al*., 2014). While the gene density in TE-rich regions is low, genes located in these regions have been shown to evolve faster than genes located in TE-poor regions (Croll & McDonald, 2012; de Jonge *et al.,* 2013). Interestingly, rapidly evolving genes in TE-rich regions have in many cases been identified as effector genes. Effectors are considered to be key elements of pathogenesis, allowing pathogens to circumvent host recognition, impede defence reactions and facilitate host invasion (Sánchez-Vallet A *et al.,* 2018). Plants have evolved strategies to recognize and counteract effectors, exposing them to a strong selection pressure by the host immune system (Stergiopoulos *et al*., 2007; Chuma *et al*., 2011; Daverdin *et al*., 2012; Rouxel and Balesdent, 2017). Indeed, in the course of the co-evolution between a pathogen and its host, the host has set up an active defence system allowing the direct or indirect recognition of some effector molecules, which activate the host immune system triggering

a local cell death, called hypersensitive reaction. Effectors that can be recognized by the host are called Avirulence proteins (Lo Presti *et al*., 2015). *Leptosphaeria maculans* 'brassicae' (hereinafter referred to as Lmb) belongs to the Dothideomycete class of Ascomycete fungi and is responsible for the stem canker of oilseed rape (*Brassica napus*). The life cycle of Lmb is complex and tightly associated to that of its host plant. Lmb displays a complex, hemibiotrophic life cycle, during which it alternates between different nutrition modes. It causes necrosis on different plant organs: leaves, more rarely on seedpods, and at the basis of the stem, causing lodging of the plant and yield losses (Rouxel and Balesdent, 2005). The most efficient method of disease control relies on the use of major resistance gene present in oilseed rape and other Brassica species. Although efficient, this control method is not sustainable, as Lmb is able to "break down" novel sources of genetic resistance rapidly (for review, Rouxel and Balesdent, 2017). So far, all described effector genes, encoding avirulence proteins, are highly expressed in the first seven days of leaf and cotyledon infection and are located in the middle of TE-rich regions (Gout *et al.*, 2006; Fudal *et al.*, 2007; Parlange *et al.,* 2009; Balesdent *et al.*, 2013; van de Wouw *et al*., 2014; Ghanbarnia *et al*., 2016; 2018; Plissonneau *et al.,* 2018; Petit-Houdenot *et al.,* 2019). Another set of putative effector genes are specifically expressed during stem infection and located in gene-rich regions (Gervais *et al*., 2017). Lmb belongs to the *L. maculans* / *Leptosphaeria biglobosa* species complex, gathering species with different host specialization and genome organizations. Within the species complex, the *L. maculans* species infecting oilseed rape, Lmb, is the only one having large regions of its genome enriched in TEs while other genomes have a low TE-content (~3% while the genome of Lmb has more than 30% of TEs; Rouxel *et al*., 2011; Grandaubert *et al*., 2014). In particular, the most closely related species to Lmb, *Leptosphaeria maculans* 'lepidii' (hereinafter referred to as Lml) is not pathogenic to oilseed rape but infects cruciferous weeds of the Lepidium genus (Mendes-Pereira *et al*., 2003). Interestingly, their genomes show a high level of macrosynteny, with only a few intra-chromosomal inversions, but differ in their TE content with Lmb having undergone a massive TE expansion 5 million years ago corresponding to the speciation date (Grandaubert *et al*., 2014). Invasion of TE in the genome of Lmb has shaped its genome, alternating TE-rich regions and gene-rich regions. On the contrary, the Lml genome has a low TE-content (~3%), with a homogeneous distribution along the chromosomes. There are increasing insights regarding how dynamic changes of DNA accessibility play fundamental role in adaptation of different individuals to abiotic and biotic stresses for instance (Gomes and Pelosi, 2013; Zogli and Libault, 2017). Importantly, evidence is accumulating that transcriptional reprogramming of effector genes or secondary metabolite gene clusters is tightly controlled by chromatin-based regulatory mechanisms as shown in Lmb, but also in distantly related fungi with different infection strategies (e.g. in *Fusarium graminearum*, *Epichloe festucae*, *L. maculans*; Connolly *et al*., 2013; Chujo and Scott, 2014; Soyer *et al*., 2014; Soyer *et al*., 2015a; Soyer *et al*., 2019). In Lmb, location of effector genes in TE-rich regions has an influence on their evolution under selection pressure and on regulation of their expression via deposition of a histone modification typical for constitutive heterochromatin, the tri-methylation of the lysine 9 of histone H3 (H3K9me3), as shown locally for two avirulence genes (*AvrLm1* and *AvrLm4-7*; Soyer *et al*., 2014). Lmb has a complex organization of its genome and involvement of the histone modification H3K9me3 has been demonstrated in the regulation of two avirulence genes. The most closely related species of Lmb, Lml, displays a well-conserved macrosynteny at the chromosomal level but devoid of the contrasted chromosomal landscapes typical of Lmb (Grandaubert *et al*., 2014). Comparative epigenomic analyses, at the intra- or inter-species levels, are very sparse and remain an

Université Paris-Saclay
Espace Technologique / Immeuble Discovery
Route de l'Orme aux Merisiers RD 128 / 91190 Saint-Aubin,
France

underexplored field of study, at least in fungi. In that context, the subspecies Lmb and Lml represent a promising model for the comparison of chromatin organization. We present here the first comparative epigenomic analysis in two closely related phytopathogenic fungi, in Lmb and Lml. We have performed ChIP-seq, during axenic culture, aiming at deciphering and comparing the distribution of three histone modifications, i.e. the di-methylation of the lysine 4 of histone H3, typical for euchromatin, and two histone modifications typical for heterochromatin, H3K9me3 and the tri-methylation of the lysine 27 of histone H3 (H3K27me3). We have investigated whether chromatin organization is conserved between Lmb and Lml notably by investigating whether orthologue genes are located in similar chromatin domains. The genome-wide histone modifications map generated *in vitro* also allowed investigating whether all known avirulence genes of Lmb are all located in heterochromatin domains and whether this pattern is conserved for all putative effector genes of Lmb and Lml.

MATERIAL AND METHODS

Fungal isolates

The isolate v23.1.3 of *L. maculans* 'brassicae' (hereinafter referred to as Lmb) and isolate IBCN84 of *L. maculans* 'lepidii' (hereinafter referred to as Lml) were used throughout the analyses (Rouxel *et al.,* 2011; Grandaubert *et al.,* 2014). Fungal cultures were maintained as described previously (Ansan-Melayah *et al*., 1995). For chromatin immunoprecipitation and transcriptomic analyses performed during *in vitro* growth, mycelium of Lmb and Lml were grown on V8 agar medium at 25°C for seven days then 10 plugs of mycelium were inoculated into 100 ml of Fries liquid medium in Roux bottle. Tissue was harvested after growing for 7 days at 25°C, immediately placed in liquid nitrogen until further used.

Chromatin immunoprecipitation and high-throughput sequencing

ChIP was performed on mycelium grown in Fries liquid culture after seven days, as described in Soyer *et al*. (2015b), with minor modifications. ChIP was performed on native material (without crosslinking) using antibodies targeting histone modifications H3K4me2 (Merck ref. 07-030), H3K9me3 (Active Motif, Carlsbad, CA, USA; ref. 39161), H3K27me3 (Active Motif, Carlsbad, CA, USA; ref. 39155). Three different ChIP (i.e. three biological replicates) were performed for each of the histone modifications. Libraries were prepared from all biological replicates, individually, according to the Illumina TruSeq protocol "Ultra Low Input DNA library". Libraries were sequenced on an Illumina HiSeq 2000 genome analyzer at the Max Planck Genome centre Cologne (Germany). Sequencing data are available under the SRA accession number xxxx.

Read mapping and identification of significantly enriched domains

Analysis of ChIP-seq datasets was performed as described in Schotanus *et al*. (2015). Quality of Illumina reads was analysed using FastQC (https://www.bioinformatics.babraham.ac.uk/projects/fastqc/). Based on results of this analysis, ten bp were trimmed from the 5' end. Processed reads were mapped on the reference genome of Lmb (Dutreux *et al*., 2018) or Lml (Grandaubert *et al*., 2014) using Bowtie2 (Langmead and Salzberg, 2012) with default parameters. Peak calling analysis was performed on each ChIP sequencing dataset, to identify significantly

Université Paris-Saclay
Espace Technologique / Immeuble Discovery
Route de l'Orme aux Merisiers RD 128 / 91190 Saint-Aubin,
France

enriched domains for either H3K4me2, H3K9me3 or H3K27me3, using RSEG (Song and Smith, 2011). A significant domain for any of the histone modification was considered only when the domain was identified in at least two out of the three biological replicates. The Integrative Genome Viewer (Thorvaldsdóttir *et al.,* 2013) was used to visualize location of each domains along genomes of Lmb and Lml according to other genome features (gene annotation, TE-annotation, GC content). Coverage of any of the histone modifications was assessed in 10 kb non-overlapping sliding windows along the supercontigs and correlation analyses, using Kendall's Ƭ correlation coefficient, was performed between biological replicates to check for reproducibility of the biological replicates. In order to assess whether H3K4me2-, H3K9me3- or H3K27me3-domains are significantly enriched in certain categories of genes (such as effector genes, secondary metabolite encoding genes), a Chi² test was applied to compare the expected proportion of a given category of genes across the entire genome to the observed distribution of the gene category in the H3K4me2-, H3K9me3- or H3K27me3-domains (Soyer *et al*., 2019). Enrichment was considered significant with a *P value* < 0.01; analyses were done in R (www.r-project.org).

RNA extraction, RNA-sequencing and expression analysis

Total RNA was extracted from mycelium grown for one week in Fries liquid medium as previously described (Fudal *et al*., 2007). For Lmb, RNA-seq libraries were prepared with the TruSeq Stranded mRNA kit (Illumina, San Diego, CA, USA) and was sequenced using 101 bp paired end reads on a HiSeq2000 Illumina sequencer. For Lml, the NEBNext Ultra Directional RNA Library Prep Kit for Illumina (cat. # E7420L New England BioLabs) was used to prepare RNA-seq libraries and sequencing was performed on an HiSeq 4000 Illumina using 50 paired end reads. Raw reads were then pre-processed with Trimmomatic (Bolger *et al*., 2014) to remove short reads (<30 bp) and eliminate sequencing adaptors. Cleaned reads were then mapped against each genome using STAR default parameters (Dobin and Gingeras, 2015). Sequencing data are available under the SRA accession number xxxx.

Identification of orthologues and annotation of genes encoding SSP in Lmb and Lml

Based on the new assembly and annotation available for the genome of Lmb (Dutreux *et al*., 2018), an updated repertoire of putative effector genes has been predicted. Therefore, to compare effector repertoires of Lmb and Lml, the same pipeline for the prediction of putative effector-encoding genes was applied to both species. Signal peptide and subcellular localization were predicted by SignalP version 4.1 and TargetP version 1.1 respectively. Transmembrane domains were predicted by TMHMM version 2.0. The predicted secretome contains all proteins which have at most one transmembrane domain and either a predicted signal peptide or an extracellular localization. The final effector repertoires were created by applying a size cut-off of 300 amino acid on the predicted secretome. In parallel, EffectorP version 1.0 was used on the predicted secretome and, for Lml, four proteins were predicted as effector with a size superior to 300 amino-acid, these four proteins were added to the SSP set. This predicted a repertoire of 1,080 and 892 SSP-encoding genes respectively for Lmb and for Lml.

The genome of Lmb encodes 13,126 proteins and that of Lml encodes 11,272 proteins (Dutreux *et al.,* 2018; Grandaubert *et al.,* 2014). In order to find orthologues between Lmb and Lml, proteins of these two species were groups using OrthoFinder with default parameters (Emms and Kelly, 2015).

Université Paris-Saclay
Espace Technologique / Immeuble Discovery
Route de l'Orme aux Merisiers RD 128 / 91190 Saint-Aubin, France

GO analysis and enrichment analysis

GO annotation of the Lmb and Lml encoding genes were retrieved from Dutreux *et al*. (2018) and Grandaubert *et al*. (2014) respectively. Gene Ontology (GO) term enrichment analysis of the H3K4me2-, H3K9me3- and H3K27me3-associated genes was performed with the plug-in Biological networks Gene ontology (BinGo; v3.0.3) of the cytoscape software (Shannon *et al*., 2003). List of genes submitted to BINGO were considered as significantly enriched for a given GO term with an associated a False Discovery Rate ≤ 0.01 for the biological processes.

A Chi² test, or a Fisher's exact test for small sized-population, were applied to identify significant enrichment of H3K4me2-, H3K9me3- or H3K27me3-domains for certain categories of genes: the expected proportion of a given category of genes across the entire genomes of Lmb or Lml was compared to the observed distribution of the gene category in the H3K4me2-, H3K9me3- or H3K27me3-domains. Enrichment was considered significant with a *P value* < 0.01. All analyses were done in R (www.r-project.org).

RESULTS

Identification of H3K4me2-, H3K9me3- and H3K27me3-enriched domains in the genomes of Lmb and Lml during axenic growth

In order to get a genome-wide view of the epigenomic landscapes in the genomes of Lmb and Lml during axenic growth, we have performed a ChIP-seq experiment using antibodies against histone modifications H3K4me2, H3K9me3 and H3K27me3 (**Table S1**). Mapping of the sequencing data was followed by identification of the significantly enriched domains, for any of the histone modifications targeted, in the genomes of Lmb and Lml (see Materials and Methods). Three different precipitation experiments were done for each histone modification to assess the robustness of the domains identified with RSEG (Song and Smith, 2011). Domains identified for one of the H3K9me3 replicate performed for Lml were inconsistent with domains identified for this modification with the two other replicates (**Table S2**) and was therefore not considered for subsequent analyses. For all other biological replicates aiming at identifying H3K4me2-, H3K9me3- and H3K27me3-domains in the genomes of Lmb and Lml, location of domains was consistent (**Table S2**, **S3**; Kendall's T >0.74, P <2.2.10^{-16}). Hence, for subsequent analyses, domains were considered as being significantly enriched when identified with at least two out of the three replicates, except for H3K9me3-domains of Lml for which domains were considered enriched when identified with both replicates kept for analysis. Based on the coordinates of the location of H3K4me2-, H3K9me3- or H3K27me3-domains, the number of bases associated with any of the three histone modifications was assessed, for each genome, in 1 kb sliding-windows. In the genomes of Lmb and Lml, the proportion of H3K4me2 and H3K27me3 was similar in both species while proportion of H3K9me3 in the genome of Lmb was higher compared to that of Lml (33% and 4% respectively for Lmb and Lml); (**Tables S4, S5**).

TE-rich domains are associated with H3K9me3 while gene-rich regions are enriched in H3K4me2

In the genomes of Lmb and Lml, H3K4me2 and H3K9me3 domains are exclusive and not associated with the same genomic regions (Kendall's T: -0.57 and -0.16, P < 2.2.10^{-16} for respectively Lmb and Lml; **Figure S1**; **Tables S6** and **S7**). A positive correlation was measured between TEs and H3K9me3-domains (Kendall's T: 0.87 and 0.68, P

Université Paris-Saclay
Espace Technologique / Immeuble Discovery
Route de l'Orme aux Merisiers RD 128 / 91190 Saint-Aubin,
France

< $2.2.10^{-16}$ for respectively Lmb and Lml; **Figure 1A**, **1C**; **Figure S1**; **Table S6** and S7) and between CDS and H3K4me2 (Kendall's *T*: 0.55 and 0.25, *P* < $2.2.10^{-16}$ for respectively Lmb and Lml; **Figure 1A, 1C; Figure S1; Tables S6** and **S7**) in both genomes. In the genome of Lmb, a weak correlation was measured between CDS and H3K27me3 domains (Kendall's *T*: 0.12, *P* < $2.2.10^{-16}$) while no clear pattern regarding location of H3K27me3 was identified, on the genome-wide scale, in the genome of Lml (**Figure S1; Tables S6, S7**). In accordance with the association of H3K9me3 with TE, the proportion of H3K9me3 is consistent with the TE-content of both genomes (36% and 2.8% TE in the genomes of Lmb and Lml, respectively). The high TE-content in the Lmb genome has an impact at the structural level, as large AT-isochores corresponding to stretches of TE-rich regions and GC-isochores alternate along the genome while it is not the case in the Lml genome, with a homogeneous repartition of the TEs (example in **Figure 2**). Hence, while the median size of the domains were similar in both genomes, Lmb genome displays extremely large H3K9me3-domains, with a size up to 230 kb, while the maximum size for the H3K9me3-domains is 12 Kb in the genome of Lml (**Figure 3**).

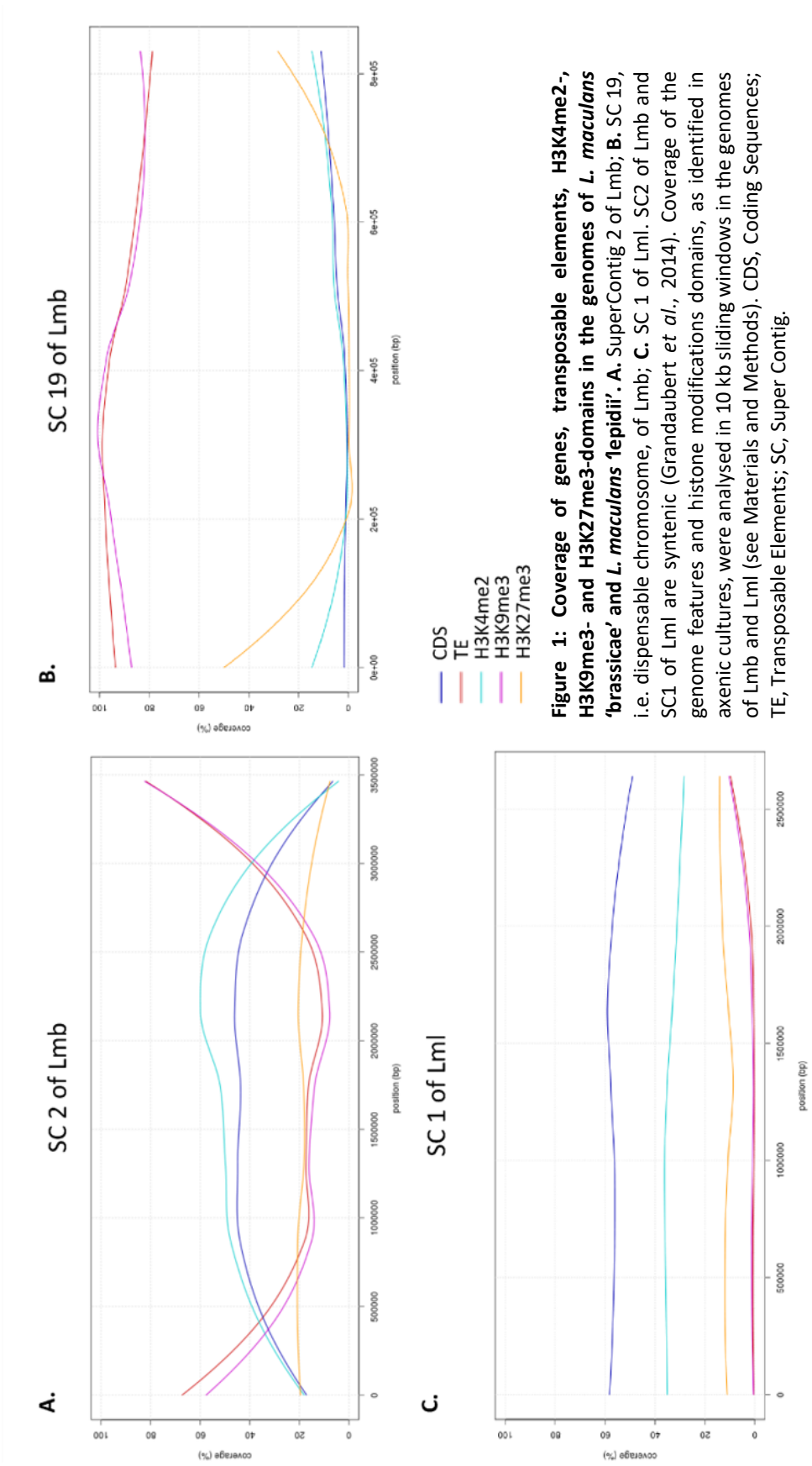

Figure 1: Coverage of genes, transposable elements, H3K4me2-, H3K9me3- and H3K27me3-domains in the genomes of *L. maculans* 'brassicae' and *L. maculans* 'lepidii'. A. SuperContig 2 of Lmb; **B.** SC 19, i.e. dispensable chromosome, of Lmb; **C.** SC 1 of Lml. SC2 of Lmb and SC1 of Lml are syntenic (Grandaubert *et al.*, 2014). Coverage of the genome features and histone modifications domains, as identified in axenic cultures, were analysed in 10 kb sliding windows in the genomes of Lmb and Lml (see Materials and Methods). CDS, Coding Sequences; TE, Transposable Elements; SC, Super Contig.

Université Paris-Saclay
Espace Technologique / Immeuble Discovery
Route de l'Orme aux Merisiers RD 128 / 91190 Saint-Aubin, France

188

189

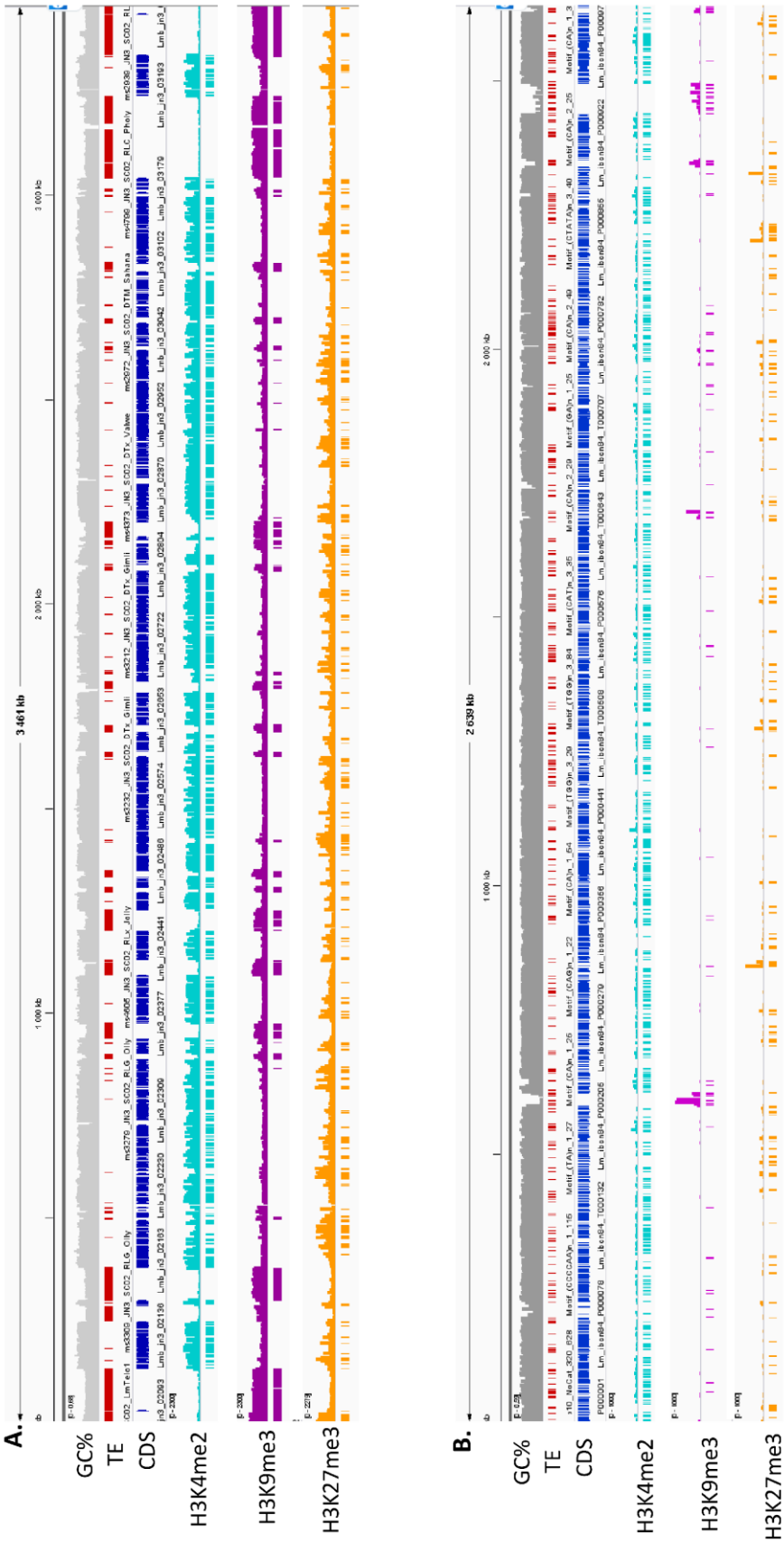

Figure 2. Genome of *L. maculans* 'brassicae' harbors large TE-rich, H3K9me3-domains compared to *L. maculans* 'lepidii'. A. Example of SC 2 of Lmb; **B.** SC 1 of Lml. ChIP-seq was performed with antibodies targeting H3K4me2 (cyan), H3K9me3 (purple) or H3K27me3 (orange); rectangles indicate location of significantly enriched domains regions for were identified with RSEG (Song and Smith, 2011) and the number below the rectangles indicate the number of biological replicates for which the domain was identified as significantly enriched (Materials and Methods). GC%, percentage of GC along the SC; TE, Transposable element; H3K4me2, di-methylation of lysine 4 of histone H3; H3K9me3, tri-methylation of lysine 9 of the histone H3; H3K27me3, tri-methylation of the lysine 27 of histone H3.

Université Paris-Saclay
Espace Technologique / Immeuble Discovery
Route de l'Orme aux Merisiers RD 128 / 91190 Saint-Aubin, France

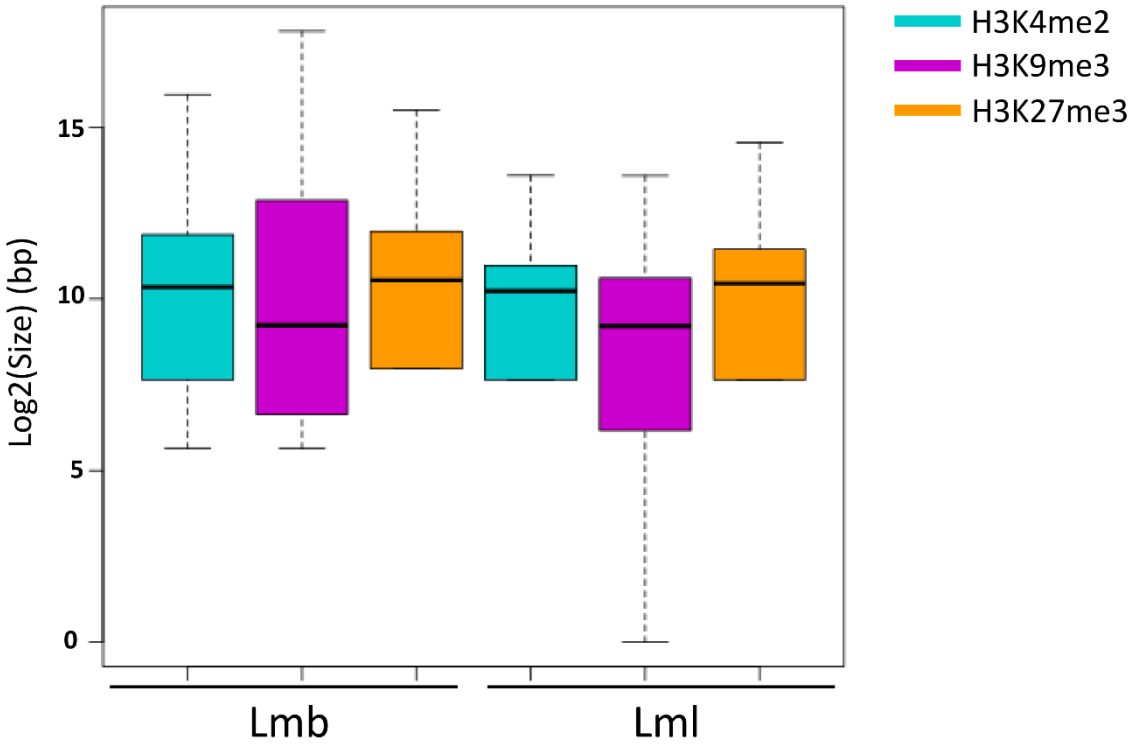

Figure 3: Size of the H3K4me2-, H3K9me3-, H3K27me3-domains in the genomes of *Leptosphaeria maculans* 'brassicae' (Lmb) and *L. maculans* 'lepidii' (Lml). Log2 of the Size of the domains was estimated based on the coordinates of the location of the domains, identified using RSEG (Song and Smith, 2011). Blue: H3K4me2; Purple: H3K9me3; Orange: H3K27me3. Lmb, *L. maculans* 'brassicae'; Lml, *L. maculans* 'lepidii'.

In the genome of Lmb, a dispensable chromosome, carrying the avirulence gene *AvrLm11*, has been identified (Leclair *et al*., 1996; Balesdent *et al*., 2013; Grandaubert *et al*., 2014), while no such accessory chromosomes was identified in the genome of Lml. The dispensable chromosome is enriched in TEs compared to the rest of the genome (35% of TEs in the core genome and 93% of TEs in the dispensable chromosome). Consistently, a strong enrichment in H3K9me3 is observed on the dispensable chromosome (32% in the core genome and 90% on the dispensable chromosome), with only a few H3K4me2- and H3K27me3-domains (**Figure 1A** and **1B**; **Figure 2**). Contrary to the genome of Lml which is not fully assembled with large gaps remaining in its genome sequence (Grandaubert *et al*., 2014), the complete assembly of the Lmb genome allows analysis of the sub-telomeric regions (Dutreux *et al*., 2018). Sub-telomeric regions of the Lmb genome, corresponding to large repeat sequences, are highly associated with H3K9me3 and H3K27me3 overlap with H3K9me3 in the telomeric regions, while they do not on chromosome arms (**Figure 1A** and **Figure 2**).

Université Paris-Saclay
Espace Technologique / Immeuble Discovery
Route de l'Orme aux Merisiers RD 128 / 91190 Saint-Aubin, France

H3K4me2- and H3K27me3-domains shelter genes involved in distinct activities

Based on the location of H3K4me2-, H3K9me3- and H3K27me3-domains in the genomes of Lmb and Lml during axenic cultures, genes associated with any of these modifications were identified. Overall, the number of genes associated with any of the histone post-translational modification is similar in both species with more than 50% of the predicted genes associated with H3K4me2, ~14% of the genes associated with H3K27me3 and only a few genes associated with H3K9me3 (**Figure 4**).

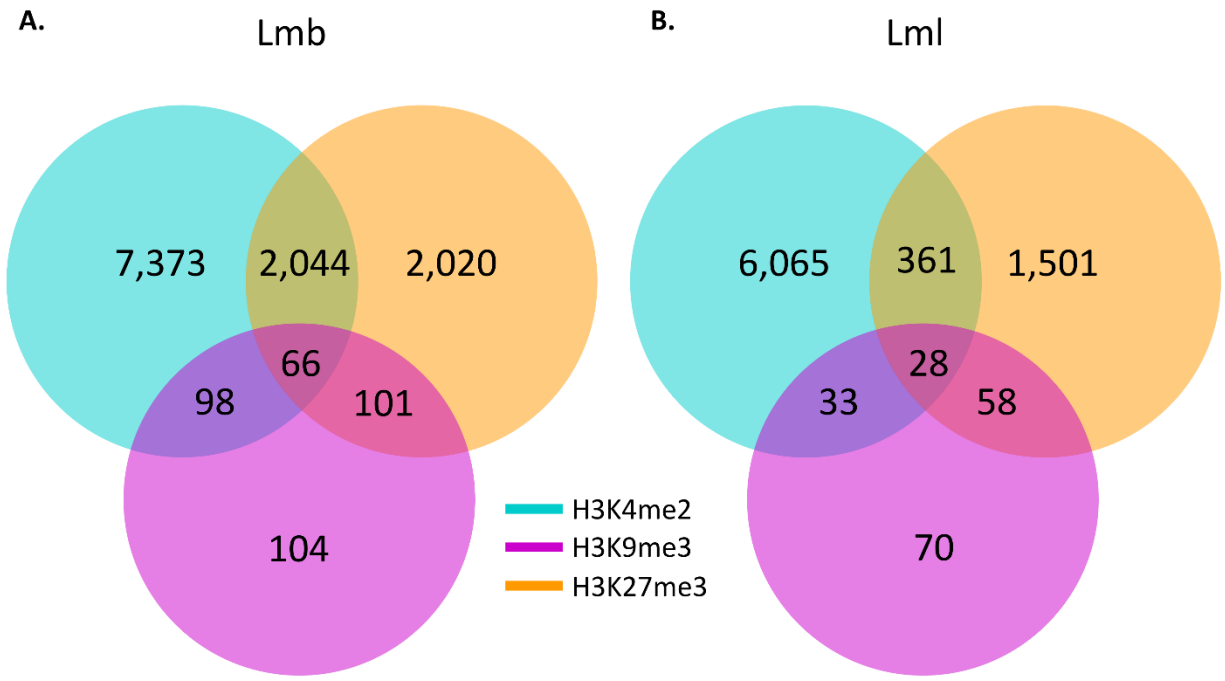

Figure 4: Number of genes associated with H3K4me2, H3K9me3 or H3K27me3 during axenic growth in A. *Leptosphaeria maculans* 'brassicae' (Lmb) and B. *L. maculans* 'lepidii'. Location of histone modifications in the genome of Lmb and Lml were identified using RSEG (Song and Smith, 2011). Blue: H3K4me2; Purple: H3K9me3; Orange: H3K27me3. Genes were considered as associated with any of the histone modifications when at least one pb of the gene was found within the borders of the domain. Lmb, *L. maculans* 'brassicae'; Lml, *L. maculans* 'lepidii'.

In the genome of Lmb, a GO annotation was assigned to 5,076 genes (i.e. 39% of the predicted genes). 3,276 genes located within a H3K4me2-domain had a GO annotation (i.e. 44% of the genes located in a H3K4me2-domain) while 572 genes located in a H3K27me3-domain (i.e. 28% of the genes associated with H3K27me3) and none of the genes located in a H3K9me3-domain had an annotation. This shows that genes located in heterochromatin are enriched in genes with no functional annotation (X^2 test, $P < 2.2.10^{-16}$). H3K27me3-associated genes mainly encode proteins of unknown function and only a few GO terms were identified among genes associated with this fraction of the genome. Nevertheless, these genes are significantly enriched in GO terms involved in carbohydrate metabolic process (GO:0005975; 82 genes associated with H3K27me), oxydo-reduction process (GO:0055114; 149 genes) and transmembrane transport (GO:0055085; 104 genes), ($P \leq 0.01$); (**Table S8**). This suggests that genes associated with H3K27me3 *in vitro* might encode proteins involved in pathogenesis-related function such as secretion of molecules, degradation of organic compounds, and defence against oxydo-reductant stress. On the contrary, genes associated with H3K4me2 display a wide variety of annotated function involved in primary metabolism (**Table S9**).

Université Paris-Saclay
Espace Technologique / Immeuble Discovery
Route de l'Orme aux Merisiers RD 128 / 91190 Saint-Aubin, France

In the genome of Lml, 3,725 genes had a GO annotation (i.e. 33% of the annotated genes). As for Lmb, genes associated with heterochromatin *in vitro* were enriched in genes with no GO annotation as only 19% of the genes associated with H3K27me3 and none of the genes associated with H3K9me3 had a GO annotation (X^2 test, $P < 2.2.10^{-16}$). On the contrary, H3K4me2-domains were enriched in genes having a GO annotation (42% of these genes). As it is the case for genes associated with H3K4me2 in Lmb, genes associated with H3K4me2 are also enriched in genes having a GO annotation involved in primary metabolism and basic cellular functions, such as translation (GO:0006412; 206 genes) or cellular protein metabolic process (GO: 44267; 477 genes); (**Table S10**). As for Lmb, only a few G0 annotation enrichments was detected for genes associated with H3K27me3-domains *in vitro*. Only one GO enrichment was found in common with Lmb, i.e. carbohydrate metabolic process (GO:0005975; 41 genes). Apart from that, all other enrichments were redundant in terms of definition: response to chemical (GO: 42221; 20 genes), response to nitrogen compound (GO:1901698; 10 genes), response to organophosphorus (GO: 46683, 10 genes) and others. All these GO terms indicate an enrichment in genes involved in a change of state or activity of an organism (in terms of movement, secretion, enzyme production, gene expression, etc.) as a result of different chemical stimuli. For instance, organophosphorus compounds are toxic cholinesterase inhibitors. Although most GO enrichments found among sets of genes associated with H3K27me3 in Lmb and Lml do not overlap, both types of enrichments suggest that H3K27me3-associated genes might be involved in a stress response mechanism, whether it might be an infection-related process or a defence against toxic compounds, or both. On the contrary, in both organisms, proteins encoded by the genes sheltered in H3K4me2-domains in Lmb and Lml are involved in similar biological processes involved in maintenance of basic cellular functions.

Heterochromatin domains are enriched in effector genes and secondary metabolite-encoding genes

In Lmb, so far, all cloned avirulence genes, which are highly expressed during asymptomatic infection of oilseed rape (at seven days post infection), are located within TE-rich regions of the genome. We assessed whether the particular location of known avirulence genes within TE-rich regions is also associated with a location in domains enriched for histone modifications typical for heterochromatin and whether this is a conserved feature for different sets of genes encoding pathogenicity-related proteins. In the genome of Lmb, 1,080 genes encoding effectors (including known avirulence genes; i.e. 8.2% of the genes predicted in the genome) were predicted (Dutreux *et al*., 2018; Gay *et al*., in prep.). In the genome of Lmb, 2,478 genes (i.e. 12% of the genes) are associated with TE-rich regions (located within a 2 kb distance of a TE sequence), including 289 genes encoding effectors. Hence, while a new prediction of the effector repertoire was performed based on the new assembly of the Lmb genome, TE-rich regions are significantly enriched in effector genes, as already shown by Rouxel *et al*. (2011; X^2 test, $P = 9.6.10^{-16}$). Similarly, H3K9me3- and H3K27me3-associated genes are significantly enriched in genes encoding effectors, as effector genes represent respectively 36% and 14% of the genes associated with these histone modifications *in vitro* (X^2 test, $P = 9.6.10^{-16}$; **Table 1**).

Université Paris-Saclay
Espace Technologique / Immeuble Discovery
Route de l'Orme aux Merisiers RD 128 / 91190 Saint-Aubin, France

On the contrary, H3K4me2-associated genes contain significantly less effector genes than the rest of the genome (i.e. 6% of the genes located in H3K4me2-domains encode putative effectors; **Table 1**). In the genome of Lml, the proportion of effector genes is similar to that of Lmb (892 of the genes encode for putative effectors, i.e. 7.9% of the genome). Likewise, TE-rich regions, H3K9me3- and H3K27me3-domains are significantly enriched in putative effector genes while H3K4me2-domains are significantly deprived in such genes compared to the rest of the genome (**Table 1**).

Table 1. Number of effector genes located in different genomic compartments in *L. maculans* 'brassicae' and *L. maculans* 'lepidii'

		genome	TE-associated genes[a]	H3K4me2-domains[b]	H3K9me3-domains[b]	H3K27me3-domains[b]	H3K9+H3K27me3-domains[b]
Lmb	number of genes	13,047	2,478	7,373	104	2,020	101
	number of effectors	1,080	289	433	38	286	24
	proportion	$8.2.10^{-2}$	$1.2.10^{-1}$	$5.8.10^{-2}$	$3.6.10^{-1}$	$1.4.10^{-1}$	$2.4.10^{-1}$
	P value[c]	-	$9.6.10^{-16}$	$6.7.10^{-14}$	$2.2.10^{-16}$	$2.2.10^{-16}$	$1.6.10^{-8}$
Lml	number of genes	11,273	641	6,065	70	1,501	58
	number of effectors	892	79	266	14	217	18
	proportion	$7.9.10^{-2}$	$1.2.10^{-1}$	$4.4.10^{-2}$	2.10^{-1}	$1.45.10^{-1}$	$3.1.10^{-1}$
	P value[c]	-	$3.5.10^{-5}$	$2.2.10^{-16}$	$1.8.10^{-4}$	$2.2.10^{-16}$	$6.9.10^{-11}$

[a]Genes located up to 2 kb upstream or downstream of a transposable element sequence;
[b]Genes located in a H3K4me2-, H3K9me3-, H3K27me3- or H3K9me3/H3K27me3-domain *in vitro*;
[c]A X^2 test was applied to compare proportion of effector genes in the genome and in the genomic compartment analysed (Materials and Methods).

The genome also encodes secondary metabolites, synthesised by clusters encoding PKS/NRPS (Polyketide Synthases and Non-Ribosomal Peptide Synthases). Twenty-nine such genes have been predicted in Lmb (Rouxel *et al*., 2011; Elliott *et al*., 2013; Grandaubert *et al*., 2014). Among them, only one has been detected so far to be highly up-regulated at 7 days post-infection, and located within AT-isochores of the genome of Lmb, i.e. *pks5* involved in the synthesis of the abscisic-acid, along with the other genes of this cluster (Darma *et al*., 2019). Regarding the twenty-nine genes encoding PKS/NRPS. For Lmb, H3K27me3-domains are enriched in such genes as 68% are located in such domains (20 PKS/NRPS; Fisher's exact test, $P= 1.3.10^{-7}$). This included the cluster encoding abscisic acid, embedded in the middle of TEs, and for which five genes of the cluster are located in a H3K27me3-domain, including the transcription factor regulating the cluster and the PKS, while three other genes of the cluster are associated with both H3K9me3 and H3K27me3 (our results; Darma *et al*., 2019). The gene encoding the sirodesmin, having antibacterial and antifungal properties (SirP; Gardiner *et al*., 2004; Elliott *et al*., 2007) is also located in a H3K27me3 domain, while not located in the middle of an AT-isochore; this gene is expressed during the infection of oilseed rape stem (Elliott *et al*., 2007). The PKS gene encoding phomenoic acid, *PKS7*, highly expressed during axenic culture (Elliott *et al*., 2013), is located in a GC-isochore and associated with H3K27me3. In the genome of Lml, 25 genes are predicted as PKS/NRPS

Université Paris-Saclay
Espace Technologique / Immeuble Discovery
Route de l'Orme aux Merisiers RD 128 / 91190 Saint-Aubin, France

(Grandaubert *et al*., 2014). Similarly to Lmb, H3K27me3-domains of the genome of Lml are enriched in PKS/NRPS encoding genes (11 PKS/NRPS; Fisher's exact test, $P = 1.7.10^{-4}$).

Heterochromatin domains of the *L. maculans* 'brassicae' and *L. maculans* 'lepidii' genomes shelter subspecies-specific genes

Comparative genomic analyses of the Lmb and Lml genes identified that 7,393 genes were conserved between both species using Orthofinder (Emms and Kelly, 2015). We assessed location of these conserved genes and identified that H3K4me2-domains are enriched in genes conserved between Lmb and Lml (66 and 64% of the conserved genes respectively in Lmb and Lml; X^2 test, $P < 2.2.10\text{-}16$). On the contrary, H3K27me3- and H3K9me3-domains are significantly enriched in genes which are not conserved between Lmb and Lml (genes conserved between both species represent less than 1% of the genes located in these domains; X^2 test, $P < 2.2.10^{-16}$).

Regarding effectors, 1,080 and 892 genes in the genome of respectively Lmb and Lml encode putative effectors, among which 274 were conserved between both sub-species (i.e. genes having an orthologue in the sister species and being predicted as a putative effector). Hence, more than two third of their effector repertoire is specific, as already described (Grandaubert *et al.,* 2014) but confirmed here with a new prediction of this repertoire. Effector genes of both species are less conserved than the rest of the predicted genes (X^2 test, $P < 2.2.10^{-16}$) and H3K9me3- and H3K27me3-domains are enriched in sub-species-specific effector genes. Five genes encoding avirulence proteins located in the middle of a large TE-rich region of Lmb are also conserved in Lml. Four out of these five genes are located in a sub-telomeric region, including three neighbour genes (ID *Lmb_jn3_05822*, *Lmb_jn3_05823*, *Lmb_jn3_05824*) and consistently associated either with H3K9me3, H3K27me3 or with both histone modifications. These three putative effectors are conserved, although inverted, in Lml and are also in located a sub-telomeric region, and associated with H3K27me3. One avirulence gene of Lmb, AvrLm10A, is conserved in Lml. In Lmb, this gene is located in a sub-telomeric region and associated with a H3K9me3-domain. In Lml, the AvrLm10A orthologue is not located in a sub-telomeric region but is associated with H3K27me3.

All cloned Avirulence genes of *L. maculans* 'brassicae' are located in H3K9me3-domains *in vitro*

H3K4me2 is typically considered as permissive for gene expression while H3K9me3 and H3K27me3 are considered as inducing gene silencing. We performed a genome-wide transcriptomic analysis *in vitro*, in parallel to the analysis of histone modifications, in order to determine the role of histone modifications on the control of gene expression and whether that role was conserved between Lmb and Lml. In Lmb, 11,525 genes (i.e. 88% of the predicted genes) are expressed during *in vitro* growth (i.e. FPKM ≥ 2). Considering the 100 most expressed genes during axenic culture, 91% of them are associated with H3K4me2 while five are located within a H3K27me3-domain and none in a H3K9me3-domain. This observation was confirmed on the genome-wide scale as H3K4me2-domains are enriched in gene expressed (7,191 of the genes associated with H3K4me2 are expressed; $P < 2.2.10^{-16}$) during axenic culture while H3K9me3- and H3K27me3-domains are enriched in genes silenced *in vitro* (56 and 1290 of the genes located respectively in a H3K9me3- or a H3K27me3-domain are expressed, $P < 2.2.10^{-16}$); (**Figure 5**). The influence of the histone modifications on gene expression is similar in Lml as, among the 100 most expressed genes during axenic

Université Paris-Saclay
Espace Technologique / Immeuble Discovery
Route de l'Orme aux Merisiers RD 128 / 91190 Saint-Aubin,
France

culture, 71 are located within a H3K4me2-domain while five are located in a H3K27me3-domain. This pattern is confirmed on the genome-wide scale, as among the 7,735 genes expressed *in vitro* by Lml (i.e. 69% of the predicted genes), H3K4me2-domains are enriched in genes expressed (5,472 of the genes expressed during axenic culture are located in a H3K4me2-domain; $P < 2.2.10^{-16}$). On the contrary, H3K9me3- and H3K27me3-domains are enriched in genes which are silenced during axenic culture (17 and 403 genes expressed *in vitro* are located respectively in a H3K9me3- or a H3K27me3-domain *in vitro*; $P < 2.2.10^{-16}$). This transcriptomic analysis confirmed, in both species, that genes located in a H3K4me2-domain were more likely to be expressed while H3K9me3- and H3K27me27-domains are enriched in silent genes.

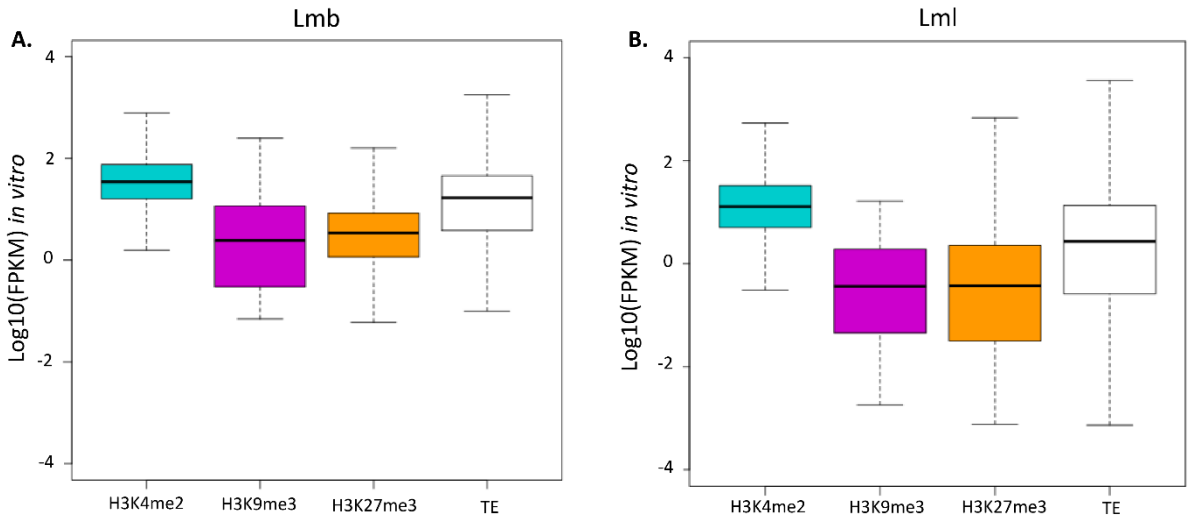

Figure 5: Genes associated with heterochromatin are less expressed than genes associated with euchromatin in the genomes of *L. maculans* 'brassicae' and *L. maculans* 'lepidii'. Location of histone modifications in the genome of Lmb and Lml were identified using RSEG (Song and Smith, 2011), during axenic culture. RNA-seq was performed from Lmb or Lml grown one week in FRIES media (see Materials and methods). Blue: H3K4me2; Purple: H3K9me3; Orange: H3K27me3; White: genes located within a 2 kb distance of a transposable element. Lmb, *L. maculans* 'brassicae'; Lml, *L. maculans* 'lepidii'.

So far, pathogenicity assays are not feasible with Lml, hence transcriptomic data *in planta* are not available. Considering Lmb, expression profile of avirulence genes is well documented during infection of oilseed rape cotyledons, showing that these genes are not, or lowly, expressed *in vitro* and highly expressed during infection of oilseed rape cotyledons, with a peak of expression seven days post-infection (Rouxel *et al.*, 2011). All the avirulence genes cloned so far in Lmb are located in a H3K9me3-domain *in vitro* consistently with the fact that these genes are located in TE-rich compartments of the genome in Lmb. Besides these avirulence genes expressed during the early stages of oilseed rape infection, 307 putative effector genes expressed during stem infection were recently described (Gervais *et al.*, 2017). A new version of the Lmb genome is now available, with a new annotation and a new effector gene prediction (Dutreux *et al.*, 2018; Gay *et al.*, in prep.), downsizing this repertoire of putative 'late' effectors to 86 candidates. In contrast to avirulence genes, most of these 'late' effector genes are located in GC-isochores, as already observed by Gervais *et al.* (2017). Only 19 of these genes are located in H3K4me2-domains while 49 are located in a H3K9me3- or H3K27me3-domain ($P < 2.10^{-5}$). Altogether, these data show that, independently of the infection stage, putative effector genes are enriched in either H3K9me3 or H3K27me3 *in vitro*.

Université Paris-Saclay
Espace Technologique / Immeuble Discovery
Route de l'Orme aux Merisiers RD 128 / 91190 Saint-Aubin, France

DISCUSSION

We present here the first comparative analysis of the location of three different histone modifications, typically associated with either euchromatin or heterochromatin, at the genome-wide scale, in two closely related phytopathogenic fungi displaying considerable differences in terms of genomic organisation as well as host range. Aim of this analysis was to question whether different genome organisations would shape the underlying associated epigenomic landscape and to identify conserved, or unique, features.

As for other fungi, domains enriched in H3K4me2, indicative of euchromatin regions, and domains enriched in H3K9me3, indicative of a heterochromatin region, are mutually exclusive in the genomes of Lmb and Lml. This was also shown for instance in *Neurospora crassa*, *Fusarium fujikuroi*, and *Zymoseptoria tritici* (Smith *et al*., 2008; Jamieson *et al*., 2013; Wiemann *et al*., 2013; Schotanus *et al*., 2015). Regarding other features, such as association of repeats with H3K9me3 or H3K27me3 or organization of the accessory chromosomes, there appears to be more and more exceptions as data are gathered. So far, H3K9me3 has always been found associated with transposable elements, whether or not sequences of transposable element span very large domains, as it is the case in Lmb (e.g. in *Z. tritici*; *Schizosaccharomyces pombe*, *F. fujikuroi*; Cam *et al*., 2005; Schotanus *et al*., 2015; Wiemann *et al*., 2013). In sub-telomeric regions of Lmb, H3K9me3 and H3K27me3-domains overlap over repetitive sequences, which is a classic feature observed also in *N. crassa* or *Z. tritici* (Smith *et al*., 2008; Connolly *et al*., 2013; Jamieson *et al*., 2013; Schotanus *et al*., 2015). Only H3K27me3 has been shown to locate in sub-telomeric areas in *F. graminearum* although a genome-wide analysis of the location of H3K9me3 (although present in its genome) has not been performed yet for this fungus (Connolly *et al*., 2013). In the genomes of Lmb and Lml, TEs consist in heterochromatin regions enriched in H3K9me3 and contrary to sub-telomeric regions, no enrichment of H3K27me3 was detected associated with TEs on chromosomal arms. This is dissimilar to the organization of TE-rich regions in *Z. tritici*, enriched in both heterochromatin modifications (Schotanus *et al*., 2015). The situation is also different for *Fusarium oxysporum*, in which most TE sequences are embedded in a H3K27me3-domain. It is worth noting that location of H3K9me3 in the genome of this fungus has not been investigated yet (Fokkens *et al*., 2018). One can envision that, once investigated, the situation of the transposons of *F. oxysporum* might be identical to those of *Z. tritici*. In *Z. tritici*, the overlap between H3K9me3 and H3K27me3 in TE-rich regions was postulated to be a consequence of the lack of cytosine DNA methylation (Schotanus *et al*., 2015), as the *dim-2* encoding gene is inactivated due to mutations caused by the RIP mechanisms (Dhillon *et al*., 2010). In the genome of Lmb, almost no cytosine DNA methylation was detected as well (Bewick *et al*., 2019), nevertheless the two heterochromatin modifications do not overlap in TE-rich regions. Therefore, overlapping of H3K9me3 and H3K27me3 observed in TE-rich regions of *Z. tritici* cannot be explained by a genome-wide lack of DNA methylation. In other fungi, such as *Aspergillus nidulans*, no H3K27me3 has been detected while H3K4me3 is associated with gene-rich regions and H3K9me3 flanks sub-telomeric regions (Gacek-Matthews *et al*., 2016; Freitag, 2017). For some other phytopathogenic fungi, such as *Botrytis cinerea*, epigenomic analysis have been set up and data from western blot analysis have helped detect H3K9me3 and H3K27me3 but a precise location is lacking so far (Schumacher *et al*., 2019). All these data tend to indicate that epigenomic analyses are of a major interest for the scientific community interested in plant-pathogenic fungi.

Université Paris-Saclay
Espace Technologique / Immeuble Discovery
Route de l'Orme aux Merisiers RD 128 / 91190 Saint-Aubin,
France

An extreme feature of fungi, although not limited to this kingdom, is the prevalence of accessory chromosomes (also called B chromosomes or dispensable chromosomes) in their genome (Galazka and Freitag, 2014; Soyer *et al*., 2018). So far, most studies regarding accessory chromosomes have pointed them out in plant-interacting Ascomycetes although this might be a bias because their detection can be delicate. Some species harbor TE-rich accessory chromosome(s) (e.g. in Lmb*, Z. tritici*, *F. oxysporum*; Ma *et al*., 2010; Rouxel *et al*., 2011; Balesdent *et al.*, 2013; Dhillon *et al.,* 2014; Grandaubert *et al*., 2015). Their heterochromatin nature is uncovered through the advent of ChIP-seq analyses. Accessory chromosomes of *Z. tritici*, *F. oxysporum* or *F. fujikuroi, F. asiaticum* are enriched in H3K27me3 (Wiemann *et al*., 2013; Galazka and Freitag, 2014; Schotanus *et al*., 2015; Studt *et al*., 2016; Fokkens *et al*., 2018) as are those of *F. graminearum* while not enriched in TEs (Connolly *et al*., 2013). Interestingly, here we shown for Lmb that its accessory chromosome is TE-rich and almost entirely associated with H3K9me3, which is different to other fungi.

Dogmas regarding conventional definitions of facultative or constitutive heterochromatin seem not to be valid in all plant pathogenic fungi. While histone modifications H3K9me3 and H3K27me3 are both a signature of heterochromatin, H3K9me3 is considered to be typical for constitutive heterochromatin, as associated with repeats and involved in genome stability (Möller *et al*., 2019), and H3K27me3 is considered to be associated with facultative heterochromatin and considered to be easily reversed toward a euchromatin state under some stresses from the environment. As H3K9me3 is found associated with TE-rich regions, the proportion of H3K9me3 in a genome strictly reflects the TE content, as described in *Z. tritici* for instance (Schotanus *et al*., 2015). This is also the case for Lmb and Lml. In Lmb, having >30% TE, 33% of the genome is associated with H3K9me3 while the genome of Lml, having a low TE content, presents a low enrichment in H3K9me3 (4% of H3K9me3 in the Lml genome). The unique dispensable chromosome of Lmb is mostly repetitive and 90% of this chromosome is associated with H3K9me3 (Rouxel *et al.,* 2011; Balesdent *et al*., 2013; Our study). Co-location of H3K9me3 and TEs is in favor of a "constitutive" nature of this modification together with the fact that H3K9me3-domains encompass a small number of genes in Lmb and Lml (respectively 70 and 104 genes), as in *Z. tritici* (86 genes; Schotanus *et al.,* 2015; Soyer *et al*., 2019). Genes associated with H3K9me3 are amost all located in the middle of repetitive elements, in sub-telomeric areas, or very close to the edge of regions enriched in repeated elements. This is in accordance with the fact that TEs are targeted by H3K9me3 which might leak to neighbor genes. Nevertheless, some of these genes are heavily transcribed upon host infection (Soyer *et al*., 2019; Chujo and Scott, 2014; Soyer *et al*., 2014; Our study). This does not match the "constitutive" nature of this modification. Even though the largest proportion of genes is found associated with H3K4me2 from detailed ChIP-seq analyses performed so far *in vitro* in plant-interacting fungi (i.e. *F. graminearum*, *F. oxysporum*, *Z. tritici*, Lmb and Lml; Connolly *et al*., 2013; Schotanus *et al*., 2015; Fokkens *et al*., 2018; Soyer *et al*., 2019; Our study), a significant proportion of the predicted genes are found associated with H3K27me3. This is in accordance with the "facultative" nature of this histone modification. On the other side, some evidence is in favor of its important role in genome organization and stability. For instance, dispensable chromosomes of *Z. tritici* are twice as rich in TEs as core chromosomes, but although no significant enrichment of these chromosomes in H3K9me3 has been identified, they are entirely covered by H3K27me3 (Schotanus *et al*., 2015). Besides, loss of H3K27me3 in *Z. tritici* increases stability of

Université Paris-Saclay
Espace Technologique / Immeuble Discovery
Route de l'Orme aux Merisiers RD 128 / 91190 Saint-Aubin,
France

some accessory chromosomes (Möller *et al*., 2019). Altogether, these features seem to indicate that although H3K27me3 is an important regulator of gene expression involved in development or response to various stresses, it might also play a role in the maintenance of some parts of fungal genomes.

The comparative epigenomic analysis corroborates previous comparative genomic analysis and previous epigenetic studies in this species complex (Grandaubert *et al.,* 2014; Soyer *et al*., 2014). Difference in terms of genome organization between Lmb and Lml (i.e. alternation of large stretches of TEs and large gene-rich compartments in Lmb vs. little TE content, no bipartite organization of the genome of Lml) is consistent with the organization of the epigenomic landscape between both species. In Lmb, very large H3K9me3-domains are present, spanning large TE-rich regions (the largest one being found on the dispensable chromosome of Lmb), while such extremely large H3K9me3-domains are not observed in the Lml genome. It is already known, for Lmb and other plant-interacting fungi, that TE-rich compartments of fungal genomes are enriched in genes encoding putative effectors or secondary metabolites (e.g. Ma *et al*., 2010; Rouxel *et al*., 2011; Grandaubert *et al*., 2014; Faino *et al*., 2016; Vlaardingerbroek *et al*., 2016; Dallery *et al*., 2017). Here we show that all cloned avirulence genes of Lmb are associated with H3K9me3 *in vitro*. Our finding regarding the genome-wide analysis of the epigenome of Lmb corroborates previous targeted epigenetic analyses performed by Soyer *et al*. (2014), in which two avirulence genes were identified associated with H3K9me3 *in vitro*, consistently with the fact that these genes are silent *in vitro*. Even outside of TE-rich regions, heterochromatin is always found associated with pathogenicity-related genes, whether they are genes encoding effectors or metabolites (Connolly *et al*., 2013; Wiemann *et al*., 2013; Chujo and Scott, 2014; Schotanus *et al*., 2015; Fokkens *et al.,* 2018; Soyer *et al*., 2019). Importantly, sets of genes up-regulated during host infection are found associated with heterochromatin, *in vitro* (Fokkens *et al*., 2018; Soyer *et al*., 2019). This supports our previous hypothesis that location of pathogenicity-related genes in flexible epigenomic compartments of the genome represents an efficient way to regulated expression of sets of genes scattered throughout the genomes and involved in similar biological processes (Soyer *et al.,* 2015a).

While importance of histone modifications in the regulation of the expression of a few effector or secondary metabolite gene clusters has already been demonstrated by ChIP-qPCR *in planta* (Chujo & Scott, 2014; Soyer *et al*., 2019) a complete view of the *in planta* chromatin dynamics of a plant-associated fungus has not been generated yet. Previous studies have assessed histone modifications at a few genomic loci of secondary metabolite gene clusters in the symbiotic fungus, *E. festucae* (Chujo and Scott, 2014). We have also performed a ChIP-qPCR analysis of targeted effector genes in *Z. tritici* during infection of wheat leaves. The experiment performed on infected wheat leaves has shown, for three putative effector genes, that their high expression at 13 dpi (corresponding to the switch from asymptomatic growth to necrotrophy for *Z. tritici*) compared to axenic culture was associated with a modification of the histone methylation patterns in their genomic environment. At 13 dpi, the level of H3K9me3 and/or H3K27me3 decreased (Soyer *et al*., 2019). Altogether, these analyses of distantly related fungi confirm that during host interaction, the specific induction of secondary metabolites / effector genes, located within heterochromatin domains *in vitro*, is associated with a dynamic re-organization of the histone modifications at their loci. So far, genome-wide scale epigenomic analyses of plant-interacting fungi have only been performed during axenic growth (Connolly *et al*.,

Université Paris-Saclay
Espace Technologique / Immeuble Discovery
Route de l'Orme aux Merisiers RD 128 / 91190 Saint-Aubin,
France

2013; Schotanus *et al*., 2015; Fokkens *et al*., 2018). This lack of a global comprehensive view of the chromatin dynamics of the fungal genome during plant interaction is currently due to technical limitations as discussed by Winter *et al.* (2018). Indeed, the success of performing such epigenomic analyses is jeopardized by the low amount of fungal biomass during plant infection combined with the fact that fungal genomes are small compared to massive host genomes. Our next challenge to be tackled now is to assess the chromatin dynamics *in planta* to decipher influence of histone modifications in the regulation of (effector) gene expression.

CONCLUSION

To the best of our knowledge, comparative analysis of histone modifications has been performed in model organisms such as mouse, in different cell types for instance (Mikkelsen *et al.,* 2010). None has been set up in phytopathogenic fungi, and nothing is known regarding how much differences in terms of location of these modifications in the genome might influence gene expression or pathogenesis. Comparative genomics has allowed analyses regarding the evolution of genes encoding effectors, their location in genomes, or secondary metabolites, of species according to their lifestyles, or the diversity of the effector repertoires according to host specialisation. The role of the epigenome is increasingly recognized in plant-pathogenic fungi, as an important regulator of the genome structure (Möller *et al*., 2019) and the expression of genes encoding effectors (Soyer *et al*., 2014; Chujo and Scott, 2014; Soyer *et al*., 2019). The next step forward is to set up comparative epigenomics to understand the impact of the epigenomic landscape on adaptation toward environmental rapid changes, modulation of interactions with the holobiont, host adaptation and specialization. This first comparative epigenomic analysis represent an important corpus of data to set the basis for further work aiming at investigating, on the genome wide scale, influence of histone modifications on gene evolution under selection pressure or host adaptation.

AUTHORS CONTRIBUTION

Conceived and designed the experiments: JLS, IF, EHS. Performed the experiments: JLS. Analysis of the data: JLS, CC, EJG, NL. Interpretation of the data: JLS, CC, IF, TR, EHS, IF. Writing of the draft: JLS. Editing of the draft: JLS, CC, TR, IF, EHS.

ACKNOWLEDGEMENT

Authors wish to thank all members of the "Environmental Genomics" and the "Effectors and Pathogenesis of *L. maculans*" groups, and M. Freitag and J. Grandaubert, for fruitful discussions. J. L. Soyer was founded by a "Contrat Jeune Scientifique" grant from INRA.

REFERENCES

Ansan-Melayah D., Balesdent M.-H., Buee M., Rouxel T., 1995. Genetic characterization of *AvrLm1*, the first avirulence gene of *Leptosphaeria maculans*. Phytopathology 85, 1525–1529.

Balesdent M.-H., Fudal I., Ollivier B., Bally P., Grandaubert J., Eber F., Chèvre A.-M., Leflon M;, Rouxel T., 2013. The dispensable chromosome of *Leptosphaeria maculans* shelters an effector gene conferring avirulence towards *Brassica rapa*. The New Phytologist. 198, 887–898.

Bewick A.J., Hofmeister B.T., Powers R.A., Mondo S.J., Grigoriev I.V., James T.Y., Stajich J.E., Schmitz R.J., 2019. Diversity of cytosine methylation across the fungal tree of life. Nature Ecology & Evolution. 3, 479–490.

Bolger A.M., Lohse M., Usadel B., 2014. Trimmomatic: a flexible trimmer for Illumina sequence data. Bioinformatics. 30, 2114–2120.

Cam H.P., Sugiyama T., Chen E.S., Chen X., FitzGerald P.C., Grewal S.I., 2005. Comprehensive analysis of heterochromatin- and RNAi-mediated epigenetic control of the fission yeast genome. Nature Genetics. 37, 809–819.

Chujo T., Scott B., 2014. Histone H3K9 and H3K27 methylation regulates fungal alkaloid biosynthesis in a fungal endophyte-plant symbiosis: K9 and K27 methylation regulates symbiosis. Molecular Microbiology 92, 413–434.

Chuma I., Isobe C., Hotta Y., Ibaragi K., Futamata N., Kusaba M., Yoshida K., Terauchi R., Fujita Y., Nakayashiki H., Valent B., Tosa Y., 2011. Multiple translocation of the *AVR-Pita* effector gene among chromosomes of the rice blast fungus *Magnaporthe oryzae* and related species. PLoS Pathogens. 7, e1002147.

Connolly L.R., Smith K.M., and Freitag M., 2013. The *Fusarium graminearum* histone H3K27 methyltransferase KMT6 regulates development and expression of secondary metabolite gene clusters. PLoS Genetics. 9, e1003916.

Croll D., McDonald B.A., 2012. The accessory genome as a cradle for adaptive evolution in pathogens. PLoS Pathogens. 8, e1002608.

Dallery J.F., Lapalu N., Zampounis A., Pigné S., Luyten I., Amselem J., Wittenberg A.H.J., Zhou S., de Queiroz M.V., Robin G.P., Auger A., Hainaut M., Henrissat B., Kim K.T., Lee Y.J, Lespinet O, Schwartz D.C., Thon M.R., O'Connell R.J., 2017. Gapless genome assembly of *Colletotrichum higginsianum* reveals chromosome structure and association of transposable elements with secondary metabolite gene clusters. BMC Genomics. 18, 667.

Darma R., Lutz A., Elliott C.E., Idnurm A.2., 2019. Identification of a gene cluster for the synthesis of the plant hormone abscisic acid in the plant pathogen *Leptosphaeria maculans*. Fungal Genetics and Biology. 130, 62–71.

Daverdin G., Rouxel T., Gout L., Aubertot J.N., Fudal I., Meyer M., Parlange F., Carpezat J., Balesdent M.H., 2012. Genome structure and reproductive behaviour influence the evolutionary potential of a fungal phytopathogen. PLoS Pathogens. 8, 1003020.

de Jonge R., Bolton M.D., Kombrink A., van den Berg G.C., Yadeta K.A., Thomma B.P., 2013. Extensive chromosomal reshuffling drives evolution of virulence in an asexual pathogen. Genome Research. 23, 1271–1282.

Dhillon B., Cavaletto J.R., Wood K.V., Goodwin S.B., 2010. Accidental amplification and inactivation of a methyltransferase gene eliminates cytosine methylation in *Mycosphaerella graminicola*. Genetics. 186, 67–77.

Université Paris-Saclay
Espace Technologique / Immeuble Discovery
Route de l'Orme aux Merisiers RD 128 / 91190 Saint-Aubin, France

Dhillon B., Gill N., Hamelin R.C., Goodwin S.B., 2014. The landscape of transposable elements in the finished genome of the fungal wheat pathogen *Mycosphaerella graminicola*. BMC Genomics. 15, 1132.

Dobin A., Gingeras T.R., 2015. Mapping RNA-seq Reads with STAR. Current protocols in bioinformatics. 51, 11.14.1-19.

Dutreux F., Da Silva C., d'Agata L., Couloux A., Gay E.J., Istace B., Lapalu N., Lemainque A., Linglin J., Noel B., Wincker P., Cruaud C., Rouxel T., Balesdent M.-H., Aury J.-M., 2018. De novo assembly and annotation of three *Leptosphaeria* genomes using Oxford Nanopore MinION sequencing. Scientific Data. 5, 180235.

Elliott C.E., Gardiner D.M., Thomas G., Cozijnsen A., Van De Wouw A., Howlett B.J., 2007. Production of the toxin sirodesmin PL by *Leptosphaeria maculans* during infection of *Brassica napus*. Molecular Plant Pathology. 8, 791–802.

Elliott C.E., Callahan D.L., Schwenk D., Nett M., Hoffmeister D., Howlett B.J., 2013. A gene cluster responsible for biosynthesis of phomenoic acid in the plant pathogenic fungus, *Leptosphaeria maculans*. Fungal Genetics and Biology. 53, 50–58.

Emms D.M., Kelly S., 2015. OrthoFinder: solving fundamental biases in whole genome comparisons dramatically improves orthogroup inference accuracy. Genome Biology. 16, 157.

Faino L., Seidl M.F., Shi-Kunne X., Pauper M., van den Berg G.C., Wittenberg A.H., Thomma B.P., 2016. Transposons passively and actively contribute to evolution of the two-speed genome of a fungal pathogen. Genome Research. 26, 1091–1100.

Fisher M.C., Hawkins N.J., Sanglard D., Gurr S.J., 2018. Worldwide emergence of resistance to antifungal drugs challenges human health and food security. Science. 360, 739–742.

Fokkens L., Shahi S., Connolly L.R., Stam R., Schmidt S.M., Smith K.M., Freitag M., Rep M., 2018. The multi-speed genome of *Fusarium oxysporum* reveals association of histone modifications with sequence divergence and footprints of past horizontal chromosome transfer events. BioRXiv.

Freitag M., 2017. Histone methylation by SET domain proteins in Fungi. Annual Review of Microbiology 71, 413–439.

Fudal I., Ross S., Gout L., Blaise F., Kuhn M.L., Eckert M.R., Cattolico L., Bernard-Samain S., Balesdent M.H., Rouxel T., 2007. Heterochromatin-like regions as ecological niches for avirulence genes in the *Leptosphaeria maculans* genome: map-based cloning of *AvrLm6*. Molecular Plant-Microbe Interactions. 20, 459–470.

Gacek-Matthews A., Berger H., Sasaki T., Wittstein K., Gruber C., Lewis Z.A., Strauss J., 2016. KdmB, a Jumonji Histone H3 demethylase, regulates genome-wide H3K4 trimethylation and is required for normal induction of secondary metabolism in *Aspergillus nidulans*. PLOS Genetics. 12, e1006222.

Galazka J.M., Freitag M., 2014. Variability of chromosome structure in pathogenic fungi--of 'ends and odds'. Curr Opin Microbiol. 20, 19–26.

Gardiner D.M., Cozijnsen A.J., Wilson L.M., Pedras M.S., Howlett B.J., 2004. The sirodesmin biosynthetic gene cluster of the plant pathogenic fungus *Leptosphaeria maculans*. Molecular Microbiology. 53, 1307–1318.

Ghanbarnia K., Fudal I., Larkan NJ., Links MG., Balesdent MH., Profotova B., Fernando WG., Rouxel T., Borhan M.H. 2015, Rapid identification of the *Leptosphaeria maculans* avirulence gene *AvrLm2* using an intraspecific comparative genomics approach. Molecular Plant Pathology. 16,699–709.

Ghanbarnia K., Ma L., Larkan N.J., Haddadi P., Fernando W.G.D., Borhan M.-H., 2018. *Leptosphaeria maculans* AvrLm9: a new player in the game of hide and seek with AvrLm4-7. Molecular Plant Pathology. 19: 1754–1764.

Gervais J., Plissonneau C., Linglin J., Meyer M., Labadie K., Cruaud C., Fudal I., Rouxel T., Balesdent M.-H., 2017. Different waves of effector genes with contrasted genomic location are expressed by *Leptosphaeria maculans* during cotyledon and stem colonization of oilseed rape. Molecular Plant Pathology. 18, 1113–1126.

Gomes M.V., Pelosi G.G., 2013. Epigenetic vulnerability and the environmental influence on health. Experimental biology and medicine / Society for Experimental Biology and Medicine. 238, 859–865.

Gout L., Fudal I., Kuhn M.-L., Blaise F., Eckert M., Cattolico L., Balesdent M.-H., Rouxel T., 2006. Lost in the middle of nowhere: the *AvrLm1* avirulence gene of the Dothideomycete *Leptosphaeria maculans*. Molecular Microbiology. 60,67–80.

Grandaubert J., Lowe R.G., Soyer J.L., Schoch C.L., Van de Wouw A.P., Fudal I., Robbertse B., Lapalu N., Links M.G., Ollivier B., Linglin J., Barbe V., Mangenot S., Cruaud C., Borhan H., Howlett B.J., Balesdent M.H., Rouxel T, 2014. Transposable element-assisted evolution and adaptation to host plant within the *Leptosphaeria maculans-Leptosphaeria biglobosa* species complex of fungal pathogens. BMC Genomics. 15, 891.

Grandaubert J., Bhattacharyya A., Stukenbrock E.H., 2015. RNA-seq-based gene annotation and comparative genomics of four fungal grass pathogens in the genus *Zymoseptoria* identify novel orphan genes and species-specific invasions of transposable elements. G3 (Bethesda). 5, 1323–1333.

Jamieson K., Rountree M.R., Lewis Z.A., Stajich J.E., and Selker E.U., 2013. Regional control of histone H3 lysine 27 methylation in *Neurospora*. Proceedings of the National Academy of Sciences of the United States of America. 110, 6027–6032.

Langmead B., Salzberg S.L., 2012. Fast gapped-read alignment with Bowtie 2. Nature Methods. 9, 357–359.

Leclair S., Ansan-Melayah D., Rouxel T., Balesdent M., 1996. Meiotic behaviour of the minichromosome in the phytopathogenic ascomycete *Leptosphaeria maculans*. Current Genetics. 30, 541–548.

Lo Presti L., Lanver D., Schweizer G., Tanaka S., Liang L., Tollot M., Zuccaro A., Reissmann S., Kahmann R., 2015. Fungal effectors and plant susceptibility. Annual Review of Plant Biology. 66, 513–545.

Université Paris-Saclay
Espace Technologique / Immeuble Discovery
Route de l'Orme aux Merisiers RD 128 / 91190 Saint-Aubin, France

Ma L.J., van der Does H.C., Borkovich K.A., Coleman J.J., Daboussi M.J., Di Pietro A. *et al*., 2010. Comparative genomics reveals mobile pathogenicity chromosomes in *Fusarium*. Nature. 464,367–373.

Mendes-Pereira E., Balesdent M.-H., Brun H., Rouxel T., 2003. Molecular phylogeny of the *Leptosphaeria maculans-L. biglobosa* species complex. Mycological Research. 107, 1287–1304.

Mikkelsen T.S., Xu Z., Zhang X., Wang L., Gimble J.M., Lander E.S., Rosen E.D., 2010. Comparative epigenomic analysis of murine and human adipogenesis. Cell. 143, 156–169.

Möller M., Schotanus K., Soyer J.L., Haueisen J., Happ K., Stralucke M., Happel P., Smith K.M., Connolly L.R., Freitag M., Stukenbrock E.H., 2019. Destabilization of chromosome structure by histone H3 lysine 27 methylation. PLoS Genetics. 15, e1008093.

Ohm R.A., Feau N., Henrissat B., Schoch C.L., Horwitz B.A., Barry K.W., Condon B.J., Copeland A.C., Dhillon B., Glaser F., Hesse C.N., Kosti I., LaButti K., Lindquist E.A., Lucas S., Salamov A.A., Bradshaw R.E., Ciuffetti L., Hamelin R.C., Kema G.H., Lawrence C., Scott J.A., Spatafora J.W., Turgeon B.G., de Wit P.J., Zhong S., Goodwin S.B, Grigoriev I.V., 2012. Diverse lifestyles and strategies of plant pathogenesis encoded in the genomes of eighteen Dothideomycetes fungi. PLoS Pathogens. 8, e1003037.

Parlange F., Daverdin G., Fuda I., Kuhn M.-L., Balesden M.-H., Blaise, F., Grezes-Besset B., Rouxel T., 2009. *Leptosphaeria maculans* avirulence gene *AvrLm4-7* confers a dual recognition specificity by the *Rlm4* and *Rlm7* resistance genes of oilseed rape, and circumvents Rlm4-mediated recognition through a single amino acid change. Molecular Microbioliogy 71, 851–863.

Petit-Houdenot Y., Degrave A., Meye M., Blaise F., Ollivier B., Marais C.-L., Jauneau A., Audran C., Rivas S., Veneault-Fourrey C., Brun H., Rouxel T., Fudal I., Balesdent M.-H., 2019. A two genes - for - one gene interaction between *Leptosphaeria maculans* and *Brassica napus*. New Phytologist. 223, 397–411.

Plissonneau C., Rouxel T., Chèvre A.-M., Van De Wouw A.P., Balesdent M.-H., 2018. One gene-one name: the *AvrLmJ1* avirulence gene of *Leptosphaeria maculans* is *AvrLm5*. Molecular Plant Pathology. 19,1012-1016.

Rouxel T., Balesdent M.H., 2005. The stem canker (blackleg) fungus, Leptosphaeria maculans, enters the genomic era. Molecular Plant Pathology. 6, 225–241.

Rouxel T., Grandaubert J., Hane J.K., Hoede C., van de Wouw A.P., Couloux A., Dominguez V., Anthouard V., Bally P., Bourras S., Cozijnsen A.J., Ciuffetti L.M., Degrave A., Dilmaghani A., Duret L., Fudal I., Goodwin S.B., Gout L., Glaser N., Linglin J., Kema G.H.J., Lapalu N., Lawrence C.B., May K., Meyer M., Ollivier B., Poulain J., Schoch C.L., Simon A., Spatafora J.W., Stachowiak A., Turgeon B.G., Tyler B.M., Vincent D., Weissenbach J., Amselem J., Quesneville H., Oliver R.P., Wincker P., Balesdent M.-H., Howlett B.J., 2011. Effector diversification within compartments of the *Leptosphaeria maculans* genome affected by Repeat-Induced Point mutations. Nature Communications 2.

Rouxel T., Balesdent M.H., 2017. Life, death and rebirth of avirulence effectors in a fungal pathogen of Brassica crops, *Leptosphaeria maculans*. New Phytologist. 214, 526–532.

Université Paris-Saclay
Espace Technologique / Immeuble Discovery
Route de l'Orme aux Merisiers RD 128 / 91190 Saint-Aubin,
France

Sánchez-Vallet A., Fouché S., Fudal I., Hartmann F.E., Soyer J.L., Tellier A., Croll D., 2018. The genome biology of effector gene evolution in filamentous plant pathogens. Annual Review of Phytopathology 56, 21–40.

Schotanus K., Soyer J.L., Connolly L.R., Grandaubert J., Happel P., Smith K.M., Freitag M., Stukenbrock E.H., 2015. Histone modifications rather than the novel regional centromeres of *Zymoseptoria tritici* distinguish core and accessory chromosomes. Epigenetics and Chromatin. 8, 41.

Schumacher J., Studt L., Tudzynski P., 2019. The putative H3K36 demethylase BcKDM1 affects virulence, stress responses and photomorphogenesis in *Botrytis cinerea*. Fungal Genetics and Biology 123, 14–24.

Shannon P., Markiel A., Ozier O., Baliga N.S., Wang J.T., Ramage D., Amin N., Schwikowski B., Ideker T., 2003. Cytoscape: a software environment for integrated models of biomolecular interaction networks. Genome Research 13: 2498-2504.

Smith K.M., Kothe G.O., Matsen C.B., Khlafallah T.K., Adhvaryu K.K., Hemphill M., Freitag M., Motamedi M.R., Selker E.U. 2008, The fungus *Neurospora crassa* displays telomeric silencing mediated by multiple sirtuins and by methylation of histone H3 lysine 9. Epigenetics and Chromatin. 1, 5.

Song Q., Smith A.D., 2011. Identifying dispersed epigenomic domains from ChIP-Seq data. Bioinformatics 27, 870–871.

Soyer J.L., El Ghalid M., Glaser N., Ollivier B., Linglin J., Grandaubert J., Balesdent M.-H., Connolly L.R., Freitag M., Rouxel T., Fudal I., 2014. Epigenetic control of effector gene expression in the plant pathogenic fungus *Leptosphaeria maculans*. PLoS Genetics. 10, e1004227.

Soyer J.L., Rouxel T., Fudal I., 2015a. A. Chromatin-based control of effector gene expression in plant-associated fungi. Current Opinion in Plant Biology. 26, 51–56.

Soyer J.L., Möller M., Schotanus K., Connolly L.R., Galazka J.M., Freitag M., Stukenbrock E.H., 2015b. Chromatin analyses of *Zymoseptoria tritici*: Methods for chromatin immunoprecipitation followed by high-throughput sequencing (ChIP-seq). Fungal Genetics and Biology. 79: 63–70.

Soyer J.L., Balesdent M.H., Rouxel T., Dean R.A., 2018. To B or not to B: a tale of unorthodox chromosomes. Current Opinion in Microbiology. 46, 50–57.

Soyer J.L., Grandaubert J., Haueisen J., Schotanus K., Stukenbrock E.H., 2019. *In planta* chromatin immunoprecipitation in *Zymoseptoria tritici* reveals chromatin-based regulation of putative effector gene expression. bioRxiv, 544627.

Stergiopoulos I., De Kock M.J., Lindhout P., De Wit P.J., 2007. Allelic variation in the effector genes of the tomato pathogen *Cladosporium fulvum* reveals different modes of adaptive evolution. Molecular Plant-Microbe Interactions. 20, 1271–1283.

Université Paris-Saclay
Espace Technologique / Immeuble Discovery
Route de l'Orme aux Merisiers RD 128 / 91190 Saint-Aubin, France

Studt L., Rösler S.M., Burkhardt I., Arndt B., Freitag M., Humpf H.U., Dickschat J.S., Tudzynski B., 2016. Knock-down of the methyltransferase Kmt6 relieves H3K27me3 and results in induction of cryptic and otherwise silent secondary metabolite gene clusters in *Fusarium fujikuroi*. Environnemental Microbiology. 18, 4037–4054.

Stukenbrock E.H., Bataillon T., Dutheil J.Y., Hansen T.T., Li R., Zala M., McDonald B.A., Wang J., Schierup MH, 2011. The making of a new pathogen: insights from comparative population genomics of the domesticated wheat pathogen *Mycosphaerella graminicola* and its wild sister species. Genome Research. 21, 2157–2166.

Thorvaldsdóttir H., Robinson J.T., Mesirov J.P., 2013. Integrative Genomics Viewer (IGV): high-performance genomics data visualization and exploration. Briefings in Bioinformatics. 14, 178–192.

Van de Wouw A.P., Lowe R.G., Elliott C.E., Dubois D.J., Howlett B.J. 2014, An avirulence gene, *AvrLmJ1*, from the blackleg fungus, *Leptosphaeria maculans*, confers avirulence to *Brassica juncea* cultivars. Molecular Plant Pathology. 15, 523–530.

Vlaardingerbroek I., Beerens B., Schmidt S.M., Cornelissen B.J., Rep M., 2016. Dispensable chromosomes in *Fusarium oxysporum* f. sp. lycopersici. Molecular Plant Pathology. 17, 1455–1466.

Wiemann P., Sieber C.M., von Bargen K.W., Studt L., Niehaus E.M., Espino J.J., Huß K., Michielse C.B., Albermann S., Wagner D., Bergner S.V., Connolly L.R., Fischer A., Reuter G., Kleigrewe K., Bald T., Wingfield B.D., Ophir R., Freeman S., Hippler M., Smith K.M., Brown D.W., Proctor R.H., Münsterkötter M., Freitag M., Humpf H.U., Güldener U., Tudzynski B., 2013. Deciphering the cryptic genome: genome-wide analyses of the rice pathogen *Fusarium fujikuroi* reveal complex regulation of secondary metabolism and novel metabolites. PLoS Pathogens.9, e1003475.

Zogli P., Libault M., 2017. Plant response to biotic stress: Is there a common epigenetic response during plant-pathogenic and symbiotic interactions? Plant Sciences. 263, 89–93.

SUPPLEMENTARY DATA

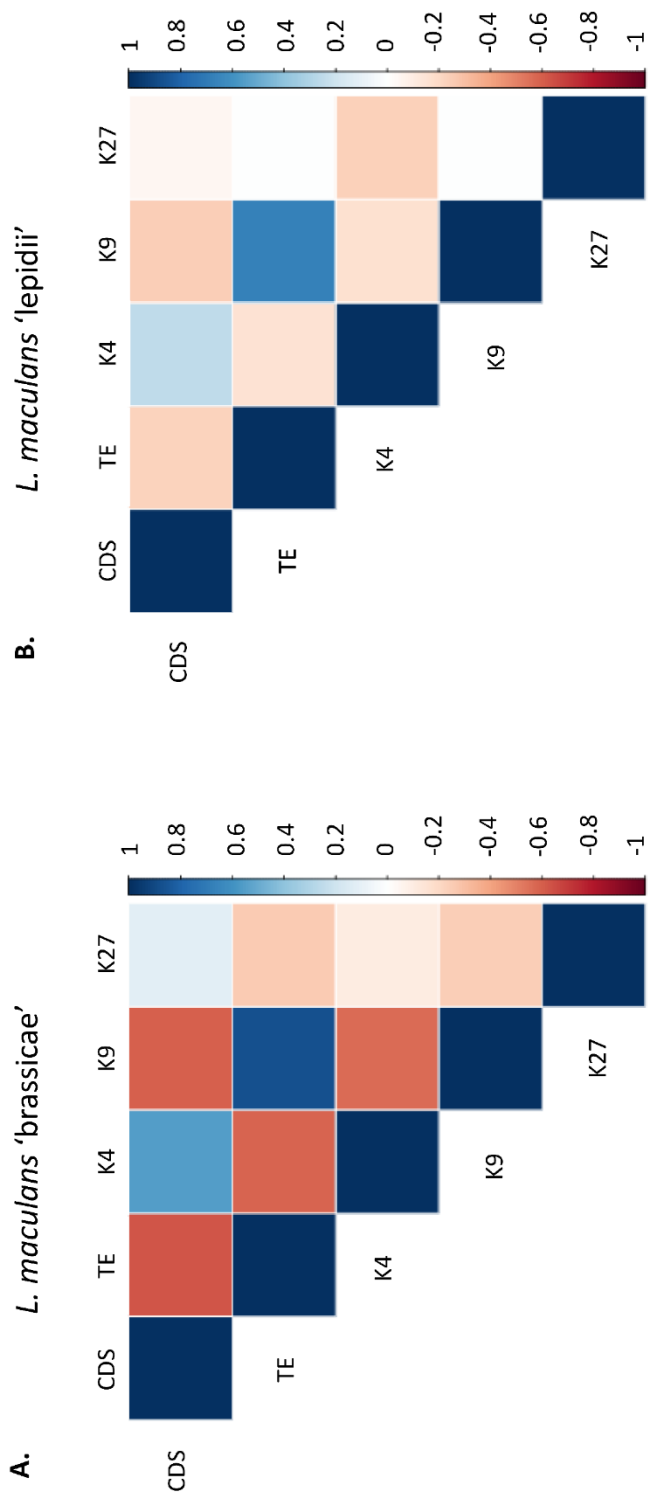

Figure S1. Correlation analysis of the location of genes, transposable elements and domains enriched for H3K4me2, H3K9me3 and H3K27me3 in the genomes of A. *Leptosphaeria maculans* 'brassicae'; B. *Leptosphaeria maculans* 'lepidii'.
Regions significantly enriched for any of the three histone modifications analysed were identified through ChIP-seq performed during axenic culture; correlation analyses were performed using a Kendall's T (see Materials and Methods). K4: H3K4me2; K9: H3K9me3; K27: H3K27me3; CDS: Coding sequences; TE: Transposable Elements.

Université Paris-Saclay
Espace Technologique / Immeuble Discovery
Route de l'Orme aux Merisiers RD 128 / 91190 Saint-Aubin, France

Université Paris-Saclay
Espace Technologique / Immeuble Discovery
Route de l'Orme aux Merisiers RD 128 / 91190 Saint-Aubin, France

650

651

Table S1: Statistics of ChIP-seq and RNA-seq datasets and alignments

Experiment	sample	ID	nb of reads	Nb not aligned	% not aligned	Nb aligned exactly one time	% aligned exactly one time	Nb aligned > 1 time	% aligned > 1 time	overall alignement rate
ChIP-seq_Lmb	Lmb_A_K4	1999_A	9395841	158895	1.69	9009443	95.89	227503	2.42	98.31
	Lmb_A_K9	1999_B	10919762	136322	1.25	1730751	15.85	9052689	82.9	98.75
	Lmb_A_K27	1999_C	10529291	124737	1.18	9039896	85.85	1364658	12.96	98.82
	Lmb_B_K4	1999_D	10534991	87375	0.83	10211829	96.93	235787	2.24	99.17
	Lmb_B_K9	1999_E	10654189	85037	0.80	1472180	13.82	9096972	85.38	99.2
	Lmb_B_K27	1999_F	10635233	56652	0.53	9449772	88.85	1128809	10.61	99.47
	Lmb_C_K4	1999_G	10346671	84083	0.81	10076434	97.39	186154	1.8	99.19
	Lmb_C_K9	1999_H	10459367	75082	0.72	1089336	10.41	9294949	88.87	99.28
	Lmb_C_K27	1999_I	10710240	65549	0.61	9566489	89.32	1078202	10.07	99.39
ChIP-seq_Lml	Lml_A_K4	1999_J	11555456	514684	4.45	11014396	95.32	26376	0.23	95.55
	Lml_A_K9	1999_K	9204550	1292960	14.05	5376256	58.41	2535334	27.54	85.95
	Lml_A_K27	1999_L	10555063	993082	9.41	9370385	88.78	191596	1.82	90.59
	Lml_B_K4	1999_M	10535483	519320	4.93	9999115	94.91	17048	0.16	95.07
	Lml_B_K9	1999_N	10850527	1895009	17.46	6719265	61.93	2236253	20.61	82.54
	Lml_B_K27	1999_O	10828748	983723	9.08	9680618	89.4	164407	1.52	90.92
	Lml_C_K4	1999_P	10734950	358237	3.34	10364563	96.55	12150	0.11	96.66
	Lml_C_K9	1999_Q	10875975	1278587	11.76	4634043	42.61	4963345	45.64	88.24
	Lml_C_K27	1999_R	11402138	823586	7.22	10308659	90.41	269893	2.37	92.78
RNA-seq_Lml	Lml_A	NDPS10	52095284	1776449	3.41	50195802	96.35	120413	0.23	96.58
	Lml_B	NDPS11	50886249	1638537	3.22	49097848	96.49	151034	0.3	96.79
	Lml_C	NDPS12	50800169	1661166	3.27	49014722	96.49	121596	0.24	96.73
RNA-seq_Lmb	Lmb_A	AMI	16800535	315850	1.88	16389267	97.55	91856	0.55	98.1
	Lmb_B	AQI	18160771	468547	2.58	17579303	96.8	110214	0.61	97.41

ChIP-seq reads were mapped against the reference genomes using Bowtie2 with default parameters; RNA-seq reads were mapped against the reference genomes using STAR (Langmead and Salzberg, 2013; Dobin and Gingeras, 2015; see Materials and Methods). Table shows the number of reads used for the alignment, the number of reads mapping only at one location, number of reads aligned more than once and the unmapped reads against the genome of *L. maculans* 'brassicae' (Dutreux *et al*., 2018) or *L. maculans* 'lepidii' (Grandaubert *et al.*, 2014).

652

653

654

Table S2: Correlation analysis between the different ChIP experiments generated with antibodies targeting histone modifications H3K4me2, H3K9me3 and H3K27me3 in the *L. maculans* 'lepidii', during *in vitro* growth.

		H3K4me2			H3K9me3			H3K27me3		
		1999_J	1999_M	1999_P	1999_K	1999_N	1999_Q	1999_L	1999_O	1999_R
	1999_J	1.00								
H3K4me2	1999_M	0.94	1.00							
	1999_P	0.89	0.90	1.00						
	1999_K	-0.21	-0.21	-0.23	1.00					
H3K9me3	1999_N	0.22	0.23	0.24	-0.88	1.00				
	1999_Q	-0.26	-0.26	-0.28	0.78	-0.77	1.00			
	1999_L	-0.21	-0.21	-0.22	-0.05	0.08	0.07	1.00		
H3K27me3	1999_O	-0.22	-0.22	-0.23	-0.06	0.09	0.05	0.89	1.00	
	1999_R	-0.30	-0.30	-0.31	-0.05	0.07	0.05	0.74	0.80	1.00

Correlation analyses were performed to analyze location of the significantly enriched domains, identified using RSEG (Song and Smith, 2011), from the three different biological replicates generated and analyzed separately. A Kendall's T correlation test was performed using R.

655

Table S3: Correlation analysis between the different ChIP experiments generated with antibodies targeting histone modifications H3K4me2, H3K9me3 and H3K27me3 in the *L. maculans* 'brassicae', during *in vitro* growth.

		H3K4me2			H3K9me3			H3K27me3		
		1999_A	1999_D	1999_G	1999_B	1999_E	1999_H	1999_C	1999_F	1999_I
	1999_A	1								
H3K4me2	1999_D	0.90	1.00							
	1999_G	0.87	0.91	1.00						
	1999_B	-0.62	-0.58	-0.55	1.00					
H3K9me3	1999_E	-0.61	-0.58	-0.55	0.97	1.00				
	1999_H	-0.62	-0.58	-0.56	0.98	0.97	1.00			
	1999_C	-0.11	-0.13	-0.14	-0.23	-0.24	-0.24	1.00		
H3K27me3	1999_F	-0.11	-0.12	-0.14	-0.25	-0.25	-0.25	0.94	1.00	
	1999_I	-0.10	-0.11	-0.13	-0.25	-0.26	-0.25	0.95	0.94	1.00

Correlation analyses were performed to analyze location of the significantly enriched domains, identified using RSEG (Song and Smith, 2011), from the three different biological replicates generated and analyzed separately. A Kendall's T correlation test was performed using R.

656

657

658

659

Table S4: Coverage of histone modifications H3K4me2, H3K9me3 and H3K27me3 in the genome of *Leptosphaeria maculans* 'brassicae'.

ID_SC[a]	SC size (bp)[a]	H3K4me2[b]		H3K9me3[b]		H3K27me3[b]	
		bp	%	bp	%	bp	%
JN3_BAC01	21008	0	0.00	21000	99.96	1251	5.95
JN3_SC00	3635781	1307171	35.95	1102622	30.33	762986	20.99
JN3_SC01	3650661	1483193	40.63	1047969	28.71	687488	18.83
JN3_SC02	3465289	1568755	45.27	821441	23.70	640962	18.50
JN3_SC03	3116548	1193866	38.31	999254	32.06	574441	18.43
JN3_SC04	3080038	1425610	46.29	665755	21.62	540171	17.54
JN3_SC05	2723307	963377	35.38	963038	35.36	579405	21.28
JN3_SC06	2669349	1086759	40.71	921773	34.53	488919	18.32
JN3_SC07	2437616	1197276	49.12	522765	21.45	587443	24.10
JN3_SC08	2329530	727752	31.24	1123307	48.22	306359	13.15
JN3_SC09	2121901	748451	35.27	886766	41.79	379620	17.89
JN3_SC10	1953324	918611	47.03	482165	24.68	439910	22.52
JN3_SC11	1933728	1000894	51.76	400992	20.74	273848	14.16
JN3_SC12	1809099	748253	41.36	486740	26.91	486379	26.89
JN3_SC13	1787499	765814	42.84	565221	31.62	372365	20.83
JN3_SC14	1545248	808577	52.33	318036	20.58	342119	22.14
JN3_SC15	1485921	587315	39.53	451809	30.41	387118	26.05
JN3_SC16	1416674	556218	39.26	545236	38.49	243093	17.16
JN3_SC17	1391278	480336	34.52	588903	42.33	415859	29.89
JN3_SC18	1351186	562433	41.63	490141	36.27	258335	19.12
JN3_SC19	832888	44716	5.37	748487	89.87	56517	6.79
JN3_SC20	252801	0	0.00	197121	77.97	32524	12.87
JN3_SC21	237616	0	0.00	197118	82.96	18507	7.79
JN3_SC22	206368	0	0.00	178511	86.50	4003	1.94
JN3_SC23	157065	0	0.00	0	0.00	0	0.00
JN3_SC24	81359	0	0.00	54108	66.51	751	0.92
JN3_SC25	68927	0	0.00	65503	95.03	5502	7.98
JN3_SC26	58575	0	0.00	57354	97.92	3254	5.56
JN3_SC27	50646	0	0.00	26005	51.35	1502	2.97
JN3_SC28	36829	0	0.00	34500	93.68	6753	18.34
JN3_SC29	33591	0	0.00	22753	67.74	15503	46.15
JN3_SC30	23239	0	0.00	20901	89.94	0	0.00
JN3_SC31	21588	0	0.00	21001	97.28	0	0.00
genome	45986477	18175377	39.52	15028295	32.68	8912887	19.38

[a]Genome as published in Dutreux *et al*. (2018). [b]Location of H3K4me2, H3K9me3 and H3K27me3 was determined through ChIP-seq analysis, in vitro, and regions significantly enriched for any of the modifications was identified using RSEG (Song and Smith, 2011).

660

661

662

663

Table S5: Coverage of histone modifications H3K4me2, H3K9me3 and H3K27me3 in the genome of *L. maculans* 'lepidii'.

ID_SC[a]	SC size[a]	H3K4me2[b]		H3K9me3[b]		H3K27me3[b]	
		bp	%	bp	%	bp	%
scaffold00001	2643178	888592	33.62	59684	2.26	313773	11.87
scaffold00002	1959821	699265	35.68	58666	2.99	233310	11.90
scaffold00003	1983546	608230	30.66	41111	2.07	242118	12.21
scaffold00004	1736283	575205	33.13	62432	3.60	172672	9.94
scaffold00005	1623222	501923	30.92	65093	4.01	189501	11.67
scaffold00006	1544579	536762	34.75	12113	0.78	153263	9.92
scaffold00007	1533342	565981	36.91	36346	2.37	120062	7.83
scaffold00008	1418419	388288	27.37	18392	1.30	190887	13.46
scaffold00009	1356343	424898	31.33	45357	3.34	231893	17.10
scaffold00010	1127952	315229	27.95	32413	2.87	165274	14.65
scaffold00011	1096957	373438	34.04	17581	1.60	137278	12.51
scaffold00012	1109454	444873	40.10	5018	0.45	87649	7.90
scaffold00013	1030750	285020	27.65	66076	6.41	138272	13.41
scaffold00014	907115	319426	35.21	33535	3.70	97454	10.74
scaffold00015	913738	323415	35.39	29781	3.26	74040	8.10
scaffold00016	782495	246356	31.48	46437	5.93	105244	13.45
scaffold00017	748245	222170	29.69	28898	3.86	92057	12.30
scaffold00018	696173	219971	31.60	5438	0.78	92845	13.34
scaffold00019	605627	248734	41.07	35469	5.86	219071	36.17
scaffold00020	573543	186512	32.52	28680	5.00	67433	11.76
…	…	…	…	…	…	…	…
scaffold00111	2197	0	0	2000	91.03	0	0
scaffold00112	2174	0	0	2000	92.00	0	0
scaffold00113	2174	0	0	2000	92.00	0	0
scaffold00114	2171	1001	46.11	0	0	0	0
scaffold00115	2150	0	0	2000	93.02	0	0
scaffold00116	2137	0	0	2000	93.59	800	37.44
scaffold00117	2134	0	0	1001	46.91	0	0
scaffold00118	2111	0	0	2000	94.74	0	0
scaffold00119	2093	0	0	2000	95.56	0	0
scaffold00120	2077	0	0	2000	96.29	0	0
scaffold00121	2060	0	0	2000	97.09	1000	48.54
scaffold00122	2041	801	39.25	951	46.59	0	0
scaffold00123	2008	0	0	951	47.36	0	0
genome	31530973	10147334	32.18	1232561	3.91	3989471	12.65

[a]Genome as published in Grandaubert *et al.* (2014). [b]Location of H3K4me2, H3K9me3 and H3K27me3 was determined through ChIP-seq analysis, in vitro, and regions significantly enriched for any of the modifications was identified using RSEG (Song and Smith, 2011).

Université Paris-Saclay
Espace Technologique / Immeuble Discovery
Route de l'Orme aux Merisiers RD 128 / 91190 Saint-Aubin, France

664

665

666

667

668

Table S6: Correlation analysis between the coverage of transposable elements (TE) and coding sequences (CDS) location, H3K4me2-, H3K9me3- and H3K27me3-domains in the L. maculans 'brassicae' genome.

	CDS	TE	H3K4me2	H3K9me3	H3K27me3
CDS	1	-0.63	0.55	-0.60	0.12
TE	-0.63	1	-0.58	0.87	-0.25
H3K4me2	0.55	-0.58	1	-0.57	-0.11
H3K9me3	-0.60	0.87	-0.57	1	-0.24
H3K27me3	0.12	-0.25	-0.11	-0.24	1

The coverage of transposable elements (TE), coding sequences (CDS) and histone modifications (H3K9me3, H3K27me3, H3K4me2) along the genome of *L. maculans* 'brassicae' was analyzed in 1000 pb sliding windows. A Kendall's T correlation analysis was done using R (Materials and Methods).

Table S7: Correlation analysis between the coverage of transposable elements (TE) and coding sequences (CDS) location, H3K4me2-, H3K9me3- and H3K27me3-domains in the *L. maculans* 'lepidii' genome.

	CDS	TE	H3K4me2	H3K9me3	H3K27me3
CDS	1.00	-0.22	0.25	-0.25	-0.05
TE	-0.22	1.00	-0.16	0.68	0.00
H3K4me2	0.25	-0.16	1.00	-0.16	-0.23
H3K9me3	-0.25	0.68	-0.16	1.00	0.01
H3K27me3	-0.05	0.00	-0.23	0.01	1.00

The coverage of transposable elements (TE), coding sequences (CDS) and histone modifications (H3K9me3, H3K27me3, H3K4me2) along the genome of *L. maculans* 'lepidii' was analyzed in 1000 pb sliding windows. A Kendall's T correlation analysis was done using R (Materials and Methods).

Université Paris-Saclay
Espace Technologique / Immeuble Discovery
Route de l'Orme aux Merisiers RD 128 / 91190 Saint-Aubin, France

669

670

Table S8: GO categories enriched in genes associated with H3K27me3 during axenic culture of *L. maculans* 'brassicae'.

GO-ID	FDR	nb. of genes with the GO term within H3K27me3	nb. of genes with a GO annotation within H3K27me3	proportion in the H3K27me3 -genes	nb. of genes with the given GO term in the genome	nb. of genes with a GO annotation in the genome	proportion in the genome	description
005975	1.54E-06	82	572	1.43E-01	362	5076	7.13E-02	carbohydrate metabolic process
0055114	4.08E-04	149	572	2.60E-01	911	5076	1.79E-01	oxidation reduction process
0055085	3.10E-03	104	572	1.82E-01	608	5076	1.20E-01	transmembrane transport

GO annotation of the Lmb genes were retrieved from Dutreux *et al.* (2018). Analysis of GO enrichment among the genes associated with H3K27me3 during axenic culture of Lmb was performed using Cytoscape (Shannon *et al.*, 2003).

671

672

Table S9: GO categories enriched in genes associated with H3K4me2 during axenic culture of *L. maculans* 'brassicae'.

GO-ID	FDR	nb. of genes with the GO term within H3K4me2	nb. of genes with a GO annotation within H3K4me2	proportion in the H3K4me2-genes	nb. of genes with the given GO in the genome	nb. of genes with a GO annotation in the genome	proportion in the genome	description
9987	3.60E-13	1976	3276	6.03E-01	2700	5076	5.32E-01	cellular_process
44237	6.85E-06	1585	3276	4.84E-01	2203	5076	4.34E-01	cellular_metabolic_process
71840	6.85E-06	540	3276	1.65E-01	661	5076	1.30E-01	cellular_component_organization_or_biogenesis
10467	1.10E-05	498	3276	1.52E-01	606	5076	1.19E-01	gene_expression
1901576	4.13E-05	698	3276	2.13E-01	899	5076	1.77E-01	organic_substance_biosynthetic
44249	4.13E-05	690	3276	2.11E-01	888	5076	1.75E-01	cellular_biosynthetic_process
44085	4.76E-05	336	3276	1.03E-01	392	5076	7.72E-02	cellular_component_biogenesis
6807	1.06E-04	1498	3276	4.57E-01	2102	5076	4.14E-01	nitrogen_compound_metabolic
9058	1.06E-04	727	3276	2.22E-01	950	5076	1.87E-01	biosynthetic_process
34645	2.43E-04	398	3276	1.21E-01	487	5076	9.59E-02	cellular_macromolecule_biosynthetic
9059	4.92E-04	402	3276	1.23E-01	497	5076	9.79E-02	macromolecule_biosynthetic_process
44271	4.92E-04	475	3276	1.45E-01	600	5076	1.18E-01	cellular_nitrogen_compound_biosynthetic_process
44267	6.15E-04	562	3276	1.72E-01	726	5076	1.43E-01	cellular_protein_metabolic_process
44260	1.37E-03	834	3276	2.55E-01	1129	5076	2.22E-01	cellular_macromolecule_metabolic
1901566	1.44E-03	445	3276	1.36E-01	565	5076	1.11E-01	nitrogen_compound_biosynthetic

GO annotation of the Lmb genes were retrieved from Dutreux *et al*. (2018). Analysis of GO enrichment among the genes associated with H3K27me3 during axenic culture of Lmb was performed using Cytoscape (Shannon *et al*., 2003).

Université Paris-Saclay
Espace Technologique / Immeuble Discovery
Route de l'Orme aux Merisiers RD 128 / 91190 Saint-Aubin, France

Table S10.: GO categories enriched in genes associated with H3K4me2 during axenic culture of *L. maculans* 'lepidii'.

GO-ID	FDR	nb. of genes with the GO term within H3K4me2	nb. of genes with a GO annotation within H3K4me2	proportion in the H3K4me2-genes	nb. of genes with the given GO in the genome	nb. of genes with a GO annotation in the genome	proportion in the genome	description
9987	3.69E-06	1564	2581	6.06E-01	2044	3725	5.49E-01	cellular_process
44267	4.48E-04	477	2581	1.85E-01	557	3725	1.50E-01	cellular_protein_metabolic_process
6807	1.25E-03	1107	2581	4.29E-01	1433	3725	3.85E-01	nitrogen_compound_metabolic_process
1901564	1.83E-03	829	2581	3.21E-01	1048	3725	2.81E-01	organonitrogen_compound_metabolic_process
1901566	1.87E-03	414	2581	1.60E-01	486	3725	1.30E-01	organonitrogen_compound_biosynthetic_process
44237	1.87E-03	1291	2581	5.00E-01	1704	3725	4.57E-01	cellular_metabolic_process
19538	2.97E-03	580	2581	2.25E-01	713	3725	1.91E-01	protein_metabolic_process
1901576	3.65E-03	585	2581	2.27E-01	722	3725	1.94E-01	organic_substance_biosynthetic_process
44260	3.68E-03	647	2581	2.51E-01	808	3725	2.17E-01	cellular_macromolecule_metabolic_process
43170	3.68E-03	863	2581	3.34E-01	1108	3725	2.97E-01	macromolecule_metabolic_process

GO annotation of the Lmb genes were retrieved from Grandaubert *et al*. (2014). Analysis of GO enrichment among the genes associated with H3K4me2 during axenic culture of Lml was performed using Cytoscape (Shannon *et al*., 2003).

Université Paris-Saclay
Espace Technologique / Immeuble Discovery
Route de l'Orme aux Merisiers RD 128 / 91190 Saint-Aubin, France

1

2

Table S11: GO categories enriched in genes associated with H3K27me3 during axenic culture of *L. maculans* 'lepidii'.

GO-ID	FDR	nb. of genes with the GO term among the genes associated with H3K27me3	nb. of genes with a GO annotation among the genes associated with H3K27me3	proportion in the H3K27me3-genes	nb. of genes with the given GO in the genome	nb. of genes with a GO annotation in the genome	proportion in the genome	description
5975	2.44E-03	41	288	1.42E-01	250	3725	6.71E-02	carbohydrate metabolic process
42221	2.44E-03	20	288	6.94E-02	88	3725	2.36E-02	response to chemical
51591	2.44E-03	10	288	3.47E-02	25	3725	6.71E-03	response to cAMP
46683	2.44E-03	10	288	3.47E-02	25	3725	6.71E-03	response to organophosphorus
10033	2.44E-03	11	288	3.82E-02	31	3725	8.32E-03	response to organic substance
10243	2.44E-03	10	288	3.47E-02	26	3725	6.98E-03	response to organonitrogen compound
1901698	2.44E-03	10	288	3.47E-02	26	3725	6.98E-03	response to nitrogen compound
14070	2.44E-03	10	288	3.47E-02	26	3725	6.98E-03	response to organic cyclic compound
14074	2.44E-03	10	288	3.47E-02	26	3725	6.98E-03	response to purine-containing compound

GO annotation of the Lmb genes were retrieved from Grandaubert *et al*. (2014). Analysis of GO enrichment among the genes associated with H3K27me3 during axenic culture of Lml was performed using Cytoscape (Shannon *et al*., 2003).

Université Paris-Saclay
Espace Technologique / Immeuble Discovery
Route de l'Orme aux Merisiers RD 128 / 91190 Saint-Aubin, France

Université Paris-Saclay
Espace Technologique / Immeuble Discovery
Route de l'Orme aux Merisiers RD 128 / 91190 Saint-Aubin, France

CHAPITRE II

Protéines modificatrices d'histone

INTRODUCTION

Dans le chapitre II, nous aborderons l'implication d'acteurs clefs de la régulation chromatinienne de l'expression des gènes via une approche d'analyse fonctionnelle. Pour cela j'ai transféré la technique de mutagenèse CRISPR-Cas9, mise au point pour *L. maculans* par A. Idnurm (Idnurm *et al.,* 2017), avec succès au laboratoire. Nous avons choisi d'inactiver plusieurs HMEs et déméthylases d'histones et d'étudier l'impact de leur inactivation sur la régulation génique et la structure du génome. Les protéines modificatrices d'histones sont de plus en plus étudiées et il s'avère que leur capacité à réguler des mécanismes complexes ainsi que des pans entiers du métabolisme chez les champignons filamenteux est de plus en plus documenté. L'objectif des analyses fonctionnelles menées chez *L. maculans* est de valider de façon expérimentale les conclusions que nous pouvons faire basées sur les analyses « genome-wide » quant à l'importance de l'organisation du génome sur la régulation de la pathogénie. A mon arrivée au laboratoire, les plasmides CRISPR-Cas9 n'étaient pas encore disponibles. J'ai donc initié des expériences de RNAi, puis ai réalisé en deuxième année de thèse l'inactivation des gènes quand les vecteurs ont été disponibles. J'ai ainsi mené les expériences d'inactivation génique, la caractérisation des transformants obtenus, et généré des échantillons afin d'obtenir des données de ChIP-Seq, RNA-Seq et Hi-C-Seq pour aller plus loin dans la caractérisation des transformants obtenus. Le séquençage des échantillons pour les analyses ChIP-Seq, RNA-Seq et Hi-C-Seq est actuellement en cours.

Dans une première partie, que j'ai rédigée sous forme d'article, je présenterai l'effet de l'inactivation de *KMT1* et *KMT6* responsables respectivement de la mise en place des marques répressives H3K9me3 et H3K27me3, sur la croissance mycélienne, la sporulation, la capacité à infecter le colza et la régulation de l'expression des gènes codant des effecteurs. Ces résultats sont préliminaires et les expériences de séquençage en cours apporterons beaucoup à l'avancée de ce projet.

Dans une deuxième partie, nous aborderons l'influence de Kdm8, une histone déméthylase dont le profil d'expression correspond à celui des gènes *AVR* clonés et dont la fonction est encore inconnue chez *L. maculans*. Le gène codant Kdm8 a été inactivé et les mutants ainsi obtenus ont été testé pour leur capacité à infecter le colza, leur croissance et la régulation de gènes codant des effecteurs.

Université Paris-Saclay
Espace Technologique / Immeuble Discovery
Route de l'Orme aux Merisiers RD 128 / 91190 Saint-Aubin,
France

RESULTATS

ARTICLE 3

Histone methyltransferases KMT1 and KMT6 regulate effector gene expression and pathogenicity in the plant-pathogenic fungus *Leptosphaeria maculans*

Université Paris-Saclay
Espace Technologique / Immeuble Discovery
Route de l'Orme aux Merisiers RD 128 / 91190 Saint-Aubin, France

Histone methyltransferases KMT1 and KMT6 regulate effector gene expression and pathogenicity in the plant-pathogenic fungus *Leptosphaeria maculans*

C. Clairet[1,2], F. Blaise[1] ,J.L. Soyer[1*] and I. Fudal[1*]

[1]UMR BIOGER, INRA, AgroParisTech, Université Paris-Saclay, Avenue Lucien Brétignières, BP 01, F-78850 Thiverval-Grignon, France

[2]Université Paris-Sud, Orsay, France

* To whom correspondence should be addressed.

INTRODUCTION

During infection, plant pathogenic fungi secrete a set of molecules, collectively known as effectors, targeting the apoplast or the cytoplasm of the plant where they are mainly involved in overcoming the host immune defense system, nutrient uptake and, eventually, symptom development (Lo Presti *et al.,* 2015; Lo Presti and Kahmann, 2017). In some cases, effectors are recognized by specific resistance genes from the plant, triggering plant defense reactions, and are then called avirulence proteins. Proteinaceous effectors are referred to as Small Secreted Proteins (SSPs) as they mainly correspond to small proteins, potentially secreted, often cysteine-rich, with no homology to other known proteins in the databases (Stergiopoulos and de Wit, 2009). Effector genes of filamentous plant pathogens are often located close to dispersed transposable elements (TEs) or in TE-rich regions of the genome, such as dispensable chromosomes, subtelomeric regions or AT-isochores (Rouxel *et al.,* 2011; Sánchez-Vallet *et al.,* 2018). Analyses of transcriptomic data, generated at different stages of infection, over the course of infection in different pathosystems highlighted concerted waves of effector gene expression (Sánchez-Vallet *et al.,* 2018). The regulation of such sets of genes expressed concertedly during infection remains poorly understood. In fungi, a few transcription factors (TFs) have been identified as regulating expression of effector genes or secondary metabolites (for review, see Tan and Oliver, 2017). As effector or secondary metabolite encoding genes are often found in TE-rich compartments of the fungal genomes, histone modifying enzymes have recently been investigated for their role in effector gene regulation. Two different histone methylations typical for heterochromatin formation have attracted attention in fungi, the tri-methylation of the lysine 9 of histone H3 (H3K9me3) and the tri-methylation of the lysine 27 of histone H3 (H3K27me3), respectively deposited by KMT1 and KMT6. Recent studies tend to prove that these two histone methylransferases are able to control effector gene and secondary metabolite gene cluster expression in several plant-associated fungi (Connolly *et al.,* 2013; Chujo and Scott, 2014; Soyer *et al.,* 2014). *Leptosphaeria maculans* is an ideal model to study involvement of these histone modifications in the control of effector gene expression: (i) *L. maculans* is a hemibiotrophic fungus causing stem canker (blackleg disease) on oilseed rape. Its complex life cycle presents alternating phases of saprophytism, biotrophy and necrotrophy. It first infects oilseed rape leaves and undergo an asexual sporulation leading to leaf spots. Then, the fungus grows into the stem without visible symptom and finally provokes stem canker at the end of the oilseed rape growing season (Rouxel and Balesdent, 2005). (ii) The *L. maculans* genome displays a bipartite structure with gene-rich regions (GC-isochores) and transposable element (TE)-rich regions (AT-isochores). One hundred and twenty-two putative effector-encoding genes were predicted in its

genome, and regions enriched in histone modifications typical for heterochromatin are significantly found in such genes (Dutreux *et al.,* 2018; Gay *et al*., in prep.; Soyer *et al*., in prep., **Article 2, Chapter 1**). *L. maculans* expresses several waves of effector genes during infection (Rouxel *et al.,* 2011; Gervais *et al.,* 2017; Gay *et al.*, in prep.). Of particular interest, all known avirulence genes are expressed concertedly during asymptomatic stage occurring on both leaves and stems. Avirulence genes of *L. maculans* are specifically located in TE-rich regions, associated with H3K9me3 (Rouxel and Balesdent, 2017; Soyer *et al.*, in prep., **Chapter 1; Article 2**). In contrast, gene-rich regions contain three hundred and seven 'late' effector candidates, enriched in H3K27me3-domains and under-expressed in the early colonization stages and over-expressed in the infected stems (Gervais *et al.,* 2017; Soyer *et al.,* unpublished). In *L. maculans*, RNAi-silencing of *KMT1* led to an over-expression of more than 30% of the genes located in TE-rich environments, normally silenced *in vitro* in the WT strain, notably effector genes. ChIP-qPCR analyses showed that over-expression of at least two avirulence genes was associated with a decrease of the repressive histone modification H3K9me3 in the genomic environment of these genes (Soyer *et al.*, 2014). The silenced transformants used by Soyer *et al.* (2014) still expressed ~20% of *KMT1* which did not allow an in-depth investigation of a complete lack of H3K9me3 on the chromatin structure and gene expression. The CRISPR-Cas9 technology has recently been established for *L. maculans* to generate knock-out mutants (Idnurm *et al*., 2017). We used that technology to inactivate *KMT1*, and also *KMT6*, responsible for H3K27me3 deposition, since H3K27me3 domains were enriched in 'late' effector genes *in vitro*. We also generated *KMT1/KMT6* double mutant. Mutants were characterized for their ability to grow in axenic culture and *in planta*. Pathogenicity and effector gene expression was also assessed in the mutants and compared to the WT. In this study we present preliminary results on chromatin-based regulation of effector genes by two histone methylase, KMT1 and KMT6. Part of the results about KMT1 regulation are presented in the **chapter 3** (**Article 4**).

MATERIAL AND METHODS

Fungal culture

The reference isolate JN3 was used as host for genetic transformations (Balesdent *et al*., 2001). Fungal cultures and conidia production were performed as previously described (Ansan-Melayah *et al.,* 1995). For DNA/RNA extractions, mycelium was grown on V8-juice agar medium at 25°C in the dark for seven days and then plugs were transferred into 150 ml of Fries liquid medium in 500 ml Roux flasks. Tissues were harvested after growing for seven days at 25°C.

Pathogenicity and growth assays

Pathogenicity assays were performed on cotyledons of 15-day-old plantlets of a susceptible cultivar of *B. napus*, Es-Astrid. Plants were incubated in a growth chamber at 16/24°C (night/day) with a 16h photoperiod. Symptoms were scored on 10-12 plants, with two biological replicates, 13 days post inoculation (dpi) using the IMASCORE rating scale comprising six infection classes (IC), where IC1 to IC3 correspond to various levels of resistance of the plant and IC4 to IC6 to susceptibility (Balesdent *et al.*, 2001). Pathogenicity on adult plants was tested by infecting one-month old susceptible oilseed rape (Bristol) plants as described in Gervais *et al.* (2017). Growth assays were performed by deposition of a 5 mm plug at the center of 90 mm Petri dish (containing 20 ml of V8-juice

Université Paris-Saclay
Espace Technologique / Immeuble Discovery
Route de l'Orme aux Merisiers RD 128 / 91190 Saint-Aubin,
France

agar medium or MMII medium) and radial growth was measured nine days after incubation in a growth chamber (25°C) on four biological replicates. Statistical analyses were performed using Kruskal-Wallis test (Guo *et al.,* 2013)

DNA and RNA manipulation

For PCR, genomic DNA was extracted from conidia or from mycelium grown in Fries liquid culture with the DNAeasy 96 plant Kit (Qiagen S.A., Courtaboeuf, France). PCR amplifications were performed as previously described (Fudal *et al.,* 2007). To identify mutation arising in the sequence of the gene targeted by the CRISPR-Cas9 strategy, sequencing was performed by Eurofins Genomics (Anzinger, Ebersberg, Germany). Total RNA was extracted from mycelium grown for one week in Fries liquid medium, from cotyledons of Es-Astrid infected by *L. maculans* at seven dpi and from stems infected by *L. maculans* at 14 dpi as previously described (Fudal *et al.,* 2007). Total gDNA was extracted for biomass quantification from 28 days infected oilseed rape stems as described in Fudal *et al.* (2007) using alkaline phenol instead of acid phenol and treating with RNAse instead of DNAse.

Gene annotation and domain prediction

The KMT6 orthologue of *L. maculans* was identified by using the KMT6 protein from *N. crassa* (Jamieson *et al.*, 2013) and the NCBI BLAST program (Altschul *et al.,* 1990). Functional domains were identified using Pfam as described in Finn *et al.* (2014) (https://pfam.xfam.org/). Alignments were performed with COBALT (Papadopoulos and Agarwala, 2007).

Vector construction and fungal transformation

Vectors pLAU2 and pLAU53 conferring respectively hygromycin and geneticin resistance were used to perform CRISPR-Cas9 gene inactivation, as described by Idnurm *et al.* (2017). DNA fragments coding for guide RNA which target gene of interest were designed using the CRISPOR prediction tool and *L. maculans* as reference genome (http://crispor.tefor.net/; **Table S1**; Dutreux *et al*., 2018). The guide RNA were chosen not to match on any other genes. The DNA fragment coding for guide RNA was amplified using primers MAI0309 and MAI0310 and then inserted into the *Xho*I site of plasmid pLAU53 using Gibson assembly (**Table S1**; Silayeva and Barnes, 2018). Hence, plasmid pLAU53-KMT6 was generated to inactivate *KMT6*. pLAU2 containing *Cas9* gene was used without modification.

Complementation plasmids were obtained using pBht2 vector conferring resistance to hygromycin (Mullins *et al*., 2001). Native sequences of *KMT1* and *KMT6* were amplified with ComplKMT1_F, ComplKMT1_R, ComplKMT6_F, ComplKMT6_R primers using genomic DNA of JN3 isolate and then inserted into *Hind*III digested pBht2 using Gibson assembly (New England Biolabs; **Table S1**) to obtain pBht2-complKMT1 or pBht2-complKMT6 vectors.

The constructs were introduced into the *Agrobacterium tumefaciens* strain C58-pGV2260 by electroporation (1.5 kV, 200 ohms and 25 mF). *A. tumefaciens* mediated transformation (ATMT) of *L. maculans* was performed as previously described (Gout *et al.,* 2006). Transformants were plated on minimal medium complemented with geneticin (50 mg/l) for pLAU53-gRNA or hygromycin (50 mg/l) for pLAU2-Cas9 and cefotaxime (250 mg/l). For the CRISPR-Cas9 gene inactivation, construct containing Cas9 (pLAU2-Cas9) was first introduced into a WT strain JN3 and transformants were selected for hygromycin resistance. Transformants transformed with pLAU2-Cas9 construct were then

Université Paris-Saclay
Espace Technologique / Immeuble Discovery
Route de l'Orme aux Merisiers RD 128 / 91190 Saint-Aubin, France

transformed with pLAU53-gRNA directed against *KMT6*. Transformants were selected for geneticin, hygromycin and cefotaxime resistance. Mutations in the targeted gene were checked in the transformations by PCR amplifying with specific primers (**Table S1**) and sequencing.

Fungal crosses

Purifications in order to eliminate *Cas9* gene and guide RNA coding gene from CRISPR-Cas9 mutants were performed by crossing mutants with a WT isolate from the opposite mating type (**Table S2**). Crosses were performed as described in Balesdent *et al.* (2002). Progeny was harvested and plated on V8-juice agar medium. Mycelium was collected and DNA extracted. PCR and sequencing were performed to select progeny without *Cas9* and guide RNA which had integrated the CRISPR-Cas9 mutation.

Quantitative RT-PCR

Quantitative RT-PCR (qRT-PCR) were performed using a model CFX96 Real Time System (BIORAD; Hercules, CA, USA) and Absolute SYBR Green ROX dUTP Mix (ABgene, Courtaboeuf, France) as previously described (Fudal *et al.,* 2007). For each condition tested, two different RNA extractions from two different biological samples and two reverse transcriptions for each biological replicate were performed. Primers used for qRT-PCR are described in **Table S1**. Ct values were analyzed as described by Muller *et al.* (2002) or using the $2^{-\Delta\Delta Ct}$ method (Livak and Schittgen, 2001). *β-tubulin* was used as a constitutively expressed reference gene. Biomass of *L. maculans* in infected plants was analyzed by generating a standard curve with known concentrations of *L. maculans* and *B. napus* gDNA. Total gDNA was extracted from adult plants 28 dpi and a 10^{-1} dilution was used for qPCR. The Ct values obtained were reported on the standard curve in order to determine fungal and plant gDNA proportion.

Native Chromatin Immunoprecipitation (N-ChIP)

We subjected *L. maculans* to ‘‘native” ChIP (no crosslinking) and isolated mono- and dinucleosomes after digesting 150 mg of mycelium per sample with micrococcal nuclease (MNase) for 13 min at 37°C (Soyer *et al.,* 2015). For immunoprecipitation, three antibodies were used, against H3K9me3 and H3K27me3 (respectively Active Motif #39161 and Active Motif #39155). The Input material, i.e. the DNA extracted directly after digestion, was used to normalize data for qPCR, as described in Soyer *et al.* (2014).

Université Paris-Saclay
Espace Technologique / Immeuble Discovery
Route de l'Orme aux Merisiers RD 128 / 91190 Saint-Aubin, France

Western Blot

Total proteins were extracted from 10-100 mg lyophilized mycelium. Mycelium was ground using tungsten beads and Mixer Mill MM 400 (Retsch, Éragny, France). Total proteins were treated as described in Petit-Houdenot *et al.* (2019). Proteins were transferred on a PVDF membrane according to the manufacturer's protocol (Trans-Blot® Turbo™ Rapid Transfer System, BIORAD, Les-Ulis, France) using a small protein transfer program. The PVDF membrane was incubated in TBS 1X containing 5% milk, 0.05% tween 20 for one hour to saturate membrane. The membrane was then incubated at 4°C over-night in TBS 1% containing 0.05% Tween 20, milk 1% and H3K9me3 antibody (1:5000; 39062 ActiveMotif, La Hulpe, Belgium Germany). PVDF membrane was washed as described in Petit-Houdenot *et al.* (2019) and was then incubated in TBS 1X + 0.05% Tween 20 + milk 1% + antiRabbit IgG II^{R} (goat anti-rabbit, Santa Cruz Biotechnology, Heidelberg, Allemagne) and washed as previously. Finally, membrane was incubated 1min in 1 mL enzyme solution (Clarity™ Western ECL, BIORAD, Les-Ulis, France) and 1 mL Luminol/enhancer solution (Clarity™ Western ECL, BIORAD, Les-Ulis, France) and observed using ChemiDoc (ChemiDoc™ Imaging Systems, BIORAD, Les-Ulis, France).

Table 1: Effect of *Lmkmt1* inactivation and *LmPf2* inactivation or over-expression on in vitro growth. conidia production. pathogenicity and effector gene expression.

Isolates/ transformants[a]	radial growth 9 Days V8 (mm)	conidiation	Effector gene expression[d]			
			AvrLm6	AvrLm4-7	*Lmb_jn3_11364*	*Lmb_jn3_00284*
JN3	46 (±0.9)	normal	1	1	1	1
Δkmt1_A	50.25 (±1.9)	normal	9.70E-02 (± 0.22)	2.37E+02 (± 27)	4.78E-02 (±0.03)	9.16E-01(±0.06)
Δkmt6_A	49.5 (±1.8)	normal	1.01E+00 (±0.28)	6.87E-01 (±0.13)	5.25E-01 (± 0.01)	1.10E+00 (±0.08)
Δkmt6_B	54.8 (±0.6)	normal	4.78E-02 (± 0.01)	1.79E-02 (±0.01)	1.15E+00 (±	2.07E+00 (±0.018)
Δkmt1_Δkmt6	65 (±4.2)	normal	1.60E-01 (±0.12)	2.55E+02 (±6.91)	1.23E-01 (±0.01)	6.30E+00 (±0.05)
complKMT1 3	nd*	normal	nd*	nd*	nd*	nd*
complKMT6 9	nd*	normal	1.01E+00 (±0.32)	1.07E+00 (±0.25)	3.56E-01(± 0.02)	9.07E-01 (±0.05)

[a]JN3 corresponding to WT; *Δkmt1*_A is *KMT1* mutant; *Δkmt6*_A and *Δkmt6*_B are *KMT6* mutants; *Δkmt1/Δkmt6* is *KMT1 KMT6* double mutant obtained by crossing; ComplKMT1 3 and ComplKMT6 9 are complemented mutants of respectively *KMT1* and *KMT6*.
[b]Measured *in vitro* by RNA-Seq using TMM normalisation method and represented as RPKM. nd*: not-tested.

RESULTS

Identification of the *KMT6* orthologue in *Leptosphaeria maculans*

In order to analyze involvement of KMT6 in the regulation of gene expression, we first identified *KMT6* in *L. maculans*. The gene encoding KMT6 in *N. crassa* was identified by Jamieson *et al.* (2013) and phylogenetic analysis showed that an orthologue of *NcKMT6 (*Genbank Accession XP_965043.2) was found in *L. maculans* (Genbank Accession XP_003838658.1). This Genbank Accession corresponds to gene ID *Lmb_jn3_06106* located on SuperContig 6 (Dutreux *et al.,* 2018). A bidirectional Best Hit with BLASTp was performed to confirm orthology between NcKMT6 and LmKMT6 (**Figure 1A**). The *L. maculans LmKMT6* gene (hereafter referred to as *KMT6*) encodes a 1,342 amino acids

Université Paris-Saclay
Espace Technologique / Immeuble Discovery
Route de l'Orme aux Merisiers RD 128 / 91190 Saint-Aubin, France

protein sharing 26.3% identity with *NcKMT6*. The two domain CXC and SET are conserved in both proteins (IPS51633; IPS50280; **Figure 1A**).

We investigated the expression profile of *KMT6* during axenic culture and at different stages of primary infection of oilseed rape (**Figure 1B**). We observed that this gene is strongly expressed *in vitro* during mycelium growth and poorly expressed during *in planta* infection. In our previous study, we identified that *KMT1* is inversely regulated compared to avirulence genes (Clairet *et al.,* unpublished; **Chapter III, Article 4**).

KMT6, KMT1 and KMT1/KMT6 inactivations do not induce morphology or conidiation defect in *L. maculans*

In a previous study, we determined that *KMT1* inactivation did not lead to growth or conidiation defect in *L. maculans* (Clairet *et al.,* in prep.; **Chapter III; Article 4**). Inactivation of *KMT*6 was performed using the CRISPR-Cas9 strategy as detailed in the Materials and Methods. Twenty transformants resistant to hygromycin and geneticin were obtained and sequenced for the *KMT6* gene. Out of the 20 transformants, 17 had no mutations in the coding sequence of *KMT6* compared to the WT, two had a 10-bp and one had a 2-bp deletion near the cleavage site (**Figure S1**). These mutations resulted, at the protein level, in frame-shifts leading to two different truncated proteins: 372 amino-acids and 401 amino-acids respectively for the 10-bp and the 2-bp deletions compared to the 1,342 amino-acids length of the WT protein (**Figure S1**). The two mutants were crossed with JN2 in order to obtain purified *Δkmt6* mutants without *Cas9* and CRISPR guide RNA (**Table S2**). The two corresponding mutants are hereinafter referred to as *Δkmt6_A* and *Δkmt6_B* (A corresponding to the 10-bp and B to the 2-bp deletion). The two Δ*kmt6* mutants were able to produce as conidia as the WT after 14 days of growth on V8-juice agar medium (**Table 1**). *Δkmt6_A* was then crossed with JN2

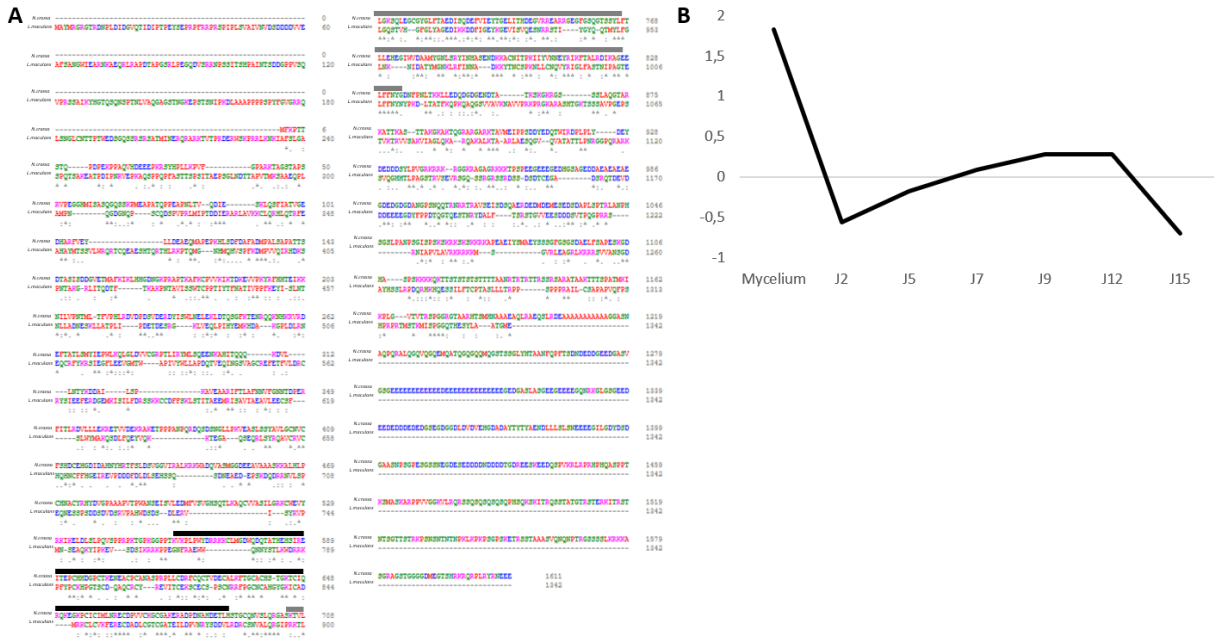

Figure 1: Identification of *KMT6* in *Leptosphaeria maculans*. A: Alignment between *KMT6* of *L. maculans* and *Neurospora crassa* was performed using COBALT (Papadopoulos and Agarwala, 2007). The black bar corresponds to the CXC domain and the grey bar corresponds to the SET domain, both identified using Pfam as described in Finn *et al.,* 2014 (https://pfam.xfam.org/). **B:** Mycelium was obtained by growing JN2 strain on V8 agar medium for 7 days. Cotyledons of the susceptible cultivar Darmor were inoculated by JN2 and sampled at 7 different time points (2, 5, 7, 9, 12 and 15 days post infection). Two biological replicates per condition were generated. Total RNA was extracted and sequenced. The expression level of *KMT6* in RNA-seq data is represented by the log2 of RPKM (Reads Per Kilobase Per Million mapped reads) (Gay *et al*., in prep.).

Université Paris-Saclay
Espace Technologique / Immeuble Discovery
Route de l'Orme aux Merisiers RD 128 / 91190 Saint-Aubin,
France

transformed with pLAU2-Cas9 and pLAUS3-KMT1. Progeny harboring the two mutations were used for subsequent analyses. We also verified that our *Δkmt1_Δkmt6* mutants were defective in H3K9me3 and H3K27me3 deposition (**Figure S1; Figure S2)**. After nine days of growth on V8-agar plate, no mutant showed growth defect indicating that KMT6 and KMT1/KMT6 deletions do not lead to growth defect. To summarize, no major defect in conidia production or growth rate was associated with the inactivation of *KMT6* or *KMT1/KMT6.*

H3K27me3 is not required for establishment of pathogenesis whereas H3K9me3 is crucial for infection establishment

After studying impact of H3K27me3 on *L. maculans* growth we wanted to investigate the impact both repressive mark H3K9me3 and H3K27me3 on pathogenicity. We previously identified that KMT1 via the deposition of H3K9me3 is crucial for pathogenesis establishment (Soyer *et al*., 2014; Clairet *et al.,* in prep.; **Chapter III; Article 4**). On the contrary, the two *Δkmt6_A* and *Δkmt6_B* mutants do not harbor any pathogenicity defect on susceptible cultivar Es-Astrid at 13 dpi (**Figure 2A, B**). The *Δkmt1_Δkmt6* double mutant produces even less symptoms on oilseed rape than *Δkmt1* (**Figure 2C**).

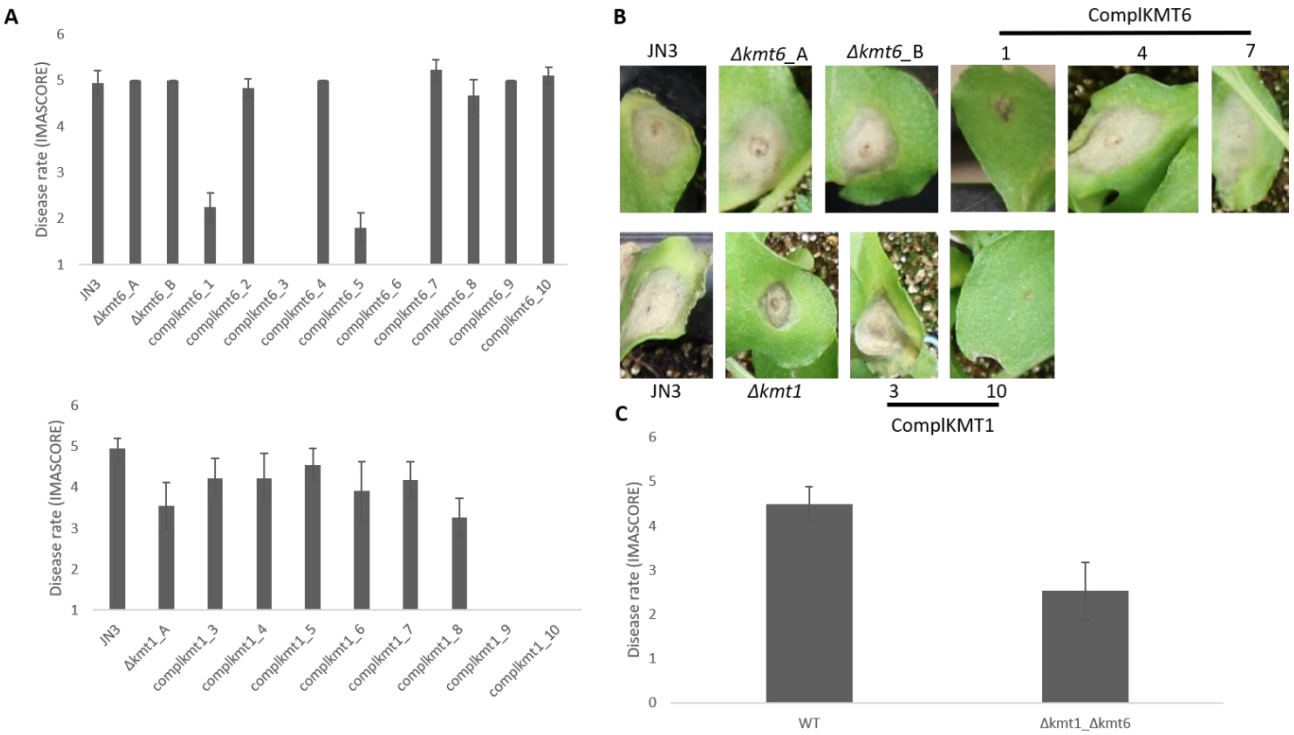

Figure 2: Effect of *Δkmt1* and *Δkmt6* inactivations on pathogenicity of *L. maculans*. A: pathogenicity assays of the selected mutants and complemented strains 14 days after inoculation on the susceptible cultivar Es-Astrid of *B. napus*. Results are expressed as a mean disease scoring using the IMASCORE rating scale comprising six infection classes (IC), where IC1 to IC3 correspond to various levels of resistance of the plant and IC4 to IC6 to susceptibility (Balesdent *et al.,* 2001). Error bars indicate the standard deviation of two biological and technical replicates. **B:** Photos of symptoms at 13 DPI on cotyledons infected by mutants, complemented mutants and WT strains. Each photo is representative of at least 24 inoculated plants. **C:** pathogenicity assays of *Δkmt1_Δkmt6* 14 days after inoculation on the susceptible cultivar Es-Astrid of *B. napus*. Results are expressed as the mean scoring using the IMASCORE rating scale as described in Balesdent *et al.* (2001). Error bars indicate the standard deviation of two biological and technical replicates.

We also infected adult plants with the mutants to study the relative impact of KMT1 and KMT6 on stem colonization. After 28 days post inoculation, fungal biomass was assessed to evaluate whether the mutants were able to colonize the stem. Plants infected with the *Δkmt1* strains contained from 5 to 10 times less fungal DNA than plants infected with the WT. Interestingly, adults plants infected with the *Δkmt6* strains contained between 1/3 and 1/2 less fungal gDNA than the plants infected with the WT. Plants infected with the *Δkmt1_Δkmt6* mutants contained even less *L. maculans* gDNA than plants infected with *Δkmt1* (**Figure 3**).

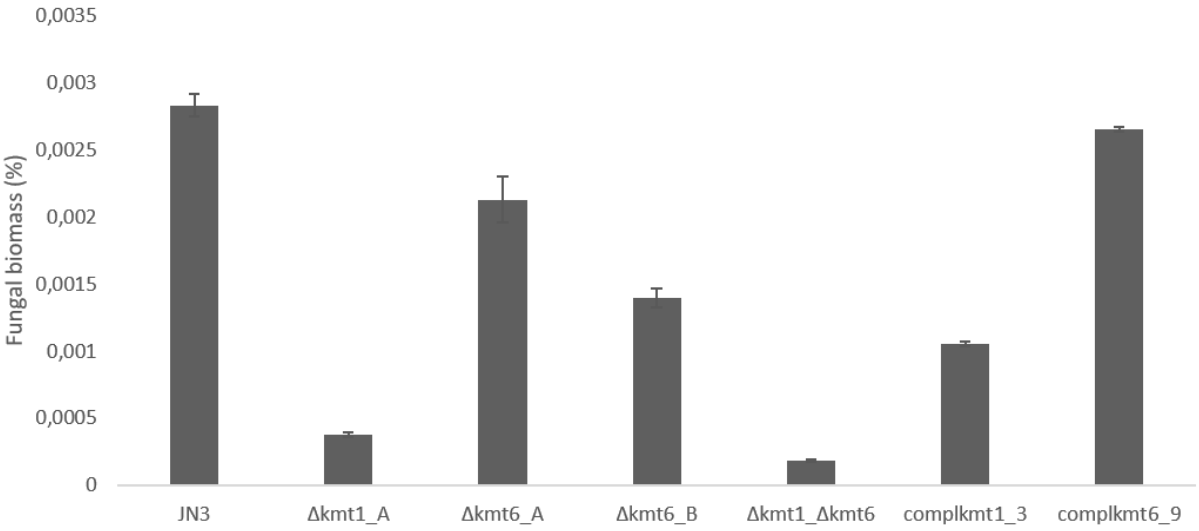

Figure 3: Effect of *KMT1* and *KMT6* inactivation on *L. maculans in planta* growth. 28 days old adult plants were inoculated with 10µL of a 10^7/mL conidia suspension as described in Gervais *et al.* (2017). Stems were then harvested after 28 days of infection and total DNA was extracted. Fungal biomass was measured by qPCR.

Effector gene expression is modified in *Δkmt1, Δkmt6* and *Δkmt1_Δkmt6* double mutants

Avirulence genes are usually not expressed during axenic growth and highly expressed during infection of cotyledons (Rouxel *et al*., 2011). Previous analyses showed these avirulence genes, located in the middle of large TE-rich regions, are associated with H3K9me3 *in vitro*, consistently with their low expression under this growth condition (Soyer *et al*., 2014; Soyer *et al*., in prep.). We measured expression of avirulence genes *AvrLm6* and *AvrLm4-7* and tardive genes *Lmb_jn3_11364* and *Lmb_jn3_00284 in vitro* in our different mutants during axenic culture. *AvrLm6* expression is not deregulated in any of the mutants (**Table 1**). Inactivation of *KMT1* increased expression of *AvrLm4-7* up to 200 times during *in vitro* growth as previously described in Clairet *et al.,* in prep. The *Δkmt1_Δkmt6* double mutant harbored the same *AvrLm4-7* up-regulation as in *Δkmt1* (**Table 1**). *Lmb_jn3_11364* and Lmb_jn3_00284 was reduced up to 20 time in *Δkmt1* and up-regulated up to 6 time in *Δkmt1_Δkmt6* while not altered in *Δkmt6* mutants (**Table 1**).

We measured expression of selected effector genes during early infection of cotyledons, in our different mutants, at 3, 7 and 13 dpi. We assessed expression of *AvrLm6* and *AvrLm4-7*, located in a H3K9me3-domain, and expression of two putative effector genes located in a H3K27me3-domains (*Lmb_jn3_00284* and *Lmb_jn3_11364*) and expressed respectively at 3 dpi of oilseed rape cotyledons and during stem infection. Inactivation of *KMT1* led to a 1.5-fold over-expression of *AvrLm4-7* and inactivation of *KMT6* increased twice its expression indicating that H3K9me3 is repressing *AvrLm4-7* expression whereas H3K27me3 is involved in correct expression of *AvrLm4-7*, but only *in planta*. The *Δkmt1_Δkmt6* double mutant did not express *AvrLm4-7*, indicating involvement of these two histone modifications in *AvrLm4-7* correct regulation (**Figure 4**). Interestingly *AvrLm6* expression was not altered by *KMT1* and *KMT6* inactivation whereas *KMT1/KMT6* double inactivation lead to four-time less expression of *AvrLm6* at 7 dpi compared to the WT indicating the involvement of these two histone modifications in *AvrLm6* correct regulation (**Figure 5**). The putative effector *Lmb_jn3_11364* is usually expressed in stems, during late stages of infection (Gervais *et al.*, 2017). Although located in a H3K27me3-domain *in vitro* (Soyer *et al.,* unpublished), inactivation of *KMT1* increased expression of this gene 40 times at 7 dpi. On the contrary, inactivation of *KMT6* did not modify expression of *Lmb_jn3_11364*. Finally, *Δkmt1_Δkmt6* double mutant was not able to express *Lmb_jn3_11364* (**Figure 6**). The *Lmb_jn3_00284* gene is expressed at early stage of infection (3 dpi). Inactivation of *KMT6* increased expression of *Lmb_jn3_00284* twice indicating that

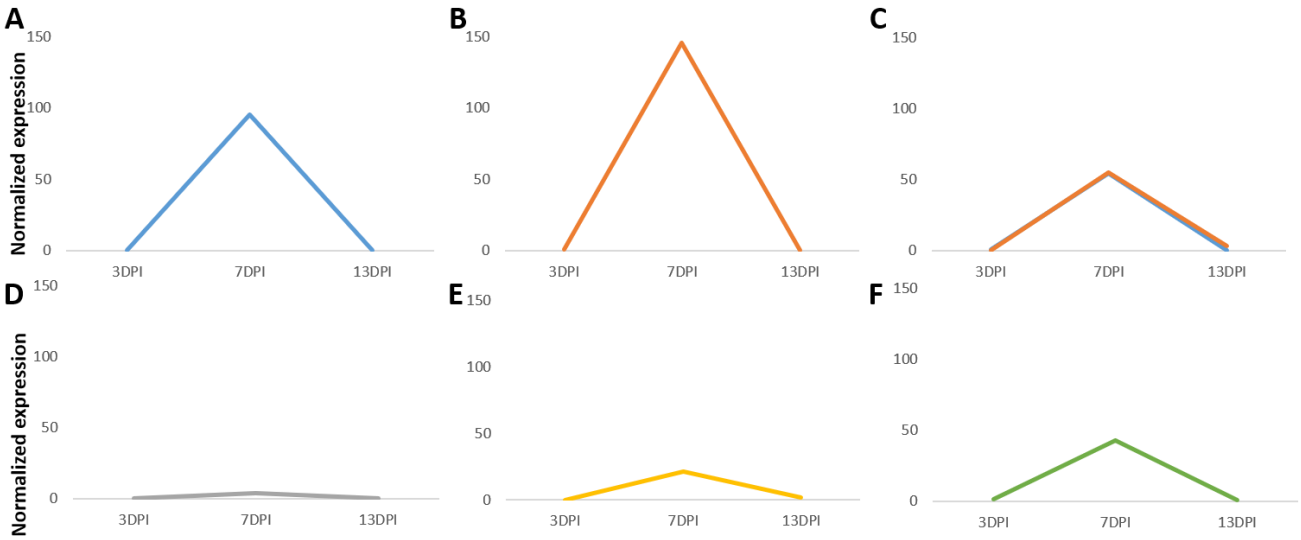

Figure 4: Effect of *KMT1*, *KMT6* and *KMT1-KMT6* deletions on *AvrLm4-7* expression pattern during early cotyledon colonization. Gene expression levels are relative to *Lmβtubulin* and calculated as described by Muller *et al.* (2002). Each value is the average of two biological replicates (two extractions from different biological replicates) and two technical replicates (two RT-PCR). Expression was measured at 3, 7 and 13 DPI. DPI= Days Post Inoculation. Expression profile (**A**) in the WT, (**B**)in the *Δkmt1* mutant, (**C**)**in** the *Δkmt6_A* and B, (**D**) in the *Δkmt1_ Δkmt6,* (**E**)in the ComplKMT1_3 and (**F**) in the ComplKMT6_9.

Université Paris-Saclay
Espace Technologique / Immeuble Discovery
Route de l'Orme aux Merisiers RD 128 / 91190 Saint-Aubin, France

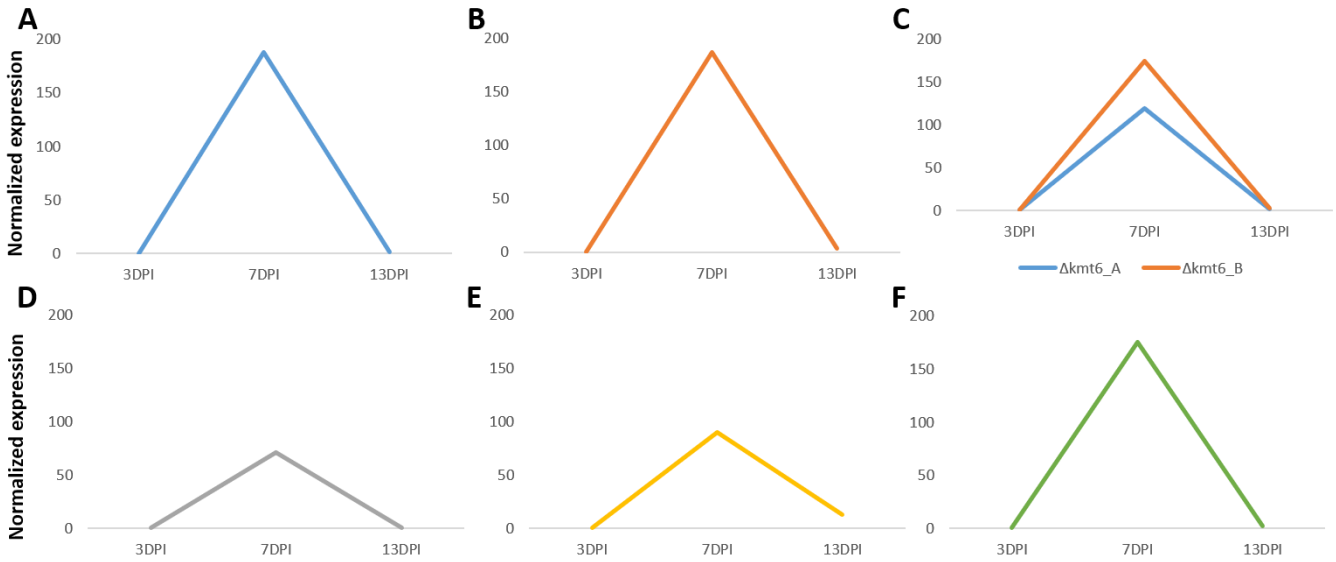

Figure 5: Effect of *KMT1*, *KMT6* and *KMT1-KMT6* deletion on *AvrLm6* expression pattern during early cotyledon colonization. Gene expression levels are relative to *Lmβtubulin* and calculated as described by Muller *et al.* (2002). Each value is the average of two biological replicates (two extractions from different biological replicates) and two technical replicates (two RT-PCR). Expression was measured at 3, 7 and 13 DPI. DPI= Days Post Inoculation. Expression profile (**A**) in the WT, (**B**)in the *Δkmt1* mutant, (**C**)in the *Δkmt6_A* and B, (**D**)in the *Δkmt1_ Δkmt6,* (**E**)in the ComplKMT1_3 and (**F**) in the ComplKMT6 9.

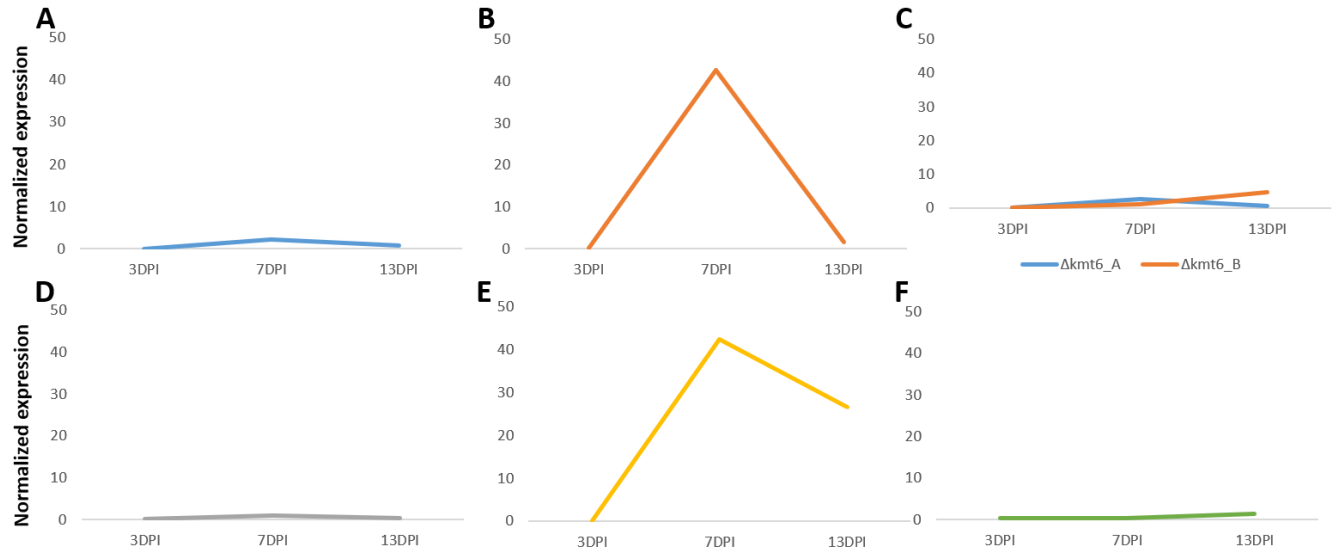

Figure 6: Effect of *KMT1*, *KMT6* and *KMT1-KMT6* deletion on *Lmb_jn3_11364* expression pattern during early cotyledon colonization. Gene expression levels are relative to *Lmβtubulin* and calculated as described by Muller *et al.* (2002). Each value is the average of two biological replicates (two extractions from different biological replicates) and two technical replicates (two RT-PCR). Expression was measured at 3, 7 and 13 DPI. DPI= Days Post Inoculation. Expression profile (**A**) in the WT, (**B**)in the *Δkmt1* mutant, (**C**)in the *Δkmt6_A* and B, (**D**)in the *Δkmt1_ Δkmt6,* (**E**)in the ComplKMT1_3 and (**F**) in the ComplKMT6_9.

H3K27me3 alone is able to repress *Lmb_jn3_00284*. Inactivation of *KMT1* had no effect on *Lmb_jn3_00284* expression (**Figure 7**). We previously determined that H3K9me3 is repressing avirulence gene expression during *in vitro* growth and that KMT1 is able to inhibit expression between 7 and 12 dpi of cotyledons (Clairet *et al.,* in prep.). To get further insight about role of KMT1 in the regulation of avirulence gene expression, we measured expression of four *AvrLm* genes in adult plants at 14 dpi of stems. As already reported, the four genes were not expressed during infection of the stem by the WT strain. Inactivation of *KMT1* induced expression of the four avirulence genes with an increase expression of up to 400 times in the mutants suggesting involvement of KMT1 in the repression of avirulence gene expression during the late stages of infection (**Figure 8**).

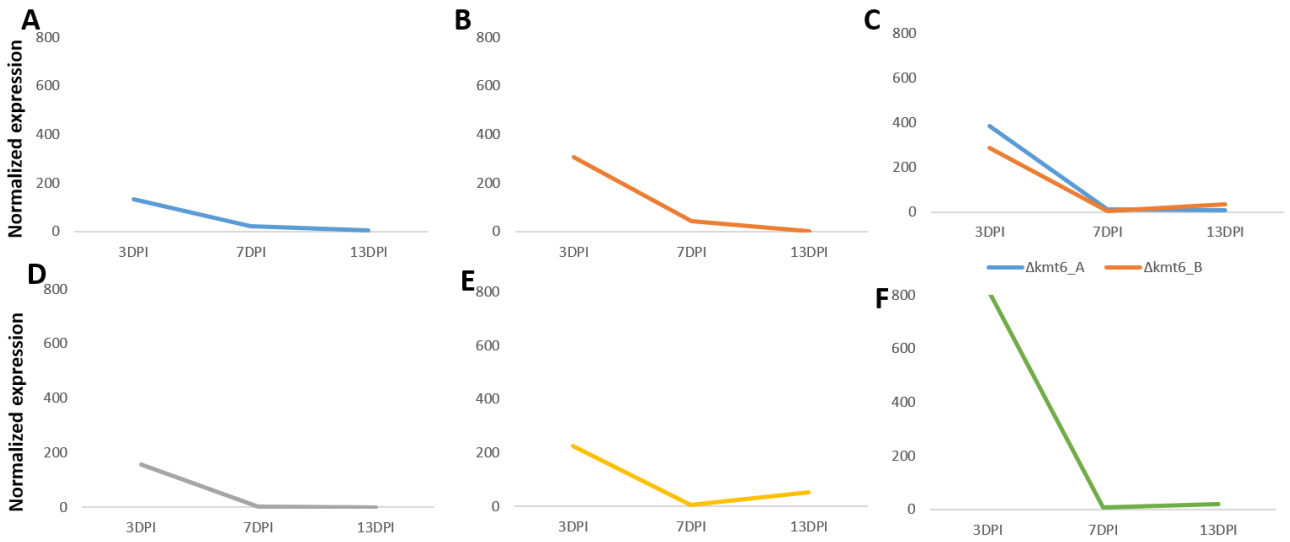

Figure 7: Effect of *KMT1*, *KMT6* and *KMT1-KMT6* deletion on *Lmb_jn3_00284* expression pattern during early cotyledon colonization. Gene expression levels are relative to *LmβtubuIin* and calculated as described by Muller *et al.* (2002). Each value is the average of two biological replicates (two extractions from different biological replicates) and two technical replicates (two RT-PCR). Expression was measured at 3, 7 and 13 DPI. DPI= Days Post Inoculation. Expression profile (**A**) in the WT, (**B**)in the *Δkmt1* mutant, (**C**)**in** the *Δkmt6_A* and B, (**D**)in the *Δkmt1_ Δkmt6,* (**E**)in the ComplKMT1_3 and (**F**) in the ComplKMT6_9.

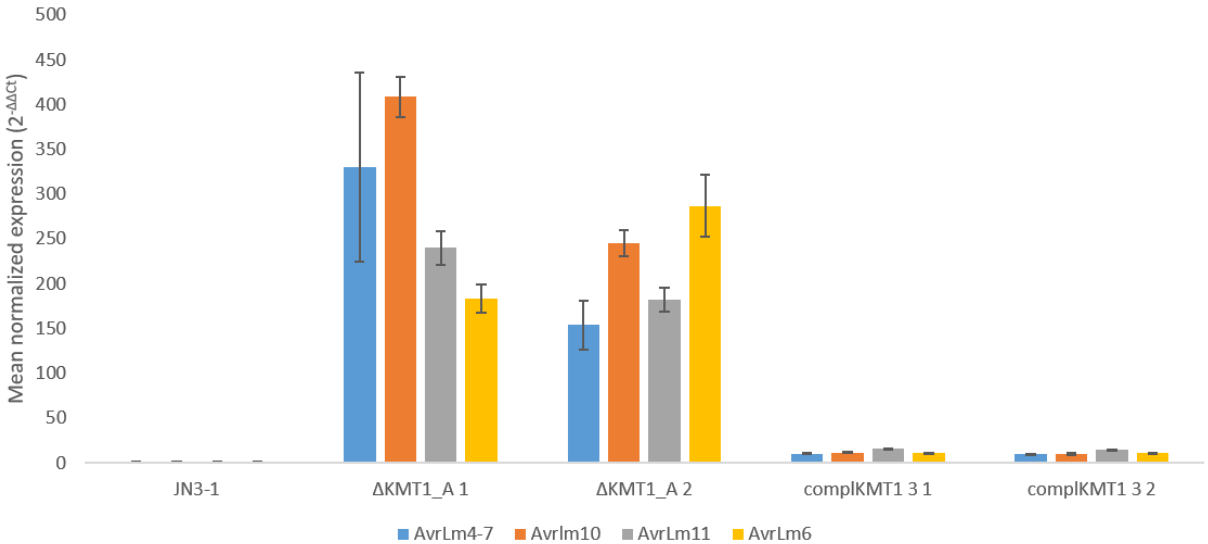

Figure 8: Effect of *KMT1* inactivation on avirulence gene expression during oilseed rape stem infection (cultivar Bristol) 14DPI. Expression of four avirulence genes was measured in the WT, *Δkmt1_A* and Compl*kmt1*_3 (complementation of *Δkmt1_A)*. Expression levels in each transformants is compared to the expression in the WT strain measured by RT-qPCR using *LmβTubulin* as a constitutive gene and using the $2^{-\Delta\Delta Ct}$ method (Livak and Schittgen, 2001). Error bars indicate the standard deviation of technical replicates.

Université Paris-Saclay
Espace Technologique / Immeuble Discovery
Route de l'Orme aux Merisiers RD 128 / 91190 Saint-Aubin,
France

Complementation of *KMT1* and *KMT6* restored the WT phenotype

Inactivated mutants were complemented using the WT genes inserted randomly in the purified mutants (**Table S1; Table S2**). This restored the ability of each protein to deposit H3K9me3 or H3K27me3 (**Figure S1**; **Figure S2**). The insertion of the WT version of the *KMT1* gene led to a partial complementation of the pathogenicity abilities. We selected two transformants, ComplKMT1_3 and ComplKMT6_9, which presented the closest pathogenicity and histone modifications phenotype to the WT (**Figure 2; Figure S1**; **Figure S2**). The two complemented transformants presented partially restored fungal biomasses during late infection on stem at 28 dpi (**Figure 3**). Interestingly, *KMT1* complementation led to *AvrLm4-7* and *AvrLm6* repression compared to the WT during cotyledon infection (**Figure 4, 5**). ComplKMT1_3 transformant also harbored altered *Lmb_jn3_11364* expression indicating that *KMT1* re-introduction do not restore correct expression (**Figure 6**). Intriguingly, Compl_KMT6_9 transformant presented *Lmb_jn3_00284* four times up-regulation indicating that *KMT6* re-introduction alter normal *Lmb_jn3_00284* expression which could be explained by the higher H3K27me3 deposition on *Lmb_jn3_00284* in ComplKMT6_9 than in the WT (**Figure 7; Figure S2**). Finally, ComplKMT1_3 transformants did not present avirulence gene up-regulation in stems at 14 dpi indicating that *KMT1* re-introduction lead to correct repression of avirulence gene between 7 dpi and 14 dpi (**Figure 8**).

DISCUSSION

Here we demonstrated that KMT1, via the deposition of H3K9me3, and KMT6, via the deposition of H3K27me3, are involved in the regulation of the expression of at least some effector genes and are key regulators of pathogenicity. On the contrary, no growth or conidiation defect were associated to loss of H3K9me3, H3K27me3 or both histone modifications.

KMT1 and KMT6 are not required for correct growth of *L. maculans*

KMT1 and KMT6 are crucial proteins in many organisms. They guarantee genome stability and integrity in *N. crassa*, *Z. tritici* and *E. festucea* (Connolly *et al*., 2013; Jamieson et al., 2013; Schotanus et al., 2015). Inactivation of *KMT1*, responsible for H3K9me3 deposition, resulted in relocation of H3K27me3 in sites normally enriched with H3K27me3 in *Z. trictici* and *N. crassa* (Basenko *et al.,* 2015; Möller et al., 2019). In contrast, lack of H3K27me3 increased stability of accessory chromosomes of Z. tritici (Möller *et al.,* 2019). In this study, we inactivated *KMT1*, *KMT6* and constructed the double *Δkmt1_Δkmt6* mutant. We did not identify any growth or conidiation defects in our mutants indicating that KMT1 and KMT6 are not crucial for correct growth of *L. maculans* during axenic culture.

KMT1 is essential for pathogenesis establishment whereas KMT6 inactivation does not alter *L. maculans* ability to produce symptoms on *B. napus*

We determined in this study that *KMT1* inactivation led to pathogenicity defects and deregulation of avirulence genes whereas *KMT6* inactivation had limited impact on pathogenicity and effector gene expression. *KMT1/KMT6* inactivation led to critical pathogenicity defects and effector gene deregulation indicating that H3K9me3 at least is critical for correct effector gene regulation. KMT1 and KMT6 are known to be able to regulate effector

Université Paris-Saclay
Espace Technologique / Immeuble Discovery
Route de l'Orme aux Merisiers RD 128 / 91190 Saint-Aubin,
France

genes and secondary metabolites gene clusters in several fungi (Gacek and Strauss, 2012; Connolly *et al.,* 2013; Chujo and Scott, 2014). Furthermore, previous studies on *L. maculans* determined that KMT1 was involved in the regulation of at least two avirulence genes (Soyer *et al.,* 2014; Clairet *et al.,* in prep). In this study, we confirmed the involvement of KMT1 is the control of *L. maculans* avirulence gene expression and determined that KMT6 is also involved in effector gene regulation but no clear involvement in the repression of avirulence gene expression. In addition, we previously determined that KMT1 is involved in the regulation of the switch between the asymptomatic colonization and the necrotrophic growth on oilseed rape cotyledons (Clairet *et al.,* in prep.; **Chapter III, Article 4**). In this study, we determined that in absence of H3K9me3, avirulence genes are not actively repressed during stem infection, and that *KMT1* complementation restored repression of these genes during stem infection.

Are H3K9me3 and H3K27me3 involved in the maintenance of genome stability in *L. maculans*?

H3K9me3- and H3K27me3-domains were recently reported for their ability to structure genome organization (Klocko *et al.,* 2016; Winter *et al.,* 2018). Furthermore, *KMT1* inactivation was associated to H3K27me3 re-localization and to genome organization destabilization in *N.crassa* and *Z. tritici* (Basenko *et al.,* 2015; Möller *et al.,* 2019). But impact of KMT1 and KMT6 on genome organization of filamentous fungi and especially on phytopathogenic fungi are poorly documented. In this study we will get cutting edge results about ability of two histone modifications to structure *L. maculans* genome and their impact on TADs (Transcriptionally Active Domains) regulation (Lanctôt *et al*., 2007). In *N. crassa,* constitutive heterochromatin domains were identified for their ability to interact together without the involvement of H3K9me3 modifications. On the contrary H3K27me3 is essential for genome stability in *N. crassa* (Klocko *et al.,* 2016). In Z. tritici, H3K27me3 have been demonstrated to be enriched in sub-telomeric compartment and to be essential to maintain interaction between telomeres and nuclear membrane. KMT1 inactivation in this species lead to massive H3K27me3 relocalisation at H3K9me3 loci leading to massive genome reorganization. At the contrary KMT6 inactivation induces limited chromosome rearrangement (Möller *et al.,* 2019). However, H3K27me3 in *Fusarium oxysporum* have been recently demonstrated to be chromatin niche for effector genes and to allow rapid evolution of this set of genes. Chromosome rearrangements can occur between core chromosomes and accessory chromosomes marked by H3K27me3 allowing rising and diversification of effector gene repertoire in two-speed genomes (Fokkens *et al.,* 2018).

ACCESSION NUMBERS

All sequenced reads have been deposited with the Short Read Archive under accession numbers XXXX.

REFERENCES

Altschul, S.F., Gish, W., Miller, W., Myers, E.W., Lipman, D.J., 1990. Basic local alignment search tool. Journal of Molecular Biology 215, 403–410.

Ansan-Melayah, D. (inra, Balesdent, M.H., Buee, M., Rouxel, T., 1995. Genetic characterization of AvrLm1, the first avirulence gene of Leptosphaeria maculans. Phytopathology (USA).

Université Paris-Saclay
Espace Technologique / Immeuble Discovery
Route de l'Orme aux Merisiers RD 128 / 91190 Saint-Aubin, France

Balesdent, M.H., Attard, A., Ansan-Melayah, D., Delourme, R., Renard, M., Rouxel, T., 2001. Genetic Control and Host Range of Avirulence Toward Brassica napus Cultivars Quinta and Jet Neuf in Leptosphaeria maculans. Phytopathology 91, 70–76.

Balesdent, M.H., Attard, A., Kühn, M.L., Rouxel, T., 2002. New Avirulence Genes in the Phytopathogenic Fungus Leptosphaeria maculans. Phytopathology 92, 1122–1133.

Basenko, E.Y., Sasaki, T., Ji, L., Prybol, C.J., Burckhardt, R.M., Schmitz, R.J., Lewis, Z.A., 2015. Genome-wide redistribution of H3K27me3 is linked to genotoxic stress and defective growth. Proceedings of the National Academy of Sciences 112, E6339–E6348.

Chujo, T., Scott, B., 2014. Histone H3K9 and H3K27 methylation regulates fungal alkaloid biosynthesis in a fungal endophyte-plant symbiosis: K9 and K27 methylation regulates symbiosis. Molecular Microbiology 92, 413–434.

Connolly, L.R., Smith, K.M., Freitag, M., 2013. The Fusarium graminearum Histone H3 K27 Methyltransferase KMT6 Regulates Development and Expression of Secondary Metabolite Gene Clusters. PLoS Genetics 9, e1003916.

Dutreux, F., Da Silva, C., d'Agata, L., Couloux, A., Gay, E.J., Istace, B., Lapalu, N., Lemainque, A., Linglin, J., Noel, B., Wincker, P., Cruaud, C., Rouxel, T., Balesdent, M.-H., Aury, J.-M., 2018. De novo assembly and annotation of three Leptosphaeria genomes using Oxford Nanopore MinION sequencing. Scientific Data 5.

Finn, R.D., Bateman, A., Clements, J., Coggill, P., Eberhardt, R.Y., Eddy, S.R., Heger, A., Hetherington, K., Holm, L., Mistry, J., Sonnhammer, E.L.L., Tate, J., Punta, M., 2014. Pfam: the protein families database. Nucleic Acids Res. 42, D222-230.

Fokkens, L., Shahi, S., Connolly, L.R., Stam, R., Schmidt, S.M., Smith, K.M., Freitag, M., Rep, M., 2018. The multi-speed genome of Fusarium oxysporum reveals association of histone modifications with sequence divergence and footprints of past horizontal chromosome transfer events. bioRxiv.

Fudal, I., Ross, S., Gout, L., Blaise, F., Kuhn, M.L., Eckert, M.R., Cattolico, L., Bernard-Samain, S., Balesdent, M.H., Rouxel, T., 2007. Heterochromatin-Like Regions as Ecological Niches for Avirulence Genes in the *Leptosphaeria maculans* Genome: Map-Based Cloning of *AvrLm6*. Molecular Plant-Microbe Interactions 20, 459–470.

Gacek, A., Strauss, J., 2012. The chromatin code of fungal secondary metabolite gene clusters. Appl Microbiol Biotechnol 95, 1389–1404.

Gervais, J., Plissonneau, C., Linglin, J., Meyer, M., Labadie, K., Cruaud, C., Fudal, I., Rouxel, T., Balesdent, M.-H., 2017. Different waves of effector genes with contrasted genomic location are expressed by Leptosphaeria maculans during cotyledon and stem colonization of oilseed rape. Molecular plant pathology 18, 1113–1126.

Gout, L., Fudal, I., Kuhn, M.-L., Blaise, F., Eckert, M., Cattolico, L., Balesdent, M.-H., Rouxel, T., 2006. Lost in the middle of nowhere: the AvrLm1 avirulence gene of the Dothideomycete Leptosphaeria maculans. Molecular Microbiology 60, 67–80.

Guo, S., Zhong, S., Zhang, A., 2013. Privacy-preserving Kruskal-Wallis test. Comput Methods Programs Biomed 112, 135–145.

Idnurm, A., Urquhart, A.S., Vummadi, D.R., Chang, S., Van de Wouw, A.P., López-Ruiz, F.J., 2017. Spontaneous and CRISPR/Cas9-induced mutation of the osmosensor histidine kinase of the canola pathogen Leptosphaeria maculans. Fungal Biology and Biotechnology 4.

Université Paris-Saclay
Espace Technologique / Immeuble Discovery
Route de l'Orme aux Merisiers RD 128 / 91190 Saint-Aubin, France

Jamieson, K., Rountree, M.R., Lewis, Z.A., Stajich, J.E., Selker, E.U., 2013. Regional control of histone H3 lysine 27 methylation in Neurospora. Proceedings of the National Academy of Sciences 110, 6027–6032.

Klocko, A.D., Ormsby, T., Galazka, J.M., Leggett, N.A., Uesaka, M., Honda, S., Freitag, M., Selker, E.U., 2016. Normal chromosome conformation depends on subtelomeric facultative heterochromatin in Neurospora crassa. PNAS 113, 15048–15053.

Lanctôt, C., Cheutin, T., Cremer, M., Cavalli, G., Cremer, T., 2007. Dynamic genome architecture in the nuclear space: regulation of gene expression in three dimensions. Nature Reviews Genetics 8, 104–115.

Livak KJ, Schmittgen TD. Analysis of relative gene expression data using real-time quantitative PCR and the 2(-Delta Delta C(T)) Method. Methods. 2001 25:402-408.

Lo Presti, L., Lanver, D., Schweizer, G., Tanaka, S., Liang, L., Tollot, M., Zuccaro, A., Reissmann, S., Kahmann, R., 2015. Fungal Effectors and Plant Susceptibility. Annual Review of Plant Biology 66, 513–545.

Lo Presti, L., Kahmann, R., 2017. How filamentous plant pathogen effectors are translocated to host cells. Current Opinion in Plant Biology 38, 19–24.

Möller, M., Schotanus, K., Soyer, J., Haueisen, J., Happ, K., Stralucke, M., Happel, P., Smith, K.M., Connolly, L.R., Freitag, M., Stukenbrock, E.H., 2019. Destabilization of chromosome structure by histone H3 lysine 27 methylation.

Muller, P.Y., Janovjak, H., Miserez, A.R., Dobbie, Z., 2002. Processing of gene expression data generated by quantitative real-time RT-PCR. BioTechniques 32, 1372–1374, 1376, 1378–1379.

Mullins, E.D., Chen, X., Romaine, P., Raina, R., Geiser, D.M., Kang, S., 2001. Agrobacterium-Mediated Transformation of Fusarium oxysporum: An Efficient Tool for Insertional Mutagenesis and Gene Transfer. Phytopathology 91, 173–180.

Papadopoulos, J.S., Agarwala, R., 2007. COBALT: constraint-based alignment tool for multiple protein sequences. Bioinformatics 23, 1073–1079.

Petit-Houdenot, Y., Degrave, A., Meyer, M., Blaise, F., Ollivier, B., Marais, C.-L., Jauneau, A., Audran, C., Rivas, S., Veneault-Fourrey, C., Brun, H., Rouxel, T., Fudal, I., Balesdent, M.-H., 2019. A two genes - for - one gene interaction between Leptosphaeria maculans and Brassica napus. New Phytol. 223, 397–411.

Rouxel, T., Balesdent, M.H., 2005. The stem canker (blackleg) fungus, Leptosphaeria maculans, enters the genomic era. Molecular Plant Pathology 6, 225–241.

Rouxel, T., Grandaubert, J., Hane, J.K., Hoede, C., van de Wouw, A.P., Couloux, A., Dominguez, V., Anthouard, V., Bally, P., Bourras, S., Cozijnsen, A.J., Ciuffetti, L.M., Degrave, A., Dilmaghani, A., Duret, L., Fudal, I., Goodwin, S.B., Gout, L., Glaser, N., Linglin, J., Kema, G.H.J., Lapalu, N., Lawrence, C.B., May, K., Meyer, M., Ollivier, B., Poulain, J., Schoch, C.L., Simon, A., Spatafora, J.W., Stachowiak, A., Turgeon, B.G., Tyler, B.M., Vincent, D., Weissenbach, J., Amselem, J., Quesneville, H., Oliver, R.P., Wincker, P., Balesdent, M.-H., Howlett, B.J., 2011. Effector diversification within compartments of the Leptosphaeria maculans genome affected by Repeat-Induced Point mutations. Nature Communications 2.

Rouxel, T., Balesdent, M.-H., 2017. Life, death and rebirth of avirulence effectors in a fungal pathogen of Brassica crops, Leptosphaeria maculans. New Phytol. 214, 526–532.

Sánchez-Vallet, A., Fouché, S., Fudal, I., Hartmann, F.E., Soyer, J.L., Tellier, A., Croll, D., 2018. The Genome Biology of Effector Gene Evolution in Filamentous Plant Pathogens. Annual Review of Phytopathology 56, 21–40.

Schotanus, K., Soyer, J.L., Connolly, L.R., Grandaubert, J., Happel, P., Smith, K.M., Freitag, M., Stukenbrock, E.H., 2015. Histone modifications rather than the novel regional centromeres of Zymoseptoria tritici distinguish core and accessory chromosomes. Epigenetics & Chromatin 8, 41.

Silayeva, O., Barnes, A.C., 2018. Gibson Assembly facilitates bacterial allelic exchange mutagenesis. J. Microbiol. Methods 144, 157–163.

Soyer, J.L., El Ghalid, M., Glaser, N., Ollivier, B., Linglin, J., Grandaubert, J., Balesdent, M.-H., Connolly, L.R., Freitag, M., Rouxel, T., Fudal, I., 2014. Epigenetic Control of Effector Gene Expression in the Plant Pathogenic Fungus Leptosphaeria maculans. PLoS Genetics 10, e1004227.

Soyer, J.L., Möller, M., Schotanus, K., Connolly, L.R., Galazka, J.M., Freitag, M., Stukenbrock, E.H., 2015. Chromatin analyses of Zymoseptoria tritici: Methods for chromatin immunoprecipitation followed by high-throughput sequencing (ChIP-seq). Fungal Genet. Biol. 79, 63–70.

Stergiopoulos, I., de Wit, P.J.G.M., 2009. Fungal Effector Proteins. Annual Review of Phytopathology 47, 233–263. https://doi.org/10.1146/annurev.phyto.112408.132637 Tamaru, H., Selker, E.U., 2001. A histone H3 methyltransferase controls DNA methylation in Neurospora crassa. Nature 414, 277.

Tan, K.-C., Oliver, R.P., 2017. Regulation of proteinaceous effector expression in phytopathogenic fungi. PLoS pathogens 13, e1006241.

Winter, D.J., Ganley, A., Young, C., Liachko, I., Schardl, C., Dupont, P., Berry, D., Ram, A., Scott, B., Cox, M., 2018. Repeat elements organize 3D genome structure and mediate transcription in the filamentous fungus Epichloë festucae. bioRxiv 339010.

Université Paris-Saclay
Espace Technologique / Immeuble Discovery
Route de l'Orme aux Merisiers RD 128 / 91190 Saint-Aubin, France

406 **SUPPLEMENTARY DATA**

407

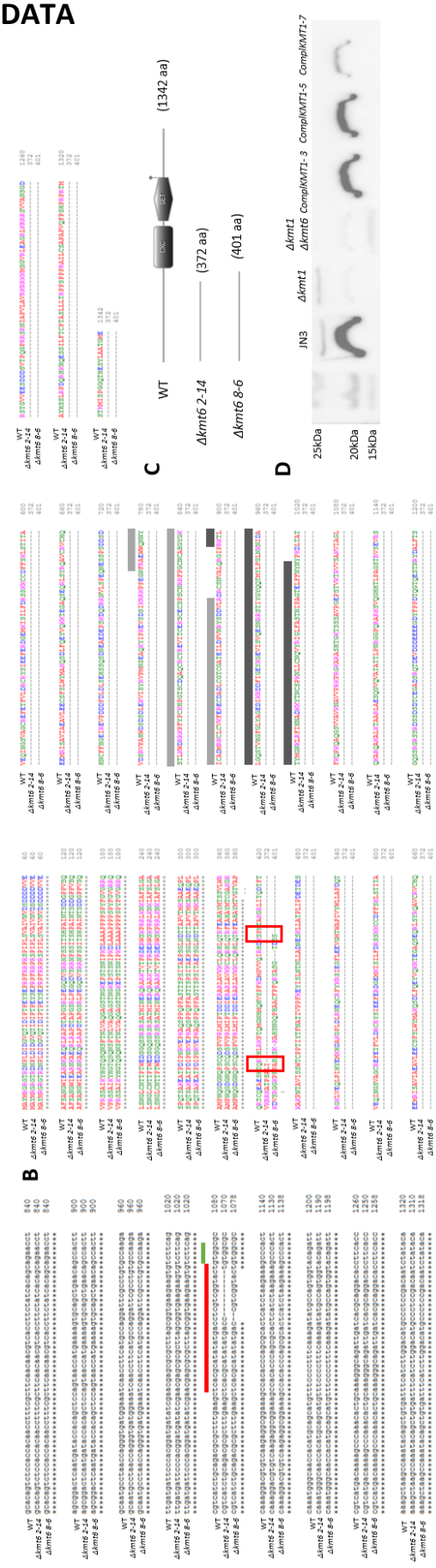

Figure S1: Effect of *Δkmt6* mutations on KMT6 protein structure and impact of kmt1 complementation on KMT1 activity. A Sequence alignment of the *KMT6* gene in the WT isolates JN2 and in two mutants Δkmt6 2-14 and 8-6 showing respectively a 10bp and 2bp deletion). The PAM (Protospacer Adjacent Motif) is highlighted in green and the region targeted by the guide RNA is highlighted in red **B:** Protein sequence of KMT6 in the WT isolate JN2 and in the two mutants. The red frame highlights the stop in the two mutant version of the protein. The WT version of the protein is 1342 aa long. Light grey bar and dark grey bar indicating respectively CXC and SET domains. **C:** KMT6 protein domains obtained with Pfam as described in Finn *et al.*, 2014 (https://pfam.xfam.org/). **D:** Western Blot analysis of H3K9 tri-methylation in JN3 (WT), *Δkmt1*, *Δkmt1_ Δkmt6* and different *kmt1* complemented strains. Nuclear protein samples were extracted from mycelium, separated by SDS-PAGE, blotted and probed with antibodies against H3K9me3.

Université Paris-Saclay
Espace Technologique / Immeuble Discovery
Route de l'Orme aux Merisiers RD 128 / 91190 Saint-Aubin, France

408

409

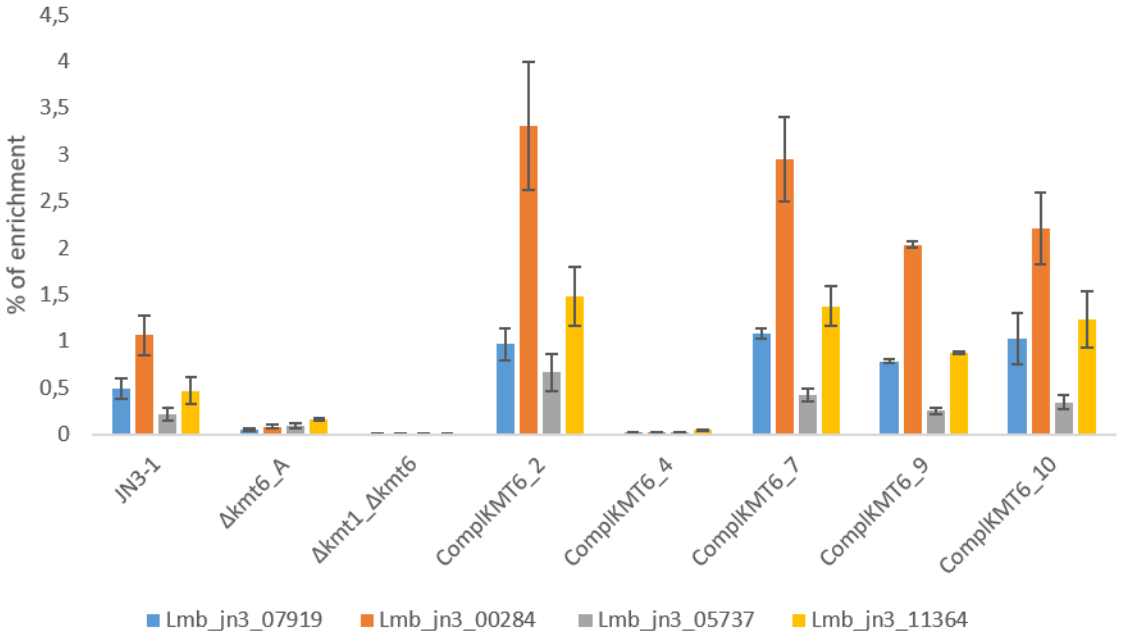

Figure S2: Trimethylation of lysine 27 of histone H3 (H3K27me3) is abolished in *Δkmt6* and *Δkmt1_Δkmt6* backgrounds and recovered in complemented 2, 7, 9 and 10 transformants. Chromatin immunoprecipitation analysis was performed to assess changes in the heterochromatic H3K27me3 mark in 'late' effector genes known to be in H3K27me3 environment in WT strain. We used avirulence genes as a negative control of H3K27me3 enrichment. Data were normalized using the ''percent of input'' method. Error bars indicate the standard deviation of two biological and technical replicates.

Université Paris-Saclay
Espace Technologique / Immeuble Discovery
Route de l'Orme aux Merisiers RD 128 / 91190 Saint-Aubin, France

Table S1: Primers used in this study

Name of the fragment	DNA sequence	function	construction
gRNA against KMT1	GAAACCTAATCAATCAACGGAGCACTGATGAGTCCGTGAGGACGAAACGAGTAAGCTCGTCTGCTCCCTTCGAACGTCTGCGTTTTAGAGCTAGAAATAGC	KMT1 CRISPR-CAS9 directed inactivation	CRISPR-CAS9 inactivation
gRNA against KMT6	GAAACCTAATCAATCAACGCGTGACTGATGAGTCCGTGAGGACGAAACGAGTAAGCTCGTCTCACGCATATATGACCTCGTGTTTTAGAGCTAGAAATAGC	KMT6 CRISPR-CAS9 directed inactivation	
MAI0309	ACCTCTAATCGAAACCTAATCAATCAAC	Amplification of gRNA coding sequence	
MAI0310	ATTTTAACTTGCTATTTCTAGCTCTAAAAC	Amplification of gRNA coding sequence	
verif_CRISPR_KMT1_F	GCCCTCCATGGTTGTGGTGC	KMT1 mutation detection	
verif_CRISPR_KMT1_R	ACCCCGGAAATGCTAGCCGA	KMT1 mutation detection	
verif_CRISPR_KMT6_F	GCGCGCTTAGCGGTGAAGAA	KMT6 mutation detection	
verif_CRISPR_KMT6_R	AGAGCCGTGGCAAGCTCGTA	KMT6 mutation detection	
Compl_KMT1_F	AGTCGACCTGCAGGCATGCACGAATGGGAAACTTTTCTGG	KMT1 amplification	gene complementation
Compl_KMT1_R	GTAAAACGACGGCCAGTGCCAACCTCCCTCGGATACTTTCTAC	KMT1 amplification	
Compl_2_KMT6_F	AGTCGACCTGCAGGCATGCATTCCTCGGGGCCCACACTAC	KMT6 amplification	
Compl_2_KMT6_R	GTAAAACGACGGCCAGTGCCAACCCGTGGCAGCAAGGTAGGA	KMT6 amplification	
verif_KMT6_F1	CATGATCAACGAAAGACAGC	KMT6 sequence verification	
verif_KMT6_F2	GGCTGTCGAGAATTTGAGAC	KMT6 sequence verification	
verif_KMT6_F3	CAATAGGTACAGTGACGACG	KMT6 sequence verification	
verif_KMT1_F1	TCGACTGGACAGGAGAAGCG	KMT1 sequence verification	
verif_KMT1_F2	GTATTGCCGGAACAAGAATG	KMT1 sequence verification	
βTubulin_F	AAGAACTCATCCTACTTCGA	qPCR	None
βTubulin_R	TGAATAGCTCCTGAATGG	qPCR	None
AvrLm4-7_F	GCCCTGCATAACTACCGAC	qPCR	None
AvrLm4-7_R	TCCTGGCCAAATATAACTCC	qPCR	None
AvrLm6_F	AAACGGCACTATTACGAAAA	qPCR	None
AvrLm6_R	GATTAGGCGAGAAGCAAGT	qPCR	None
AvrLm10.A_F	ACAGGAGAACACTGACGGCT	qPCR	None
AvrLm10.A_R	GCATGGACTATCGTAGCGTTAT	qPCR	None
AvrLm11_F	TGCGTTTCTTGCTTCCTATATTT	qPCR	None
AvrLm11_R	CAAGTTGGATCTTTCTCATTCG	qPCR	None
Lmb_jn3_11364_F	TACTGGCTGTCTTTGCTGC	qPCR	None
Lmb_jn3_11364_R	CCGCCACAGTGAACATAAT	qPCR	None
Lmb_jn3_00284_F	ACCTTCCCACACGAAACC	qPCR	None
Lmb_jn3_00284_R	CAGCCAGCTCCGCTTTTA	qPCR	None
Lmb_jn3_07919_F	ATCGCCATCCTCTCCCTT	qPCR	None
Lmb_jn3_07919_R	ACTCAGCGTTACCAGCCTC	qPCR	None
Lmb_jn3_05737_F	ACAATGTGGAGGACAAGAAG	qPCR	None
Lmb_jn3_05737_R	AGTAGTTGGGAAGAGTGACAG	qPCR	None
ActinBn_F	TCCCTCAGCACTTTCCAAC	qPCR	None
ActinBn_R	TTCAATCCCCATCTCAACAA	qPCR	None

Université Paris-Saclay
Espace Technologique / Immeuble Discovery
Route de l'Orme aux Merisiers RD 128 / 91190 Saint-Aubin, France

411

Table S2: Strains used for mutant purification.

		Purification (Crosses)			
	CRISPR-CAS9 mutation	**JN2**[a]	**JN2-GFP**[b]	**selected progeny**[c]	**Additional Transformation**[d]
Δkmt1 6-1	1 bp insertion	yes	yes	*Δkmt1_A* *Δkmt1_A*-GFP	complementation
Δkmt6 2-14	10pb deletion	yes	yes	*Δkmt6*_A *Δkmt6_A*-GFP	complementation
Δkmt6 8-6	2pb deletion	no	yes	*Δkmt6_B*-GFP *Δkmt6_B*-GFP	no
Δkmt1_Δkmt6 60-1	2pb deletion *KMT1* and 10pb del *KMT6*	no	yes	*Δkmt1/Δkmt6*	no

a: Purification by crossing with an isolate of opposite mating type with or without GFP. b: Selected progenies purified (without *Cas9* and gRNA). b: Second round of purification by crossing with JN2-GFP to obtain purified-GFP mutants. c: Names of the selected purified (without Cas9 and gRNA) descendants. d: Transformation on purified transformants (after all purification rounds).

412 ## FUNDING

413 This work was supported by the Plant Health and Environment division of the French National Institute for Agricultural
414 Research [Chromadyn Project AAP 2018].

415 ## CONFLICT OF INTEREST

416 The authors declare no conflict of interest.

417

418

419

420

421

422 # RESULTATS COMPLEMENTAIRES

Analyse fonctionnelle de KDM8, histone déméthylase putative spécifique de H3K36me2

Certaines protéines sont capables de retirer les modifications chimiques des queues d'histones et ainsi de réguler l'expression génique (Kronholm *et al.,* 2016), et certaines déméthylases ont été identifiées comme régulatrice de processus infectieux. Il a notamment été montré que certaines déméthylases d'histones étaient impliquées dans le contrôle du métabolisme secondaire chez certains champignons filamenteux. C'est le cas de KdmA et KdmB, responsables respectivement de l'enlèvement d'une marques répressive, H3K9me3, et d'une marque activatrice, H3K4me3, jouent un rôle dans la régulation du switch entre métabolisme primaire et secondaire chez *Aspergillus nidulans* (Gacek-Matthews *et al.,* 2015 ; Gacek-Matthews *et al.,* 2016). Parmi les sept déméthylases d'histones prédites chez *L. maculans* (Pratx and Zurletto, Pers. Comm), Kmd8, est spécifiquement sur-exprimée pendant les étapes précoces de l'infection de cotylédons de colza (**Figure 1**). Son homologue chez *B. cinerea, BcKdm1* (42 % identité) a été identifiée comme impliquée dans de nombreux processus physiologiques et notamment dans la pénétration de l'hôte (Schumacher *et al.,* 2019). Pour étudier son implication dans la régulation des gènes codant des effecteurs, j'ai réalisé une mutagénèse dirigée en utilisant la technique CRISPR-Cas9 contre le gène codant cette protéine. J'ai ainsi identifié deux mutants indépendants, ayant respectivement 2 et 3 pb délétées dans la partie 5' du gène. L'une des délétions entraîne au niveau protéique la perte du domaine fonctionnel Jumonji de la protéine, alors que la seconde délétion n'entraine qu'une perte d'un acide aminé et ne modifie que très légèrement la séquence protéique (**Figure 2**). J'ai ensuite croisé les mutants ainsi obtenus avec une souche sauvage pour éliminer le gène codant la Cas9 et l'ARN guide. Les mutants purifiés ont été respectivement nommés *ΔKdm8_A* et *ΔKdm8_B.* J'ai ensuite caractérisé les mutants pour leur croissance et leur pathogénie sur cultivar sensible de colza (**Figure 3**). Aucun défaut de pathogénie ou croissance

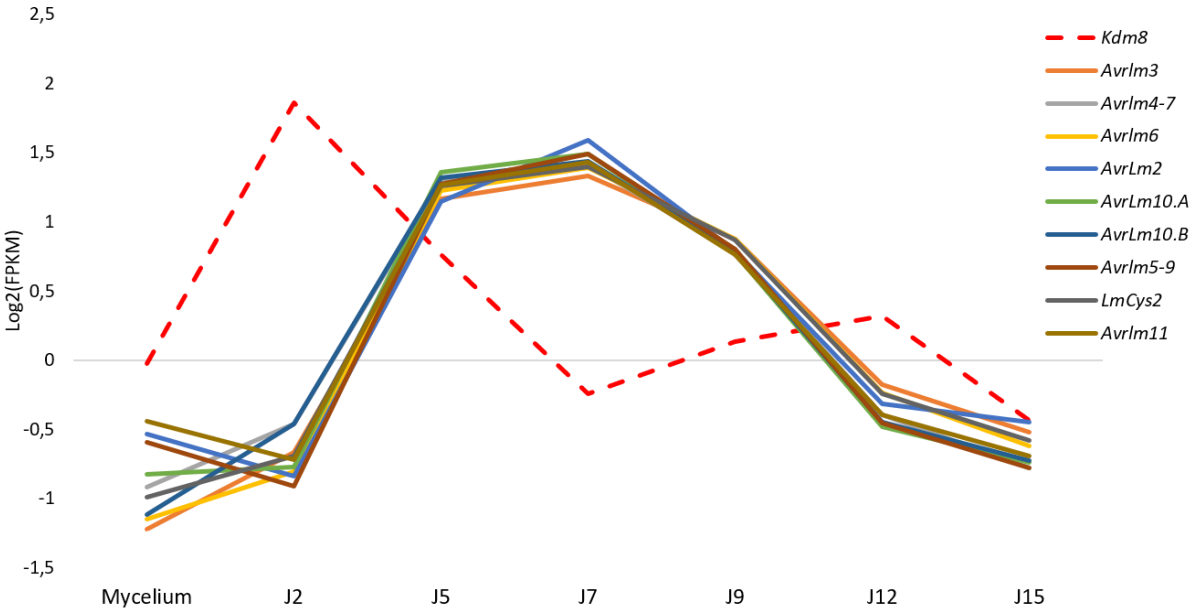

Figure 1: Expression profile of *Leptosphaeria maculans* avirulence genes and *Kdm8* during axenic growth and infection of oilseed rape cotyledons. Mycelium was obtained by growing JN2 strain on V8-agar medium for 7 days. Cotyledons of the susceptible cultivar Darmor were inoculated by JN2 and sampled at seven different time points (2, 5, 7, 9, 12 and 15 days post infection). Two biological replicates per condition were generated. Total RNA was extracted and sequenced. The expression level of eight avirulence genes and *Kdm8* is represented by the log2 of FPKM (Fragments Per Kilobase per Million mapped reads) (Gay *et al*., ongoing thesis).

Université Paris-Saclay
Espace Technologique / Immeuble Discovery
Route de l'Orme aux Merisiers RD 128 / 91190 Saint-Aubin,
France

n'a été observé. Nous avons ensuite cherché à savoir si le mutant *ΔKdm8_6* ayant perdu le domaine fonctionnel de Kdm8, était affecté pour l'expression de gènes codant des effecteurs *in vitro* et *in planta*. J'ai donc testé par RT-qPCR l'expression de différents gènes codant effecteurs pendant la croissance axénique et pendant l'infection primaire. Je n'ai mis en évidence aucune altération d'expression des effecteurs testés (**Figures 4** et **5**).

423

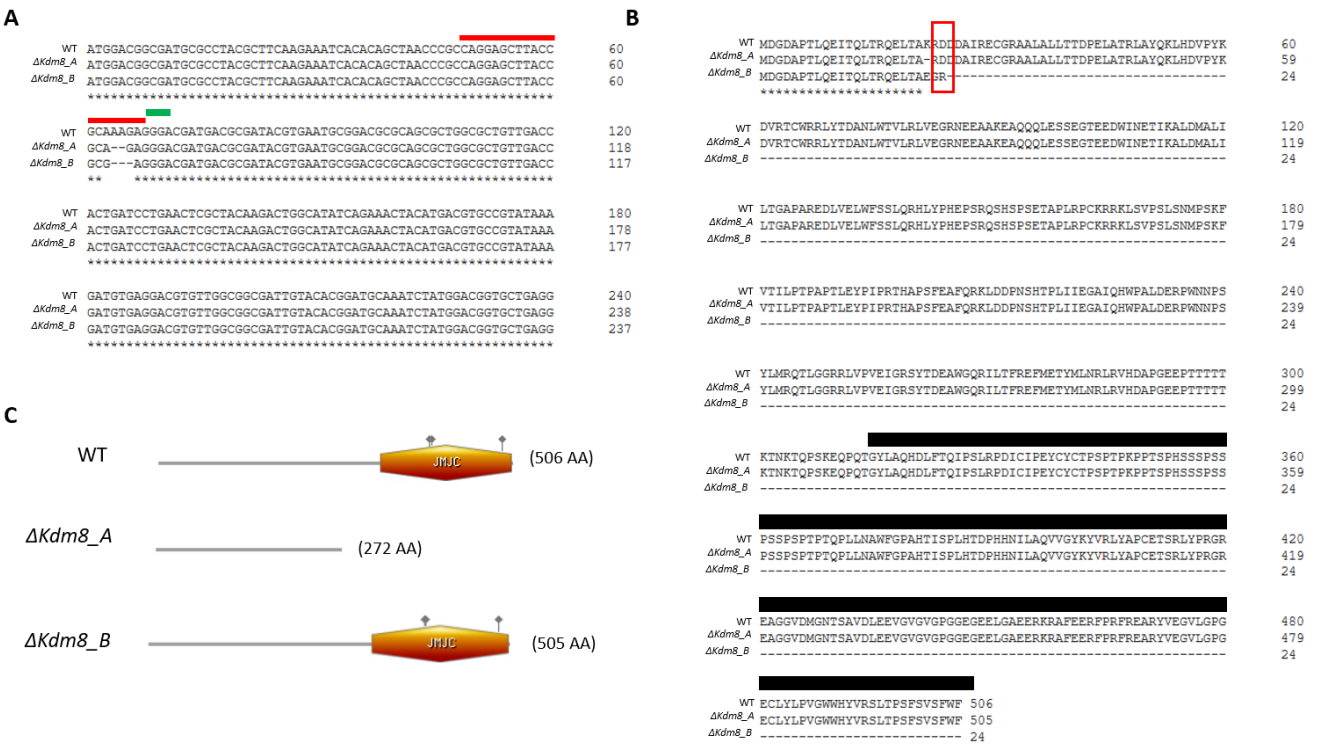

Figure 2: Effect of the *Kdm8* mutations on Kdm8 protein structure. A: Sequence alignment of the *Kdm8* gene in the WT isolate JN2 and in two mutants (*ΔKdm8_A* and (*ΔKdm8_B* showing respectively a 2-bp and 3-bp deletion). The PAM (Protospacer Adjacent Motif) is highlighted in green and the region targeted by the guide RNA is highlighted in red. **B:** Protein sequence of Kdm8 in the WT isolate JN2 and in the two mutants. The Jumanji domain is indicated by a black bar. The red frame indicates the location of the stop codon in the mutant version of the protein. **C:** Kdm8 protein length and domains identified with Pfam as described in Finn *et al.,* 2014 (https://pfam.xfam.org/).

Université Paris-Saclay
Espace Technologique / Immeuble Discovery
Route de l'Orme aux Merisiers RD 128 / 91190 Saint-Aubin, France

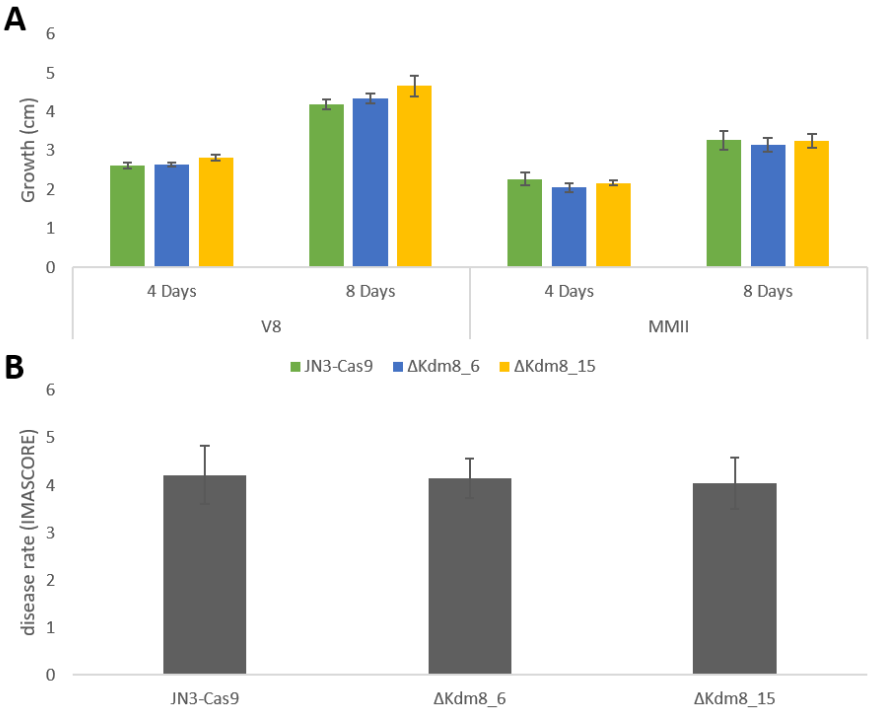

Figure 3: Effect of *kdm8* inactivation on mycelial growth and pathogenicity of *Leptosphaeria maculans*. A: Growth assay on kdm8 mutants and WT strain JN3 with or without Cas9 gene. Mycelial growth was measured at 4 days and 8 days post inoculation on two different agar media, V8 and MMII. **B:** Pathogenicity tests were performed on the susceptible cultivar Es-Astrid at 13DPI. Disease rate is expressed as the mean scoring using the IMASCORE rating scale comprising six infection classes (IC), where IC1 to IC3 corresponded to resistance and IC4 to IC6, to susceptibility. DPI= Days Post Inoculation.

Université Paris-Saclay
Espace Technologique / Immeuble Discovery
Route de l'Orme aux Merisiers RD 128 / 91190 Saint-Aubin, France

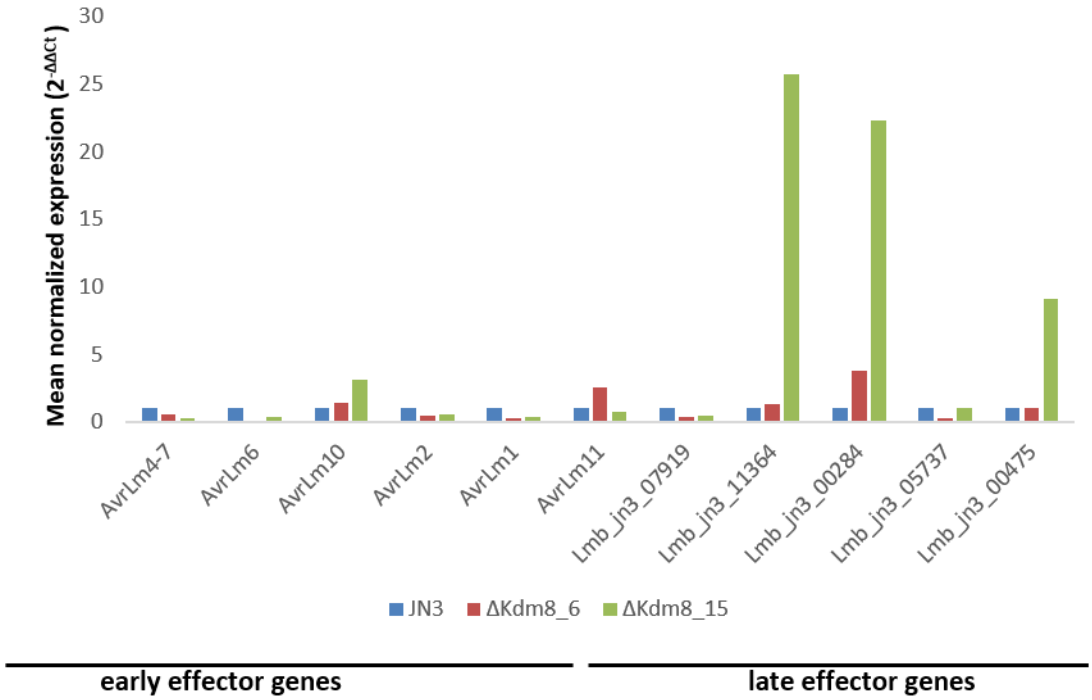

Figure 4: Influence of *Kdm8* inactivation on expression of several *L. maculans* 'early' and 'late' effector genes *in vitro*. Mycelium was obtained by growing JN3-Cas9 strain and transformants in Fries liquid medium for 7 days. Two biological replicates per condition were generated. Total RNA was extracted. Expression of 'early' and 'late' effector genes was measured by qRT-PCR and expressed relatively to *LmβTubulin* expression and to expression of the same genes in JN3 using the $2^{-\Delta\Delta Ct}$ method.

Université Paris-Saclay
Espace Technologique / Immeuble Discovery
Route de l'Orme aux Merisiers RD 128 / 91190 Saint-Aubin, France

Université Paris-Saclay
Espace Technologique / Immeuble Discovery
Route de l'Orme aux Merisiers RD 128 / 91190 Saint-Aubin, France

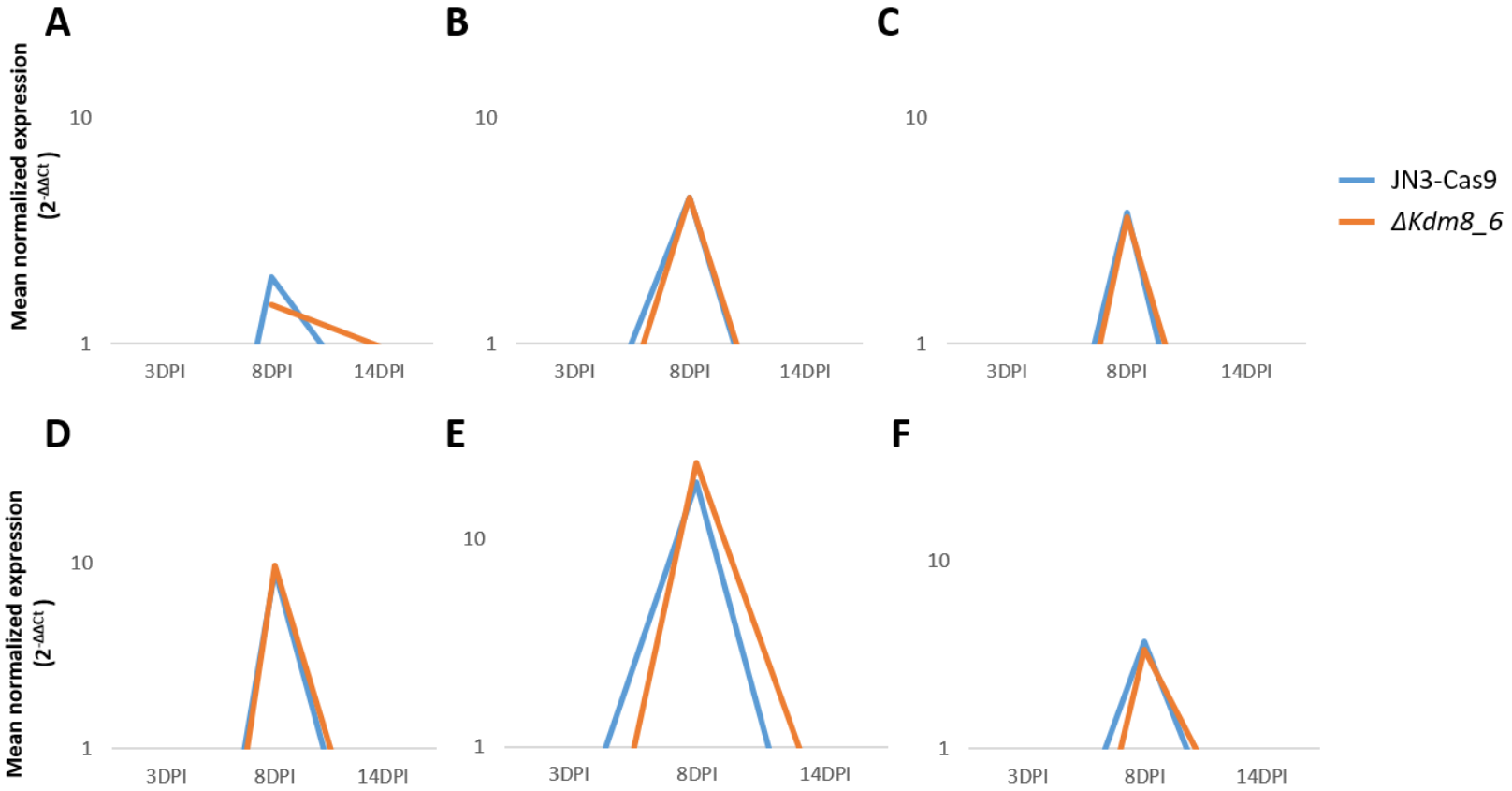

Figure 5: Influence of *Kdm8* inactivation on the expression of six *L. maculans* avirulence genes during infection of oilseed rape. Oilseed rape susceptible cultivar ES Astrid was inoculated with JN3-Cas9 and ΔKdm8 mutant. Cotyledons were harvested 5, 8 and 14 dpi. Expression of *Lmb_jn3_11364* (A) *AvrLm10A* (B) *; AvrLm4-7* (C) ; *AvrLm6* (D) ; *AvrLm11* (E); *AvrLm2* (F) was measured by qRT-PCR level using *LmβTubulin* as a constitutive reporter gene and expression in JN3-Cas9 as reference ($2^{-\Delta\Delta Ct}$ method). Each value is the average of two biological replicates (two extractions from different biological replicates) and two technical replicates (two RT-PCR).

CHAPITRE III

Régulation transcriptionnelle

INTRODUCTION

Dans le chapitre III sera abordée la question de la régulation transcriptionnelle de l'expression des gènes codant des effecteurs chez *L. maculans*. Pour cette étude, nous avons identifié un facteur de transcription (LmPf2) impliqué dans le contrôle des effecteurs fongiques et de la pathogénie chez plusieurs Dothideomycetes phytopathogènes et conservé chez *L. maculans*. Grâce à l'exploitation de données RNA-Seq générées dans le cadre d'un autre projet et couvrant tout le cycle de vie de *L. maculans* au champ et en conditions contrôlées, nous avons pu observer que ce FT avait un profil d'expression similaire à celui des gènes d'avirulence. J'ai réalisé l'inactivation de *LmPf2* par la technique CRISPR-Cas9. J'ai également réalisé des constructions permettant la sur-expression de *LmPf2*. J'ai caractérisé les transformants ainsi obtenus pour leur croissance, leur sporulation et leur capacité à infecter le colza. J'ai également mené des analyses RNA-Seq afin d'identifier les gènes directement ou indirectement régulés par LmPf2. L'inactivation de *LmPf2* mène à une perte de pouvoir pathogène ainsi qu'à une absence d'expression des effecteurs exprimés durant les phases précoces de l'infection *in planta*. La sur-expression de *LmPf2* dans deux fonds génétiques distincts, un fond sauvage et un fond *Δkmt1* dans lequel la marque répressive H3K9me3 était absente, nous a permis de montrer que la sur-expression de *LmPf2* selon l'état de compaction de la chromatine va être capable de réguler différents sets de gènes selon des vagues concertées. J'ai rédigé les résultats obtenus sous forme d'un article dont je suis premier auteur (première partie du chapitre). Dans une deuxième partie, je présenterai les résultats obtenus lors de l'inactivation de deux autres FTs spécifiques de *L*. maculans, également surexprimés pendant les étapes précoces d'infection.

Université Paris-Saclay
Espace Technologique / Immeuble Discovery
Route de l'Orme aux Merisiers RD 128 / 91190 Saint-Aubin, France

ARTICLE IV

Regulation of effector gene expression as concerted waves in Leptosphaeria maculans: a two-players game

Université Paris-Saclay
Espace Technologique / Immeuble Discovery
Route de l'Orme aux Merisiers RD 128 / 91190 Saint-Aubin, France

Regulation of effector gene expression as concerted waves in *Leptosphaeria maculans*: a two-players game

C. Clairet[12], E.J. Gay[12], A. Simon[1], N. Lapalu[1], F. Blaise[1], C.L. Marais[1], J.L. Soyer[1,*] and I. Fudal[1,*]

[1] UMR BIOGER, INRA, AgroParisTech, Université Paris-Saclay, Avenue Lucien Brétignières, BP 01, F-78850 Thiverval-Grignon, France

[2] Université Paris-Sud, 91405, Orsay, France

* To whom correspondence should be addressed.

E-mail: jessica.soyer@inra.fr; isabelle.fudal@inra.fr

ABSTRACT

Phytopathogenic fungi secrete during infection a set of molecules collectively known as effectors, involved in overcoming the host immune defense system and in disease establishment. In *Leptosphaeria maculans*, the causal agent of oilseed rape stem canker, we established that the histone modification H3K9me3, deposited by Kmt1, was involved in the regulation of expression of genes highly expressed during infection, including effectors expressed during the early stages of infection. Effector genes are concertedly expressed as waves during infection. These concerted patterns of effector gene expression suggest a tight regulation of their expression involving both chromatin remodeling proteins and specific transcription factors (TFs). Pf2, a TF belonging to the Zn2Cys6 fungal specific TF family, was described in several Dothideomycete species as essential for pathogenicity and effector gene expression. Here, we identified the protein orthologous to Pf2 in *L.* maculans, LmPf2. To investigate the role of LmPf2 together with Kmt1 in *L. maculans*, we inactivated *LmPf2* and over-expressed *LmPf2* in a WT and a *Δkmt1* backgrounds. Functional analyses of the corresponding transformants highlighted an essential role of LmPf2 in the establishment of pathogenesis. It also showed that LmPf2 is involved in the control of effector gene expression, particularly in a *Δkmt1* background. Transcriptomic analyses, using RNA-seq, during axenic growth helped deciphering the complex regulatory roles of LmPf2 and KMT1 on effector gene expression. Altogether, our findings allowed us to establish an effector gene regulatory model both *in planta* and *in vitro*.

INTRODUCTION

During infection, plant pathogenic fungi secrete a set of molecules, collectively known as effectors, involved in overcoming the host immune defense system, nutrient uptake and, eventually, symptom development (Lo Presti *et al.,* 2015). Effectors mainly correspond to small secreted proteins, generally cysteine-rich, with no homology to other known proteins in the databases (SSPs; Stergiopoulos and de Wit, 2009). Effector genes of filamentous plant pathogens are often located in transposable elements (TEs)-rich regions of the genomes, such as dispensable chromosomes or telomeres (Sánchez-Vallet *et al*., 2018). Transcriptomic data generated during different stages of plant infection highlighted concerted waves of effector gene expression over the course of infection, according to the infection structure, to the host-plant infected or to the species or strain studied (Sanchez-Vallet *et al*., 2018). Little is

known about how coordinated expression of effector genes is regulated. Based on observation that many effector genes are located in TE-rich regions, and up-regulated during host penetration/infection, the role of chromatin remodeling in the regulation of these genes was recently investigated. Many proteins were as involved in chromatin remodeling, and analyses in plant pathogenic fungi have shed light on two histone methyltransferases, KMT1 and KMT6. These two proteins are involved in the trimethylation of the lysine 9 of histone H3 (H3K9me3) and of the trimethylation of the lysine 27 of histone H3 (H3K27me3), typical for the tightly packed portion of the chromatin, the heterochromatin, and associated with gene repression. The role of KMT1 and KMT6 in the regulation of the expression of genes encoding pathogenicity determinants (effector and secondary metabolite-encoding genes) has been demonstrated in distantly related fungi, for instance in *Leptosphaeria maculans* and in *Epichloe festucae* (Chujo & Scott 2014; Soyer *et al*., 2014). In *L. maculans*, the causal agent of stem canker of oilseed rape (*Brassica napus*), inactivation of *KMT1*, led to an over-expression of more than 30% of the genes located in TE-rich environments, normally silenced *in vitro* in the WT strain, specifically effector genes, compared to the wild type strain. ChIP-qPCR analyses showed that over-expression of at least two effector genes was associated with a decrease of the repressive histone modification H3K9me3 in the genomic environment of these genes (Soyer *et al.*, 2014). In a recent study we constructed the map of H3K4me2 activating modification, H3K9me3 and H3K27me3 repressive modification respective repartitions on *L. maculans* genomes (Soyer *et al.,* 2019). We used this map to get further insight in chromatin modifications involvement in gene regulation and more specifically on effector gene regulation in *L. maculans*. Altogether, these analyses revealed that chromatin structure, via the dynamic of chromatin remodeling, was an important regulatory layer of effector genes up-regulated during host infection and located in TE-rich regions.

Leptosphaeria maculans is an ideal model to investigate the dual control of effector gene expression: (i) it displays a complex life cycle with alternating phases of saprophytism, asymptomatic growth and necrotrophy that suggest involvement of sophisticated regulation networks. It first infects oilseed rape leaves and undergoes asexual sporulation leading to leaf spots. Then, the fungus grows into the stem without visible symptom and finally provokes stem canker at the end of the oilseed rape growing season (Rouxel and Balesdent, 2005). (ii) The *L. maculans* genome displays a bipartite structure with gene-rich regions and TE-rich regions. One thousand and eighty putative effector genes are predicted in its genome, and regions enriched for histone modifications typical for heterochromatin are significantly enriched in such genes (Dutreux *et al.,* 2018; EJ. Gay, on-going PhD thesis; JL. Soyer, unpublished). During infection of oilseed rape, several waves of effector genes are expressed (Rouxel *et al.,* 2011; Gervais *et al.,* 2017; E.J. Gay, on-going PhD thesis). Of particular interest, during the asymptomatic stages occurring on both leaves and stems, a specific set of effector genes is expressed, including all know avirulence genes (*AvrLm*) identified so far, and these genes are specifically located in TE-rich regions. Avr protein coded by these genes directly or indirectly activates plant defense upon recognition mediated by corresponding plant R proteins (Biezen and Jones, 1998). iii) Involvement of the chromatin structure in the regulation of gene expression highlighted that the chromatin folding in TE-rich regions was instrumental in the regulation of effector genes (and *AvrLm* genes) located in these regions. Nevertheless, at least in *L. maculans*, inactivation of *KMT1*, while highly inducing expression of effector genes *in vitro*, did not induce expression of these genes at the same level as during infection of oilseed rape. This suggests that, although chromatin folding plays an important role in the regulatory mechanism, a second regulator, such as a transcription factor,

Université Paris-Saclay
Espace Technologique / Immeuble Discovery
Route de l'Orme aux Merisiers RD 128 / 91190 Saint-Aubin, France

might be involved. Based on the observation that loosening of the chromatin fiber alone does not result in the same expression level as during *in planta* infection, Soyer *et al.* (2015. A) proposed a model of dual control of effector gene expression: after chromatin loosening upon infection, one or several transcription factor(s) (TFs) could bind effector gene promoters resulting in their concerted expression. Synergic involvement of chromatin modifications and TF(s) remains poorly understood and an unexplored field of investigation.

In filamentous plant pathogens, only a few transcription factors influencing effector gene expression have been identified so far (see for review Tan and Oliver, 2017). Among them, AbPf2, a Zn2Cys6 TF, was first described in *Alternaria brassicicola*, in which it regulates, directly or indirectly, expression of 33 genes encoding secreted proteins including eight putative effectors (Cho *et al.,* 2013). In *Parastagonospora nodorum*, the AbPf2 orthologue PnPf2 positively regulates two necrotrophic effector genes, *SnToxA* and *SnTox3* and the orthologue of *SnToxA*, *ToxA*, is regulated by PtrPf2 in *Pyrenophora tritici-repentis* (Rybak *et al.,* 2017).

Here, we investigated the involvement of the homolog of Pf2 in *L. maculans*, LmPf2, in the control of effector gene expression. We inactivated *LmPf2* using the CRISPR-Cas9 strategy and over-expressed *LmPf2* in two different genetic backgrounds: (i) a wild type strain; (ii) a strain in which the gene encoding KMT1 (responsible for the deposition of H3K9me3) is inactivated. We characterized the corresponding transformants for their growth, sporulation and pathogenicity. We performed a RNA-seq analysis in order to decipher the respective involvement of LmPf2 and KMT1 in gene regulation. We found out that KMT1 and LmPf2 are acting together to specifically control at least part of two different sets of genes expressed as concerted waves at two infection time points.

MATERIAL AND METHODS

Fungal culture

The reference isolates JN2 and JN3 were used as hosts for genetic transformations (Balesdent *et al*., 2001). We also used a JN2 strain constitutively expressing *eGFP* (Sâsêk *et al*., 2012) which was crossed with our mutants in order to follow the colonization of oilseed rape by the mutants. Fungal cultures and conidia production were performed as previously described (Ansan-Melayah *et al.,* 1995). For DNA/RNA extractions, mycelium was grown on V8-juice agar medium at 25°C in the dark for seven days and then plugs were transferred into 150 ml of Fries liquid medium in 500 ml Roux flasks. Tissues were harvested after growing for seven days at 25°C.

Pathogenicity and growth assays

Pathogenicity assays were performed on cotyledons of 15-day-old plantlets of a susceptible cultivar of *B. napus*, Es-Astrid. Plants were incubated in a growth chamber at 16/24°C (night/day) with a 16h photoperiod. Symptoms were scored on 10-12 plants, with two biological replicates, 13 days post inoculation (dpi) using the IMASCORE rating scale comprising six infection classes (IC), where IC1 to IC3 correspond to various levels of resistance of the plant and IC4 to IC6 to susceptibility (Balesdent *et al.*, 2001). Growth assays were performed by deposition of a 5 mm plug at the center of 90 mm Petri dishes (containing 20 ml of V8-juice agar medium or MMII medium). Radial growth was measured at nine days after incubation in a growth chamber (25°C) on four biological replicates and statistical analysis were performed using Kruskal-Wallis test (Guo *et al.,* 2013).

Université Paris-Saclay
Espace Technologique / Immeuble Discovery
Route de l'Orme aux Merisiers RD 128 / 91190 Saint-Aubin, France

DNA and RNA manipulation

For PCR, genomic DNA was extracted from conidia or from mycelium grown in Fries liquid culture with the DNAeasy 96 plant Kit (Qiagen S.A., Courtaboeuf, France). PCR amplifications were performed as previously described (Fudal *et al.,* 2007). To identify mutation arising in the sequence of the gene targeted by the CRISPR-Cas9 strategy, sequencing was performed by Eurofins Genomics (Anzinger, Ebersberg, Germany). Total RNA was extracted from mycelium grown for one week in Fries liquid medium, and from cotyledons of Es-Astrid infected by *L. maculans* seven dpi as previously described (Fudal *et al.,* 2007).

Vector construction and fungal transformation

Vectors pLAU2 and pLAU53 conferring respectively hygromycin and geneticin resistance were used to perform CRISPR-Cas9 gene inactivation, as described by Idnurm *et al.* (2017). DNA fragments coding for gRNA which target genes of interest were designed using the CRISPOR prediction tool and *L. maculans* as reference genome (http://crispor.tefor.net/; **Table S1**; Dutreux *et al*., 2018). The gRNA were chosen not to match on any other genes. The DNA fragment coding for gRNA was amplified using primers MAI0309 and MAI0310 and then inserted into the *Xho*I site of plasmid pLAU53 using Gibson assembly (**Table S1**; Silayeva and Barnes, 2018). Hence, plasmids Plau2-Cas9 and Plau53-KMT1 and Plau53-LmPf2 were generated to inactivate *KMT1* and *LmPf2*. PLAU2 containing *Cas9* gene was used without modification.

Over-expression plasmids were obtained using the pBht2 vector conferring resistance to hygromycin (Mullins *et al*., 2001). *EF1α* promoter was amplified using EF1aProSac1F and EF1aProKpnIR primers and genomic DNA of JN3 isolate as template, and then inserted into *Kpn*I-*Sac*I digested pBht2 to obtain pBht2-promEF1a vector. *LmPf2* gene and his terminator were then amplified using surex_*LmPf2*_Gibs_F and surex_ *LmPf2*_Gibs_R primers and inserted in 3' of the *EF1α* promoter in the *Hin*dIII digested pBht2-promEF1a vector using Gibson assembly to obtain pBht2-surexLmPf2 (**Table S1**). JN2 and *Δkmt1* were used for the transformation.

The constructs were introduced into the *Agrobacterium tumefaciens* strain C58-pGV2260 by electroporation (1.5 kV, 200 ohms and 25 mF). *A. tumefaciens* mediated transformation (ATMT) of *L. maculans* was performed as previously described (Gout *et al.,* 2006). Transformants were plated on minimal medium complemented with geneticin (50 mg/l) for pLAU53-gRNA or hygromycin (50 mg/l) for pBht2-surex*LmPf2* and pLAU2-Cas9 and cefotaxime (250 mg/l). For the CRISPR-Cas9 gene inactivation, construct containing *Cas9* (pLAU2-Cas9) was first introduced into a JN3 strain and transformants were selected for hygromycin resistance. Transformants transformed with pLAU2-Cas9 construct were then transformed with pLAU53-gRNA directed against *KMT1* or *LmPf2*. Transformants were selected for geneticin, hygromycin and cefotaxime resistance. For the *LmPf2* over-expression, pBht2-*surexLmPf2* was introduced into JN2 and *Δkmt1.* Mutations in the targeted genes were checked in the transformants by PCR amplifying with specific primers (**Table S1**) and sequencing. Correct insertions of *surexLmPf2* construction were checked in transformants by PCR amplification.

Fungal crosses

Université Paris-Saclay
Espace Technologique / Immeuble Discovery
Route de l'Orme aux Merisiers RD 128 / 91190 Saint-Aubin, France

Purification in order to eliminate *Cas9* gene and gRNA coding gene from the CRISPR-Cas9 mutants were performed by crossing mutants with a WT isolate (expressing or not *GFP*) from the opposite mating type (**Table S2**). Crosses were performed as described by Balesdent *et al.* (2002). Progeny was harvested and plated on V8-juice agar medium. Mycelium was collected and DNA extracted. PCR and sequencing were performed to select progeny without *Cas9* and gRNA which had integrated the CRISPR-Cas9 mutation.

Quantitative RT-PCR

Quantitative RT-PCR (qRT-PCR) was performed using a model CFX96 Real Time System (BIORAD; Hercules, CA, USA) and Absolute SYBR Green ROX dUTP Mix (ABgene, Courtaboeuf, France) as previously described (Fudal *et al.,* 2007). For each condition tested, two different RNA extractions from two different biological samples and two reverse transcriptions for each biological replicate were performed. Primers used for qRT-PCR are described in (**Table S1)**. Ct values were analyzed as described by Muller *et al.* (2002) or using the $2^{-\Delta\Delta Ct}$ method (Livak and Schittgen, 2001). *β-tubulin* was used as a constitutively expressed reference gene. Biomass of *L. maculans* in infected plants was analyzed by generating a standard curve with known concentration of *L. maculans* and *B. napus* gDNA. Total gDNA was extracted from adult 28 dpi infected plants and a 10^{-1} dilution was used for qPCR. The Ct values obtained were reported on the standard curve in order to determine fugal and plant gDNA proportion.

Confocal microscopy and binocular observation

Cotyledons of a susceptible cultivar (Es-Astrid) infected by isolates expressing *GFP* were observed at two different time points (5 and 7 dpi) using a DM5500B Leica TCS SPE laser scanning confocal microscope and a 20x HCX Fluotar Leica objective lens. GFP was excited at 488 nm and emission was captured with a 505–530 nm broad-pass filter. The detector gain was set-up between 700 and 900. Calibrations of gain settings were performed with multiple control leaves and with a range of background fluorescence. All images represent at least 4 scans. Infected cotyledons were also observed at 8 and 13 dpi using a Leica MZ16F fluorescent binocular coupled with a Leica DFC300FX camera.

Western Blot

Total proteins were extracted from 10-100 mg lyophilized mycelium. Mycelium was ground using beads and Mixer Mill MM 400 (Retsch, Éragny, France). Total proteins were treated as described in Petit-Houdenot *et al.* (2019). Proteins were transferred on a PVDF membrane according to the manufacturer's protocol (Trans-Blot® Turbo™ Rapid Transfer System, BIORAD, Les-Ulis, France) using a small protein transfer program. The PVDF membrane was incubated in TBS 1X containing 5% milk, 0.05% tween 20 for one hour to saturate membrane. The membrane was then incubated at 4°C over-night in TBS 1% containing 0.05% Tween 20, milk 1% and H3K9me3 antibody (1:5000; 39062 ActiveMotif, La Hulpe, Belgium Germany). PVDF membrane was washed as described by Petit-Houdenot *et al.* (2019) and was then incubated in TBS 1X + 0.05% Tween 20 + milk 1% + antiRabbit IgG II^R (goat anti-rabbit, Santa Cruz Biotechnology, Heidelberg, Allemagne) and washed as previously. Finally, membrane was incubated 1min in 1 mL enzyme solution (Clarity™ Western ECL, BIORAD, Les-Ulis, France) and 1 mL Luminol/enhancer solution (Clarity™ Western ECL, BIORAD, Les-Ulis, France) and observed using ChemiDoc (ChemiDoc™ Imaging Systems, BIORAD, Les-Ulis, France).

Université Paris-Saclay
Espace Technologique / Immeuble Discovery
Route de l'Orme aux Merisiers RD 128 / 91190 Saint-Aubin, France

Gene annotation and domain prediction

The Pf2 orthologue of *L. maculans* had been previously identified by Rybak et al. (2017). As it was identified on a previous version of the *L. maculans* genome, we have performed a new search, using the protein sequence of Pf2 of *P. nodorum* and the NCBI BLAST program (Altschul *et al.,* 1990). Functional domains were identified using Pfam as described in Finn *et al.,* 2014 (https://pfam.xfam.org/). Alignments were performed with COBALT (Papadopoulos and Agarwala, 2007).

RNA-Seq and statistical analysis

Eight different transformants (i.e., mutants inactivated for *KMT1* or *LmPf2* and transformants in which *LmPf2* is over-expressed in a JN2 background (JN2_oPf2) or a *Δkmt1* background (*Δkmt1*_oPf, **Table 1**) were grown in Fries medium during 7 days and harvested for RNA extraction. Two RNA extraction corresponding to two biological replicates were performed for each transformant. About 150 mg of mycelium was used per extraction. Libraries were prepared from all biological replicates, individually, according to the Illumina TruSeq protocol (Illumina, San Diego, CA, USA). Libraries including polyA enrichment were performed and sequenced using 150 pb paired-end strategy on an HiSeq2000 Illumina sequencer at the Genewiz sequencing facility (Leipzig, Germany) with an input of 1µg total RNA. Raw sequencing data are available under the SRA accession number xxxx. Quality of the reads was checked and improved using Trimmomatic (Bolger *et al.,* 2014). The resulting reads were treated to remove adaptors and reads below 30 bp and filtered reads were mapped against the *L. maculans* genome using STAR (Dobin *et al.,* 2013; Dutreux *et al.,* 2018) with default parameters. Read alignments were stored in SAM format, and indexing, sorting, and conversion to BAM format were performed using SAMtoolsv0.1.19 (Li *et al.*, 2009). Genes with a number of read > 15 in at least one condition were kept for statistical analysis. Differential expression analyses were made using R (R Core Team, 2017) and the package EdgeR (Robinson *et al.,* 2010): Genes with a log2 Fold Change ≤ -1.5 or ≥ 1.5 and an associated false discovery rate ≤ 0.05 were considerated as differentially expressed (McCarthy *et al.,* 2012).

Gene Ontology enrichment analysis

Gene Ontology (GO) annotation of L. maculans encoding genes were retrieved from Dutreux et al., (2018). Gene ontology term enrichment analysis of the differentially expressed genes in our transformants was performed with the plug-in Biological networks Gene ontology (BinGo; v3.0.3) of the cytoscape software (Shannon *et al*., 2003). List of genes submitted to BINGO were considered as significantly enriched for a given GO term with an associated a False Discovery Rate ≤ 0.01 for the biological processes. All analyses were done in R (www.r-project.org).

Université Paris-Saclay
Espace Technologique / Immeuble Discovery
Route de l'Orme aux Merisiers RD 128 / 91190 Saint-Aubin, France

206

207

208

209

Table 1: Effect of *kmt1* and *LmPf2* inactivations and of *LmPf2* over-expression on mycelial growth, conidia production, pathogenicity and effector gene expression of *Leptosphaeria maculans*

Isolate / transformants[a]	Radial growth 9 days post inoculation on V8 medium (mm)	conidia/ml	Pathogenicity assay using conidia[b]	Pathogenicity assay using mycelium plugs[c]	Effector gene expression during axenic growth[d] *AvrLm6*	*AvrLm4-7*
JN2	60.5 (± 2.24)	4.50E+07	4.83 (± 0.28)	pathogenic	1	1
Δkmt1	50.25 (± 1.94)	4.00E+07	3.09 (± 0.35)	pathogenic	9.70E-02 (± 0.22)	2.37E+02 (± 27)
ΔLmPf2_A	56.13 (± 0.9)	1.53E+08	1 (± 0)	non pathogenic	4.60E-02 (± 0)	0.00E+00 (± 0)
ΔLmPf2_B	80 (± 0.8)*	1.08E+08	1 (± 0)	non pathogenic	6.30E-03 (± 0)	4.10E-03 (± 0)
JN2_oPf2_14	77.38 (± 0.76)	0.00E+00	not enough conidia	pathogenic	3.05E+00 (± 0.14)	2.50E-01 (± 0.20)
JN2_oPf2_24	73.5 (± 1.19)	0.00E+00	not enough conidia	pathogenic	2.68E+00 (± 0.19)	7.00E-02 (± 0.02)
*Δkmt1*_oPf2_8	68.38 (± 1.03)	2.00E+07	4 (± 0)	pathogenic	2.61E+01 (± 3.4)	4.73E+02 (± 8.6)
*Δkmt1*_oPf2_22	53.75 (± 1.06)	1.25E+06	not enough conidia	non pathogenic	1.30E+04 (± 107.79)	2.31E+03 (± 24.64)

a: JN2 is the WT strain; *ΔLmPf2_A* and B are LmPf2 mutants; JN2_oPf2_14 and JN2_oPf2_24 correspond to *LmPf2* over-expression transformants (with respectively 600 fold and 150 fold expression of *LmPf2* compared to JN2); *Δkmt1*_oPf2_8 and *Δkmt1*_oPf2_22 correspond to *LmPf2* over-expression transformants in a *Δkmt1* mutant background (with respectively 150 fold and 600 fold expression of *LmPf2* compared to the *Δkmt1* mutant). b: Pathogenicity tests were performed on the susceptible cultivar Es-Astrid. Disease rate is expressed as the mean scoring using the IMASCORE rating scale comprising six infection classes (IC), where IC1 to IC3 correspond to various levels of resistance of the plant and IC4 to IC6 to susceptibility (Balesdent *et al.,* 2001).c: ability to provoke symptoms on cotyledons; d: Mycelium was obtained by growing JN2 strain and transformants in Fries liquid medium for 7 days. Two biological replicates per condition were generated. Total RNA was extracted. Expression of *AvrLm6* and *AvrLm4-7* was measured by qRT-PCR and expressed relatively to *LmβTubulin* expression and to expression of *AvrLm6* or *AvrLm4-7* in JN2 using the the $2^{-\Delta\Delta Ct}$ method (Livak and Schittgen, 2001). Asterisk corresponds to transformants statistically different from the WT, Kruskal Wallis test *Pvalue*<0,05.

210

211

212

Université Paris-Saclay
Espace Technologique / Immeuble Discovery
Route de l'Orme aux Merisiers RD 128 / 91190 Saint-Aubin, France

RESULTS

Identification of a *Pf2* orthologue and analysis of *KMT1* and *LmPf2* expression in *Leptosphaeria maculans*

In order to analyze involvement of Pf2 and KMT1 in the regulation of gene expression, notably on effector genes located in TE-rich regions and highly expressed during the early stages of oilseed rape infection, we firstly identified *Pf2* in *L. maculans*. The gene encoding Pf2 in *P. nodorum*, *PnPf2*, was identified by Rybak *et al.* (2017) and phylogenetic analysis showed that the closest orthologue of *PnPf2* was found in *L. maculans* (Genbank Accession XP_003838593.1). This Genbank Accession corresponded to gene ID *Lmb_jn3_06039* of *L. maculans*, located on SuperContig6 (Dutreux *et al*., 2018). A bidirectional Best Hit with BLASTp was performed to confirm orthology between *PnPf2* and *LmPf2* (**Figure 1**). The *Pf2* gene of *L. maculans* (hereinafter referred to as *LmPf2*) encodes a 658 amino acids protein sharing 67% identity with PnPf2. A Zn2Cys6-type DNA-binding domain is predicted in both proteins (IPR001138; **Figure 1**).

Figure 1: Identification of a PnPf2 orthologue in *Leptosphaeria maculans*. Alignment between LmPf2 of *L. maculans* and *Parastagonospora nodorum* PnPf2 was performed using COBALT (Papadopoulos and Agarwala, 2007). The black bar corresponds to the Zn2Cys6-type DNA binding domain identified using Pfam as described in Finn *et al.,* 2014 (https://pfam.xfam.org/). LmPf2 and PnPf2 share 67 % identity.

Université Paris-Saclay
Espace Technologique / Immeuble Discovery
Route de l'Orme aux Merisiers RD 128 / 91190 Saint-Aubin, France

We then investigated the expression profile of *LmPf2* and *KMT1* during axenic growth and at different stages of primary infection of oilseed rape and compared their expression profiles to that of the avirulence genes of *L. maculans* (*AvrLm2*, *AvrLm3*, *AvrLm4-7*, *AvrLm5-9*, *AvrLm6*, *AvrLm10.A*, *AvrLm10.B* and *AvrLm11*; Fudal *et al.*, 2007; Parlange *et al.,* 2009; Balesdent *et al.*, 2013; van de Wouw *et al*., 2014; Plissonneau *et al.,* 2016; Ghanbarnia *et al*., 2018; Petit-Houdenot *et al.,* 2019) (**Figure 2**). As already described, expression of the avirulence genes of *L. maculans* was repressed during axenic. Expression strongly increased during the asymptomatic infection of oilseed rape cotyledons, between two and nine dpi, reaching a peak seven dpi and then, expression slowly decreased up to 12-15 dpi, when necrotic symptoms were visible (**Figure 2**). Likewise, *LmPf2* was not expressed *in vitro* while its expression increased between 5 and 7 dpi and decreased again until 15 dpi. *KMT1* was inversely expressed with high expression during axenic growth, no expression during early infection (J2 to J9), and was up-regulated at J12 when *AvrLm* gene expression decreased. To summarize, *LmPf2* showed a similar expression profile as *AvrLm* genes described so far in *L. maculans*, and *KMT1* was inversely correlated with *AvrLm* genes expression (**Figure 2**).

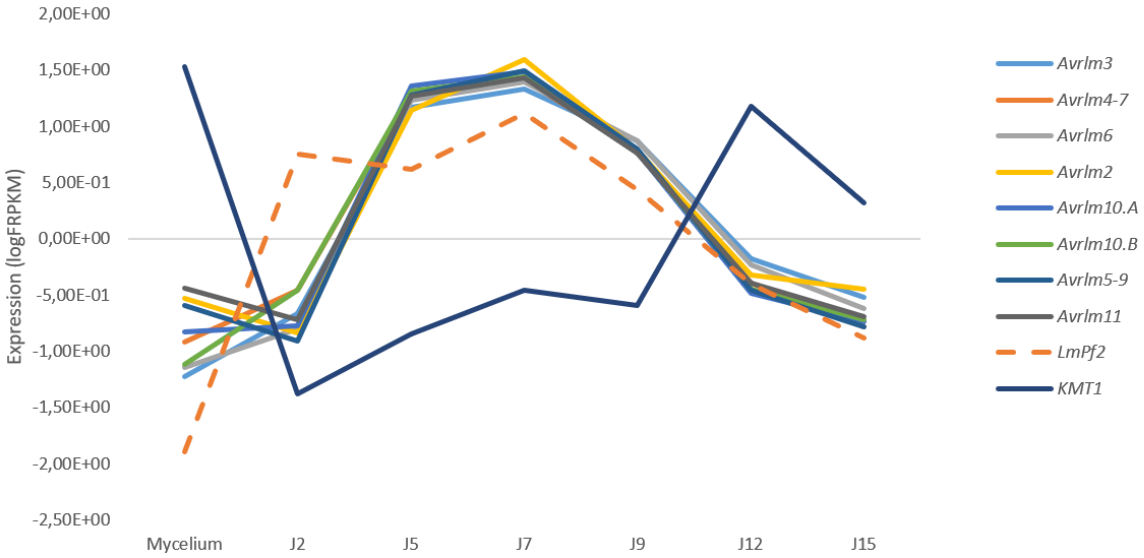

Figure 2: Expression profile of *Leptosphaeria maculans* avirulence genes, *LmPf2* transcription factor and *KMT1* during axenic growth and infection of oilseed rape cotyledons. Mycelium was obtained by growing JN2 strain on V8 agar medium for 7 days. Cotyledons of the susceptible cultivar Darmor-bzh were inoculated by JN2 and sampled at 7 different time points (2, 5, 7, 9, 12 and 15 days post infection). Two biological replicates per condition were generated. Total RNA was extracted and sequenced. The expression level of nine avirulence genes, *LmPf2* and *Kmt1* in RNA-seq data is represented by the log2 of FPKM (Reads Per Kilobase Per Million mapped reads) centered and reduced (Gay et al., in prep.).

Université Paris-Saclay
Espace Technologique / Immeuble Discovery
Route de l'Orme aux Merisiers RD 128 / 91190 Saint-Aubin, France

LmPf2 and *KMT1* inactivations do not induce morphology, conidiation or pigmentation defects while *LmPf2* over-expression induces developmental defects in *L. maculans*

We inactivated *LmPf2* in order to evaluate its involvement in the regulation of *L. maculans* avirulence genes. Inactivation of *LmPf2* was performed using the CRISPR-Cas9 strategy as detailed in the Materials and Methods section. Seventeen transformants resistant to hygromycin and geneticin were obtained and sequenced for the *LmPf2* gene. Of the 17 transformants, 12 had no mutations in *LmPf2* compared to the WT, three had a 1-bp and one had a 5-bp deletion near the cleavage site (**Figure 3A**). These mutations resulted, at the protein level, in frame-shifts leading to two different truncated proteins: 175 amino-acids and 238 amino-acids respectively for the 1-bp and the 5-bp deletions compared to the 658 amino-acids length of the WT protein (**Figure 3B**). The two mutants were crossed with JN2-GFP in order to obtain purified *ΔLmPf2* and *ΔLmPf2-GFP* mutants without *Cas9* and CRISPR guide RNA (**Table S2**). The four corresponding mutants are hereinafter referred to as *ΔLmPf2_A, ΔLmPf2_A-GFP, ΔLmPf2_B and ΔLmPf2_B-GFP* (A corresponding to the 1-bp and B to the 5-bp deletion). The four Δ*LmPf2* mutants were able to produce conidia and showed dark coloration of the hyphae, corresponding to melanin production, as the WT after 14 days of growth on V8-juice agar medium (**Figure S1**; **Table 1**). After nine days of growth on V8-agar plate, only *ΔLmPf2_B* exhibited statistically more growth than the WT indicating that *LmPf2* deletion does not lead to growth defect. To summarize, no major defect in conidia production, growth rate or morphology was associated with the inactivation of *LmPf2*.

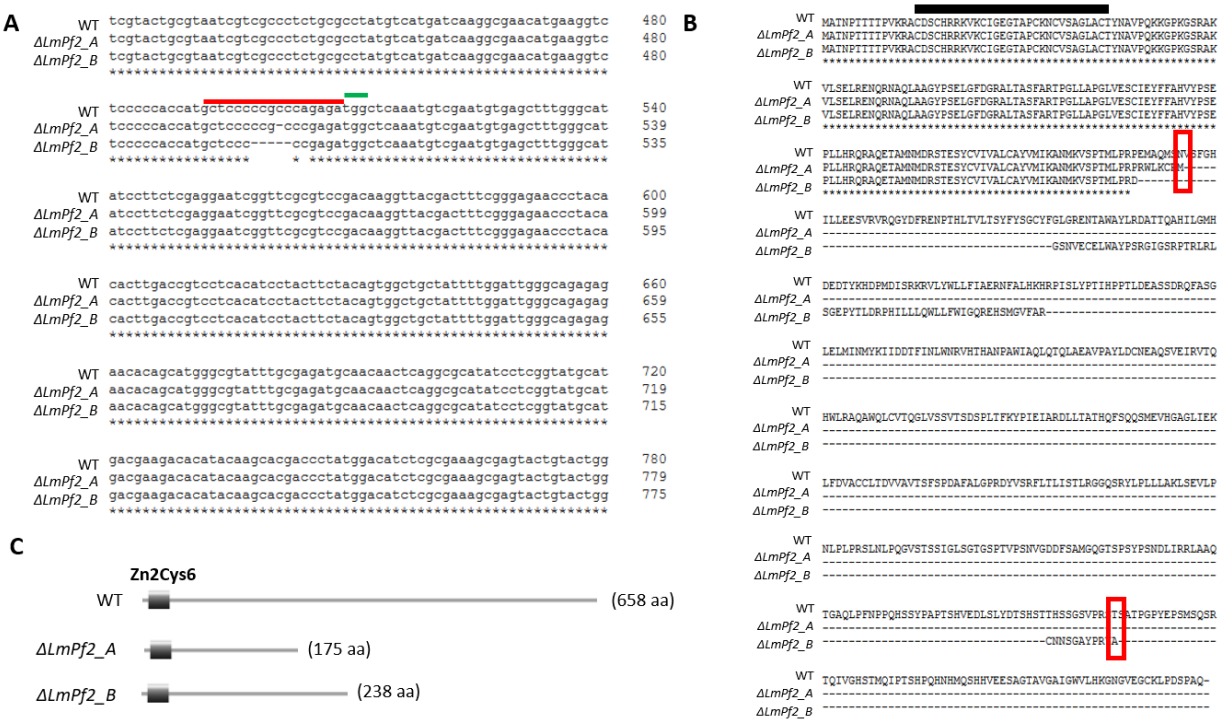

Figure 3: Effect of the *LmPf2* mutations on LmPf2 protein structure. A: Sequence alignment of the *LmPf2* gene in the WT isolates JN2 and in two mutants *ΔLmPf2_A* and B showing respectively a 1bp and 5bp deletion. The PAM (Protospacer Adjacent Motif) is highlighted in green and the region targeted by the guide RNA is highlighted in red. **B:** Protein sequence of LmPf2 in the WT isolate JN2 and in the two mutants. The DNA-binding Domain is indicated by a black bar. The red frames indicate the location of the stop codons in the mutant versions of the protein. **C:** LmPf2 protein length and domains identified with Pfam as described in Finn *et al.* (2014)(https://pfam.xfam.org/).

Université Paris-Saclay
Espace Technologique / Immeuble Discovery
Route de l'Orme aux Merisiers RD 128 / 91190 Saint-Aubin, France

In a previous study, Soyer *et al.* (2014) silenced expression of *KMT1* (with a residual expression of 16% compared to the WT). Silencing of *KMT1* led to an over-expression of effector genes located in TE-rich regions, notably avirulence genes, during axenic growth. This over-expression was associated, at least for two avirulence genes, with a decrease of H3K9me3 at their loci. Here, we took advantage of the availability of the CRISPR-Cas9 strategy to better investigate involvement of KMT1 in the regulation of *L. maculans* gene expression. Twenty-five transformants resistant to hygromycin and geneticin were obtained and sequenced for the *KMT1* gene. Of the 25 transformants, 24 had no mutations in *KMT1* compared to the WT and one had a 1-bp insertion resulting, at the protein level, in a truncated protein of 144 aa (while the WT protein had a length of 516 amino-acids; **Figure 4A and B**). Both functional domains of KMT1 (Pre-SET and SET) are absent from the truncated protein (Pfam analysis; Finn *et al.,* 2014; https://pfam.xfam.org/; **Figure 4C**) and loss of H3K9me3 was confirmed in the *Δkmt1* mutant strain by Western blot analysis (**Figure 4D; Figure S2**). The *Δkmt1* mutant was crossed with JN2-GFP in order to obtain purified *Δkmt1* and *Δkmt1*-GFP mutants without *Cas9* and CRISPR guide RNA (**Table S2**). The two corresponding mutants are hereinafter referred to as *Δkmt1* and *Δkmt1-GFP* mutants. We tested the effect of *KMT1* inactivation on growth and conidiation of *L. maculans*. *Δkmt1* was not significantly altered in its mycelial growth, conidia production and production of melanin (**Table 1; Figure S1**).

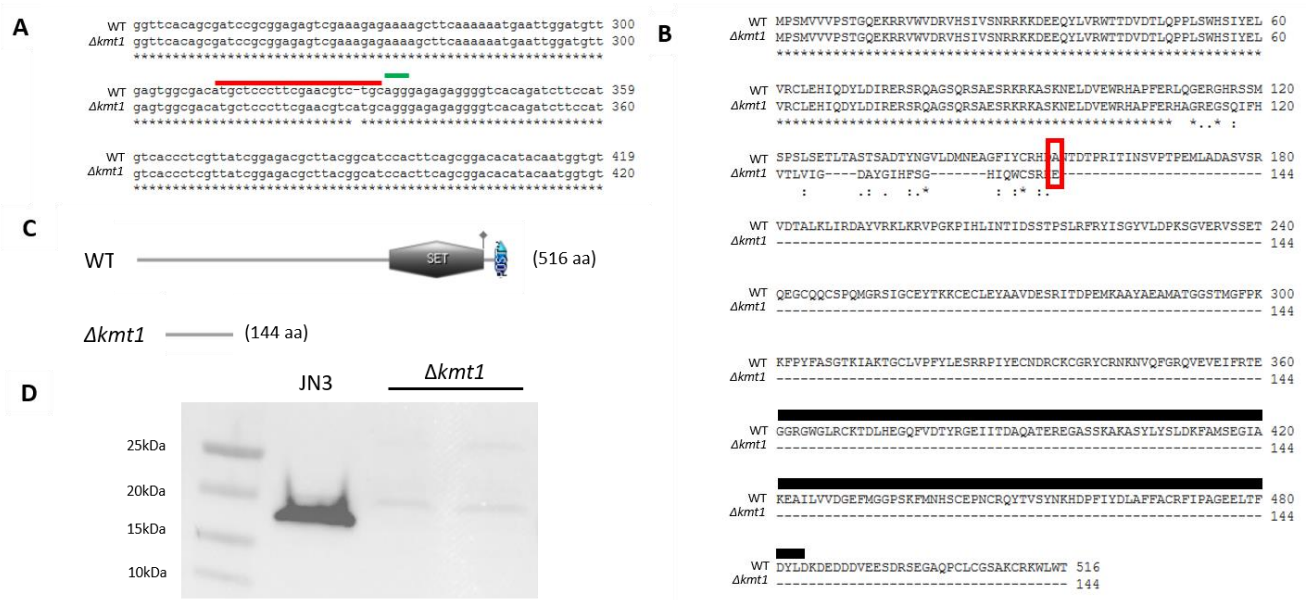

Figure 4: Effect of the *Δkmt1* mutation on the KMT1 protein structure and function. A: Nucleotide sequence alignment of the *KMT1* gene in the WT isolate and in the *Δkmt1* mutant (showing a 1bp insertion). The PAM (Protospacer Adjacent Motif) is highlighted in green and the region targeted by the guide RNA is highlighted in red. **B:** Protein sequence of KMT1 in the WT isolate JN2 and in the *Δkmt1* mutant. The red frame indicates the stop in the mutant version of the protein. The black bar indicates the SET domain which has been lost in the truncated protein. **C:** KMT1 protein length and domains identified with Pfam as described in Finn *et al.* (2014)(https://pfam.xfam.org/). **D:** Western Blot analysis of H3K9 tri-methylation in JN3 (WT) and *Δkmt1.* Nuclear proteins were extracted from mycelium, separated by SDS-PAGE, blotted and probed with antibodies against H3K9me3. *Δkmt1* proteins replicates have been used for this test.

We then expressed *LmPf2* under the control of the *EF1α* promoter. The construct was introduced in two different genetic backgrounds: the WT isolate JN2 and the *Δkmt1* mutant. Twenty-five transformants were recovered for each transformation and named respectively JN2_oPf2 and *Δkmt1*_oPf2. We measured expression of *LmPf2* during axenic growth by RT-qPCR. The JN2_oPf2 transformants showed a 15 to 18,000-fold increase of expression of *LmPf2* compared to the WT while *LmPf2* expression increased 15 to 700-fold in the *Δkmt1*_oPf2 transformants (**Figure S3**). For further analyses, we selected two transformants from each genetic background with similar *LmPf2* expression levels (150 and 600 more expression than in the JN2 or the *Δkmt1* strains; **Figure S3**): JN2_oPf2_14, JN2_oPf2_24, *Δkmt1*_oPf2_8 and *Δkmt1*_oPf2_22. Over-expression of the *LmPf2* gene in the WT strain or the *Δkmt1* strains did not induce any growth defect even though the thallus was denser and harbored a white coloration indicating that the mutants were not able to produce melanin. In addition, over-expression of *LmPf2* had critical impact on *L. maculans* conidiation (**Table 1**; **Figure S1**).

LmPf2 and KMT1 are involved in the control of effector gene expression and pathogenicity of *L. maculans*

We inoculated *ΔLmPf2, ΔLmPf2-GFP, Δkmt1*, *Δkmt1-GFP,* LmPf2-overexpressing transformants and a WT strain on cotyledons of the susceptible cultivar Es-Astrid. *ΔKmt1* and *ΔKmt1-GFP* showed reduced symptoms compared to the WT, indicating a decrease of pathogenicity (**Figure 5A; Figure S4; Table 1**). Cotyledons infected with *ΔKmt1-GFP* were observed from 5 to 13 dpi, which allowed us to distinguish living plant cells and GFP fungal hyphae, and production of pycnidia. The *Δkmt1-GFP* transformant was able to colonize the plant and to produce pycnidia but induced lesser symptoms than the WT (**Figure 5C; Figure S4**). The *ΔLmPf2* mutants were not able to invade the cotyledon further than the inoculation site, and consequently, did not induce any visible symptom (**Figure 5; Figure S4; Table 1**). *ΔLmPf2* mutants started producing pycnidia at 5 DPI at the inoculation site whereas the WT started producing pycnidia at 7 DPI (**Figure 5A, B**). These results indicate that both KMT1 and LmPf2 are involved in infection establishment. Finally, the transformants over-expressing *LmPf2* were not able to produce enough conidia, which are normally used to perform pathogenicity tests. We thus performed pathogenicity tests using plugs of mycelium and all the transformants, excepted *Δkmt1*_oPf2_22, were able to produce symptoms on oilseed rape cotyledons (**Table 1**).

Université Paris-Saclay
Espace Technologique / Immeuble Discovery
Route de l'Orme aux Merisiers RD 128 / 91190 Saint-Aubin, France

We investigated expression of two avirulence genes (*AvrLm4-7* and *AvrLm6*) in the *ΔKmt1* mutant, the *ΔLmPf2* mutant, transformants over-expressing *LmPf2* and the WT strain during axenic growth by qRT-PCR (**Figure 6; Table 1**). While expression of *Avrlm6* was comparable to that of the WT, *AvrLm4-7* was over-expressed in *ΔKmt1* compared to the WT strain (237 times more expressed; **Table 1**). *AvrLm4-7* and *AvrLm6* expression was fully abolished in both *ΔLmPf2* mutant (**Table 1**). In both genetic backgrounds of *LmPf2* over-expression, we observed an up-regulation of these genes, with a higher level of up-regulation in the *Δkmt1* background. *AvrLm4-7* expression level reach up to 172-fold change in JN2_oPf2 mutants while *AvrLm6* expression level reach up to 1,000-fold change in the JN2_oPf2 mutants and up to 20,000-fold change in the *Δkmt1*_oPf2 mutants; **Figure 6**). To investigate whether a stronger over-expression of *LmPf2* in a WT background would result in a higher increase of expression of the two avirulence genes, we also investigated expression of these avirulence genes in two JN2_oPf2 transformants in which *LmPf2* was over-expressed 10,000 and 18,000 times compared to the WT strain (**Figure S5**). The strong *LmPf2* over-expression induced an up-regulation of *AvrLm4-7* and *AvrLm6* expression. Nevertheless, it did not reach the same level as in a *Δkmt1* background (*AvrLm4-7* was induced 50-1,100-fold and *AvrLm6* 700-4,700-fold compared to the WT). We then investigated expression of four avirulence genes (*AvrLm4-7*, *AvrLm6*, *AvrLm10.A* and *AvrLm11*) in the *ΔLmPf2* and *Δkmt1* mutants and the WT strain during infection of the susceptible cultivar Es-Astrid at 7 dpi (when expression of *L. maculans* effectors reaches a peak in the WT strain). Expression of the four avirulence genes was very low in *ΔLmPf2* compared to the WT (1000 to 2000-fold less expressed than in the WT) or even not detected (**Table 2**). In *Δkmt1*, *avirulence* gene expression was not altered *in planta* (**Table 2**). Altogether, our results suggest that KMT1 is able to repress avirulence gene expression whereas LmPf2 induces their expression.

Table 2: Effect of *LmPf2* and *KMT1* inactivation on avirulence gene expression during primary oilseed rape infection

Isolate/ transformants	expression *in planta* 7DPI[a]			
	AvrLm4-7	***AvrLm6***	***AvrLm10A***	***AvrLm11***
WT	3.25E+01	7.41E+01	2.92E+01	1.96E+02
ΔLmPf2_A	nd[b]	4.58E-02	2.49E-02	7.64E-02
ΔLmPf2_B	4.08E-03	6.27E-03	3.25E-02	9.55E-02
Δkmt1	1,03E+00	4,23E+00	1,93E+00	5,23E+00

Expression of *AvrLm4-7*, *AvrLm6*, *AvrLm10.A* and *AvrLm11* at 7dpi on cotyledons of a susceptible cultivar (Es-Astrid) in *ΔLmPf2, Δkmt1* mutants and a WT isolate. Legends: [a]Gene expression levels are relative to *Lmβtubulin* and calculated as described by Muller *et al.* (2002). Each value is the average of two biological replicates (two extractions from different biological replicates) and two technical replicates (two RT-PCR). [b]nd:

Université Paris-Saclay
Espace Technologique / Immeuble Discovery
Route de l'Orme aux Merisiers RD 128 / 91190 Saint-Aubin, France

KMT1 and LmPf2 differentially control effector genes expression

Inactivation of *LmPf2* abolished expression of the avirulence genes tested *in planta* while the up-regulation of *LmPf2* strongly induced expression of these genes *in vitro*, and the effect was stronger in a *Δkmt1* background than in a WT background. Based on these observations, we generated RNA-seq data during axenic growth of all types of transformants generated, and of the WT strain (i.e., JN2, *Δkmt1*, *ΔLmPf2_A*, *ΔLmPf2_B, JN2_oPf2_14, JN2_oPf2_24, Δkmt1_oPf2_8* and *Δkmt1_oPf2_22*; **Table 1**). Eighteen million reads were obtained, on average, for each sample, that were filtered based on their quality using Trimmomatic and mapped on the *L. maculans* genome. According to the sample considered, between 79.5% and 88% paired-end reads were uniquely mapped, except for one technical replicate of the *ΔLmPf2_A* mutant for which only 39% of paired-end reads were mapped (**Table S3**). We then plotted the log2(RPKM) of each sample and observed that biological replicates of the same condition were correlated, except for *Δkmt1_oPf2_8* and *Δkmt1_oPf2_22* transformants (**Figure 7**; **Figure S6**). Based on that observation, data from biological replicates were merged, except that of *Δkmt1_oPf2_8* and *Δkmt1_oPf2_22* that were considered separately for subsequent statistical analyses.

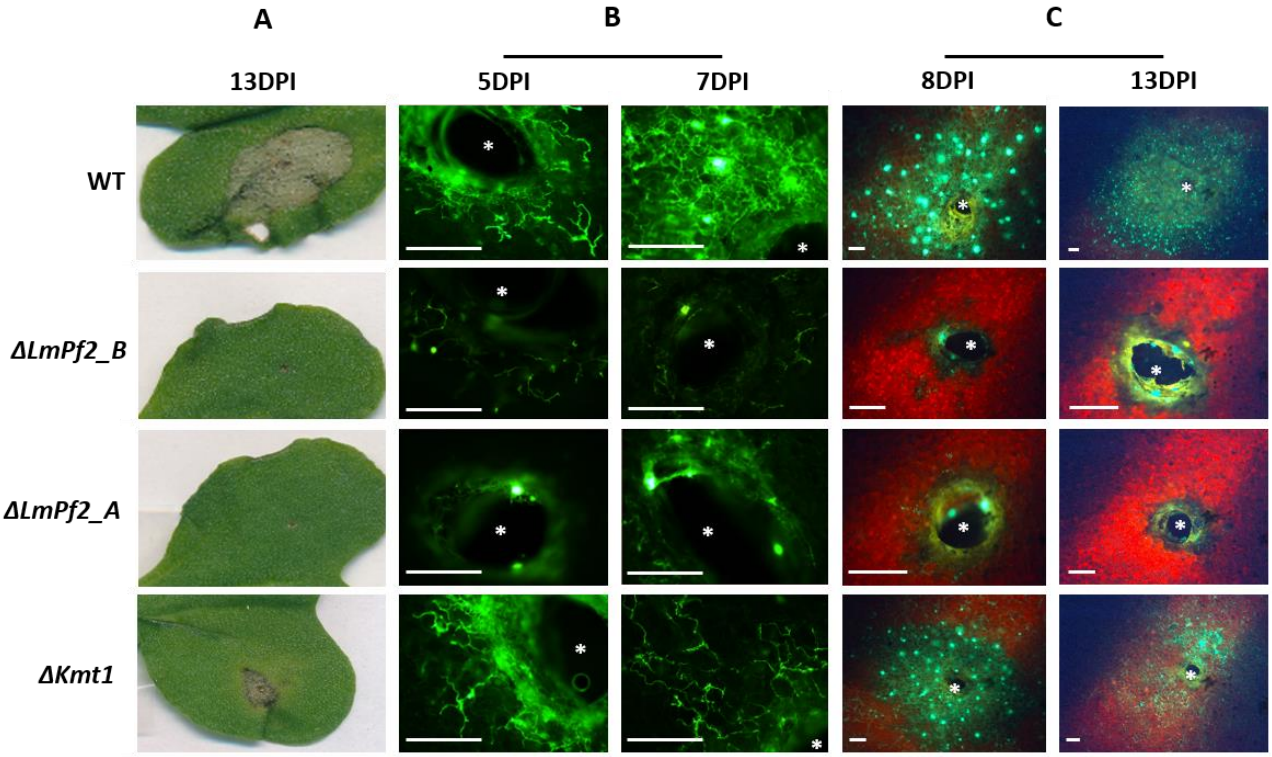

Figure 5: Effect of *LmPf2* and *LmKmt1* inactivations on pathogenicity of *L. maculans*. The WT isolate JN3 and mutants inactivated for *LmPf2* or *kmt1* were inoculated on cotyledons of a susceptible cultivar of oilseed rape (Es-Astrid). *ΔLmPf2_A* has a 1 bp deletion leading to a truncated protein of 175 aa. *ΔLmPf2_B* has a 5 bp deletion leading to a truncated protein of 238 aa. *ΔKmt1* has a 1 bp insertion leading to a truncated protein of 144 aa. **A:** Pictures of symptoms at 13 DPI. **B:** Fluorescence images of cotyledons infected by GFP mutants and WT strains at 5 and 7 DPI using a confocal microscope. **C:** Fluorescence images of cotyledons infected by GFP mutants and WT strains at 8 and 13 DPI using a fluorescence binocular. Infection site (needle hole) is indicated by a white asterisk. Scale bars represent 1 mm. DPI = Days Post Inoculation.

330

331

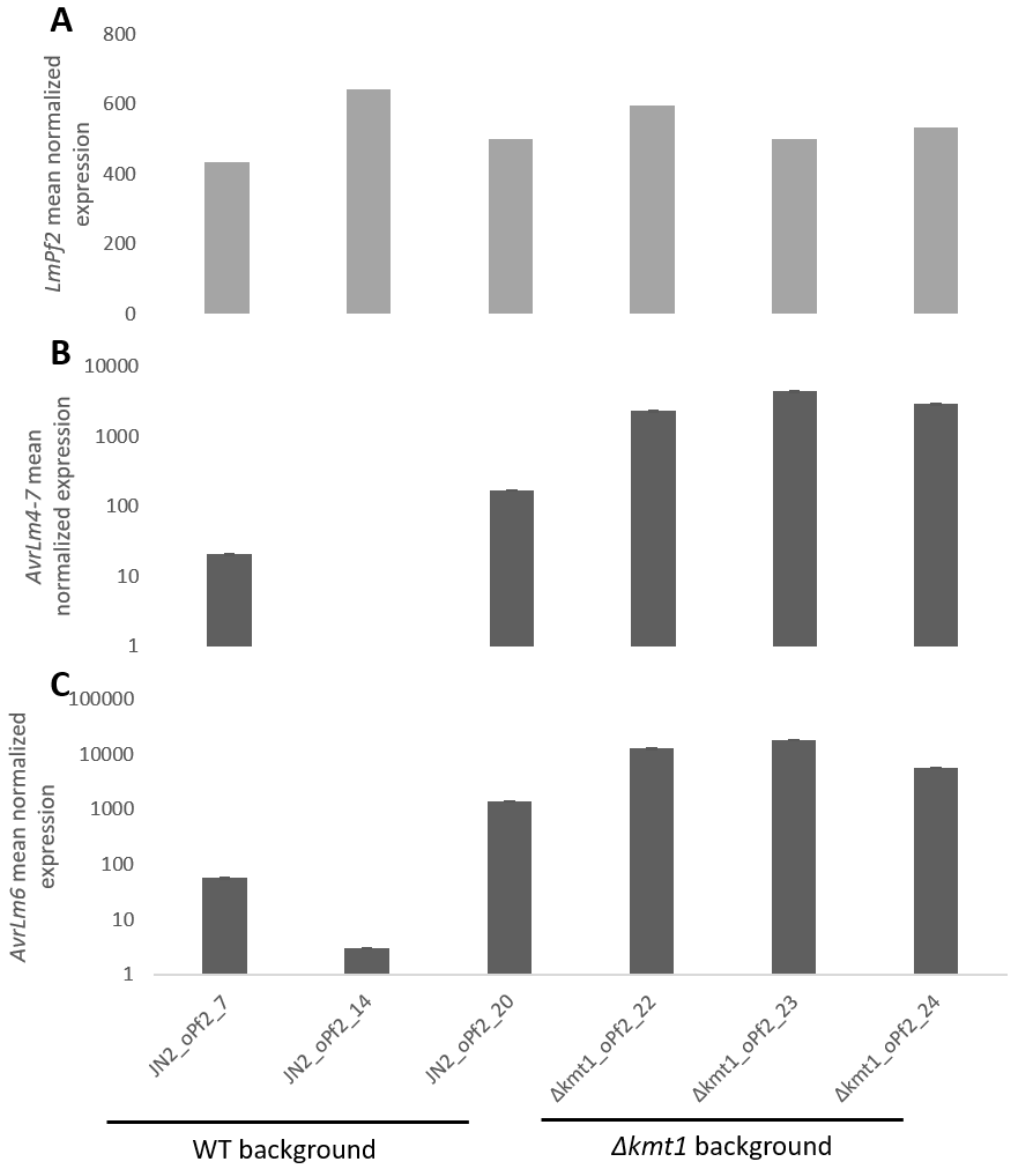

Figure 6: Influence of *LmPf2* overexpression and *KMT1* inactivation on the expression of two *L. maculans* avirulence genes during axenic growth. Mycelium was grown in Fries liquid medium during seven days. Expression of *LmPf2* (A), *AvrLm4-7 (*B) and *AvrLm6* (C) was measured by qRT-PCR level using *LmβTubulin* as a constitutive reporter gene and expression in JN2 or *Δkmt1* as reference ($2^{-\Delta\Delta Ct}$ method). Each value is the average of two biological replicates (two extractions from different biological replicates) and two technical replicates (two RT-PCR).

Université Paris-Saclay
Espace Technologique / Immeuble Discovery
Route de l'Orme aux Merisiers RD 128 / 91190 Saint-Aubin, France

We identified respectively 272, 427, 524, 433 and 1792 genes differentially expressed in *Δkmt1, ΔLmPf2, JN2_oPf2, Δkmt1_oPf_8, Δkmt1_oPf_22.* We observed respectively 129, 247, 275, 931 genes up-regulated in *Δkmt1, JN2_oPf2, Δkmt1_oPf_8, Δkmt1_oPf_22* and 129 genes down-regulated in *ΔLmPf2.* In *JN2_oPf2* we observed 247 up-regulated genes which were statistically enriched in H3K27me3 and H3K9me3/H3K27me3 genomic compartments, and statistically involved in carbohydrate metabolic process (19 genes; *Pvalue*=4.94E^{-4}) and polysaccharide metabolic process (6 genes; *Pvalue*=2.27E^{-2}; **Table S4**). Interestingly down-regulated genes in *ΔLmPf2* were statistically enriched in H3K9me3, H3K9me3/H3K27me3 and SSP-encoding genes and GOs analysis revealed that 33 of them were involved in oxidation-reduction process (*Pvalue*=8.86E-4). Finally, *Δkmt1, Δkmt1_oPf_8* and *Δkmt1_oPf_22* up-regulated genes were specifically located in H3K9me3, H3K27me3 and H3K9me3/H3K27me3 domains and were statistically enriched in SSP-encoding genes indicating that H3K9me3 and LmPf2 are able to control expression of facultative and constitutive heterochromatinian located genes and specifically SSP coding genes (**Table S4**). Up-regulated genes in *Δkmt1*_oPf2_8 were involved in starch, sucrose, disaccharide, glucan, cellular glucan, cellular polysaccharide and oligosacchide metabolic processes with 5 genes involved in each process. Finally, Up-regulated genes in *Δkmt1_oPf_22* were involved in carbohydrate metabolic processes nucleic acid phosphodiester bond hydrolysis, cell wall modification and transmembrane transport. Altogether these results indicate that *KMT1* inactivation and *LmPf2* over-expression in two different background lead to the same metabolic process enrichment and that the more *LmPf2* is expressed the more we get differentially regulated metabolic processes.

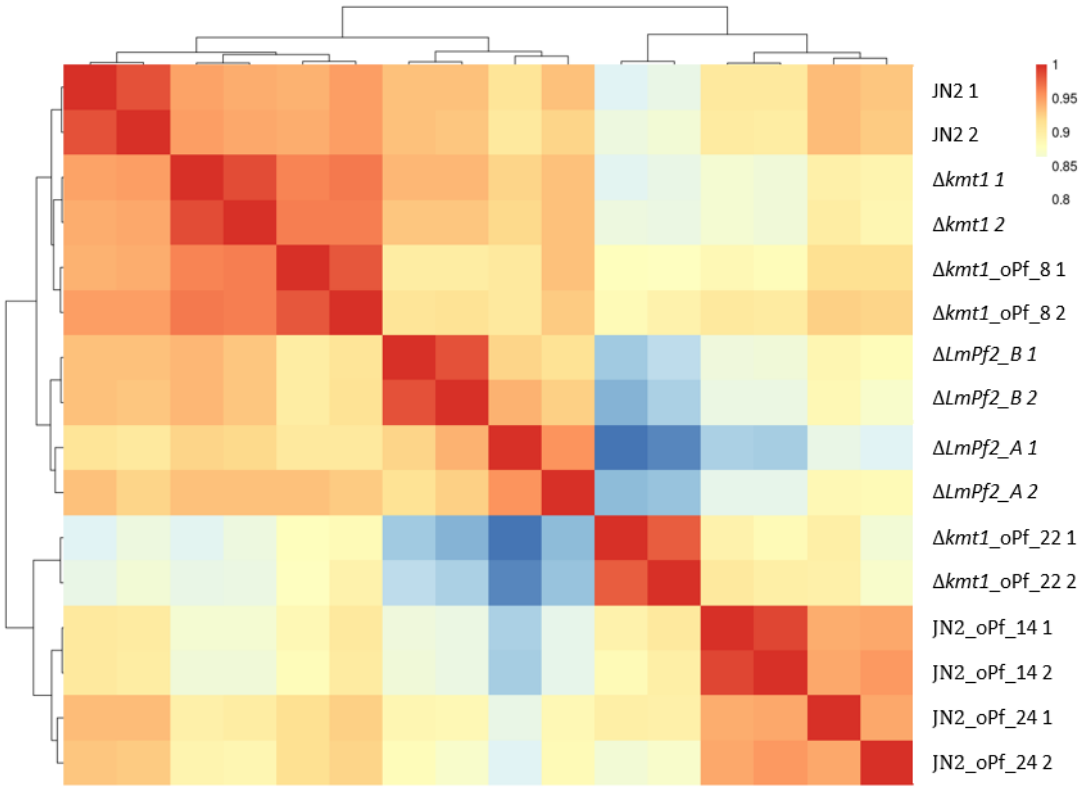

Figure 7: Hierarchical clustering of the pairwise Pearson correlation between the 18 RNA-Seq conditions. Heatmap of log2(RPKM) of each RNA-Seq biological and technical replicate plotted using Pearson correlation. JN2 is the WT strain; ΔLmPf2_A and B are LmPf2 mutants; JN2_oPf2_14 and JN2_oPf2_24 correspond to *LmPf2* over-expression transformants (with respectively 600 fold and 150 fold expression of *LmPf2* compared to JN2); Δkmt1_oPf2_8 and Δkmt1_oPf2_22 correspond to *LmPf2* over-expression transformants in a *Δkmt1* mutant background (with respectively 150 fold and 600 fold expression of *LmPf2* compared to the *Δkmt1* mutant).

Université Paris-Saclay
Espace Technologique / Immeuble Discovery
Route de l'Orme aux Merisiers RD 128 / 91190 Saint-Aubin,
France

Recent transcriptomic analyses throughout the life cycle of *L. maculans* have highlighted that synchronous waves of genes, including effector genes, are expressed (Gay et al., in prep.). Among these waves, four were specifically expressed during oilseed rape infection. Here, we investigated two of the four waves of genes concertedly expressed during infection and determined whether they were up-regulated in *Δkmt1*, *Δkmt1*_oPf2_22 or JN2_oPf2 or down-regulated in *ΔLmPf2* to investigate the respective effect of H3K9me3 removal and LmPf2 involvement in gene regulation. Respectively 4, 9 and 14 genes of wave 2 were differentially regulated in Δkmt1, JN2_oPf2 and *ΔLmPf2* indicating that H3K9me3 removal or *LmPf2* over-expression alone lead to limited wave 2 effector genes up-regulation. In contrast, sixty-six genes from wave 2 (71%) were specifically up-regulated in *Δkmt1_oPf2_22* on 931 genes up-regulated in total representing a 9.94-time enrichment in wave 2 effector genes (Khi^2; *pValue*=$2.20E^{-16}$). Interestingly, half of these genes were located in H3K27me3 or in no particular compartment indicating that H3K9me3 removal and *LmPf2* over-expression do not only target H3K9me3 enriched genes. We did not identify any genes of wave 3 up-regulated in Δkmt1 indicating that H3K9me3 do not actively repress these genes. Surprisingly, we identified 16, 19 and 20 of wave 3 genes respectively up-regulated in JN2_oPf2, *ΔLmPf2* and Δ*kmt1*_oPf2_22 confirming the limited impact of H3K9me3 removal on this set of genes. Furthermore, the 16 and 19 genes specifically up-regulated in JN2_oPf2 and *ΔLmPf2* transformants represented respectively an 11.6-time enrichment and an 15-time enrichment (Khi^2; *pValue*=$2.20E^{-16}$) whereas the 20 genes of wave 3 up-regulated in Δ*kmt1*_oPf2_22 represented a 3.8-time enrichment

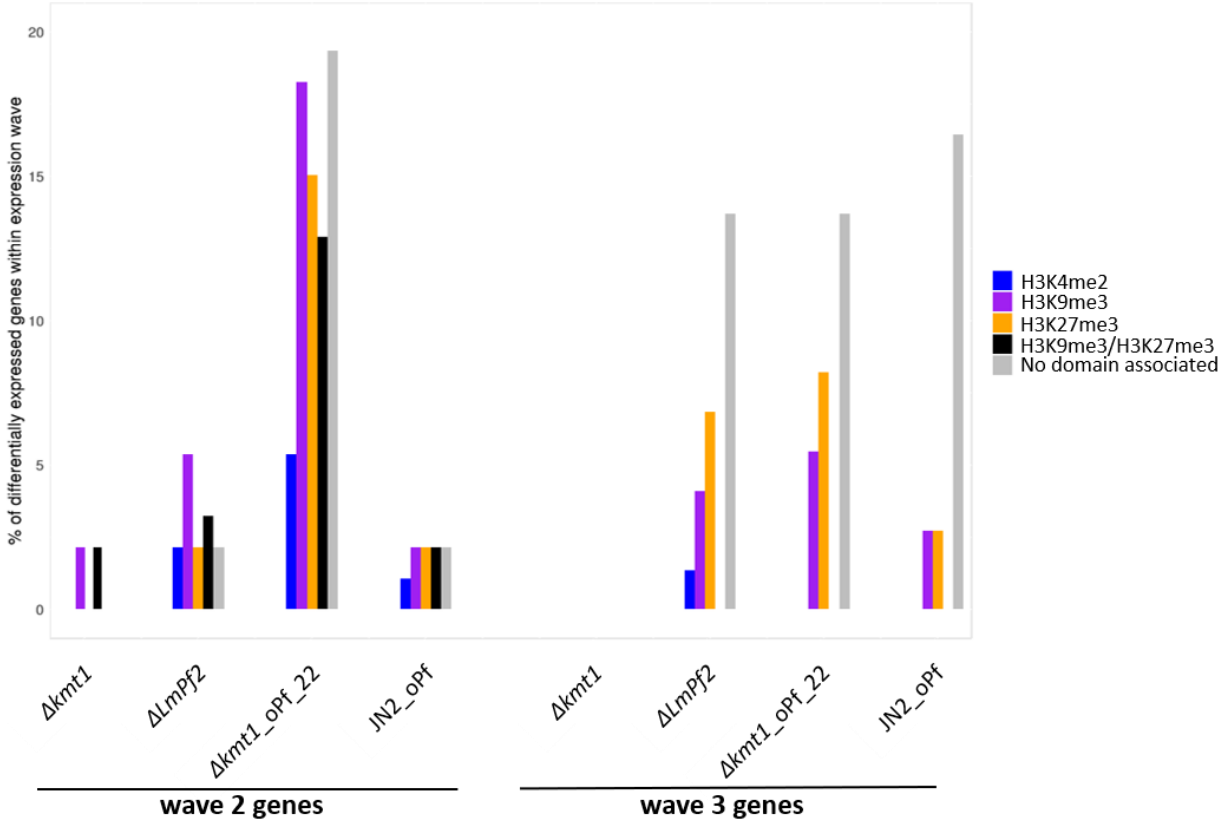

Figure 8: Influence of KMT1 and LmPf2 on expression of genes specifically expressed during infection. RNA-Seq analysis of differentially up-regulated genes in *Δkmt1*, *Δkmt1*_oPf2_22 and JN2_oPf2 transformants and down-regulated in *ΔLmPf2* depending on their chromatinian environnement and compared to genes concertedly expressed as wave 2 and wave 3 during *Leptosphaeria maculans* life-cycle. Histograms representing % of genes belonging to each wave of concertedly expressed genes in each transformant depending on their chromatin environment. On the left, genes concertedly expressed at 7 DPI during early infection on cotyledons of susceptible cultivar Darmor (including avirulence genes; wave 2). On the right, genes concertedly expressed between 9 and 12 DPI (wave 3) during early infection on cotyledons of a susceptible cultivar Darmor-bzh. DPI = Days Post Inoculation.

Université Paris-Saclay
Espace Technologique / Immeuble Discovery
Route de l'Orme aux Merisiers RD 128 / 91190 Saint-Aubin, France

(Khi²; *pValue*= 3,68E^{-10} ; **Figure 8**). Altogether these results indicate that genes of wave 2 are under H3K9me3 and LmPf2 double control whereas genes of wave 3 are under LmPf2 control only.

In order to get insight on how concerted effector gene expression could be controlled by H3K9me3 and LmPf2 in *planta*, we plotted the expression of *KMT1* and *LmPf2* during different stages of *L. maculans* life cycle. We observed that at least at three time points (Cotyledons 9-12DPI; Petioles 7-14DPI; and Stems between May and October) *KMT1* and *LmPf2* are conversely expressed indicating an inverted control exerted by these two genes (**Figure 9**). Interestingly, each time the *LmPf2* and *KMT1* expression was inverted, we observed a switch between sets of concertedly expressed genes.

Finally, we investigated whether TF-encoding genes were up-regulated in case of *LmPf2* over-expression. Surprisingly, we identified 21 TF-encoding genes up-regulated in Δ*kmt1*_oPf2_22 and 6 in JN2_oPf2 with only 2 of them in common (**Table S5**). We conclude that LmPf2 could act as a master regulator and activate different sets of TF depending on the chromatin context.

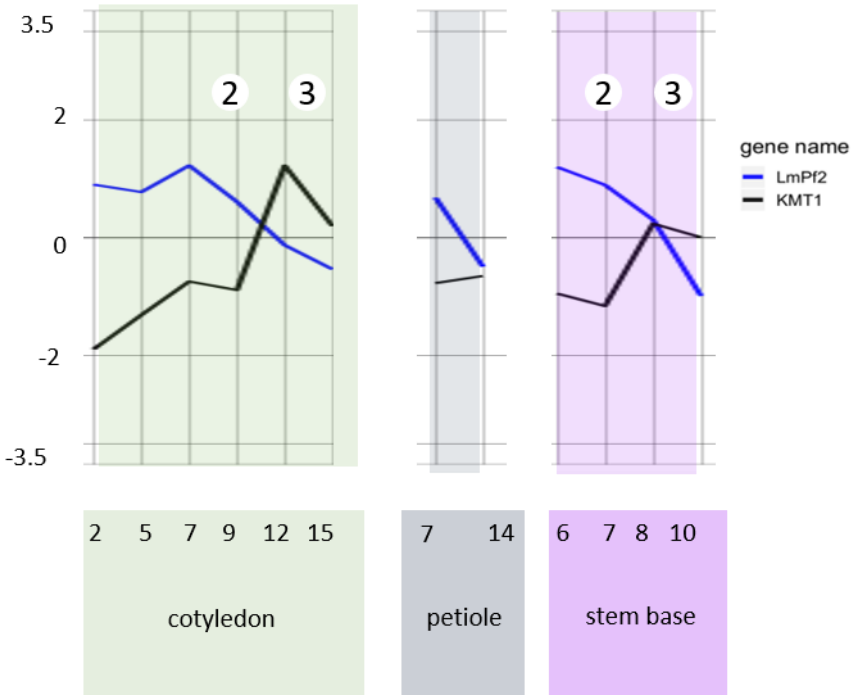

Figure 9: Inverted regulation of *KMT1* and *LmPf2* during *Leptosphaeria maculans* life cycle. Expression obtained by RNA-Seq in different *in planta* conditions. Expression corresponding to scalled log2(FPKM). The black line corresponds to *KMT1* expression and the blue line to *LmPf2* expression. Numbers at the top corresponding to concerted effector waves expressed depending on the infection time. Green part of the graph corresponding to infection of Darmor-bzh cotyledons between 2 and 15DPI. Grey part of the graph corresponding to petioles infected by the JN2 in controlled conditions at two time points 7 and 14DPI. The purple part of the graph corresponding to stem harvested in the field between June (6) and October (10).

Université Paris-Saclay
Espace Technologique / Immeuble Discovery
Route de l'Orme aux Merisiers RD 128 / 91190 Saint-Aubin, France

DISCUSSION

Here we demonstrated that LmPf2, a Zn2Cys6 TF, is involved in the establishment of infection and in the control of effector gene expression in *L. maculans*. We also determined that this TF is able to differentially regulate two sets of effector genes, expressed at different time points, depending on the chromatinin condensation state regulated by H3K9me3 deposition via KMT1. Furthermore, *LmPf2* presents an inverted expression profile compared to *KMT1* which suggests an opposite role on effector gene expression. To our knowledge, this is the first evidence of a double control involving both the chromatin structure and specific TF on expression of effector genes in a fungal species. Altogether, these results allowed us to draw a model for the double control of effector gene expression mediated by KMT1 and LmPf2 in *L. maculans*. The next step forward will be to investigate whether LmPf2 directly binds on effector gene promoters.

LmPf2* and *KMT1* inactivations lead to pathogenicity defects in *L. maculans

In this study, we investigated function of *LmPf2* and *KMT1* in *L. maculans*. CRISPR-Cas9 inactivation of *LmPf2* and *KMT1* induced pathogenicity defects while the mutants were not altered in their growth or conidiation. We conclude that, in *L. maculans*, LmPf*2* and KMT1 are specifically involved in the establishment of oilseed rape infection by *L. maculans.* This is in accordance with previous results obtained for three other Pleosporales species *A. brassicicola*, *P. tritici repentis* and *P. nodorum* in which Pf2 is also essential for establishment of infection (Cho *et al.,* 2013; Rybak *et al.,* 2017). Other fungal TF were also reported as involved in the establishment of infection (Michielse *et al.,* 2009, IpCho *et al.,* 2010; Zahiri *et al*., 2010; Soyer *et al.,* 2015. B). KMT1 was also demonstrated to be involved in several cellular processes in fungi. Histone modifications enzymes are more and more documented for their ability to express concertedly, large portion of genomic compartments (Gacek and Strauss, 2012). In a fungal endophyte, *Epichloë festucea*, KMT1 is able to regulate symbiosis-specific alkaloids bioprotective metabolites synthesis and to be crucial for mutualistic interaction establishment (Chujo and Scott, 2014). Despite the fact that KMT1 has been demonstrated to be crucial for pathogenicity establishment and effector and pathogenicity gene regulation in *B. cinerea* and *L. maculans* (Soyer *et al.,* 2014; Zhang *et al.,* 2016). The role of KMT1 in phytopathogenic fungi during infection remain poorly understood. H3K9me3 has also been described to regulate secondary metabolism, via the inactivation of the KdmA demethylase responsible for H3K9me3 removal in *A. nidulans* (Gacek-Matthews *et al.,* 2015).

***LmPf2* and *KMT1* inactivations lead to changes in effector gene expression**

Δkmt1 mutant exhibited *AvrLm6* up-regulation *in vitro*. This is consistent with our previous finding that *DIM5* (*KMT1*) partial inactivation via RNAi led to avirulence genes up-regulation and H3K9me3 depletion. H3K9me3 is known to regulate secondary metabolism and alkaloid production in several fungi and even in a species related to *L. maculans*, *Epichloe festucae*, harboring a bipartite genome structure as well (Gacek and Strauss, 2012; Chujo et Scott, 2014). Soyer *et al.* (2014) determined that the silencing of KMT1 allowed up-regulation of 30% of the genes specifically located in H3K9me3 whereas in this study we only identified five genes located in a H3K9me3 context specifically up-regulated in the Δ*kmt1* mutant. Soyer et al. (2014) were using DNA oligoarrays for their transcriptomic analysis and a previous annotation of *L. maculans* genome. Furthermore, the complete inactivation of *KMT1* could have led to

Université Paris-Saclay
Espace Technologique / Immeuble Discovery
Route de l'Orme aux Merisiers RD 128 / 91190 Saint-Aubin,
France

H3K27me3 relocation at H3K9me3 previous emplacements, as previously reported for *Neurospora crassa* or *Zymoseptoria tritici*, that phenomenon being less pronounced after silencing of *KMT1* (Basenko *et al.,* 2015; Möller *et al.,* 2019). The inactivation of KMT1 also induced expression of genes which were located in H3K4me2 and in no particular environment indicating that H3K9me3 removal not only modify gene expression in its environment but also in other compartments due to a structural role of H3K9me3 in genome organization as previously described in *N. crassa* (Winter *et al.,* 2018).

In this study, we also determined that *LmPf2* inactivation led to effector gene expression defect *in planta*. Furthermore, *LmPf2* over-expression led to effector genes up-regulation. Altogether these results indicate that LmPf2 specifically regulates effector gene expression in *L. maculans*. Once again, these results are in accordance with previous studies that described Pf2 as a regulator of effector gene expression in three Pleosporales species. Pf2, was reported to regulates, expression of 33 genes encoding secreted proteins including eight putative effectors in *Alternaria brassicicola* (Cho *et al.,* 2013). In *Parastagonospora nodorum*, PnPf2 positively regulates two necrotrophic effector genes, *SnToxA* and *SnTox3* and the orthologue of *SnToxA*, *ToxA*, is regulated by PtrPf2 in *Pyrenophora tritici-repentis* (Rybak *et al.,* 2017). This can confirm the conserved function of Pf2 on effector gene regulation in several phytopathogenic fungi.

***LmPf2* over-expression leads to an up-regulation of effector-encoding genes and genes in an heterochromatin context**

In this study, we observed that up-regulated genes in JN2_oPf2 transformants were statistically enriched in SSP-encoding genes, and genes located in a heterochromatin context (enriched in H3K9me3 or H3K27me3). Furthermore, we determined that the inactivation of KMT1 combined with an over-expression of *LmPf2* induced expression of avirulence genes. We thus conclude that LmPf2 specifically regulate effector genes which are mostly located in H3K9me3 and H3K27me3 environments. In addition, avirulence genes up-regulation was much higher in a Δ*kmt1* than in a WT background. Finally, we observed that *LmPf2* and *KMT1* were inversely expressed during infection. This indicate that *AvrLm* genes in *L. maculans* are under double control of both H3K9me3 and LmPf2. Histone modifications H3K9me3 and H3K27me3 have been identified as important regulators of effector and secondary metabolism gene expression in some fungi (Strauss and Reyes-Dominguez, 2011; Chujo and Scott, 2014; Connolly *et al.,* 2013; Soyer *et al.,* 2015. A). But to our knowledge this is the first study focusing on both a transcription factor and a chromatinin remodeler. We now need to determine if that model of double control of effector gene expression involving a specific TF and a chromatin remodeler could be generalized to other pathogenic fungi with two speed genome structures or if it remains very specific of *L. maculans*. In *F. oxysporum*, two specific transcription factors, FTF1 and FTF2, have been described for their ability to regulate all effector genes located on a particular pathogenicity dispensable chromosome (van der Does *et al.,* 2016). Such differences in effector genes regulation could indicate that phytopathogenic fungi use their incredible genome plasticity in very different ways to regulates effector genes during infection.

LmPf2 controls different sets of genes according to their chromatin context

Effector genes are known to need a tight regulation to permit fungus escaping plant recognition and manipulating host cell (Raffaele et Kamoun, 2012; Hacquard *et al.,* 2012; O'Connell *et al.,* 2012; Gervais *et al.,* 2017; Haueisen *et al.,* 2018). In this study, we determined the respective impact of chromatin remodeling and LmPf2 on effector gene expression. We determined that, in a WT background, *LmPf2* over-expression leads to over-expression of wave 3 effector genes. In contrast, in a ∆kmt1 background, *LmPf2* over-expression leads to over-expression of wave 2 effector genes including six of the nine cloned avirulence genes. Since *KMT1* is lowly expressed at the peak of expression of wave 2 effector genes (7DPI), we can hypothesize that H3K9me3 is removed at these effector gene loci during early infection and allow direct or indirect control by LmPf2. Furthermore, the inverted expression of *KMT1* and *LmPf2* during *L. maculans* life cycle supports our model of the double regulation. Other specific TFs could act in addition to LmPf2 to concertedly express all genes of wave 2. We propose the following regulation model: (i) *in vitro*, wave 2 and 3 genes are tightly repressed by H3K9me3 deposited by KMT1. (ii) at the onset of infection, H3K9me3 is removed and *LmPf2* is highly expressed, specifically activating wave 2 genes possibly because of a better direct or indirect affinity for wave 2 promoters. (iii) At 9 DPI, *KMT1* starts being re-expressed leading to a deposition of H3K9me3 on wave 2 genes first, possibly because of their high level of H3K9me3 *in vitro* or their specific localization in TE-rich compartments. At this stage, LmPf2 is not involved anymore on the control of wave 2 gene expression and starts activating wave 3 genes (**Figure 10**). These different sets of genes could be differentially controlled by LmPf2 indirectly taking into account the diversity of TF-encoding genes differentially expressed depending on the chromatinin condensation state.

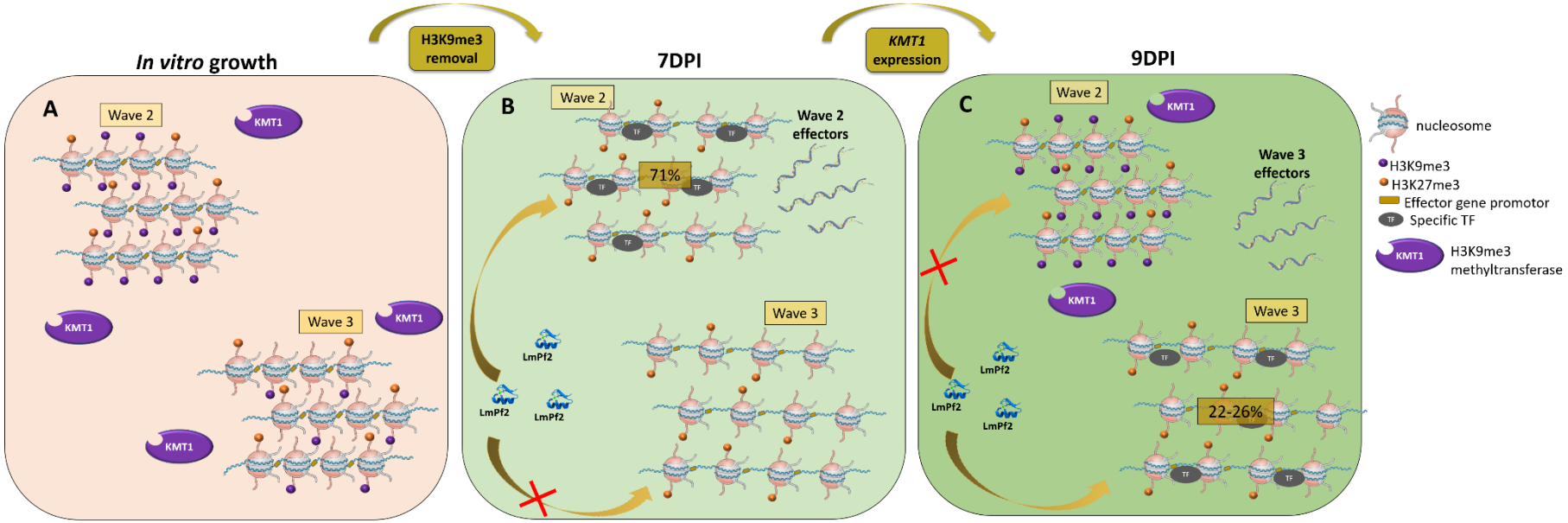

Figure 10: Model of key players of effector gene regulation as concerted waves during the early stage of *Leptosphaeria maculans* colonization of oilseed rape and *in vitro* growth. During *Leptosphaeria maculans'* life cycle, LmPf2 and KMT1 are able to regulate effector gene expression respectively acting on effector gene expression activation and chromatin condensation. **A:** During axenic growth effector waves repertoire are tightly repressed by H3K9me3 maintained by KMT1. **B:** At 7 DPi H3K9me3 is fully removed and heterochromatin is loosened. At this stage *LmPf2* is highly expressed and is able to regulate specifically 71% of Wave 2 effector genes probably because of a better affinity for wave 2 effector promotors. Between 7 DPI and 9 DPI *KMT1* is being expressed and start heterochromatin recondensation by H3K9me3 redeposition. **C:** Wave 2 effector genes are being recondense and LmPf2 start acting on (22 -26%) of Wave 3 effector genes, provoking their up-regulation. DPI = Days Post Inoculation.

Université Paris-Saclay
Espace Technologique / Immeuble Discovery
Route de l'Orme aux Merisiers RD 128 / 91190 Saint-Aubin, France

ACCESSION NUMBERS

All sequenced reads have been deposited with the Short Read Archive under accession numbers XXXX.

REFERENCES

Altschul, S.F., Gish, W., Miller, W., Myers, E.W., Lipman, D.J., 1990. Basic local alignment search tool. Journal of Molecular Biology 215, 403–410.

Ansan-Melayah, D. (inra, Balesdent, M.H., Buee, M., Rouxel, T., 1995. Genetic characterization of AvrLm1, the first avirulence gene of Leptosphaeria maculans. Phytopathology (USA).

Balesdent, M.H., Attard, A., Ansan-Melayah, D., Delourme, R., Renard, M., Rouxel, T., 2001. Genetic Control and Host Range of Avirulence Toward Brassica napus Cultivars Quinta and Jet Neuf in Leptosphaeria maculans. Phytopathology 91, 70–76.

Balesdent, M.H., Attard, A., Kühn, M.L., Rouxel, T., 2002. New Avirulence Genes in the Phytopathogenic Fungus Leptosphaeria maculans. Phytopathology 92, 1122–1133.

Balesdent, M.-H., Fudal, I., Ollivier, B., Bally, P., Grandaubert, J., Eber, F., Chèvre, A.-M., Leflon, M., Rouxel, T., 2013. The dispensable chromosome of Leptosphaeria maculans shelters an effector gene conferring avirulence towards Brassica rapa. New Phytologist 198, 887–898.

Basenko, E.Y., Sasaki, T., Ji, L., Prybol, C.J., Burckhardt, R.M., Schmitz, R.J., Lewis, Z.A., 2015. Genome-wide redistribution of H3K27me3 is linked to genotoxic stress and defective growth. Proceedings of the National Academy of Sciences 112, E6339–E6348.

Bolger, A.M., Lohse, M., Usadel, B., 2014. Trimmomatic: a flexible trimmer for Illumina sequence data. Bioinformatics 30, 2114–2120.

Van der Biezen, E.A., Jones, J.D., 1998. Plant disease-resistance proteins and the gene-for-gene concept. Trends Biochem. Sci. 23, 454–456.

Cho, Y., Ohm, R.A., Grigoriev, I.V., Srivastava, A., 2013. Fungal-specific transcription factor AbPf2 activates pathogenicity in Alternaria brassicicola. The Plant Journal 75, 498–514.

Chujo, T., Scott, B., 2014. Histone H3K9 and H3K27 methylation regulates fungal alkaloid biosynthesis in a fungal endophyte-plant symbiosis: K9 and K27 methylation regulates symbiosis. Molecular Microbiology 92, 413–434.

Connolly, L.R., Smith, K.M., Freitag, M., 2013. The Fusarium graminearum Histone H3 K27 Methyltransferase KMT6 Regulates Development and Expression of Secondary Metabolite Gene Clusters. PLoS Genetics 9, e1003916.

Dobin, A., Davis, C.A., Schlesinger, F., Drenkow, J., Zaleski, C., Jha, S., Batut, P., Chaisson, M., Gingeras, T.R., 2013. STAR: ultrafast universal RNA-seq aligner. Bioinformatics 29, 15–21.

van der Does, H.C., Fokkens, L., Yang, A., Schmidt, S.M., Langereis, L., Lukasiewicz, J.M., Hughes, T.R., Rep, M., 2016. Transcription factors encoded on core and accessory chromosomes of Fusarium oxysporum induce expression of effector genes. PLoS genetics 12, e1006401.

Université Paris-Saclay
Espace Technologique / Immeuble Discovery
Route de l'Orme aux Merisiers RD 128 / 91190 Saint-Aubin, France

Dutreux, F., Da Silva, C., d'Agata, L., Couloux, A., Gay, E.J., Istace, B., Lapalu, N., Lemainque, A., Linglin, J., Noel, B., Wincker, P., Cruaud, C., Rouxel, T., Balesdent, M.-H., Aury, J.-M., 2018. De novo assembly and annotation of three Leptosphaeria genomes using Oxford Nanopore MinION sequencing. Scientific Data 5.

Finn, R.D., Bateman, A., Clements, J., Coggill, P., Eberhardt, R.Y., Eddy, S.R., Heger, A., Hetherington, K., Holm, L., Mistry, J., Sonnhammer, E.L.L., Tate, J., Punta, M., 2014. Pfam: the protein families database. Nucleic Acids Res. 42, D222-230.

Fudal, I., Ross, S., Gout, L., Blaise, F., Kuhn, M.L., Eckert, M.R., Cattolico, L., Bernard-Samain, S., Balesdent, M.H., Rouxel, T., 2007. Heterochromatin-Like Regions as Ecological Niches for Avirulence Genes in the *Leptosphaeria maculans* Genome: Map-Based Cloning of *AvrLm6*. Molecular Plant-Microbe Interactions 20, 459–470.

Gacek, A., Strauss, J., 2012. The chromatin code of fungal secondary metabolite gene clusters. Appl Microbiol Biotechnol 95, 1389–1404.

Gacek-Matthews, A., Noble, L.M., Gruber, C., Berger, H., Sulyok, M., Marcos, A.T., Strauss, J., Andrianopoulos, A., 2015. KdmA, a histone H3 demethylase with bipartite function, differentially regulates primary and secondary metabolism in A spergillus nidulans: Histone H3K9 demethylase function in growth. Molecular Microbiology 96, 839–860.

Ghanbarnia, K., Ma, L., Larkan, N.J., Haddadi, P., Fernando, W.G.D., Borhan, M.H., 2018. Leptosphaeria maculans AvrLm9: a new player in the game of hide and seek with AvrLm4-7. Molecular Plant Pathology 19, 1754–1764.

Gervais, J., Plissonneau, C., Linglin, J., Meyer, M., Labadie, K., Cruaud, C., Fudal, I., Rouxel, T., Balesdent, M.-H., 2017. Different waves of effector genes with contrasted genomic location are expressed by Leptosphaeria maculans during cotyledon and stem colonization of oilseed rape. Molecular plant pathology 18, 1113–1126.

Gout, L., Fudal, I., Kuhn, M.-L., Blaise, F., Eckert, M., Cattolico, L., Balesdent, M.-H., Rouxel, T., 2006. Lost in the middle of nowhere: the AvrLm1 avirulence gene of the Dothideomycete Leptosphaeria maculans. Molecular Microbiology 60, 67–80.

Guo, S., Zhong, S., Zhang, A., 2013. Privacy-preserving Kruskal-Wallis test. Comput Methods Programs Biomed 112, 135–145.

Hacquard, S., Joly, D.L., Lin, Y.-C., Tisserant, E., Feau, N., Delaruelle, C., Legué, V., Kohler, A., Tanguay, P., Petre, B., Frey, P., Van de Peer, Y., Rouzé, P., Martin, F., Hamelin, R.C., Duplessis, S., 2012. A comprehensive analysis of genes encoding small secreted proteins identifies candidate effectors in Melampsora larici-populina (poplar leaf rust). Mol. Plant Microbe Interact. 25, 279–293.

Haueisen, J., Möller, M., Eschenbrenner, C.J., Grandaubert, J., Seybold, H., Adamiak, H., Stukenbrock, E.H., 2019. Highly flexible infection programs in a specialized wheat pathogen. Ecology and Evolution 9, 275–294.

Idnurm, A., Urquhart, A.S., Vummadi, D.R., Chang, S., Van de Wouw, A.P., López-Ruiz, F.J., 2017. Spontaneous and CRISPR/Cas9-induced mutation of the osmosensor histidine kinase of the canola pathogen Leptosphaeria maculans. Fungal Biology and Biotechnology 4.

IpCho, S.V.S., Tan, K.-C., Koh, G., Gummer, J., Oliver, R.P., Trengove, R.D., Solomon, P.S., 2010. The Transcription Factor StuA Regulates Central Carbon Metabolism, Mycotoxin Production, and Effector Gene Expression in the Wheat Pathogen Stagonospora nodorum. Eukaryotic Cell 9, 1100–1108.

Li, H., Handsaker, B., Wysoker, A., Fennell, T., Ruan, J., Homer, N., Marth, G., Abecasis, G., Durbin, R., 2009. The Sequence Alignment/Map format and SAMtools. Bioinformatics 25, 2078–2079.

Livak KJ, Schmittgen TD. Analysis of relative gene expression data using real-time quantitative PCR and the 2(-Delta Delta C(T)) Method. Methods. 2001 25:402-408.

Lo Presti, L., Lanver, D., Schweizer, G., Tanaka, S., Liang, L., Tollot, M., Zuccaro, A., Reissmann, S., Kahmann, R., 2015. Fungal Effectors and Plant Susceptibility. Annual Review of Plant Biology 66, 513–545.

McCarthy, D.J., Chen, Y., Smyth, G.K., 2012. Differential expression analysis of multifactor RNA-Seq experiments with respect to biological variation. Nucleic Acids Res 40, 4288–4297.

Michielse, C.B., van Wijk, R., Reijnen, L., Manders, E.M.M., Boas, S., Olivain, C., Alabouvette, C., Rep, M., 2009. The Nuclear Protein Sge1 of Fusarium oxysporum Is Required for Parasitic Growth. PLoS Pathogens 5, e1000637.

Möller, M., Schotanus, K., Soyer, J., Haueisen, J., Happ, K., Stralucke, M., Happel, P., Smith, K.M., Connolly, L.R., Freitag, M., Stukenbrock, E.H., 2019. Destabilization of chromosome structure by histone H3 lysine 27 methylation.

Muller, P.Y., Janovjak, H., Miserez, A.R., Dobbie, Z., 2002. Processing of gene expression data generated by quantitative real-time RT-PCR. BioTechniques 32, 1372–1374, 1376, 1378–1379.

Mullins, E.D., Chen, X., Romaine, P., Raina, R., Geiser, D.M., Kang, S., 2001. Agrobacterium-Mediated Transformation of Fusarium oxysporum: An Efficient Tool for Insertional Mutagenesis and Gene Transfer. Phytopathology 91, 173–180.

O'Connell, R.J., Thon, M.R., Hacquard, S., Amyotte, S.G., Kleemann, J., 2012. Lifestyle transitions in plant pathogenic Colletotrichum fungi deciphered by genome and transcriptome analyses. Nature Genetics 44, 1060–1065.

Papadopoulos, J.S., Agarwala, R., 2007. COBALT: constraint-based alignment tool for multiple protein sequences. Bioinformatics 23, 1073–1079.

Parlange, F., Daverdin, G., Fudal, I., Kuhn, M.-L., Balesdent, M.-H., Blaise, F., Grezes-Besset, B., Rouxel, T., 2009. Leptosphaeria maculans avirulence gene AvrLm4-7 confers a dual recognition specificity by the Rlm4 and Rlm7 resistance genes of oilseed rape, and circumvents Rlm4-mediated recognition through a single amino acid change. Mol. Microbiol. 71, 851–863.

Petit-Houdenot, Y., Degrave, A., Meyer, M., Blaise, F., Ollivier, B., Marais, C.-L., Jauneau, A., Audran, C., Rivas, S., Veneault-Fourrey, C., Brun, H., Rouxel, T., Fudal, I., Balesdent, M.-H., 2019. A two genes - for - one gene interaction between Leptosphaeria maculans and Brassica napus. New Phytol. 223, 397–411.

Plissonneau, C., Rouxel, T., Chèvre, A.-M., Van De Wouw, A.P., Balesdent, M.-H., 2018. One gene-one name: the AvrLmJ1 avirulence gene of Leptosphaeria maculans is AvrLm5. Molecular plant pathology 19, 1012–1016.

Robinson, M.D., McCarthy, D.J., Smyth, G.K., 2010. edgeR: a Bioconductor package for differential expression analysis of digital gene expression data. Bioinformatics 26, 139–140.

Rouxel, T., Balesdent, M.H., 2005. The stem canker (blackleg) fungus, Leptosphaeria maculans, enters the genomic era. Molecular Plant Pathology 6, 225–241.

Université Paris-Saclay
Espace Technologique / Immeuble Discovery
Route de l'Orme aux Merisiers RD 128 / 91190 Saint-Aubin,
France

Rouxel, T., Grandaubert, J., Hane, J.K., Hoede, C., van de Wouw, A.P., Couloux, A., Dominguez, V., Anthouard, V., Bally, P., Bourras, S., Cozijnsen, A.J., Ciuffetti, L.M., Degrave, A., Dilmaghani, A., Duret, L., Fudal, I., Goodwin, S.B., Gout, L., Glaser, N., Linglin, J., Kema, G.H.J., Lapalu, N., Lawrence, C.B., May, K., Meyer, M., Ollivier, B., Poulain, J., Schoch, C.L., Simon, A., Spatafora, J.W., Stachowiak, A., Turgeon, B.G., Tyler, B.M., Vincent, D., Weissenbach, J., Amselem, J., Quesneville, H., Oliver, R.P., Wincker, P., Balesdent, M.-H., Howlett, B.J., 2011. Effector diversification within compartments of the Leptosphaeria maculans genome affected by Repeat-Induced Point mutations. Nature Communications 2.

Rybak, K., See, P.T., Phan, H.T., Syme, R.A., Moffat, C.S., Oliver, R.P., Tan, K.-C., 2017. A functionally conserved Zn2Cys6 binuclear cluster transcription factor class regulates necrotrophic effector gene expression and host-specific virulence of two major Pleosporales fungal pathogens of wheat. Molecular plant pathology 18, 420–434.

Sánchez-Vallet, A., Fouché, S., Fudal, I., Hartmann, F.E., Soyer, J.L., Tellier, A., Croll, D., 2018. The Genome Biology of Effector Gene Evolution in Filamentous Plant Pathogens. Annual Review of Phytopathology 56, 21–40.

Šašek, V., Nováková, M., Dobrev, P.I., Valentová, O., and Burketová, L. (2012). β-aminobutyric acid protects Brassica napus plants from infection by Leptosphaeria maculans. Resistance induction or a direct antifungal effect? Eur. J. Plant Pathol. 133, 279–289.

Shannon, P., Markiel, A., Ozier, O., Baliga, N.S., Wang, J.T., Ramage, D., Amin, N., Schwikowski, B., Ideker, T., 2003. Cytoscape: a software environment for integrated models of biomolecular interaction networks. Genome Res. 13, 2498–2504.

Silayeva, O., Barnes, A.C., 2018. Gibson Assembly facilitates bacterial allelic exchange mutagenesis. J. Microbiol. Methods 144, 157–163.

Soyer, J.L., El Ghalid, M., Glaser, N., Ollivier, B., Linglin, J., Grandaubert, J., Balesdent, M.-H., Connolly, L.R., Freitag, M., Rouxel, T., Fudal, I., 2014. Epigenetic Control of Effector Gene Expression in the Plant Pathogenic Fungus Leptosphaeria maculans. PLoS Genetics 10, e1004227.

Soyer, J.L., Rouxel, T., Fudal, I., 2015. A Chromatin-based control of effector gene expression in plant-associated fungi. Current Opinion in Plant Biology 26, 51–56.

Soyer, J.L., Hamiot, A., Ollivier, B., Balesdent, M.-H., Rouxel, T., Fudal, I., 2015. B The APSES transcription factor LmStuA is required for sporulation, pathogenic development and effector gene expression in *Leptosphaeria maculans*: Functional analysis of LmStuA from *L. maculans*. Molecular Plant Pathology 16, 1000–1005.

Soyer, J.L., Grandaubert, J., Haueisen, J., Schotanus, K., Stukenbrock, E.H., 2019. In planta chromatin immunoprecipitation in Zymoseptoria tritici reveals chromatin-based regulation of putative effector gene expression. bioRxiv 544627.

Stergiopoulos, I., de Wit, P.J.G.M., 2009. Fungal Effector Proteins. Annual Review of Phytopathology 47, 233–263.

Strauss, J., Reyes-Dominguez, Y., 2011. Regulation of secondary metabolism by chromatin structure and epigenetic codes. Fungal Genetics and Biology 48, 62–69.

Tan, K.-C., Oliver, R.P., 2017. Regulation of proteinaceous effector expression in phytopathogenic fungi. PLoS pathogens 13, e1006241.

Université Paris-Saclay
Espace Technologique / Immeuble Discovery
Route de l'Orme aux Merisiers RD 128 / 91190 Saint-Aubin, France

Winter, D.J., Ganley, A., Young, C., Liachko, I., Schardl, C., Dupont, P., Berry, D., Ram, A., Scott, B., Cox, M., 2018. Repeat elements organize 3D genome structure and mediate transcription in the filamentous fungus Epichloë festucae. bioRxiv 339010.

Wouw, A.P.V. de, Lowe, R.G.T., Elliott, C.E., Dubois, D.J., Howlett, B.J., 2014. An avirulence gene, AvrLmJ1, from the blackleg fungus, Leptosphaeria maculans, confers avirulence to Brassica juncea cultivars. Molecular Plant Pathology 15, 523–530.

Zahiri, A., Heimel, K., Wahl, R., Rath, M., Kämper, J., 2010. The *Ustilago maydis* Forkhead Transcription Factor Fox1 Is Involved in the Regulation of Genes Required for the Attenuation of Plant Defenses During Pathogenic Development. Molecular Plant-Microbe Interactions 23, 1118–1129.

Zhang, X., Liu, X., Zhao, Y., Cheng, J., Xie, J., Fu, Y., Jiang, D., Chen, T., 2016. Histone H3 Lysine 9 Methyltransferase DIM5 Is Required for the Development and Virulence of Botrytis cinerea. Frontiers in Microbiology 7.

SUPPLEMENTARY DATA

Supplementary Data are available at NAR online.

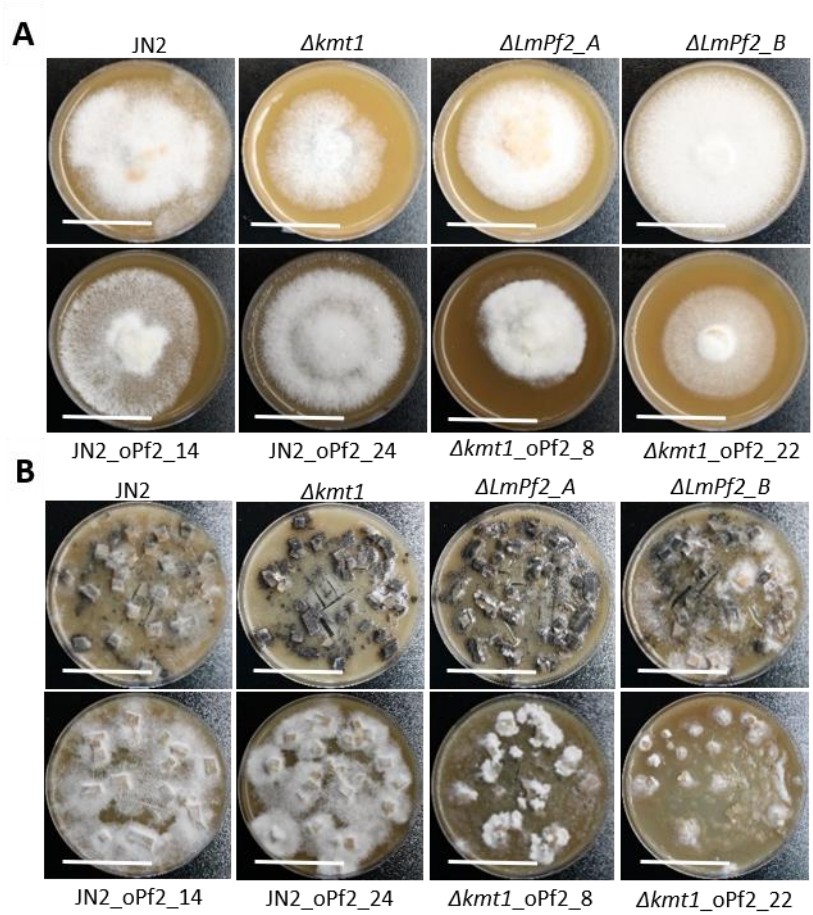

Figure S1: Morphological characterization of *LmPf2* mutants and over-expression transformants. The over-expression transformants have been obtained in a WT background (JN2) and in a *Δkmt1* background. **A:** Transformant thallus morphology on V8 agar medium at 6 days after inoculation. Scale bars corresponding to 50 mm. **B:** Transformant thallus morphology during conidiation on V8 agar 14 days after inoculation. Scale bars corresponding to 90 mm.

Université Paris-Saclay
Espace Technologique / Immeuble Discovery
Route de l'Orme aux Merisiers RD 128 / 91190 Saint-Aubin, France

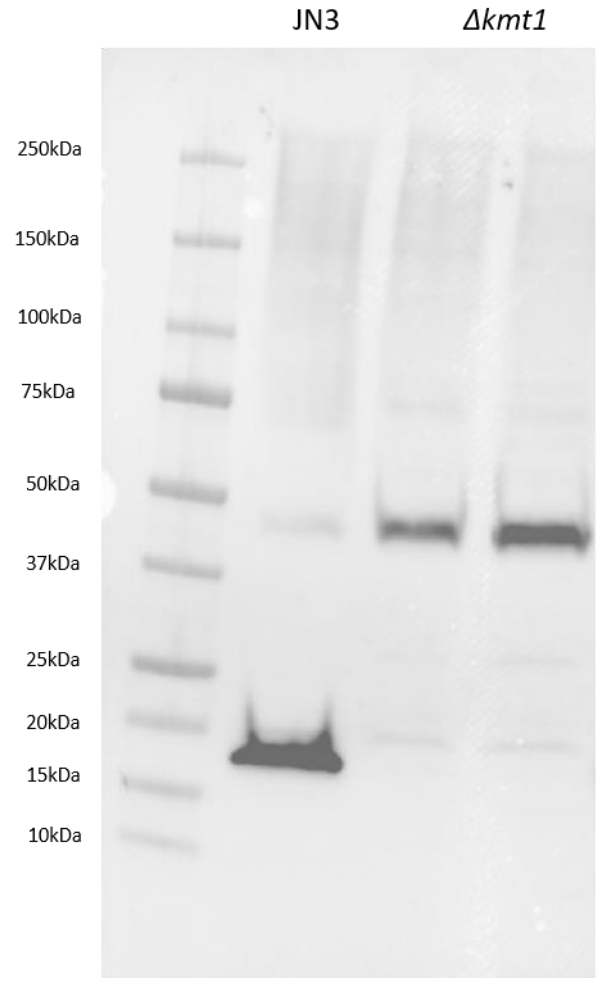

Figure S2: Immunoblot analysis showing presence of H3K9me3. Protein extracts were analysed by immunoblotting with anti-H3K9me3 antibodies. *Δkmt1* have been tested using two replicates of total protein extract.

Université Paris-Saclay
Espace Technologique / Immeuble Discovery
Route de l'Orme aux Merisiers RD 128 / 91190 Saint-Aubin, France

658

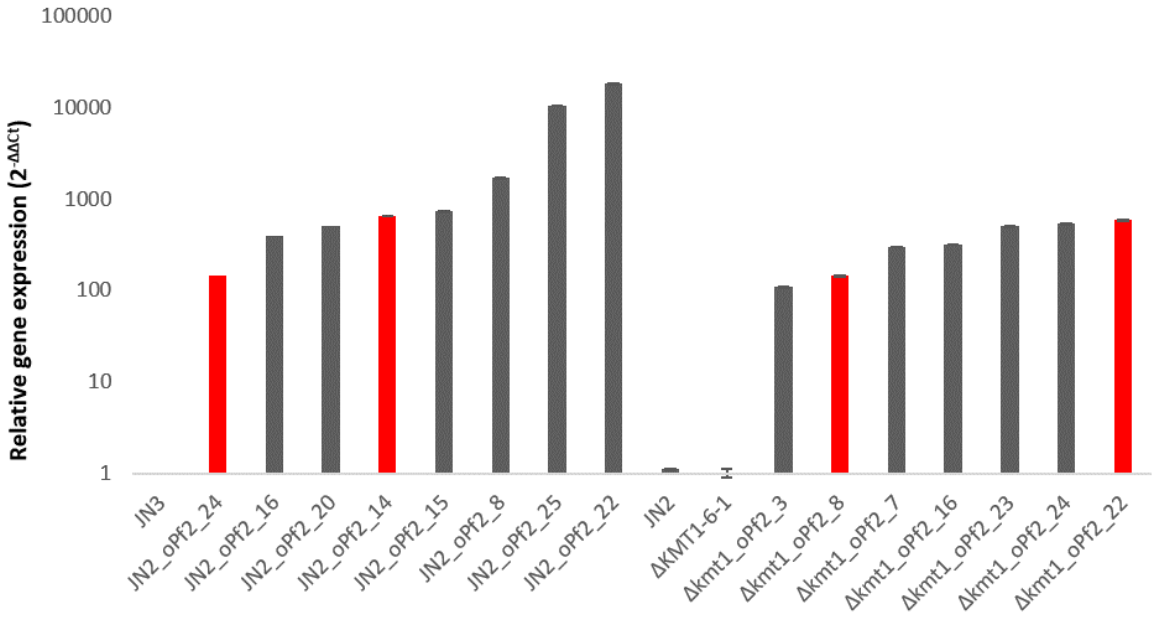

Figure S3: Level of *LmPf2* expression in the *L. maculans* transformants over-expressing *LmPf2* during axenic growth. Mycelium was obtained by growing JN2 and JN3 strains and transformants in Fries liquid medium for 7 days. Two biological replicates per condition were generated. Total RNA was extracted. Expression of *LmPf2* was measured by qRT-PCR and expressed relatively to *LmβTubulin* expression and to expression of *LmPf2* in the strain before transformation using the $2^{-\Delta\Delta Ct}$ method (Livak and Schittgen, 2001). Red bars correspond to transformants which were selected for further characterization (JN2_oPf2_14, JN2_oPf2_24, *Δkmt1*_oPf2_8 and *Δkmt1*_oPf2_22).

Université Paris-Saclay
Espace Technologique / Immeuble Discovery
Route de l'Orme aux Merisiers RD 128 / 91190 Saint-Aubin, France

659

660

661

662

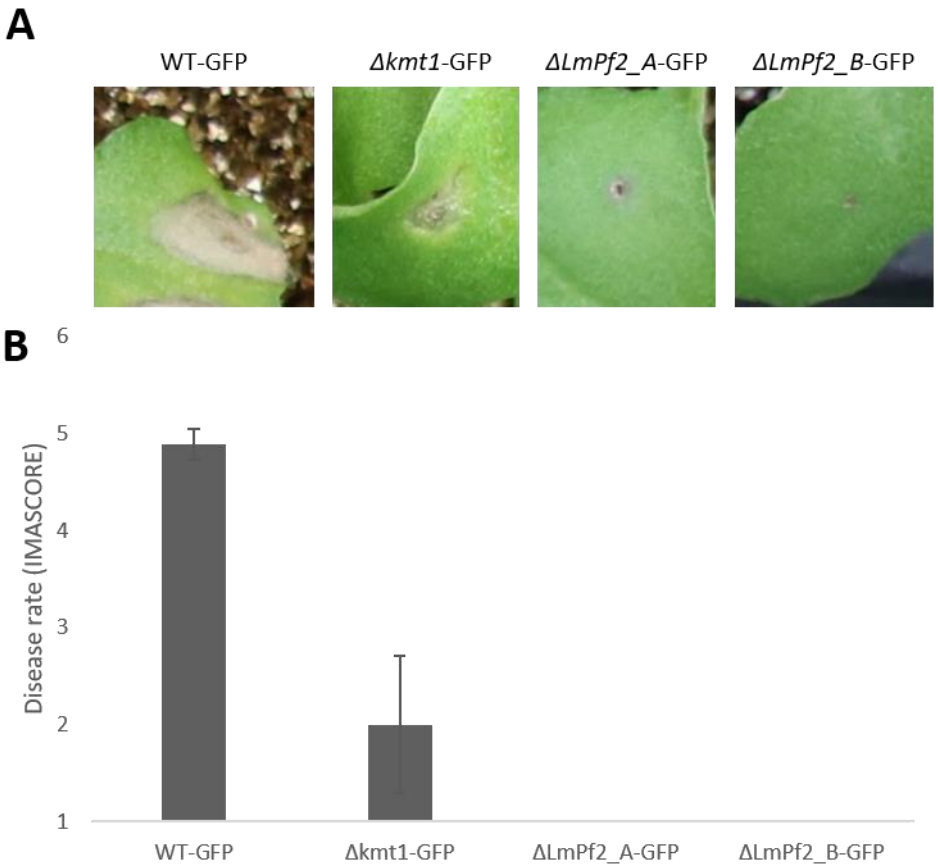

Figure S4: Pathogenicity assays on WT, *Δkmt1* and *ΔLmPf2* transformants after crossing with JN2-GFP. A: Photos of symptoms on Es-Astrid at 14 DPI. **B:** Pathogenicity test of three different CRISPR-Cas9 mutants on oilseed rape cotyledons of a susceptible cultivar (Es-Astrid) at 13 DPI. Disease rate is expressed as the mean scoring using the IMASCORE rating scale comprising six infection classes (IC), where IC1 to IC3 correspond to various levels of resistance of the plant and IC4 to IC6 to susceptibility (Balesdent *et al.,* 2001).

663

664

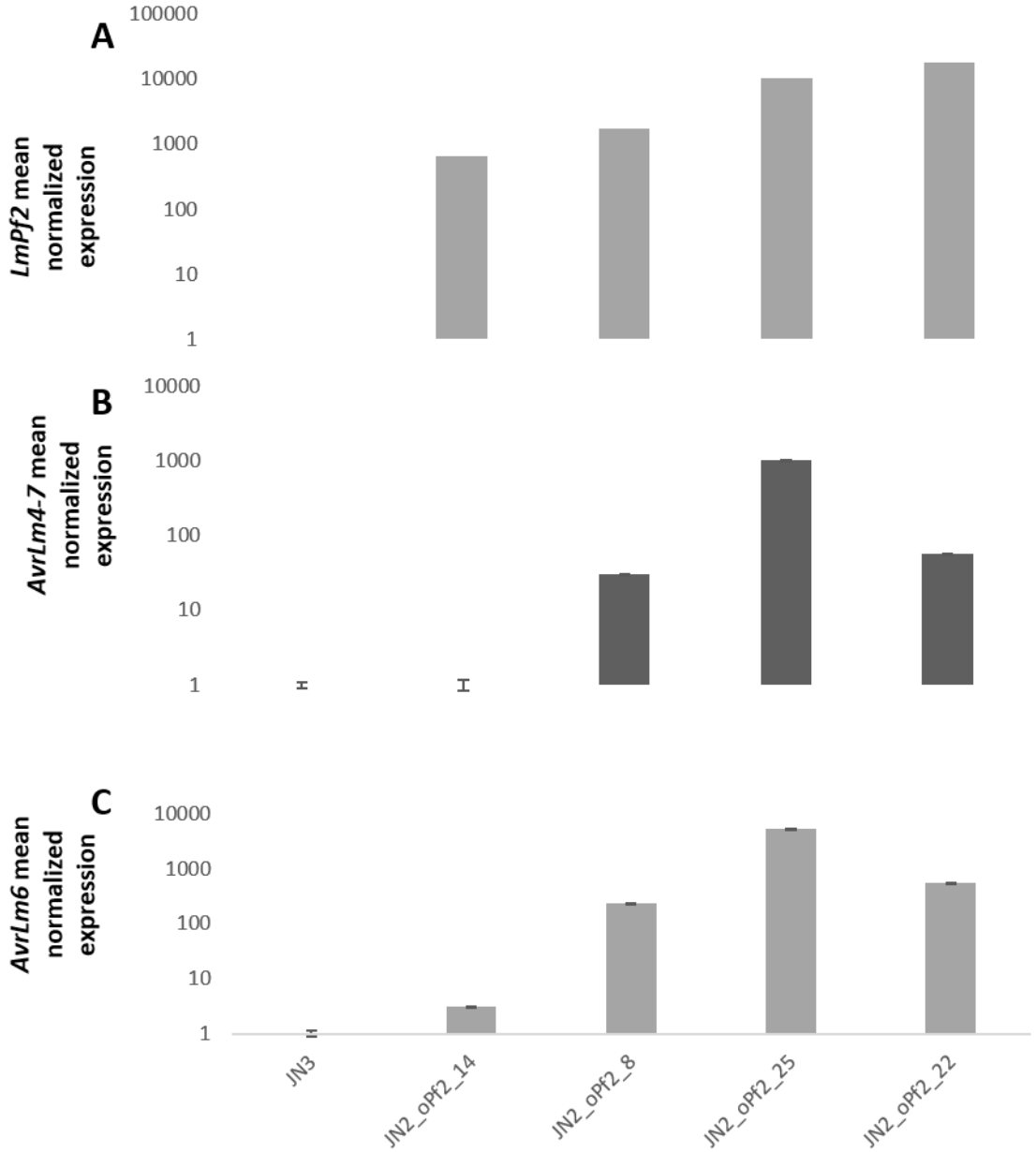

Figure S5: Influence of *LmPf2* over-expression on the expression of two *L. maculans* avirulence genes during axenic growth. Mycelium was grown in Fries liquid medium during seven days. Expression of *LmPf2* (A), *AvrLm4-7 (*B) and *AvrLm6* (C) was measured by qRT-PCR level using *LmβTubulin* as a constitutive reporter gene and expression in JN2 as reference ($2^{-\Delta\Delta Ct}$ method). Each value is the average of two biological replicates (two extractions from different biological replicates) and two technical replicates (two RT-PCR).

Université Paris-Saclay
Espace Technologique / Immeuble Discovery
Route de l'Orme aux Merisiers RD 128 / 91190 Saint-Aubin, France

665

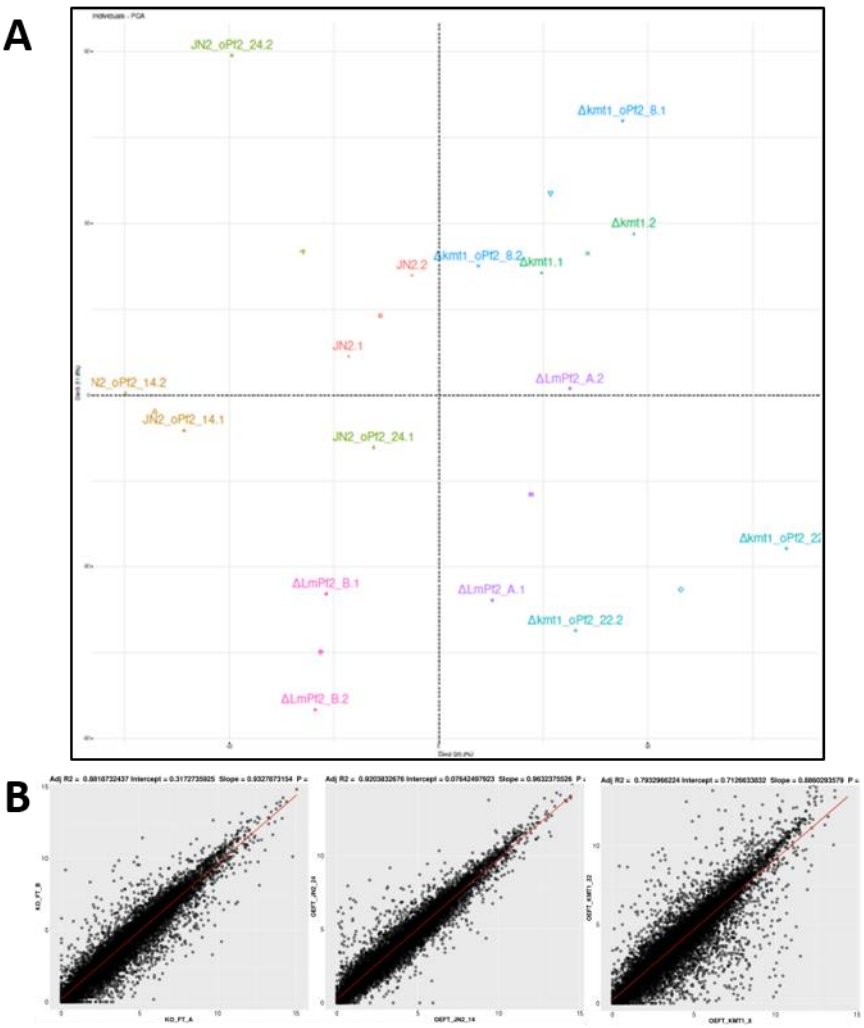

Figure S6: Reproducibility of RNA-Seq replicates. A: log2(RPKM) PCA of all samples. Legend labels: WT = JN2; Δ*kmt1*_X = Δ*kmt1_A* and B; Δ*LmPf2*_X = Δ*LmPf2_A* and B*;* JN2_oPf2_X = JN2_oPf2_14 and 24 ; and Δ*kmt1*_oPf2_X = *Δkmt1*_oPf_8 and 22. **B:** Scatterplot obtained with Log2(RPKM) of three biological replicates. Left panel = Δ*LmPf2_A* vs Δ*LmPf2_B;* middle panel = JN2_oPf2_14 vs JN2_oPf2_24*;* and right panel = *Δkmt1*_oPf2_8 vs Δ*kmt1*_oPf2_22.

Université Paris-Saclay
Espace Technologique / Immeuble Discovery
Route de l'Orme aux Merisiers RD 128 / 91190 Saint-Aubin, France

Table S1: Primers used in the study

Name of the fragment	DNA sequence	function	construction
gRNA against *LmPf2*	GAAACCTAATCAATCAACAGCATGCTGATGAGTCCGTGAGGACGAAACGAGTAAGCTCGTCCATGCTCCCCGCCCAG	*Lmpf2* CRISPR-CAS9 directed inactivation	CRISPR-Cas9
	AGAGTTTTAGAGCTAGAAATAGC		
gRNA against *KMT1*	GAAACCTAATCAATCAACGGAGCACTGATGAGTCCGTGAGGACGAAACGAGTAAGCTCGTCTGCTCCCTTCGAACGTC	*KMT1* CRISPR-CAS9 directed inactivation	
	TGCGTTTTAGAGCTAGAAATAGC		
MAI0309	ACCTCTAATCGAAACCTAATCAATCAAC	Amplification of gRNA coding sequence	
MAI0310	ATTTTAACTTGCTATTTCTAGCTCTAAAAC	Amplification of gRNA coding sequence	
verif_CRISPR_LmPf2_F	CCACTCCAGTCAAGCGGGC	*LmPf2* mutation detection	
verif_CRISPR_LmPf2_R	AATTGGCGGTCGGACGATGC	*LmPf2* mutation detection	
verif_CRISPR_KMT1_F	GCCCTCCATGGTTGTGGTGC	*KMT1* mutation detection	
verif_CRISPR_KMT1_R	ACCCCGGAAATGCTAGCCGA	*KMT1* mutation detection	
EF1aProSac1F	GAGAGAGAGCTCGGCACTCGTAAGGAGTATGAGC	*Ef1a* promoter amplification and cloning	*Lmpf2* overexpression
EF1aProKpnIR	GAGAGAGGTACCGTTGGCGGTGTTGTGATGG	*Ef1a* promoter amplification and cloning	
surex_LmPf2_Gibs_F	AGTCGACCTGCAGGCATGCAATGGCTACCAATCCCACCACC	*Lmpf2* amplification and cloning	
surex_LmPf2_Gibs_R	GTAAAACGACGGCCAGTGCCAAGTTGGGGGAGAGTACATACTG	*Lmpf2* amplification and cloning	
LmPf2_primer_Up	ATGGCTACCAATCCCACCACC	*Lmpf2* sequence verification	
LmPf2_Seq1_F	CCGCCAATTCGCGTCTGGCC	*Lmpf2* sequence verification	
LmPf2_primer_Low	CAGTATGTACTCTCCCCCAAC	*Lmpf2* sequence verification	
βTubulin_F	AAGAACTCATCCTACTTCGA	qPCR	None
βTubulin_R	TGAATAGCTCCTGAATGG	qPCR	None
AvrLm4-7_F	GCCCTGCATAACTACCGAC	qPCR	None
AvrLm4-7_R	TCCTGGCCAAATATAACTCC	qPCR	None
AvrLm6_F	AAACGGCACTATTACGAAAA	qPCR	None
AvrLm6_R	GATTAGGCGAGAAGCAAGT	qPCR	None
AvrLm10.A_F	ACAGGAGAACACTGACGGCT	qPCR	None
AvrLm10.A_R	GCATGGACTATCGTAGCGTTAT	qPCR	None
AvrLm11_F	TGCGTTTCTTGCTTCCTATATTT	qPCR	None
AvrLm11_R	CAAGTTGGATCTTTCTCATTCG	qPCR	None

666

Université Paris-Saclay
Espace Technologique / Immeuble Discovery
Route de l'Orme aux Merisiers RD 128 / 91190 Saint-Aubin, France

667

Table S2: Crosses performed for mutant purification

	CRISPR-Cas9 mutation	Compatible isolate used for crosses	Name of the selected progenies[b]	Additional Transformation
Δkmt1 6-1	1 bp insertion	JN2[a]	*ΔKMT1*	*LmPf2* over-expression
		JN2-GFP	*ΔKMT1-GFP*	no
ΔLmPf2 1-2	1 bp deletion	JN2-GFP	*ΔLmPf2_A*	no
		JN2-GFP	*ΔLmPf2_A-GFP*	no
ΔLmPf2 4-2	5 bp deletion	JN2-GFP	*ΔLmPf2_B*	no
		JN2-GFP	*ΔLmPf2_B-GFP*	no

[a]Purification by crossing with an isolate of opposite mating type with or without GFP. b: Selected progenies purified (without *Cas9* and gRNA).

Université Paris-Saclay
Espace Technologique / Immeuble Discovery
Route de l'Orme aux Merisiers RD 128 / 91190 Saint-Aubin, France

668

669

Table S3: RNA-Seq read information.

	Total numbers of paired reads	Paired reads after pre-prossessing[a]	% paired kept reads	STAR mapping Uniquely mapped reads[b]
JN2-1	1.49 E+07	1.24E+07	83,28%	81.76%
JN2-2	2.35E+07	1.95E+07	83,14%	83.75%
Δkmt1-1	1.71E+07	1.42E+07	83,23%	83.12%
Δkmt1-2	1.72E+07	1.43E+07	83,06%	85.79%
ΔLmPf2_A-1	1.66E+07	1.37E+07	82,76%	83.92%
ΔLmPf2_A-2	1.59E+07	1.31E+07	82,51%	38.76%
ΔLmPf2_B-1	1.59E+07	1.32E+07	82,84%	81.68%
ΔLmPf2_B-2	1.62E+07	1.33E+07	82,17%	81.20%
JN2_oPf_14-1	2.43E+07	2.01E+07	82,73%	79.73%
JN2_oPf_14-2	2.32E+07	1.92E+07	82,86%	79.11%
JN2_oPf_24-1	2.48E+07	2.06E+07	83,02%	80.51%
JN2_oPf_24-1	2.42E+07	2.01E+07	83,17%	82.96%
Δkmt1_oPf_8-1	2.23E+07	1.85E+07	82,81%	84.44%
Δkmt1_oPf_8-2	2.23E+07	1.85E+07	83,04%	82.61%
Δkmt1_oPf_22-1	2.48E+07	2.08E+07	83,98%	75.19%
Δkmt1_oPf_22-2	2.11E+07	1.75E+07	83,00%	71.57%

[a] Paired read was treated with Trimmomatic. Sequencing adaptors and too short reads (<30 bp) were removed. [b] Reads were then mapped against *L. maculans* genome using STAR (Dobin *et al.,* 2013; Dutreux *et al.,* 2018).

Université Paris-Saclay
Espace Technologique / Immeuble Discovery
Route de l'Orme aux Merisiers RD 128 / 91190 Saint-Aubin, France

670

671

672

Table S4: Differentially expressed genes encoding small secreted proteins or located in particular chromatin domains.

		Total genes	SSP encoding genes	H3K4me2 genes	H3K9me3 genes	H3K27me3 genes	H3K9me3/H3K27me3 genes
Up-regulated	*Δkmt1*	129	22*	33#	5*	22*	2*
	ΔLmPf2	202	19	85#	4	23	5*
	JN2_oPf2	247	45	77#	5	41*	2*
	*Δkmt1*_oPf_8	275	54*	61#	16*	56*	10*
	*Δkmt1*_oPf_22	931	154*	218#	34*	152*	15*
Down-regulated	*Δkmt1*	143	25*	36#	13*	13	6*
	ΔLmPf2	225	36*	75#	10*	26	4*
	JN2_oPf2	277	19	126#	3	26	0
	*Δkmt1*_oPf_8	158	23*	41#	9*	16	8*
	*Δkmt1*_oPf_22	861	83	399#	16	80	9*

Differential expression is obtained by comparing WT expression to each transformant. We studied genes specifically coding for Small Secreted Proteins (SSPs) or specifically located in euchromatin environment marked by di-methylation of lysine 4 of histone H3 (H3K4me2) and heterochromatin environment marked by tri-methylation of lysine 9 of histone H3 (H3K9me3), tri-methylation of lysine 27 of histone H3 (H3K27me3) and both (H3K9me3/H3K27me3). # corresponds to statistically under-represented genes and * corresponds to statistically enriched genes. Statistical analysis performed using Khi², Pvalue < 0.05.

Université Paris-Saclay
Espace Technologique / Immeuble Discovery
Route de l'Orme aux Merisiers RD 128 / 91190 Saint-Aubin, France

Table S5: Differentially expressed transcription factor coding genes in *LmPf2* over-expressor harbouring different chromatinian context.

Upregulated transcription factor genes			
*Δkmt1*_oPf_22		JN2_oPf2	
ID	Fonction	ID	Fonction
Lmb_jn3_00338	zinc_finger-containing	Lmb_jn3_00032	zinc_finger_740
Lmb_jn3_00666	AN1_zinc_finger		
Lmb_jn3_01078	C2H2_type_zinc_finger_containing	Lmb_jn3_04461	C2H2_type_zinc_finger_domain_containing
Lmb_jn3_01759	zinc_knuckle	Lmb_jn3_04938	translation_factor_mitochondrial
Lmb_jn3_02114	zinc_finger_ring-type		
Lmb_jn3_03373	C6_transcription_factor	Lmb_jn3_05737	Zn(2)-C6_fungal-type_D-binding_domain
Lmb_jn3_04191	C2H2_conidiation_transcription_factor	Lmb_jn3_07527	transcription_factor_jumonji_aspartyl_beta-hydroxylase
Lmb_jn3_04849	C2H2_finger_domain-containing	Lmb_jn3_11428	C-x8-C-x5-C-x3-H_type_zinc_finger
Lmb_jn3_05461	zinc_ion_binding		
Lmb_jn3_05737	Zn(2)-C6_fungal-type_D-binding_domain		
Lmb_jn3_06942	C6_finger_domain		
Lmb_jn3_06984	transcriptiol_co-activator		
Lmb_jn3_07222	C2H2_finger_domain-containing		
Lmb_jn3_07297	C2H2_type_zinc_finger_domain-containing		
Lmb_jn3_07916	C6_Zinc_finger_domain_containing		
Lmb_jn3_08804	zinc_ion_binding		
Lmb_jn3_10400	zinc_metalloprotease		
Lmb_jn3_11010	transcription_factor_tfiiic_complex_subunit_sfc4		
Lmb_jn3_11399	zinc_ion_binding		
Lmb_jn3_11428	C-x8-C-x5-C-x3-H_type_zinc_finger		
Lmb_jn3_12660	C2H2_finger_domain		

ACKNOWLEDGEMENT

We are grateful to the Genewiz bioinformatics platform Leipzig Germany for providing computing resources.

FUNDING

CONFLICT OF INTEREST

The authors declare no conflict of interest

RESULTATS COMPLEMENTAIRES

Analyse fonctionnelle de facteurs de transcription putatifs pour leur implication dans la régulation de l'expression des gènes codant des effecteurs de *Leptosphaeria maculans*

Certains FTs sont capables de réguler la mise en place de différents processus cellulaires chez les champignons filamenteux tels que le métabolisme primaire, secondaire, la reproduction sexuée ou encore l'expression des gènes codant des effecteurs (Cho *et al.,* 2013 ; Soyer *et al.,* 2015. B; Niño-Sánchez *et al.,* 2016; Rybak *et al*., 2017). Lors de cette thèse, j'ai pu mettre en évidence le rôle majeur du FT LmPf2 dans le contrôle de l'expression des gènes codant des effecteurs de *L. maculans* (Voire **chapitre 3**). Afin d'identifier un ou des FTs contrôlant l'expression des gènes codant des effecteurs de *L. maculans*, deux approches avaient été choisies : (i) une approche avec *a priori* consistant à identifier les gènes orthologues de FTs décrits chez les champignons comme impliqués dans le contrôle de l'expression des effecteurs (e.g. *Sge1*, *StuA*, cf. **partie 5.3**) et (ii) une approche sans *a priori* consistant à prédire le répertoire de FTs de *L. maculans* et à rechercher les FTs surexprimés pendant l'infection ou spécifiques de *L. maculans* (J. Soyer, thèse). Parmi eux, j'ai sélectionné deux FTs de *L. maculans,* codant des AT-Hook (ciblant spécifiquement les régions riches en AT) et différentiellement exprimés *in planta* pour une étude fonctionnelle. Le premier gène codant un FT est spécifique de *L. maculans*, *Lmb_jn3_09123*. Le second, *Lmb_jn3_02170,* est présent chez toutes les espèces du complexe d'espèce de *L. maculans* (**Figure 1**).

J'ai inactivé ces deux facteurs de transcription par la technique CRISPR-Cas9. Le premier gène, *Lmb_jn3_09123*, est exprimé dès 2 jpi. J'ai obtenu 10 mutants indépendants présentant six types de mutations différentes menant pour cinq d'entre eux à la perte des domaines fonctionnels (**Figure 2**). Les mutants ont été caractérisés pour leur croissance et leur capacité à infecter un cultivar sensible de colza. Aucun des mutants ne présentait d'altération de croissance ou de pathogénie (**Figure 3**). Il reste cependant possible que ce FT soit impliqué dans la mise en place de l'infection étant donné son profil d'expression et les domaines prédits (deux domaines de liaison à la chitine, un domaine de liaison à l'ubiquitine et un domaine déacétylase de chitine ; **Figures 1** et **2**).

Université Paris-Saclay
Espace Technologique / Immeuble Discovery
Route de l'Orme aux Merisiers RD 128 / 91190 Saint-Aubin, France

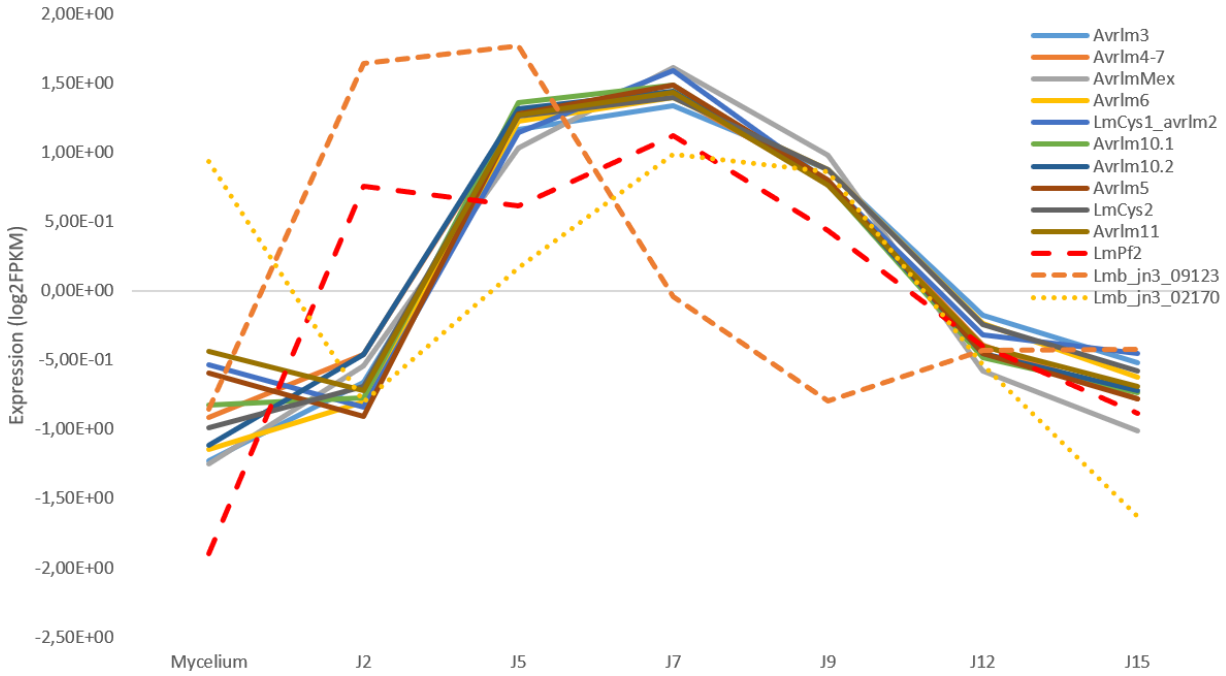

Figure 1: Expression profile of cloned effector genes and three specific transcription factors during infection and axenic growth obtained by RNA-seq. Mycelium were obtained by growing JN2 on V8 for 7 days. Cotyledons were sampled at 7 different time points (2, 5, 7, 9, 12, 15 days post infection). All samples were sequenced in two replicats. Cloned effector genes (*AvrLm4-7, AvrLm6, AvrLm2, AvrLm3, AvrLm10.1, AvrLm10.2, AvrLmCys2, AvrLm11, AvrLm5*) relative expression is plotted depending on the conditions. Transcription factors (*LmPf2, Lmb_jn3_09123 and Lmb_jn3_02170*) relative expression is plotted depending on the same conditions (EJ. Gay, on-going PhD thesis, Data extracted from Leptolife project).

Université Paris-Saclay
Espace Technologique / Immeuble Discovery
Route de l'Orme aux Merisiers RD 128 / 91190 Saint-Aubin, France

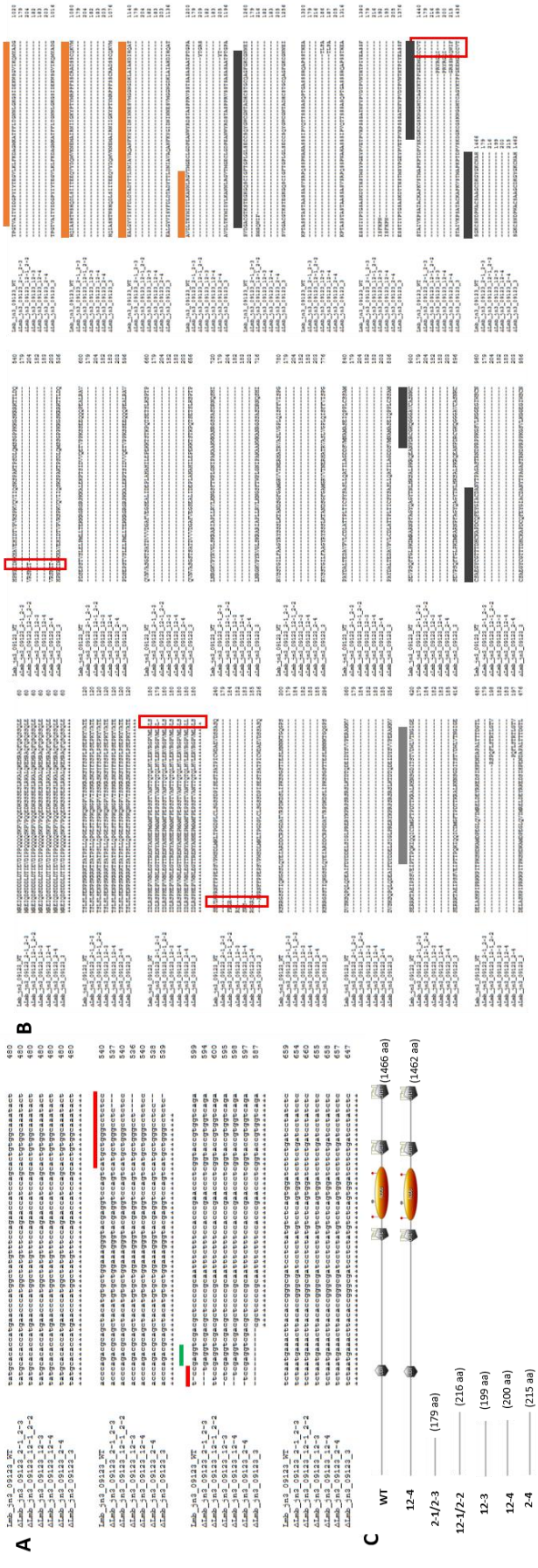

Figure 2: Effect of the *Lmb_jn3_09123* mutations on Lmb_jn3_09123 protein structure. A: Sequence alignment of the ***Lmb_jn3_09123* gene** in the WT isolate JN2 and in six mutants. The PAM (Protospacer Adjacent Motif) is highlighted in green and the region targeted by the guide RNA is highlighted in red. **B:** Protein sequence of Lmb_jn3_09123 in the WT isolate JN2 and in the six mutants. Light grey, dark greys and orange domains corresponding respectively to UBA, chitin binding domains and NODB domain. **C:** Lmb_jn3_09123 protein length and domains identified with Pfam (UBA(Ubiquitin-associated domain), three chitin binding domains and NOBD domain (chitin deacetylase domain); https://pfam.xfam.org/) .

Université Paris-Saclay
Espace Technologique / Immeuble Discovery
Route de l'Orme aux Merisiers RD 128 / 91190 Saint-Aubin, France

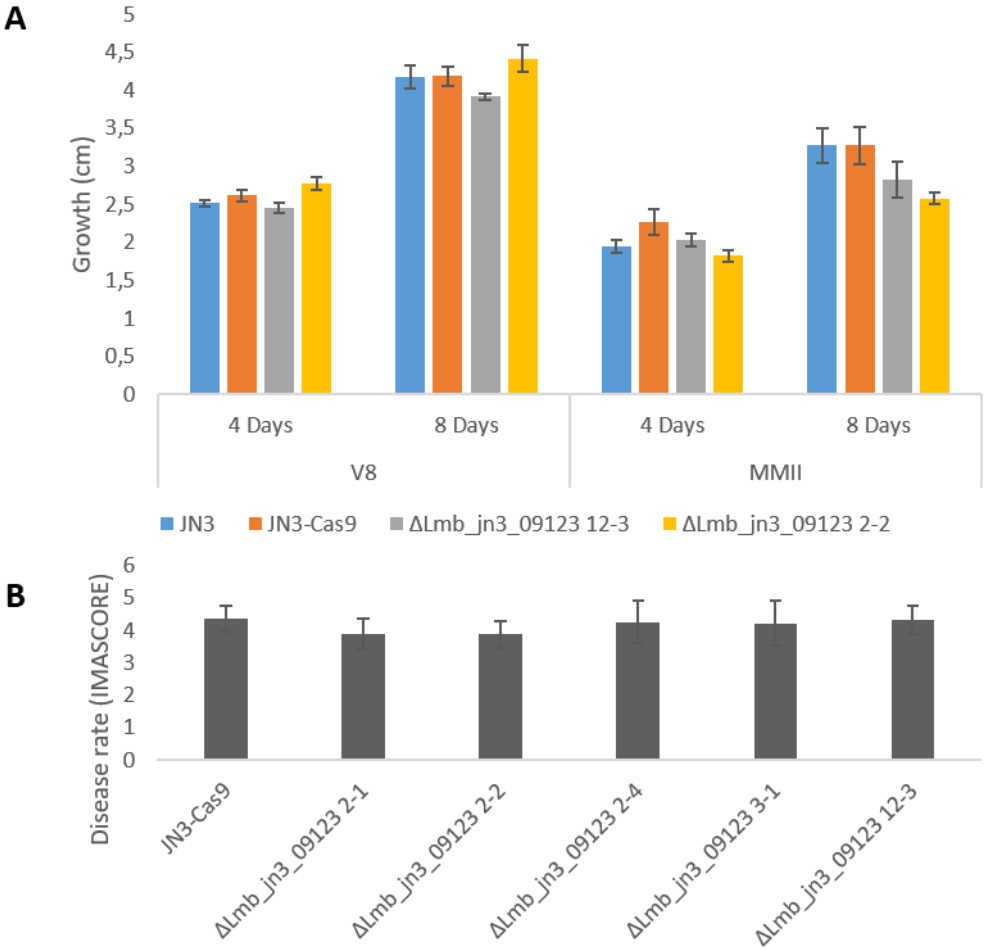

Figure 3: Effect of *Lmb_jn3_09123* inactivation on mycelial growth and pathogenicity of *Leptosphaeria maculans*. A: Growth assay on *Lmb_jn3_09123* mutants and WT strain JN3 with or without *Cas9* gene. Mycelial growth was measured at 4 days and 8 days post inoculation on two different agar media, V8 and MMII. **B:** Pathogenicity tests were performed on the susceptible cultivar Es-Astrid at 13 DPI. Disease rate is expressed as the mean scoring using the IMASCORE rating scale comprising six infection classes (IC), where IC1 to IC3 corresponded to resistance and IC4 to IC6, to susceptibility. DPI = Days Post Inoculation.

Université Paris-Saclay
Espace Technologique / Immeuble Discovery
Route de l'Orme aux Merisiers RD 128 / 91190 Saint-Aubin, France

L'autre FT que j'ai étudié, *Lmb_jn3_02170*, possède un profil d'expression corrélé avec celui des effecteurs précoces (**Figure 1**). L'inactivation de Lmb*_jn3_02170* par CRISPR-Cas9 a permis d'obtenir trois types de mutations différentes et quatre mutants indépendants. Ces trois mutations mènent à protéine tronquée de la moitié de sa taille. Ce FT ne possède pas de domaine fonctionnel prédit et il est donc difficile d'identifier sa fonction (**Figure 4**). L'inactivation de *Lmb_jn3_02170* ne conduit à aucun défaut de croissance ou de pathogénie (**Figure 5**).

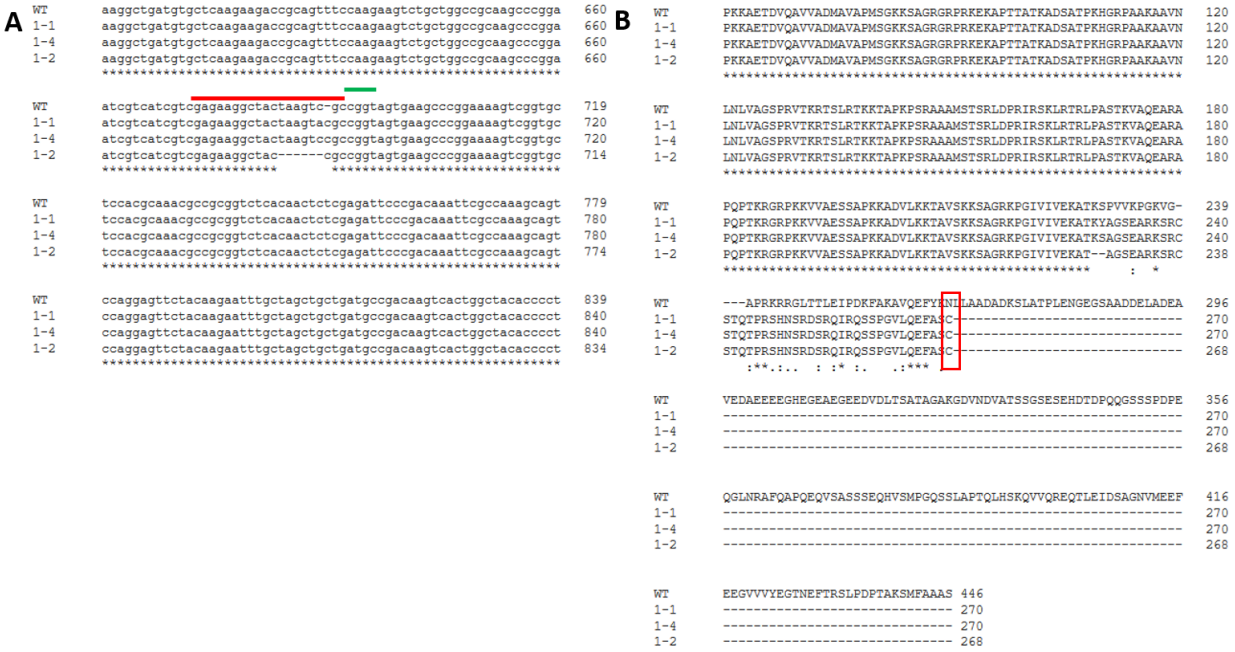

Figure 4: Effect of the *Lmb_jn3_02170* mutations on Lmb_jn3_02170 protein structure. A: Sequence alignment of the *Lmb_jn3_02170* gene in the WT isolate JN2 and in three mutants. The PAM (Protospacer Adjacent Motif) is highlighted in green and the region targeted by the guide RNA is highlighted in red. **B:** Protein sequence of Lmb_jn3_02170 in the WT isolate JN2 and in the three mutants. The red frame indicates the stop in the mutant versions of the protein. No domains have been predicted using Pfam (https://pfam.xfam.org/).

Université Paris-Saclay
Espace Technologique / Immeuble Discovery
Route de l'Orme aux Merisiers RD 128 / 91190 Saint-Aubin, France

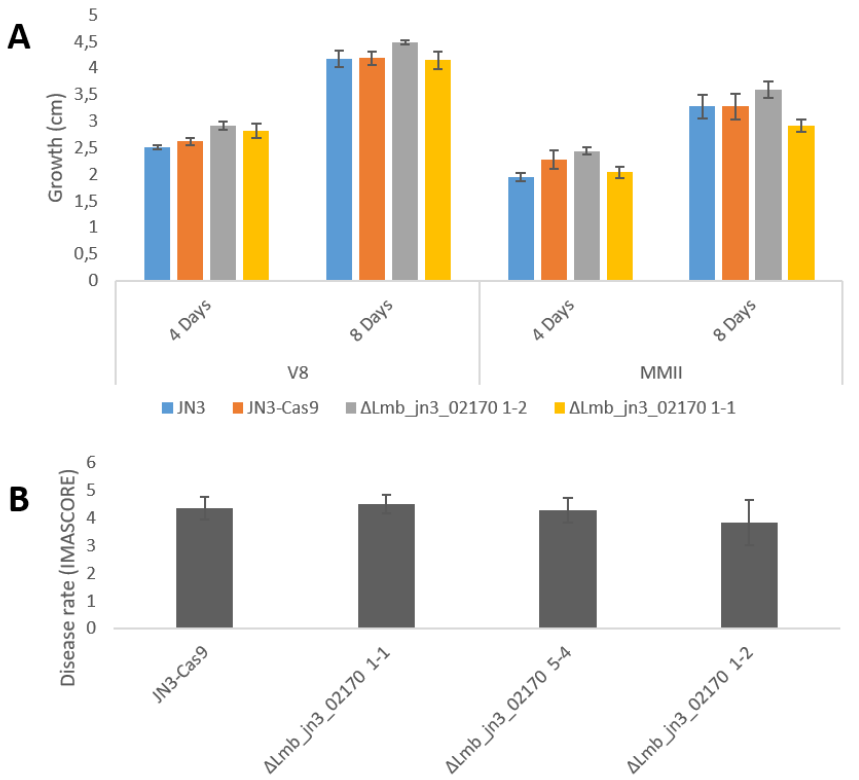

Figure 5: Effect of *Lmb_jn3_02170* inactivation on mycelial growth and pathogenicity of *Leptosphaeria maculans*. A: Growth assay on *Lmb_jn3_02170* mutants and WT strain JN3 with or without *Cas9* gene. Mycelial growth was measured at 4 days and 8 days post inoculation on two different agar media, V8 and MMII. **B:** Pathogenicity tests were performed on the susceptible cultivar Es-Astrid at 13 DPI. Disease rate is expressed as the mean scoring using the IMASCORE rating scale comprising six infection classes (IC), where IC1 to IC3 corresponded to resistance and IC4 to IC6, to susceptibility. DPI = Days Post Inoculation.

Université Paris-Saclay
Espace Technologique / Immeuble Discovery
Route de l'Orme aux Merisiers RD 128 / 91190 Saint-Aubin, France

DISCUSSION

Ce travail de thèse a été réalisé en forte interaction avec d'autres membres de l'UMR Bioger, dont l'équipe de bio-informatique de l'unité, le plateau de cytologie ainsi qu'avec Elise Gay qui réalise une thèse de bio-informatique dans notre équipe.

L'étude de l'action de protéines effectrices dans la relation entre un organisme phytopathogène et sa plante hôte est un sujet brulant (Lo Presti *et al.,* 2015 ; Lo Presti et Kahmann, 2017 ; Irieda *et al.,* 2019). Les gènes codant des effecteurs sont souvent localisés dans des régions particulières des génomes fongiques et sont souvent corégulés (Schardl *et al*., 2013 ; Soyer *et al.,* 2015,A ; van Dam *et al.,* 2017 ; Sànchez-Vallet *et al*., 2018). Précédemment à ma thèse, l'étude de la régulation chromatinienne et transcriptionnelle de l'expression des effecteurs localisés dans les régions riches en ETs chez *L. maculans* avait été initiée par I. Fudal et J. Soyer. Notre équipe avait pu identifier que les régions riches en ETs étaient enrichies en effecteurs, notamment en gènes d'avirulence, sur-exprimés pendant l'infection primaire du colza. L'inactivation par ARNi de gènes codant des protéines impliquées de la mise en place de l'hétérochromatine (KMT1, HP1) avait permis de montrer un contrôle chromatinien de l'expression d'au moins deux gènes codant des effecteurs, via l'implication de la modification H3K9me3 qui réprime l'expression de ces gènes *in vitro* (Soyer *et al.,* 2014). L'analyse d'un contrôle transcriptionnel de l'expression des effecteurs précoces via des FTs spécifiques avait également été initiée. Ainsi, l'analyse fonctionnelle de StuA, connu pour réguler de nombreuses fonctions chez les champignons filamenteux (IpCho *et al.,* 2010 ; Ohara and Tsuge, 2004 ; Tong *et al.,* 2007), avait aussi été menée par ARNi. Il avait été montré que ce FT régule, de façon directe ou indirecte, l'expression d'au moins trois gènes codant des effecteurs localisés en régions riches en ETs (Soyer *et al.,* 2015. B). Depuis les premières analyses transcriptomiques qui avaient permis de montrer une expression spécifique des gènes codant des effecteurs pendant l'infection des cotylédons de colza (Rouxel *et al.,* 2011), d'autres analyses transcriptomiques ont été menées à d'autres étapes du cycle infectieux, et ainsi, d'autres vagues d'expression d'effecteurs ont également été identifiées (Gervais *et al.,* 2017, Gay *et al*., en préparation).

L'objectif de ma thèse était de comprendre le rôle de la structure de la chromatine (à plusieurs échelles : position des nucléosomes, modification des histones et organisation intra-nucléaire des chromosomes) et de FTs dans le contrôle de l'expression concertée des gènes codant des effecteurs chez *L. maculans*, et plus globalement dans le contrôle de l'expression génique et de la pathogénie.

Pour comprendre comment ces mécanismes intervenaient dans le contrôle de l'expression génique, différentes approches ont été choisies. Une étude « genome-wide » de trois modifications des histones, de la localisation des nucléosomes, des interactions physiques du génome de *L. maculans* ont été entreprises. Une analyse *in vitro* des modifications chimiques des histones et de la localisation des nucléosomes a aussi été menée chez une espèce proche de *L. maculans* 'brassicae', *Leptosphaeria maculans* 'lepidii' (Lml), ainsi que de l'expression des gènes associés. Une étude fonctionnelle de remodeleurs chromatiniens via une inactivation par CRISPR-Cas9 chez *L. maculans* et enfin une étude fonctionnelle de FTs possiblement impliqués dans cette régulation encore une fois via

Université Paris-Saclay
Espace Technologique / Immeuble Discovery
Route de l'Orme aux Merisiers RD 128 / 91190 Saint-Aubin,
France

une inactivation par CRISPR-Cas9 et une sur-expression dans différents fonds génétiques de *L. maculans*. Cette étude m'a permis d'identifier un FT essentiel à la mise en place de la pathogénie chez *L. maculans*. De plus la surexpression de ce FT dans différents contextes chromatiniens m'a permis de mettre en évidence un double contrôle via la structure chromatinienne et ce FT spécifique de l'expression de différents sets de gènes codant notamment des effecteurs et exprimés de façon concertée tout au long du cycle de vie de *L. maculans*.

Contrôle chromatinien de l'expression des gènes codant des effecteurs

Le contrôle chromatinien de l'expression des gènes codant des effecteurs n'a commencé à être investigué que récemment. Ainsi, seuls, quelques cas de régulation des gènes codant des effecteurs protéiques ou impliqués dans des clusters de métabolisme secondaire ont été analysés jusqu'à présent. Ces études tendent à montrer que les gènes codant des effecteurs fongiques, souvent localisés dans des régions particulières des génomes, sont souvent régulés par des modifications chimiques des queues d'histones (Strauss et Reyes-Dominguez, 2011 ; Connolly *et al.,* 2013 ; Chujo and Scott, 2014 ; Soyer *et al.,* 2015. A). La cartographie des territoires nucléosomiques est également un domaine de recherche innovant pour essayer de comprendre les dynamiques régissant l'expression des gènes (Ponts *et al.,* 2010 ; Locke *et al.,* 2013 ; Chereji *et al.,* 2016), qui n'avait encore pas été développé chez les champignons phytopathogènes. L'étude réalisée dans le cadre de ma thèse est, à ce jour, le seul exemple d'analyse comparative de distribution nucléosomique chez des champignons phytopathogènes à notre connaissance (**Chapitre 1 ; Article 1**). L'étude, par ChIP-Seq, de marques chromatiniennes à l'échelles du génome de *L. maculans* a permis de mettre en évidence la localisation des gènes codant des effecteurs, exprimés pendant les phases biotrophes d'infection, en environnement hétérochromatinien H3K9me3, H3K27me3 ou H3K9me3/H3K27me3. Ainsi nous avons pu déterminer que les gènes spécifiquement exprimés à 7 jpi sur cotylédons, notamment les gènes d'avirulence, sont spécifiquement localisés en environnement H3K9me3 et H3K27me3 alors que les autres gènes codant des effecteurs et exprimés durant la phase de colonisation systémique de la tige de colza sont plutôt enrichis en domaines H3K27me3 (**Chapitre 1 ; Article 2**). De plus l'inactivation de *KMT1*, responsable du dépôt de la marque H3K9me3, a permis de déterminer que KMT1 est impliqué dans la mise en place de l'infection car le mutant *Δkmt1* induit des symptômes plus réduits que le WT. KMT1 est également impliqué dans l'expression des gènes codant des effecteurs puisque son inactivation induit l'expression de *Lmb_jn3_11364* à 7 jpi alors qu'il est normalement exprimé pendant les phases de colonisation tardives de la tige. KMT1 est également impliqué dans la répression de l'expression des gènes d'avirulence *AvrLm4-7, AvrLm6, AvrLm10.A* et d'*AvrLm11* pendant l'infection de la tige à 14 jpi. En résumé KMT1 est essentiel à l'expression du set d'effecteurs adéquat à plusieurs étapes de l'infection. KMT6 via la mise en place de la marque H3K27me3, joue un rôle plus limité dans la mise en place de l'infection et dans le contrôle de l'expression des effecteurs. Son inactivation ne mène à aucun de défaut de pathogénie sur cotylédon mais le développement de la biomasse fongique dans la tige (28 jpi) est altéré. Enfin l'inactivation de *KMT6* n'a pas permis de détecter de défaut de régulation des effecteurs testés. KMT6 est donc impliqué dans la réalisation totale du cycle infectieux mais n'influe pas directement sur l'expression des effecteurs testés / à moins qu'en cas d'inactivation de *KMT6*, une autre histone methyltransferase prenne le relai (**Chapitre 2 ; Article 3**). Ces résultats confirment ceux précédemment obtenus par l'équipe concernant la régulation des gènes d'avirulence par KMT1 et HP1 (Soyer *et al.,* 2014). L'inactivation d'une déméthylase d'histone,

Université Paris-Saclay
Espace Technologique / Immeuble Discovery
Route de l'Orme aux Merisiers RD 128 / 91190 Saint-Aubin,
France

Kdm8, présentant un profil d'expression similaire à celui des gènes d'avirulence n'a pas permis de mettre en évidence son implication dans le contrôle de l'expression de ces gènes. Il demeure néanmoins possible qu'elle soit impliquée dans le contrôle de l'expression de set de gènes non indispensables à la mise en place de l'infection. En effet l'implication de déméthylases d'histones dans la régulation de processus développementaux et dans la production de métabolites secondaires a été décrite chez *A. nidulans* (Gacek-Matthews *et al.,* 2015 ; Gacek-Matthews *et al.,* 2016).

Le contrôle de l'expression des gènes codant des effecteurs exprimés spécifiquement dans les tiges de colza semble plus complexe. En effet ces gènes sont statistiquement plus présents dans les régions marquées par la marque H3K27me3. Cependant, l'inactivation de KMT6 responsable du dépôt de cette marque n'entraine pas de surexpression spécifique de ces gènes. Il semble donc que des régulateurs agissent en plus ou même sans qu'il n'y ait besoin d'éliminer H3K27me3 pour activer l'expression concertée des gènes codant les effecteurs exprimés pendant les phases tardives de l'infection. Il est également possible que le retrait des marques H3K27me3 mène à la relocalisation de modification H3K9me3 sur les sites normalement occupés par du H3K9me3 (Möller *et al.,* 2019). L'identification de FTs présentant le même profil d'expression que les effecteurs exprimés pendant les premières étapes de l'infection a permis d'identifier *LmPf2* lors de la thèse de J. Soyer puis de réaliser son analyse fonctionnelle durant ma thèse, permettant de mettre en évidence sa capacité à réguler la pathogénie via le contrôle successif de l'expression de sets de gènes exprimés sous forme de vagues concertées. Il serait donc intéressant de réaliser le même type d'analyse pour identifier des FTs co-régulés avec les gènes codant des effecteurs exprimés pendant les phases tardives de l'infection.

Contrôle transcriptionnel de l'expression des gènes codant des effecteurs

Les FTs, représentent de 0.5 à 8% du génome des Eucaryotes et sont indispensables à la régulation du cycle de vie chez la plupart des organismes complexes (Weirauch et Hughes, 2011). Certains FTs sont généraux et régulent plusieurs mécanismes cellulaires (Ohara et Tsuge, 2004 ; Tong *et al.,* 2007 ; IpCho *et al.,* 2010). D'autres ont été identifiés comme directement impliqués dans la régulation de la pathogénie chez les Mycètes (Michielse *et al.,* 2009 ; Niño-Sánchez *et al.,* 2016). Chez les champignons phytopathogènes, la régulation du métabolisme secondaire ou de l'expression des effecteurs via des FTs spécifiques a déjà été relatée (Tollot *et al.,* 2016 ; van der Does *et al.,* 2016).

Pendant ma thèse j'ai menée l'inactivation par CRISPR-Cas9 et la surexpression de *LmPf2* décrit comme régulant la pathogénie et l'expression des effecteurs chez des Pleosporales proches de *L. maculans* (Cho *et al.,* 2013 ; Rybak *et al.,* 2017). Cette étude a permis de déterminer que ce FT est également impliqué dans la pathogénie chez *L. maculans*, son inactivation menant à une absence totale de développement de symptômes sur cotylédons de colza. De plus, cette étude a également permis de déteminer que ce FT contrôle l'expression de plusieurs sets d'effecteurs impliqués dans la phase de colonisation biotrophe du colza (**Figure 1 ; Chapitre 3 ; Article 4)**. L'inactivation de deux autres FTs ayant des profils d'expression similaires à ceux des gènes d'avirulence de *L. maculans* n'a mené à aucun défaut de pathogénie. Il reste néanmoins possible que ces FTs contrôlent l'expression d'effecteurs non-essentiels à l'établissement de la pathogénie.

Université Paris-Saclay
Espace Technologique / Immeuble Discovery
Route de l'Orme aux Merisiers RD 128 / 91190 Saint-Aubin, France

Double contrôle, chromatinien et transcriptionel, de l'expression des gènes codant des effecteurs précoces

L'étude menée pendant ma thèse est à notre connaissance la seule mettant en évidence l'implication de protéines impliquées dans le remodelage de la chromatine et de FTs dans le contrôle de l'expression des gènes codant des effecteurs protéiques chez les champignons phytopathogènes. Nous avons déterminé que la surexpression de *LmPf2* chez une souche sauvage contrôle spécifiquement les gènes de la vague 3 exprimés spécifiquement entre 9 et 12 jpi sur cotylédons alors que sa sur-expression dans un contexte *Δkmt1,* présentant une structure chromatinienne relâchée, va spécifiquement activer l'expression des gènes de la vague 2 composée de 91 gènes comportant les huit gènes d'avirulence clonés et spécifiquement exprimés à 7 jpi. Nous avons à partir de ces résultats proposé un modèle de régulation de l'expression des effecteurs chez *L. maculans* dans lequel le champignon pénètre dans la plante hôte et perçoit un signal végétal ou environnemental (demeurant inconnu). Le champignon va alors retirer les marques H3K9me3 au niveau des gènes codant des effecteurs en particulier ceux localisés dans les régions riches en ET, rendant les promoteurs de ces gènes accessibles à des FTs spécifiques tels que LmPf2. LmPf2 est alors capable d'activer successivement 71% des gènes de la vague 2. Entre 9 et 12 jours après infection, *KMT1*, codant la méthylase d'histone responsable du dépôt des marques H3K9me3, est exprimée ce qui induirait une recondensation des régions hétérochromatiniennes et bloquant ainsi l'accessibilité aux promoteurs des gènes de la vague 2. LmPf2 activerait alors 22-26 % des gènes de la vague 3. La production de ces effecteurs va permettre à *L. maculans* de coloniser les tissus de la plante en échappant à sa reconnaissance (**Figure 1 ; Chapitre 3 ; Article 4**).

Université Paris-Saclay
Espace Technologique / Immeuble Discovery
Route de l'Orme aux Merisiers RD 128 / 91190 Saint-Aubin,
France

Université Paris-Saclay
Espace Technologique / Immeuble Discovery
Route de l'Orme aux Merisiers RD 128 / 91190 Saint-Aubin, France

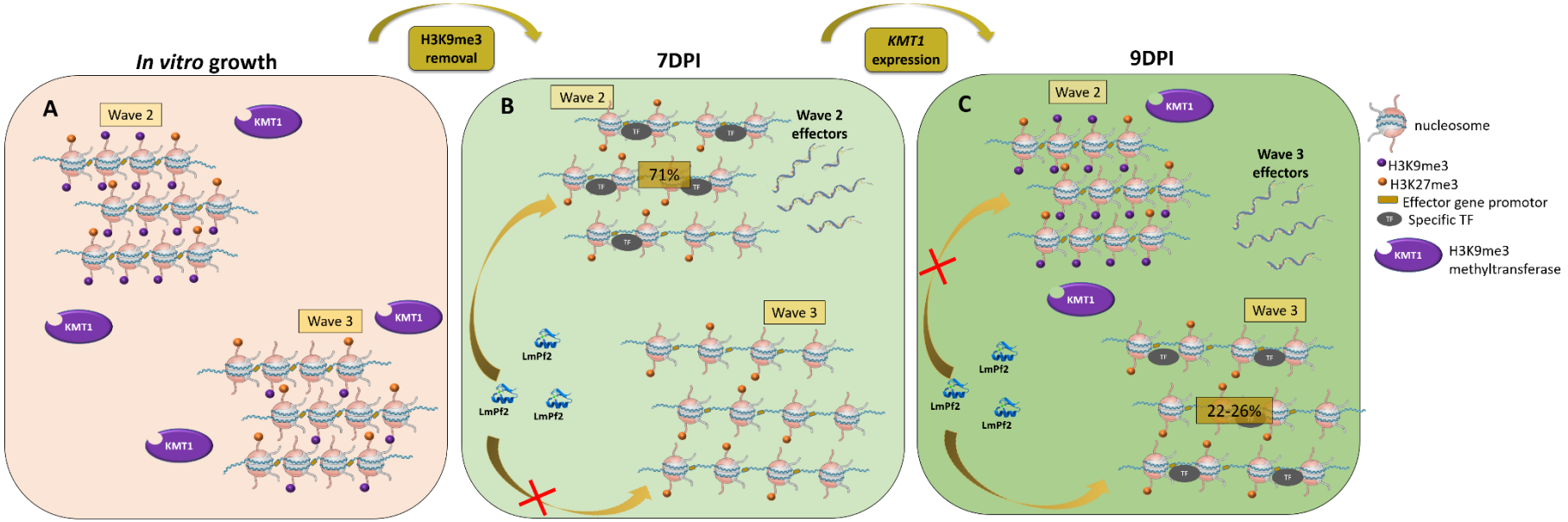

Figure 1: Model of key players of effector gene regulation as concerted waves during the early stage of *Leptosphaeria maculans* colonization of oilseed rape and *in vitro* growth. During *Leptosphaeria maculans'* life cycle, LmPf2 and KMT1 are able to regulate effector gene expression respectively acting on effector gene expression activation and chromatin condensation. **A:** During axenic growth effector waves repertoire are tightly repressed by H3K9me3 maintained by KMT1. **B:** At 7 DPi H3K9me3 is fully removed and heterochromatin is loosened. At this stage *LmPf2* is highly expressed and is able to regulate specifically 71% of Wave 2 effector genes probably because of a better affinity for wave 2 effector promotors. Between 7 DPI and 9 DPI *KMT1* is being expressed and start heterochromatin recondensation by H3K9me3 redeposition. **C:** Wave 2 effector genes are being recondense and LmPf2 start acting on (22 -26%) of Wave 3 effector genes, provoking their up-regulation. DPI = Days Post Inoculation.

PERSPECTIVES

Conformation 3D des génomes et contrôle de l'expression des gènes codant des effecteurs chez *L. maculans*

La compréhension de l'organisation 3D des génomes et le decryptage de la régulation genique par des assemblages protéiques complexes sont en pleine expansion. Il a été décrit que des parties entières de chromosomes peuvent être co-régulées en intéragissant avec différents partenaires protéiques (Lanctôt *et al.,* 2007 ; Ulianov *et al.,* 2016). Chez les champignons phytopathogènes, une étude récente a permis de mettre en évidence une structuration du génome d'*Epichloë festucae* (ayant, comme *L. maculans*, une structure de génome en isochores) par les éléments répétés constituant les Isochores AT. On retrouve les gènes différentiellement exprimés *in planta* près des régions riches en ETs, cette structuration 3D pourrait donc être impliquée dans leur expression concertée *in planta* (Winter *et al.,* 2018). Ma thèse a permis d'initié l'étude de l'impact de la structure chromosomique sur la régulation génique à travers la création de mutants HMEs et une expériences de Hi-C chez ces mutants et chez une souche sauvage (échantillons sont en cours de séquençage) afin de définir les régions génomiques intéragissant physiquement. Chez d'autres champignons filamenteux, les protéines KMT1 et KMT6 ont été montrées comme impliquées dans l'organisation des génomes. En effet, chez *N. crassa* et *E. festucea*, les méthylations H3K9me3 et H3K27me3 jouent un rôle crucial dans l'organisation du noyaux en permettant les interactions entre régions hétérochromatiniennes (Klocko *et al.,* 2016 ; Winter *et al.,* 2018). Chez *N. crassa*, l'inactivation de KMT1 mène à la relocalisation des marques H3K27me3 à l'emplacement des modifications H3K9me3 ce qui induit de larges réarangements chromosomiques. L'inactivation de KMT6 qui dépose normalement la marque H3K27me3 sur les régions subtélomériques induit une diminution des liaisons hétérochromatine-hétérochromatine, une augmentation des liaisons euchromatine-hétérochormatine et une destabilisation des liaisons entre télomères et enveloppe nucléaire (Klocko *et al.,* 2016). Chez *Z. tritici* également, on retrouve des modifications H3K27me3 sur les télomères ce qui permet leur interaction avec la membrane nucléaire. L'inactivation de KMT1 chez ce champignon induit de la même façon une relocalisation de H3K27me3 à l'emplacement des modifications H3K9me3 ce qui induit de larges réarangements chromosomiques (Möller *et al.,* 2019). Au contraire l'inactivation de KMT6 n'induit que des réarrangements chromosomiques mineurs et en faible nombre. Chez *Fusarium oxysporum*, il existe des chromosomes dispensables, fortement enrichies en gènes différentiellement exprimés pendant l'infection et fortement enrichis en modifications H3K27me3 (Ma *et al.,* 2010). Les régions enrichies en H3K27me3 étant soumises à une évolution plus rapide (« fast » génome). Enfin, une étude récente à permis d'identifier que le core génome de cette espèce peut être diviser en deux catégories, le vrai « core » génome, enrichie en gène de ménages et en modification H3K4me2 et le « fast core » génome enrichie en gènes différentiellements exprimés pendant l'infection (transport et défense). Les chromosomes dispensables, au contraire, sont spécifiquement enrichis en gènes codant des SSPs différentiellement exprimés pendant l'infection. Le génome à deux vitesse serait donc composé du vrai « core » génome et du « fast » génome constitué lui-même de plusieurs régions enrichies en H3K27me3 (chromosomes dispensables et « fast core » génome). Il serait également possible que des réarrangements entre « fast core » génome et chromosomes dispensables se produisent augmentant grandement la diversité génétique du pathogène (Fokkens *et al.,* 2018). Chez *L. maculans* qui possède aussi des chromosomes dispensables (Balesdent *et al.*, 2013). le « fast » genome pourrait être composé du « fast core » genome

Université Paris-Saclay
Espace Technologique / Immeuble Discovery
Route de l'Orme aux Merisiers RD 128 / 91190 Saint-Aubin,
France

composé des isochores AT enrichies en H3K9me3 et des régions GC-riche enrichies en H3K27me3 ce qui pourrait constituer en plus du chromosome dispensable deux types distincts de « fast » génome.

Différents répertoires d'effecteurs pour différentes phases d'infection

Lors de ce travail de thèse j'ai pu mettre en évidence que les gènes codant des effecteurs exprimés pendant les premières étapes de l'infection du colza par *L. maculans* 'brassicae' (Lmb), étaient, au moins partiellement, contrôlés par LmPf2. Les effecteurs exprimés précocement sont décrits comme impliqués dans le contournement des réactions de défense de la plante et comme facilitant le développement fongique dans la plante hôte. De plus, il a été montré que la compartimentalisation des génomes d'organismes phytopathogènes filamenteux, avec des régions génomiques enrichies en effecteurs et en TEs évoluant plus rapidement, apporte un avantage sélectif à ces derniers (Raffaele and Kamoun, 2012 ; van Dam *et al.,* 2017). Je fais donc l'hypothèse que les effecteurs exprimés durant les phases plus tardive de l'infection, localisés dans les régions riches en gènes du génome de *L. maculans* 'brassicae', constituent le répertoire d'origine de l'ancêtre commun entre *L. maculans* 'brassicae', *L. biglobosa* et 'lepidii'(Lml) mais qu'une invasion du génome de Lmb par des TEs lui a permis de diversifier son répertoire d'effecteurs et d'acquérir, progressivement, une nouvelle phase d'infection, la phase biotrophe, permettant une colonisation primaire de la plante plus efficace avant de passer à une phase nécrotrophe comme celle des autres espèces du complexe. Cette capacité aurait été obtenue en acquérant progressivement un (ou plusieurs) set d'effecteurs permettant d'échapper à la reconnaissance de la plante hôte. Cette hypothèse est soutenue par l'existence d'espèces proches ayant la même structure genomique et chromatinienne telles qu'*Epichloë festucae* qui présente un mode de vie endophyte (Winter *et al.,* 2018). Il semble donc que les Isochores AT enrichis en gènes codant des effecteurs servent au champignon à la colonisation biotrophe de leur plante hôte. Cependant, l'utilisation du modèle Lmb/Lml est limité pour comprendre ces mécanismes car nous ne possédons pas d'hôte pour étudier l'infection de Lml et celui-ci n'est pas capable d'infecter le colza. Il serait donc à l'avenir plus intéressant d'étudier la spécialisation à l'hôte et la régulation du cycle infectieux en comparant *L. maculans '*brassicae*'*/*Leptosphaeria biglobosa* 'brassicae' qui est aussi capable d'infecter le colza mais ne possède pas de grands isochores AT comme chez Lmb et n'initie pas son cycle infectieux par une phase de colonisation biotrophe. Il serait donc intéressant de comprendre si ce sont bien les isochores AT marqués par du H3K9me3 et enrichis en gènes codant des effecteurs qui sont responsables de la colonisation biotrophe initiale de l'hôte.

Applications liées à la compréhension des mécanismes épigénétiques et transcriptionnels

Bien que très fondamental, le projet de thèse que j'ai mené a tout de même des applications concrètes. En effet, la compréhension des mécanismes épigénétiques régissant l'expression des gènes codant des effecteurs et ainsi la colonisation de la plante hôte pourrait permettre de développer de nouveaux moyens de lutte contre les champignons phytopathogènes. On peut par exemple penser à des traitement chimiques agissant sur les protéines HMEs et ainsi empêcher la décondensation de la chromatine et l'expression des effecteurs. La limitation de ce type de traitements est que les HMEs sont très conservées au sein des Eucaryote et qu'il sera difficile de cibler les HMEs de l'agent pathogène sans inactiver celles de l'hôte. Cependant, il a été prouvé récemment que les plantes et leurs agents

Université Paris-Saclay
Espace Technologique / Immeuble Discovery
Route de l'Orme aux Merisiers RD 128 / 91190 Saint-Aubin, France

pathogènes sont capables de manipuler le système de défense adverse à l'aide de siRNA (Weiberg *et al.,* 2013 ; Wang *et al.,* 2016). Il est ainsi possible de créer des plantes OGM produisant des siRNA dirigés contre les domaines fonctionnels très conservés de protéines essentielles à la régulation des effecteurs (e.g. le site Zn2Cys6 de LmPf2 ou les domaines catalytiques de KMT1). Du fait du fort niveau de conservation de ce type de domaine, la possibilité de mutation et de conservation de fonction sera limitée et le contournement de la résistance sera, du même coup, difficile. Il serait également possible de traiter le champ directement avec des siRNA dirigés contre ce type de domaines fonctionnels.

Valorisation du matériel produit pendant la thèse

A mon arrivée au laboratoire, nous utilisions la technique RNAi pour étudier fonctionnellement un gène. Cette technique a prouvé son efficacité, notamment pour l'identification de gènes d'avirulence, mais également ses limites quand il s'agit de l'étude de FTs ou de protéines modificatrices d'histones (HMEs) qui sont très spécifiques, parfois vitales pour la cellule, avec des régulations complexes et des fenêtres d'expression limitées. J'ai donc au cours de ma thèse transféré l'outil de mutagénèse dirigée, CRISPR-Cas9, au laboratoire, technique qui m'a permis d'inactiver les gènes codant les FTs et HMEs que nous voulions étudier sans rencontrer de soucis relatifs au niveau d'expression du transgène. Cette technique a nécessité la transformation successive de *L. maculans* par la construction portant la Cas9 puis par la construction contenant l'ARN guide. Les transformants ont ensuite été cultivés jusqu'à ce qu'une mutation apparaisse puis croisés avec une souche sauvage (GFP ou non) pour éliminer la Cas9 et l'ARN guide. Cette méthode sera par la suite très utile à l'équipe puisque l'inactivation des gènes par recombinaison homologue au locus chez *L. maculans* est très difficile (de l'ordre de 1/300) comme chez beaucoup de champignons du fait de la présence de gènes KU70 et KU80 (Impliqués dans la recombinaison non-homologue ; Gardiner et Howlett, 2004). L'inactivation par CRISPR-Cas9 de Ku70/Ku80 pourra même par la suite permettre de réaliser des recombinaison homologues chez *L. maculans* et faciliter grandement les études fonctionnelles.

Notre équipe à l'origine développait des approches de génétique formelle pour identifier des gènes d'avirulence de *L. maculans* et les gènes de résistance associés chez le colza. Pendant ma thèse j'ai pu obtenir des transformants surexprimant *LmPf2* dans un contexte sauvage ou dans un mutant *Δkmt1.* En fonction du contexte chromatinien et du niveau d'expression de *LmPf2*, différents sets de gènes codant des effecteurs sontsur-exprimés, parfois à de très haut niveaux (20 000 fois plus). On pourrait donc faire croître ces souches en milieu liquide (Fries) et utiliser le surnageant de cultures pour obtenir des mélanges protéiques pouvant permettre de cribler des génotypes de colza pour la présence de gènes de résistance non encore identifiés. Nous pourrions également découvrir de nouvelles molécules d'intérêt, par ex. des métabolites secondaires, en inactivant et/ou surexprimant des HMEs/FTs connus pour déréguler le metabolisme secondaire chez d'autres champignons et produire des molécules habituellement non produites en condition de culture axénique.

Université Paris-Saclay
Espace Technologique / Immeuble Discovery
Route de l'Orme aux Merisiers RD 128 / 91190 Saint-Aubin,
France

CONCLUSION

Lorsque j'ai commencé ma thèse, J. Soyer avait déjà démontré l'implication de H3K9me3 déposée par KMT1 dans la répression de l'expression d'au moins deux gènes codant des effecteurs. Mais leur surexpression *in planta* n'était pas uniquement dû au retrait de modifications chromatiniennes, ce qui suggérait l'intervention de FTs spécifiques. Au cours de cette thèse, nous avons pu cartographier à l'échelle du génome : (i) trois modifications chromatiniennes dans les génomes de *L. maculans* 'brassicae' et d'une espèce proche *L. maculans* 'lepidii' et (ii) la répartition nucléosomale chez quatre espèces de champignons phytopathogènes. J'ai également pu mettre en évidence un double contrôle par KMT1 et LmPf2 de différents sets de gènes très enrichies en effecteurs et exprimés de façon concertée au cours de l'infection. C'est à ce jour la première étude mettant en lumière une double régulation génique par une HME et un FT spécifique. De plus nous avons pu déterminer l'implication de deux methylase d'histone, KMT1 et KMT6 dans la mise en place de la pathogénèse et le contrôle des gènes codant des effecteurs. Enfin nous avons initié au cours de ma thèse des expériences de Hi-C Seq couplées à du ChIp-Seq et RNA-Seq *in vitro* qui nous renseignerons grandement à la fois sur l'implication des modifications chromatiniennes sur la structure du génome et sur l'expression des gènes.

BIBLIOGRAPHIE

Andrulis, E.D., Neiman, A.M., Zappulla, D.C., Sternglanz, R., 1998. Perinuclear localization of chromatin facilitates transcriptional silencing. Nature 394, 592–595.

Antequera, F., Tamame, M., Villanueva, J.R., Santos, T., 1984. DNA methylation in the fungi. J. Biol. Chem. 259, 8033–8036.

Aramayo R., Peleg Y, Addison R, Metzenberg R., 1996. Asm-1+, a Neurospora crassa gene related to transcriptional regulators of fungal development. Genetics 144: 991-1003.

Balesdent, M.H., Fudal, I., Ollivier, B., Bally, P., Grandaubert, J., Eber, F., Chèvre, A.-M., Leflon, M., Rouxel, T., 2013. The dispensable chromosome of Leptosphaeria maculans shelters an effector gene conferring avirulence towards Brassica rapa. New Phytologist 198, 887–898.

Bannister, A.J., Kouzarides, T., 2005. Reversing histone methylation. Nature 436, 1103–1106.

Bantignies, F., Grimaud, C., Lavrov, S., Gabut, M., Cavalli, G., 2003. Inheritance of Polycomb-dependent chromosomal interactions in Drosophila. Genes Dev. 17, 2406–2420.

Basenko, E.Y., Sasaki, T., Ji, L., Prybol, C.J., Burckhardt, R.M., Schmitz, R.J., Lewis, Z.A., 2015. Genome-wide redistribution of H3K27me3 is linked to genotoxic stress and defective growth. Proceedings of the National Academy of Sciences 112, E6339–E6348.

Belaghzal, H., Dekker, J., Gibcus, J.H., 2017. HI-C 2.0: AN OPTIMIZED HI-C PROCEDURE FOR HIGH-RESOLUTION GENOME-WIDE MAPPING OF CHROMOSOME CONFORMATION. Methods 123, 56–65.

Bewick, A.J., Hofmeister, B.T., Powers, R.A., Mondo, S.J., Grigoriev, I.V., James, T.Y., Stajich, J.E., Schmitz, R.J., 2019. Diversity of cytosine methylation across the fungal tree of life. Nat Ecol Evol 3, 479–490.

Université Paris-Saclay
Espace Technologique / Immeuble Discovery
Route de l'Orme aux Merisiers RD 128 / 91190 Saint-Aubin,
France

Bird, A., 2002. DNA methylation patterns and epigenetic memory. Genes Dev. 16, 6–21.

Bonev, B., Cavalli, G., 2016. Organization and function of the 3D genome. Nature Reviews Genetics 17, 661–678.

Bonneuil, C. and Thomas, F., 2012. Semences, une histoire politique : amélioration des plantes, agriculture et alimentation en France depuis la Seconde Guerre mondiale, ECLM.

Brundrett, M.C., 2002. Coevolution of roots and mycorrhizas of land plants. New phytologist 154, 275–304.

Bunnik, E.M., Polishko, A., Prudhomme, J., Ponts, N., Gill, S.S., Lonardi, S., Le Roch, K.G., 2014. DNA-encoded nucleosome occupancy is associated with transcription levels in the human malaria parasite Plasmodium falciparum. BMC Genomics 15, 347.

Carhart-Harris, R.L., Roseman, L., Bolstridge, M., Demetriou, L., Pannekoek, J.N., 2017. Psilocybin for treatment-resistant depression: fMRI-measured brain mechanisms. Scientific Reports 7.

Carrillo, A.J., Schacht, P., Cabrera, I.E., Blahut, J., Prudhomme, L., Dietrich, S., Bekman, T., Mei, J., Carrera, C., Chen, V., Clark, I., Fierro, G., Ganzen, L., Orellana, J., Wise, S., Yang, K., Zhong, H., Borkovich, K.A., 2017. Functional Profiling of Transcription Factor Genes in Neurospora crassa. G3 (Bethesda) 7, 2945–2956.

Casolari, J.M., Brown, C.R., Komili, S., West, J., Hieronymus, H., Silver, P.A., 2004. Genome-Wide Localization of the Nuclear Transport Machinery Couples Transcriptional Status and Nuclear Organization. Cell 117, 427–439.

Cedar, H., Bergman, Y., 2009. Linking DNA methylation and histone modification: patterns and paradigms. Nature Reviews Genetics 10, 295–304.

Chalhoub, B., Denoeud, F., Liu, S., et al. 2014. Early allopolyploid evolution in the post-Neolithic Brassica napus oilseed genome. Science 345, 950–953.

Chereji, R.V., Kan, T.-W., Grudniewska, M.K., Romashchenko, A.V., Berezikov, E., Zhimulev, I.F., Guryev, V., Morozov, A.V., Moshkin, Y.M., 2016. Genome-wide profiling of nucleosome sensitivity and chromatin accessibility in Drosophila melanogaster. Nucleic Acids Research 44, 1036–1051.

Cho, Y., Ohm, R.A., Grigoriev, I.V., Srivastava, A., 2013. Fungal-specific transcription factor AbPf2 activates pathogenicity in Alternaria brassicicola. The Plant Journal 75, 498–514.

Chujo, T., Scott, B., 2014. Histone H3K9 and H3K27 methylation regulates fungal alkaloid biosynthesis in a fungal endophyte-plant symbiosis: K9 and K27 methylation regulates symbiosis. Molecular Microbiology 92, 413–434.

Coleman, J.J., Rounsley, S.D., Rodriguez-Carres, M., Kuo, A., Wasmann, C.C., Grimwood, J., Schmutz, J., Taga, M., White, G.J., Zhou, S., Schwartz, D.C., Freitag, M., Ma, L., Danchin, E.G.J., Henrissat, B., Coutinho, P.M., Nelson, D.R., Straney, D., Napoli, C.A., Barker, B.M., Gribskov, M., Rep, M., Kroken, S., Molnár, I., Rensing, C., Kennell, J.C., Zamora, J., Farman, M.L., Selker, E.U., Salamov, A., Shapiro, H., Pangilinan, J., Lindquist, E., Lamers, C., Grigoriev, I.V., Geiser, D.M., Covert, S.F., Temporini, E., VanEtten, H.D., 2009. The Genome of Nectria haematococca: Contribution of Supernumerary Chromosomes to Gene Expansion. PLOS Genetics 5, e1000618.

Collemare, J., Seidl, M.F., 2019. Chromatin-dependent regulation of secondary metabolite biosynthesis in fungi: is the picture complete? FEMS Microbiol. Rev.

Université Paris-Saclay
Espace Technologique / Immeuble Discovery
Route de l'Orme aux Merisiers RD 128 / 91190 Saint-Aubin, France

Colot, H.V., Park, G., Turner, G.E., Ringelberg, C., Crew, C.M., Litvinkova L., Weiss, R.L., Borkovich, K.A., and Dunlap, J.C., 2006. A high-throughput gene knockout procedure for Neurospora reveals functions for multiple transcription factors. PNas, 103, 10352–10357.

Connolly, L.R., Smith, K.M., Freitag, M., 2013. The Fusarium graminearum Histone H3 K27 Methyltransferase KMT6 Regulates Development and Expression of Secondary Metabolite Gene Clusters. PLoS Genetics 9, e1003916.

Cooke, R.C., Whipps, J.M., 1980. The evolution of modes of nutrition in fungi parasitic on terrestrial plants. Biological Reviews 55, 341–362.

Cremer, T., Cremer, C., 2001. Chromosome territories, nuclear architecture and gene regulation in mammalian cells. Nature Reviews Genetics 2, 292–301.

van Dam, S., Võsa, U., van der Graaf, A., Franke, L., de Magalhães, J.P., 2018. Gene co-expression analysis for functional classification and gene–disease predictions. Brief Bioinform 19, 575–592.

Deising, H.B., Werner, S., Wernitz, M., 2000. The role of fungal appressoriain plant infection. Microbes and infection 2, 1631–1641.

Dhillon, B., Cavaletto, J.R., Wood, K.V., Goodwin, S.B., 2010. Accidental amplification and inactivation of a methyltransferase gene eliminates cytosine methylation in Mycosphaerella graminicola. Genetics 186, 67–77.

Dilmaghani, A., Balesdent, M.H., Didier, J.P., Wu, C., Davey, J., Barbetti, M.J., Li, H., Moreno-Rico, O., Phillips, D., Despeghel, J.P., Vincenot, L., Gout, L., Rouxel, T., 2009. The Leptosphaeria maculans – Leptosphaeria biglobosa species complex in the American continent. Plant Pathology 58, 1044–1058.

Dilmaghani, A., Gladieux, P., Gout, L., Giraud, T., Brunner, P.C., Stachowiak, A., Balesdent, M.-H., Rouxel, T., 2012. Migration patterns and changes in population biology associated with the worldwide spread of the oilseed rape pathogen Leptosphaeria maculans. Molecular Ecology 21, 2519–2533.

van der Does, H.C., Fokkens, L., Yang, A., Schmidt, S.M., Langereis, L., Lukasiewicz, J.M., Hughes, T.R., Rep, M., 2016. Transcription factors encoded on core and accessory chromosomes of Fusarium oxysporum induce expression of effector genes. PLoS genetics 12, e1006401.

Dunlap, J.C., Borkovich, K.A., Henn, M.R., Turner, G.E., Sachs, M.S., Glass, N.L., McCluskey, K., Plamann, M., Galagan, J.E., Birren, B.W., Weiss, R.L., Townsend, J.P., Loros, J.J., Nelson, M.A., Lambreghts, R., Colot, H.V., Park, G., Collopy, P., Ringelberg, C., Crew, C., Litvinkova, L., DeCaprio, D., Hood, H.M., Curilla, S., Shi, M., Crawford, M., Koerhsen, M., Montgomery, P., Larson, L., Pearson, M., Kasuga, T., Tian, C., Baştürkmen, M., Altamirano, L., Xu, J., 2007. Enabling a Community to Dissect an Organism: Overview of the Neurospora Functional Genomics Project, in: Advances in Genetics. Elsevier, pp. 49–96.

Duplessis, S., Cuomo, C.A., Lin, Y.-C., Aerts, A., Tisserant, E., Veneault-Fourrey, C., Joly, D.L., Hacquard, S., Amselem, J., Cantarel, B.L., Chiu, R., Coutinho, P.M., Feau, N., Field, M., Frey, P., Gelhaye, E., Goldberg, J., Grabherr, M.G., Kodira, C.D., Kohler, A., Kues, U., Lindquist, E.A., Lucas, S.M., Mago, R., Mauceli, E., Morin, E., Murat, C., Pangilinan, J.L., Park, R., Pearson, M., Quesneville, H., Rouhier, N., Sakthikumar, S., Salamov, A.A., Schmutz, J., Selles, B., Shapiro, H., Tanguay, P., Tuskan, G.A., Henrissat, B., Van de Peer, Y., Rouze, P., Ellis, J.G., Dodds, P.N., Schein, J.E., Zhong, S., Hamelin, R.C., Grigoriev, I.V., Szabo, L.J., Martin, F., 2011. Obligate biotrophy features unraveled by the genomic analysis of rust fungi. Proceedings of the National Academy of Sciences 108, 9166–9171.

Université Paris-Saclay
Espace Technologique / Immeuble Discovery
Route de l'Orme aux Merisiers RD 128 / 91190 Saint-Aubin,
France

Dutreux, F., Da Silva, C., d'Agata, L., Couloux, A., Gay, E.J., Istace, B., Lapalu, N., Lemainque, A., Linglin, J., Noel, B., Wincker, P., Cruaud, C., Rouxel, T., Balesdent, M.-H., Aury, J.-M., 2018. De novo assembly and annotation of three Leptosphaeria genomes using Oxford Nanopore MinION sequencing. Scientific Data 5, 180235.

Eberharter, A., 2002. Histone acetylation: a switch between repressive and permissive chromatin: Second in review series on chromatin dynamics. EMBO Reports 3, 224–229

Farnham, P.J., 2009. Insights from genomic profiling of transcription factors. Nature Reviews Genetics 10, 605–616.

Fisher, M.C., Henk, D.A., Briggs, C.J., Brownstein, J.S., Madoff, L.C., McCraw, S.L., Gurr, S.J., 2012. Emerging fungal threats to animal, plant and ecosystem health. Nature 484, 186–194.

Fitt, B.D.L., Brun, H., Barbetti, M.J., Rimmer, S.R., 2006. World-Wide Importance of Phoma Stem Canker (Leptosphaeria maculans and L. biglobosa) on Oilseed Rape (Brassica napus). European Journal of Plant Pathology 114, 3–15.

Fokkens, L., Shahi, S., Connolly, L.R., Stam, R., Schmidt, S.M., Smith, K.M., Freitag, M., Rep, M., 2018. The multi-speed genome of Fusarium oxysporum reveals association of histone modifications with sequence divergence and footprints of past horizontal chromosome transfer events. bioRxiv.

Foss, H.M., Roberts, C.J., Claeys, K.M., Selker, E.U., 1993. Abnormal chromosome behavior in Neurospora mutants defective in DNA methylation. Science 262, 1737–1741.

Francis, N.J., Kingston, R.E., 2001. Mechanisms of transcriptional memory. Nat. Rev. Mol. Cell Biol. 2, 409–421.

Freitag, M., 2017. Histone Methylation by SET Domain Proteins in Fungi. Annual Review of Microbiology 71, 413–439.

Gacek, A., Strauss, J., 2012. The chromatin code of fungal secondary metabolite gene clusters. Appl Microbiol Biotechnol 95, 1389–1404.

Gacek-Matthews, A., Noble, L.M., Gruber, C., Berger, H., Sulyok, M., Marcos, A.T., Strauss, J., Andrianopoulos, A., 2015. KdmA, a histone H3 demethylase with bipartite function, differentially regulates primary and secondary metabolism in A spergillus nidulans: Histone H3K9 demethylase function in growth. Molecular Microbiology 96, 839–860.

Gacek-Matthews, A., Berger, H., Sasaki, T., Wittstein, K., Gruber, C., Lewis, Z.A., Strauss, J., 2016. KdmB, a Jumonji Histone H3 Demethylase, Regulates Genome-Wide H3K4 Trimethylation and Is Required for Normal Induction of Secondary Metabolism in Aspergillus nidulans. PLOS Genetics 12, e1006222.

Galagan, J.E., Selker, E.U., 2004. RIP: the evolutionary cost of genome defense. Trends in Genetics 20, 417–423.

Galazka, J.M., Klocko, A.D., Uesaka, M., Honda, S., Selker, E.U., Freitag, M., 2016. Neurospora chromosomes are organized by blocks of importin alpha-dependent heterochromatin that are largely independent of H3K9me3. Genome Research 26, 1069–1080.

Garcia-Diaz, M., Bebenek, K., 2007. Multiple Functions of DNA Polymerases. Critical Reviews in Plant Sciences 26, 105–122.

Université Paris-Saclay
Espace Technologique / Immeuble Discovery
Route de l'Orme aux Merisiers RD 128 / 91190 Saint-Aubin, France

Gardiner, D.M., Howlett, B.J., 2004. Negative selection using thymidine kinase increases the efficiency of recovery of transformants with targeted genes in the filamentous fungus Leptosphaeria maculans. Curr. Genet. 45, 249–255.

Gerke, J., Braus, G.H., 2014. Manipulation of fungal development as source of novel secondary metabolites for biotechnology. Applied Microbiology and Biotechnology 98, 8443–8455.

Gervais, J., Plissonneau, C., Linglin, J., Meyer, M., Labadie, K., 2017. Different waves of effector genes with contrasted genomic location are expressed by Leptosphaeria maculans during cotyledon and stem colonization of oilseed rape. Molecular plant pathology 18, 1113–1126.

Gimeno, CJ., Fink GR., 1994. Induction of pseudohyphal growth by overexpression of PHD1, a Saccharomyces cerevisiae gene related to transcriptional regulators of fungal development. Mol Cell Biol 14: 2100-2112.

Goyon, C., Barry, C., Grégoire, A., Faugeron, G., Rossignol, J.L., 1996. Methylation of DNA repeats of decreasing sizes in Ascobolus immersus. Mol Cell Biol 16, 3054–3065.

Gowher, H., Ehrlich, K.C., Jeltsch, A., 2001. DNA from Aspergillus flavus contains 5-methylcytosine. FEMS Microbiol Lett 205, 151–155.

Grandaubert, J., Lowe, R.G., Soyer, J.L., Schoch, C.L., Van de Wouw, A.P., 2014. Transposable element-assisted evolution and adaptation to host plant within the Leptosphaeria maculans-Leptosphaeria biglobosa species complex of fungal pathogens. BMC genomics 15, 891.

Grewal, S.I.S., Jia, S., 2007. Heterochromatin revisited. Nature Reviews Genetics 8, 35–46.

Hou, C., Li, L., Qin, Z.S., Corces, V.G., 2012. Gene Density, Transcription, and Insulators Contribute to the Partition of the Drosophila Genome into Physical Domains. Molecular Cell 48, 471–484.

Harrison, M.J., 2012. Cellular programs for arbuscular mycorrhizal symbiosis. Current Opinion in Plant Biology 15, 691–698.

Hassing, B., Winter, D., Becker, Y., Mesarich, C.H., Eaton, C.J., Scott, B., 2019. Analysis of Epichloë festucae small secreted proteins in the interaction with Lolium perenne. PLoS ONE 14, e0209463.

Hebinger, H. 2013. Le Colza, Editions France Agricole.

Heitz E., 1928. Das heterochromatin der moose. I Jahrb Wiss Botanik 69: 762-818.

Horbach, R., Navarro-Quesada, A.R., Knogge, W., Deising, H.B., 2011. When and how to kill a plant cell: Infection strategies of plant pathogenic fungi. Journal of Plant Physiology 168, 51–62.

Huisinga, K.L., Brower-Toland, B., Elgin, S.C.R., 2006. The contradictory definitions of heterochromatin: transcription and silencing. Chromosoma 115, 110–122.

IpCho, S.V.S., Tan, K.-C., Koh, G., Gummer, J., Oliver, R.P., Trengove, R.D., Solomon, P.S., 2010. The Transcription Factor StuA Regulates Central Carbon Metabolism, Mycotoxin Production, and Effector Gene Expression in the Wheat Pathogen Stagonospora nodorum. Eukaryotic Cell 9, 1100–1108.

Irieda, H., Inoue, Y., Mori, M., Yamada, K., Oshikawa, Y., Saitoh, H., Uemura, A., Terauchi, R., Kitakura, S., Kosaka, A., Singkaravanit-Ogawa, S., Takano, Y., 2019. Conserved fungal effector suppresses PAMP-triggered immunity by targeting plant immune kinases. Proceedings of the National Academy of Sciences 116, 496–505.

Université Paris-Saclay
Espace Technologique / Immeuble Discovery
Route de l'Orme aux Merisiers RD 128 / 91190 Saint-Aubin, France

Jackson, J.P., Lindroth, A.M., Cao, X., Jacobsen, S.E., 2002. Control of CpNpG DNA methylation by the KRYPTONITE histone H3 methyltransferase. Nature 416, 556–560.

Jamieson, K., Rountree, M.R., Lewis, Z.A., Stajich, J.E., Selker, E.U., 2013. Regional control of histone H3 lysine 27 methylation in Neurospora. Proceedings of the National Academy of Sciences 110, 6027–6032.

Janevska, S., Baumann, L., Sieber, C.M.K., Münsterkötter, M., Ulrich, J., Kämper, J., Güldener, U., Tudzynski, B., 2018. Elucidation of the Two H3K36me3 Histone Methyltransferases Set2 and Ash1 in Fusarium fujikuroi Unravels Their Different Chromosomal Targets and a Major Impact of Ash1 on Genome Stability. Genetics 208, 153–171.

Jenuwein, T., Allis, C.D., 2001. Translating the histone code. Science 293, 1074–1080.

Jeon, J., Choi, J., Lee, G.-W., Park, S.-Y., Huh, A., Dean, R.A., Lee, Y.-H., 2015. Genome-wide profiling of DNA methylation provides insights into epigenetic regulation of fungal development in a plant pathogenic fungus, Magnaporthe oryzae. Scientific Reports 5, 8567.

Jupe, J., Stam, R., Howden A.J.M., Morris J.A., Zhang R., 2013. Phytophthora capsici-tomato interaction features dramatic shifts in gene expression associated with a hemi-biotrophic lifestyle. Genome Biology,14:R63

van Kan, J.A.L., 2006. Licensed to kill: the lifestyle of a necrotrophic plant pathogen. Trends in Plant Science 11, 247–253.

Khatter, H., Vorländer, M.K., Müller, C.W., 2017. RNA polymerase I and III: similar yet unique. Current Opinion in Structural Biology 47, 88–94.

Kim, J.-A., Kwon, M., Kim, J., 2019. Allosteric Regulation of Chromatin-Modifying Enzymes. Biochemistry 58, 15–23.

Klocko, A.D., Ormsby, T., Galazka, J.M., Leggett, N.A., Uesaka, M., Honda, S., Freitag, M., Selker, E.U., 2016. Normal chromosome conformation depends on subtelomeric facultative heterochromatin in Neurospora crassa. PNAS 113, 15048–15053.

Kouzarides, T., 2007. Chromatin Modifications and Their Function. Cell 128, 693–705.

Kouzminova, E., Selker, E.U., 2001. dim-2 encodes a DNA methyltransferase responsible for all known cytosine methylation in Neurospora. EMBO J. 20, 4309–4323.

Kronholm, I., Johannesson, H., Ketola, T., 2016. Epigenetic Control of Phenotypic Plasticity in the Filamentous Fungus Neurospora crassa; Genes|Genomes|Genetics.

Kubartová, A., Ranger, J., Berthelin, J., Beguiristain, T., 2009. Diversity and Decomposing Ability of Saprophytic Fungi from Temperate Forest Litter. Microbial Ecology 58, 98–107.

Lanctôt, C., Cheutin, T., Cremer, M., Cavalli, G., Cremer, T., 2007. Dynamic genome architecture in the nuclear space: regulation of gene expression in three dimensions. Nature Reviews Genetics 8, 104–115.

Latchman, D.S., 1997. Transcription factors: An overview. The International Journal of Biochemistry & Cell Biology 29, 1305–1312.

Law, J.A., Jacobsen, S.E., 2010. Establishing, maintaining and modifying DNA methylation patterns in plants and animals. Nature Reviews Genetics 11, 204–220.

Levine, M., Tjian, R., 2003. Transcription regulation and animal diversity. Nature 424, 147–151.

Université Paris-Saclay
Espace Technologique / Immeuble Discovery
Route de l'Orme aux Merisiers RD 128 / 91190 Saint-Aubin, France

Li, E., Beard, C., Forster, A.C., Bestor, T.H., Jaenisch, R., 1993. DNA Methylation, Genomic Imprinting, and Mammalian Development. Cold Spring Harb Symp Quant Biol 58, 297–305.

Lieberman-Aiden, E., van Berkum, N.L., Williams, L., Imakaev, M., Ragoczy, T., Telling, A., Amit, I., Lajoie, B.R., Sabo, P.J., Dorschner, M.O., Sandstrom, R., Bernstein, B., Bender, M.A., Groudine, M., Gnirke, A., Stamatoyannopoulos, J., Mirny, L.A., Lander, E.S., Dekker, J., 2009. Comprehensive mapping of long-range interactions reveals folding principles of the human genome. Science 326, 289–293.

Lindequist, U., Niedermeyer, T.H.J., Jülich, W.-D., 2005. The Pharmacological Potential of Mushrooms. Evidence-Based Complementary and Alternative Medicine 2, 285–299.

Locke, G., Haberman, D., Johnson, S.M., Morozov, A.V., 2013. Global remodeling of nucleosome positions in C. elegans. BMC genomics 14, 284.

Lomvardas, S., Barnea, G., Pisapia, D.J., Mendelsohn, M., Kirkland, J., Axel, R., 2006. Interchromosomal Interactions and Olfactory Receptor Choice. Cell 126, 403–413.

Lo Presti, L., Lanver, D., Schweizer, G., Tanaka, S., Liang, L., Tollot, M., Zuccaro, A., Reissmann, S., Kahmann, R., 2015. Fungal Effectors and Plant Susceptibility. Annual Review of Plant Biology 66, 513–545.

Lo Presti, L., Kahmann, R., 2017. How filamentous plant pathogen effectors are translocated to host cells. Current Opinion in Plant Biology 38, 19–24.

Luger, K., Mäder, A.W., Richmond, R.K., Sargent, D.F., Richmond, T.J., 1997. Crystal structure of the nucleosome core particle at 2.8 Å resolution. Nature 389, 251.

Luger, K., Richmond, T.J., 1998. The histone tails of the nucleosome. Current Opinion in Genetics & Development 8, 140–146.

Ma, L.-J., van der Does, H.C., Borkovich, K.A., Coleman, J.J., Daboussi, M.-J., Di Pietro, A., Dufresne, M., Freitag, M., Grabherr, M., Henrissat, B., Houterman, P.M., Kang, S., Shim, W.-B., Woloshuk, C., Xie, X., Xu, J.-R., Antoniw, J., Baker, S.E., Bluhm, B.H., Breakspear, A., Brown, D.W., Butchko, R.A.E., Chapman, S., Coulson, R., Coutinho, P.M., Danchin, E.G.J., Diener, A., Gale, L.R., Gardiner, D.M., Goff, S., Hammond-Kosack, K.E., Hilburn, K., Hua-Van, A., Jonkers, W., Kazan, K., Kodira, C.D., Koehrsen, M., Kumar, L., Lee, Y.-H., Li, L., Manners, J.M., Miranda-Saavedra, D., Mukherjee, M., Park, G., Park, J., Park, S.-Y., Proctor, R.H., Regev, A., Ruiz-Roldan, M.C., Sain, D., Sakthikumar, S., Sykes, S., Schwartz, D.C., Turgeon, B.G., Wapinski, I., Yoder, O., Young, S., Zeng, Q., Zhou, S., Galagan, J., Cuomo, C.A., Kistler, H.C., Rep, M., 2010. Comparative genomics reveals mobile pathogenicity chromosomes in Fusarium. Nature 464, 367–373.

Marino-Ramirez, L., Levine, K.M., Morales, M., Zhang, S., Moreland, R.T., Baxevanis, A.D., Landsman, D., 2011. The Histone Database: an integrated resource for histones and histone fold-containing proteins. Database 2011, bar048-bar048.

Mauser, R., Kungulovski, G., Keup, C., Reinhardt, R., Jeltsch, A., 2017. Application of dual reading domains as novel reagents in chromatin biology reveals a new H3K9me3 and H3K36me2/3 bivalent chromatin state. Epigenetics & Chromatin 10.

McGee DC & Petrie GA. 1978. Variability of Leptosphaeria maculans in relation to blackleg of oilseed rape. Phytopathology 68: 47-52.

Université Paris-Saclay
Espace Technologique / Immeuble Discovery
Route de l'Orme aux Merisiers RD 128 / 91190 Saint-Aubin, France

Mendes-Pereira E., Balesdent M.H., Brun H., Rouxel T., 2003. Molecular phylogeny of the Leptosphaeria maculans-L. biglobosa species complex. Mycol Res 107:1287-1304.

Michielse, C.B., van Wijk, R., Reijnen, L., Manders, E.M.M., Boas, S., Olivain, C., Alabouvette, C., Rep, M., 2009. The Nuclear Protein Sge1 of Fusarium oxysporum Is Required for Parasitic Growth. PLoS Pathogens 5, e1000637.

Möller, M., Schotanus, K., Soyer, J.L., Haueisen, J., Happ, K., Stralucke, M., Happel, P., Smith, K.M., Connolly, L.R., Freitag, M., Stukenbrock, E.H., 2019. Destabilization of chromosome structure by histone H3 lysine 27 methylation. PLOS Genetics 15, e1008093.

Motlagh, H.N., Wrabl, J.O., Li, J., Hilser, V.J., 2014. The ensemble nature of allostery. Nature 508, 331–339.

Muggia, L., Grube, M., 2018. Fungal Diversity in Lichens: From Extremotolerance to Interactions with Algae. Life 8, 15.

Niño-Sánchez, J., Castillo, C.-D., Tello, V., Vega-Bartol, D., José, J., Ramos, B., Sukno, S.A., Díaz Mínguez, J.M., 2016. The FTF gene family regulates virulence and expression of SIX effectors in Fusarium oxysporum. Molecular plant pathology 17, 1124–1139.

Nishida, H., Motoyama, T., Yamamoto, S., Aburatani, H., Osada, H., 2009. Genome-wide maps of mono- and di-nucleosomes of Aspergillus fumigatus. Bioinformatics 25, 2295–2297.

O'Connell, R.J., Panstruga, R., 2006. Tete a tete inside a plant cell: establishing compatibility between plants and biotrophic fungi and oomycetes. New Phytologist 171, 699–718.

O'Connell, R.J., Thon, M.R., Hacquard, S., Amyotte, S.G., Kleemann, J., 2012. Lifestyle transitions in plant pathogenic Colletotrichum fungi deciphered by genome and transcriptome analyses. Nature Genetics 44, 1060–1065.

Ohara, T., Tsuge, T., 2004. FoSTUA, Encoding a Basic Helix-Loop-Helix Protein, Differentially Regulates Development of Three Kinds of Asexual Spores, Macroconidia, Microconidia, and Chlamydospores, in the Fungal Plant Pathogen Fusarium oxysporum. Eukaryot Cell 3, 1412–1422.

Ohm, R.A., Feau, N., Henrissat, B., Schoch, C.L., Horwitz, B.A., Barry, K.W., Condon, B.J., Copeland, A.C., Dhillon, B., Glaser, F., Hesse, C.N., Kosti, I., LaButti, K., Lindquist, E.A., Lucas, S., Salamov, A.A., Bradshaw, R.E., Ciuffetti, L., Hamelin, R.C., Kema, G.H.J., Lawrence, C., Scott, J.A., Spatafora, J.W., Turgeon, B.G., Wit, P.J.G.M. de, Zhong, S., Goodwin, S.B., Grigoriev, I.V., 2012. Diverse Lifestyles and Strategies of Plant Pathogenesis Encoded in the Genomes of Eighteen Dothideomycetes Fungi. PLOS Pathogens 8, e1003037.

Osborne, C.S., Chakalova, L., Brown, K.E., Carter, D., Horton, A., Debrand, E., Goyenechea, B., Mitchell, J.A., Lopes, S., Reik, W., Fraser, P., 2004. Active genes dynamically colocalize to shared sites of ongoing transcription. Nat. Genet. 36, 1065–1071.

Pabo, C.O., Sauer, R.T., 1992. Transcription Factors: Structural Families and Principles of DNA Recognition 43.

Pais, P., Costa, C., Cavalheiro, M., Romão, D., Teixeira, M.C., 2016. Transcriptional Control of Drug Resistance, Virulence and Immune System Evasion in Pathogenic Fungi: A Cross-Species Comparison. Front Cell Infect Microbiol 6, 131.

Park, J., Park, J., Jang, S., Kim, S., Kong, S., Choi, J., Ahn, K., Kim, J., Lee, S., Kim, S., Park, B., Jung, K., Kim, S., Kang, S., Lee, Y.-H., 2008. FTFD: an informatics pipeline supporting phylogenomic analysis of fungal transcription factors. Bioinformatics 24, 1024–1025.

Université Paris-Saclay
Espace Technologique / Immeuble Discovery
Route de l'Orme aux Merisiers RD 128 / 91190 Saint-Aubin, France

Papamichos-Chronakis, M., Peterson, C.L., 2013. Chromatin and the genome integrity network. Nature Reviews Genetics 14, 62–75.

Patikoglou, G., Burley, S.K., 1997. Eukaryotic transcription factor-DNA complexes. Annu Rev Biophys Biomol Struct 26, 289–325.

Ponts, N., Harris, E.Y., Prudhomme, J., Wick, I., Eckhardt-Ludka, C., Hicks, G.R., Hardiman, G., Lonardi, S., Le Roch, K.G., 2010. Nucleosome landscape and control of transcription in the human malaria parasite. Genome Research 20, 228–238.

Radman-Livaja M., Rando Q.J., 2010. Nucleosome positioning: how is it established and why does it matter? Dev. Biol. 339: 258-266.

Raffaele, S., Kamoun, S., 2012. Genome evolution in filamentous plant pathogens: why bigger can be better. Nature Reviews Microbiology 10, 417–430.

Remy, W., Taylor, T.N., Hass, H., Kerp, H., 1994. Four hundred-million-year-old vesicular arbuscular mycorrhizae. Proceedings of the National Academy of Sciences 91, 11841–11843.

Richards, E.J., Elgin, S.C.R., 2002. Epigenetic codes for heterochromatin formation and silencing: rounding up the usual suspects. Cell 108, 489–500.

Rohe, M., Gierlich, A., Hermann, H., Hahn, M., Schmidt, B., 1995. The race-specific elicitor, NIP1, from the barley pathogen, Rhynchosporium secalis, determines avirulence on host plants of the Rrs1 resistance genotype. The EMBO Journal 14, 4168–4177.

Rossetto, D., Avvakumov, N., Côté, J., 2012. Histone phosphorylation: A chromatin modification involved in diverse nuclear events. Epigenetics 7, 1098–1108.

Rouxel T, Mendes-Pereira E, Brun H, Balesdent MH. 2004. Species complex of fungal phytopathogens: the Leptosphaeria maculans-L. biglobosa case study. In: Plant Genome: Diversity and Evolution. Vol. 2: Cryptogams. AK Sharma & A Sharma (Eds.), Science Publishers, Inc., Enfield, USA, pp.33-75.

Rouxel, T., Grandaubert, J., Hane, J.K., Hoede, C., van de Wouw, A.P., Couloux, A., Dominguez, V., Anthouard, V., Bally, P., Bourras, S., Cozijnsen, A.J., Ciuffetti, L.M., Degrave, A., Dilmaghani, A., Duret, L., Fudal, I., Goodwin, S.B., Gout, L., Glaser, N., Linglin, J., Kema, G.H.J., Lapalu, N., Lawrence, C.B., May, K., Meyer, M., Ollivier, B., Poulain, J., Schoch, C.L., Simon, A., Spatafora, J.W., Stachowiak, A., Turgeon, B.G., Tyler, B.M., Vincent, D., Weissenbach, J., Amselem, J., Quesneville, H., Oliver, R.P., Wincker, P., Balesdent, M.-H., Howlett, B.J., 2011. Effector diversification within compartments of the Leptosphaeria maculans genome affected by Repeat-Induced Point mutations. Nature Communications 2.

Ruthenburg, A.J., Allis, C.D., Wysocka, J., 2007. Methylation of Lysine 4 on Histone H3: Intricacy of Writing and Reading a Single Epigenetic Mark. Molecular Cell 25, 15–30.

Rybak, K., See, P.T., Phan, H.T., Syme, R.A., Moffat, C.S., 2017. A functionally conserved Zn2Cys6 binuclear cluster transcription factor class regulates necrotrophic effector gene expression and host-specific virulence of two major Pleosporales fungal pathogens of wheat. Molecular plant pathology 18, 420–434.

Saksouk, N., Simboeck, E., Déjardin, J., 2015. Constitutive heterochromatin formation and transcription in mammals. Epigenetics & Chromatin 8, 3.

Université Paris-Saclay
Espace Technologique / Immeuble Discovery
Route de l'Orme aux Merisiers RD 128 / 91190 Saint-Aubin, France

Sánchez-Vallet, A., Fouché, S., Fudal, I., Hartmann, F.E., Soyer, J.L., Tellier, A., Croll, D., 2018. The Genome Biology of Effector Gene Evolution in Filamentous Plant Pathogens. Annual Review of Phytopathology 56, 21–40.

Savitsky, P., Krojer, T., Fujisawa, T., Lambert, J.-P., Picaud, S., Wang, C.-Y., Shanle, E.K., Krajewski, K., Friedrichsen, H., Kanapin, A., Goding, C., Schapira, M., Samsonova, A., Strahl, B.D., Gingras, A.-C., Filippakopoulos, P., 2016. Multivalent Histone and DNA Engagement by a PHD/BRD/PWWP Triple Reader Cassette Recruits ZMYND8 to K14ac-Rich Chromatin. Cell Reports 17, 2724–2737.

Selker, E.U., Stevens, J.N., 1985. DNA methylation at asymmetric sites is associated with numerous transition mutations. Proc. Natl. Acad. Sci. U.S.A. 82, 8114–8118.

Selker, E.U., Richardson, G.A., Garrett-Engele, P.W., Singer, M.J., Miao, V., 1993. Dissection of the Signal for DNA Methylation in the ζ-η Region of Neurospora. Cold Spring Harb Symp Quant Biol 58, 323–329.

Selker, E.U. 2002. Repeat-induced gene silencing in fungi. Advances in genetics 46:439-450.

Selker, E.U., Tountas, N.A., Cross, S.H., Margolin, B.S., Murphy, J.G., Bird, A.P., Freitag, M., 2003. The methylated component of the Neurospora crassa genome. Nature 422, 893–897.

Shelest, E., 2008. Transcription factors in fungi. FEMS Microbiology Letters 286, 145–151.

Sheppard, D.C., Doedt, T., Chiang, L.Y., Kim, H.S., Chen, D., Nierman, W.C., Filler, S.G., 2005. The Aspergillus fumigatus StuA Protein Governs the Up- Regulation of a Discrete Transcriptional Program during the Acquisition of Developmental Competence□D. Molecular Biology of the Cell 16, 14.

Schardl, C.L., Young, C.A., Hesse, U., Amyotte, S.G., Andreeva, K., Calie, P.J., Fleetwood, D.J., Haws, D.C., Moore, N., Oeser, B., Panaccione, D.G., Schweri, K.K., Voisey, C.R., Farman, M.L., Jaromczyk, J.W., Roe, B.A., O'Sullivan, D.M., Scott, B., Tudzynski, P., An, Z., Arnaoudova, E.G., Bullock, C.T., Charlton, N.D., Chen, L., Cox, M., Dinkins, R.D., Florea, S., Glenn, A.E., Gordon, A., Güldener, U., Harris, D.R., Hollin, W., Jaromczyk, J., Johnson, R.D., Khan, A.K., Leistner, E., Leuchtmann, A., Li, C., Liu, JinGe, Liu, Jinze, Liu, M., Mace, W., Machado, C., Nagabhyru, P., Pan, J., Schmid, J., Sugawara, K., Steiner, U., Takach, J.E., Tanaka, E., Webb, J.S., Wilson, E.V., Wiseman, J.L., Yoshida, R., Zeng, Z., 2013. Plant-Symbiotic Fungi as Chemical Engineers: Multi-Genome Analysis of the Clavicipitaceae Reveals Dynamics of Alkaloid Loci. PLOS Genetics 9, e1003323.

Schmid, M., Arib, G., Laemmli, C., Nishikawa, J., Durussel, T., Laemmli, U.K., 2006. Nup-PI: The Nucleopore-Promoter Interaction of Genes in Yeast. Molecular Cell 21, 379–391.

Schotanus, K., Soyer, J.L., Connolly, L.R., Grandaubert, J., Happel, P., Smith, K.M., Freitag, M., Stukenbrock, E.H., 2015. Histone modifications rather than the novel regional centromeres of Zymoseptoria tritici distinguish core and accessory chromosomes. Epigenetics & Chromatin 8, 41.

Schumacher, J., Studt, L., Tudzynski, P., 2019. The putative H3K36 demethylase BcKDM1 affects virulence, stress responses and photomorphogenesis in Botrytis cinerea. Fungal Genetics and Biology 123, 14–24.

Shoemaker R.A. & Brun H., 2001. The telemorph of the weakly aggressive segregate of Leptosphaeria maculans. Can J Bot 79: 412-419.

Silar et Malagnac, Les champignons redécouverts, Paris, Belin, Hors collection, 2013, 0-231.

Skibbens, R.V., 2019. Condensins and cohesins - one of these things is not like the other! J. Cell. Sci. 132.

Smith, M.M., 1991. Histone structure and function. Current opinion in cell biology 3, 429–437.

Université Paris-Saclay
Espace Technologique / Immeuble Discovery
Route de l'Orme aux Merisiers RD 128 / 91190 Saint-Aubin, France

Smith, K.M., Galazka, J.M., Phatale, P.A., Connolly, L.R., Freitag, M., 2012. Centromeres of filamentous fungi. Chromosome Res 20, 635–656.

Soyer, J.L., El Ghalid, M., Glaser, N., Ollivier, B., Linglin, J., Grandaubert, J., Balesdent, M.-H., Connolly, L.R., Freitag, M., Rouxel, T., Fudal, I., 2014. Epigenetic Control of Effector Gene Expression in the Plant Pathogenic Fungus Leptosphaeria maculans. PLoS Genetics 10, e1004227.

Soyer, J.L., Rouxel, T., Fudal, I., 2015. A. Chromatin-based control of effector gene expression in plant-associated fungi. Current Opinion in Plant Biology 26, 51–56.

Soyer, J.L., Hamiot, A., Ollivier, B., Balesdent, M.-H., Rouxel, T., Fudal, I., 2015. B. The APSES transcription factor LmStuA is required for sporulation, pathogenic development and effector gene expression in Leptosphaeria maculans: Functional analysis of LmStuA from L. maculans. Molecular Plant Pathology 16, 1000–1005.

Soyer, J.L., Grandaubert, J., Haueisen, J., Schotanus, K., Stukenbrock, E.H., 2019. In planta chromatin immunoprecipitation in Zymoseptoria tritici reveals chromatin-based regulation of putative effector gene expression. bioRxiv 544627.

Spanu, P.D., Abbott, J.C., Amselem, J., Burgis, T.A., Soanes, D.M., Stüber, K., Themaat, E.V.L. van, Brown, J.K.M., Butcher, S.A., Gurr, S.J., Lebrun, M.-H., Ridout, C.J., Schulze-Lefert, P., Talbot, N.J., Ahmadinejad, N., Ametz, C., Barton, G.R., Benjdia, M., Bidzinski, P., Bindschedler, L.V., Both, M., Brewer, M.T., Cadle-Davidson, L., Cadle-Davidson, M.M., Collemare, J., Cramer, R., Frenkel, O., Godfrey, D., Harriman, J., Hoede, C., King, B.C., Klages, S., Kleemann, J., Knoll, D., Koti, P.S., Kreplak, J., López-Ruiz, F.J., Lu, X., Maekawa, T., Mahanil, S., Micali, C., Milgroom, M.G., Montana, G., Noir, S., O'Connell, R.J., Oberhaensli, S., Parlange, F., Pedersen, C., Quesneville, H., Reinhardt, R., Rott, M., Sacristán, S., Schmidt, S.M., Schön, M., Skamnioti, P., Sommer, H., Stephens, A., Takahara, H., Thordal-Christensen, H., Vigouroux, M., Weßling, R., Wicker, T., Panstruga, R., 2010. Genome Expansion and Gene Loss in Powdery Mildew Fungi Reveal Tradeoffs in Extreme Parasitism. Science 330, 1543–1546.

Strauss, J., Reyes-Dominguez, Y., 2011. Regulation of secondary metabolism by chromatin structure and epigenetic codes. Fungal Genetics and Biology 48, 62–69.

Struhl, K., Segal, E., 2013. Determinants of nucleosome positioning. Nature Structural & Molecular Biology 20, 267–273.

Stukenbrock, E.H., Banke, S., Javan-Nikkhah, M., McDonald, B.A., 2007. Origin and domestication of the fungal wheat pathogen Mycosphaerella graminicola via sympatric speciation. Mol. Biol. Evol. 24, 398–411.

Tamaru, H., Selker, E.U., 2001. A histone H3 methyltransferase controls DNA methylation in Neurospora crassa. Nature 414, 277.

Tan, K.-C., Oliver, R.P., 2017. Regulation of proteinaceous effector expression in phytopathogenic fungi. PLoS pathogens 13, e1006241.

Tanizawa, H., Kim, K.-D., Iwasaki, O., Noma, K., 2017. Architectural alterations of the fission yeast genome during the cell cycle. Nature Structural & Molecular Biology 24, 965–976.

Taylor, T.N., Osborn, J.M., 1996. The importance of fungi in shaping the paleoecosystem. Review of Palaeobotany and Palynology 90, 249–262.

Université Paris-Saclay
Espace Technologique / Immeuble Discovery
Route de l'Orme aux Merisiers RD 128 / 91190 Saint-Aubin, France

Thomas, M.C., Chiang, C.-M., 2006. The General Transcription Machinery and General Cofactors. Critical Reviews in Biochemistry and Molecular Biology 41, 105–178.

Tong, X., Zhang, X., Plummer, K.M., Stowell, K.M., Sullivan, P.A., Farley, P.C., 2007. GcSTUA, an APSES Transcription Factor, Is Required for Generation of Appressorial Turgor Pressure and Full Pathogenicity of Glomerella cingulata. Molecular Plant-Microbe Interactions 20, 1102–1111.

Tollot, M., Assmann, D., Becker, C., Altmüller, J., Dutheil, J.Y., Wegner, C.-E., Kahmann, R., 2016. The WOPR Protein Ros1 Is a Master Regulator of Sporogenesis and Late Effector Gene Expression in the Maize Pathogen Ustilago maydis. PLOS Pathogens 12, e1005697.

Trojer, P., Reinberg, D., 2007. Facultative Heterochromatin: Is There a Distinctive Molecular Signature? Molecular Cell 28, 1–13.

Tsankov, A.M., Thompson, D.A., Socha, A., Regev, A., Rando, O.J., 2010. The Role of Nucleosome Positioning in the Evolution of Gene Regulation. PLoS Biology 8, e1000414.

Ulianov, S.V., Khrameeva, E.E., Gavrilov, A.A., Flyamer, I.M., Kos, P., Mikhaleva, E.A., Penin, A.A., Logacheva, M.D., Imakaev, M.V., Chertovich, A., Gelfand, M.S., Shevelyov, Y.Y., Razin, S.V., 2016. Active chromatin and transcription play a key role in chromosome partitioning into topologically associating domains. Genome Res. 26, 70–84.

Vincenot, L., Balesdent, M.H., Li, H., Barbetti, M.J., Sivasithamparam, K., Gout, L., Rouxel, T., 2008. Occurrence of a New Subclade of Leptosphaeria biglobosa in Western Australia. Phytopathology 98, 321–329.

Voigt, K., Cozijnsen, A.J., Kroymann, J., Pöggeler, S., Howlett, B.J., 2005. Phylogenetic relationships between members of the crucifer pathogenic Leptosphaeria maculans species complex as shown by mating type (MAT1-2), actin, and beta-tubulin sequences. Mol. Phylogenet. Evol. 37, 541–557.

De Wit, P.J.G.M., Mehrabi, R., Van Den Burg, H.A., Stergiopoulos, I., 2009. Fungal effector proteins: past, present and future. Molecular Plant Pathology 10, 735–747.

Wang, M., Weiberg, A., Jin, H., 2015. Pathogen small RNAs: a new class of effectors for pathogen attacks: Pathogen small RNAs at attack. Molecular Plant Pathology 16, 219–223.

Wang, M., Weiberg, A., Lin, F.-M., Thomma, B.P.H.J., Huang, H.-D., Jin, H., 2016. Bidirectional cross-kingdom RNAi and fungal uptake of external RNAs confer plant protection. Nature Plants 2, 16151.

Weiberg, A., Wang, M., Lin, F.-M., Zhao, H., Zhang, Z., Kaloshian, I., Huang, H.-D., Jin, H., 2013. Fungal Small RNAs Suppress Plant Immunity by Hijacking Host RNA Interference Pathways. Science 342, 118–123.

Weirauch, M.T., Hughes, T.R., 2011. A Catalogue of Eukaryotic Transcription Factor Types, Their Evolutionary Origin, and Species Distribution, in: Hughes, Timothy R. (Ed.), A Handbook of Transcription Factors, Subcellular Biochemistry. Springer Netherlands, Dordrecht, pp. 25–73.

West, J.S., Fitt, B.D.L., Leech, P.K., Biddulph, J.E., Huang, Y.-J., Balesdent, M.-H., 2002. Effects of timing of Leptosphaeria maculans ascospore release and fungicide regime on phoma leaf spot and phoma stem canker development on winter oilseed rape (Brassica napus) in southern England. Plant Pathology 51, 454–463.

Williams RH & Fitt BDL. 1999. Differentiating A and B groups of Leptosphaeria maculans,
causal agent of stem canker (blackleg) of oilseed rape. Plant Pathology 48: 161-175.

Université Paris-Saclay
Espace Technologique / Immeuble Discovery
Route de l'Orme aux Merisiers RD 128 / 91190 Saint-Aubin,
France

Wipf, D., Krajinski, F., Tuinen, D. van, Recorbet, G., Courty, P.-E., 2019. Trading on the arbuscular mycorrhiza market: from arbuscules to common mycorrhizal networks. New Phytologist 223, 1127–1142.

Winter, D.J., Ganley, A., Young, C., Liachko, I., Schardl, C., Dupont, P., Berry, D., Ram, A., Scott, B., Cox, M., 2018. Repeat elements organize 3D genome structure and mediate transcription in the filamentous fungus Epichloë festucae. bioRxiv 339010.

Wolter, F., Schindele, P., Puchta, H., 2019. Plant breeding at the speed of light: the power of CRISPR/Cas to generate directed genetic diversity at multiple sites. BMC Plant Biology 19.

Wouw, A.P.V. de, Marcroft, S.J., Barbetti, M.J., Hua, L., Salisbury, P.A., Gout, L., Rouxel, T., Howlett, B.J., Balesdent, M.H., 2009. Dual control of avirulence in Leptosphaeria maculans towards a Brassica napus cultivar with 'sylvestris-derived' resistance suggests involvement of two resistance genes. Plant Pathology 58, 305–313.

Wunderlich, Z., Mirny, L.A., 2009. Different gene regulation strategies revealed by analysis of binding motifs. Trends in Genetics 25, 434–440.

Yadav, T., Quivy, J.-P., Almouzni, G., 2018. Chromatin plasticity: A versatile landscape that underlies cell fate and identity. Science 361, 1332–1336.

Zolan ME, Pukkila PJ (1985) DNA methylation in Coprinus cinereus, pp. 333-344 in Molecular Genetics of Filamentous Fungi, edited by W. TIMBERLAKE. Alan R. Liss, New-York.

Zuccaro, A., Lahrmann, U., Langen, G., 2014. Broad compatibility in fungal root symbioses. Current Opinion in Plant Biology 20, 135–145.

Université Paris-Saclay
Espace Technologique / Immeuble Discovery
Route de l'Orme aux Merisiers RD 128 / 91190 Saint-Aubin, France

ANNEXES

Poster

Investigating the involvement of the chromatin state in the control of gene expression in *Leptospharia maculans*

Colin Clairet[1,2], Jessica L. Soyer[1], Elise J. Gay[1,2], Nicolas Lapalu[1], Adeline Simon[1], Françoise Blaise[1], Eva H. Stukenbrock[3] and Isabelle Fudal[1]

[1]UMR BIOGER, INRA, AgroParisTech, Université Paris-Saclay, Thiverval-Grignon, France

[2]Université Paris-Sud, Orsay, France

[3]Max Planck Institute for Evolutionary Biology, Plön, and Christian-Albrechts University of Kiel, Germany

Leptosphaeria maculans, a hemibiotrophic fungus responsible for stem canker, colonises oilseed rape in two stages: an early stage of cotyledon or leaf colonisation, and a late colonisation stage during which the fungus colonises systemically without visible symptom the plant before stem canker appears. *L. maculans* presents a bipartite genome structure alternating gene-rich and transposable element (TE)-rich region. While TE-rich regions are enriched in putative effector-encoding genes strongly over-expressed during early infection ('early' effectors), gene-rich regions contain putative effector-encoding genes specifically expressed during late infection ('late' effectors). Here, we analyzed nucleosome positioning, chromatin structure and gene expression at the genome scale combining MAINE-seq, ChIP-seq and RNA-seq data during axenic growth and performed functional analysis of two players of heterochromatin assembly (KMT1 and KMT6). We analyzed *in vitro* ChIP-seq data targeting two heterochromatin modifications, H3K9me3 and H3K27me3, and a euchromatin modification, H3K4me2, and found that gene-rich regions are associated with H3K4me2 and H3K27me3 while TE-rich regions are associated with H3K9me3. Analysis of *in vitro* MAINE-seq data showed distinct nucleosome organization for genes located in TE-rich or gene-rich regions, and according to gene expression level. CRISPR-Cas9 mutants of *KMT1* and *KMT6* have been generated and are currently characterized for their ability to infect leaves and stems of oilseed rape, and to express effector genes.

Presented at:

40th Symposium of New phytologist (Vienne, Austria)

19th Fungal Genetics conference (Asilomar, Ca, USA)

Investigating the involvement of the chromatin state in the control of effector gene expression in *Leptosphaeria maculans*

Colin Clairet[1,2], Jessica L. Soyer[1,3], Elise J. Gay[1,2], Nicolas Lapalu[1], Adeline Simon[1], Françoise Blaise[1], Eva H. Stukenbrock[3] and Isabelle Fudal[1]
[1]INRA BIOGER[2], Thiverval-Grignon, Université Paris Saclay and Université Paris-Sud[1], Orsay France
[2]Université Paris-Sud, Orsay, France
[3]Max Planck Institute for Evolutionary Biology, Plön, and Christian-Albrechts University of Kiel, Germany

Poster Number: 648T

1/Context: *Leptosphaeria* life cycle and control of effector gene expression

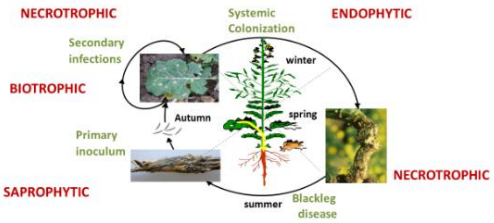

Leptosphaeria maculans, a hemibiotrophic fungus responsible for stem canker, colonizes oilseed rape in two stages: an early stage of cotyledon or leaf colonization, and a late colonization stage during which the fungus colonizes, systemically, without visible symptom, the plant before stem canker appears.

Rouxel, Grandaubert et al., 2011

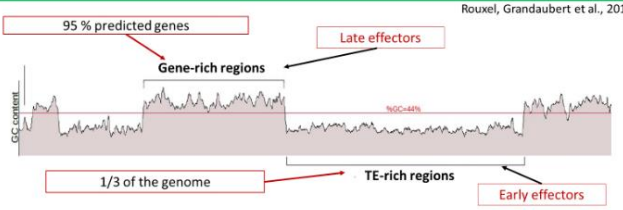

L. maculans presents a bipartite genome structure alternating gene-rich and transposable element (TE)-rich regions. TE-rich regions are enriched in putative effector-encoding genes that are expressed specifically in an early stage of infection ('early effectors'). In contrast, gene-rich regions were recently reported to contain putative effector-encoding genes specifically expressed during the late stages of stem infection ('late' effectors).

2/Strategy to decipher the role of chromatin structure on effector gene expression *in vitro*

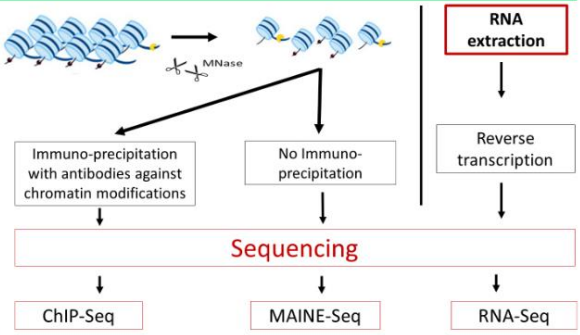

➡ Comparison of all the data to get an integrated view of chromatin based regulation of gene expression.

3/Localization of chromatin marks on *Leptosphaeria* genome

Soyer et al., unpublished

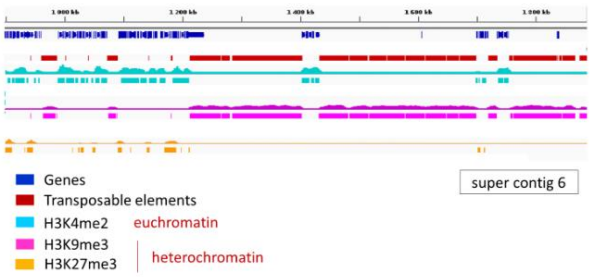

Gene-rich regions are enriched in an euchromatin mark, H3K4me2. Both TE-rich and gene-rich regions are enriched in heterochromatin marks, but these marks are distinct. While TE-rich regions are enriched in H3K9me3, gene-rich regions are enriched in H3K27me3.

4/Chromatin marks at late and early effector loci

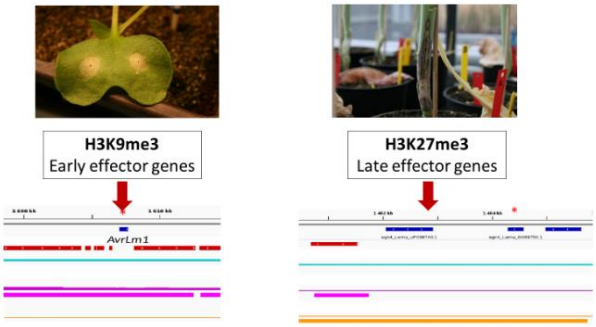

Early effector genes are statistically associated to H3K9me3 compartments. Late effector genes on the contrary are specifically associated to H3K27me3 compartments. The differential time of expression of these genes sets can be led by these different type of marks.

5/Nucleosome positioning on genes depending on regions and expression level

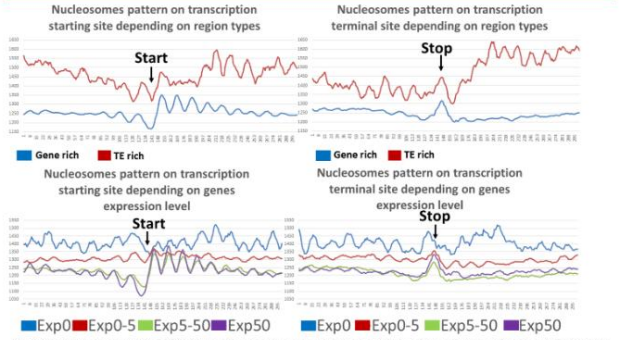

Nucleosomes have well defined positions on transcription starting site and stop of gene-rich regions unlike nucleosomes on TE-rich regions. Nucleosomes have also better positioning on well expressed genes than on poorly expressed genes. These observations are clearer on nucleosomes localized just after the start which are crucial for transcription efficiency. With Exp corresponding to expression level in TPM (transcript per million).

6/Effector concerted expression model and perspectives

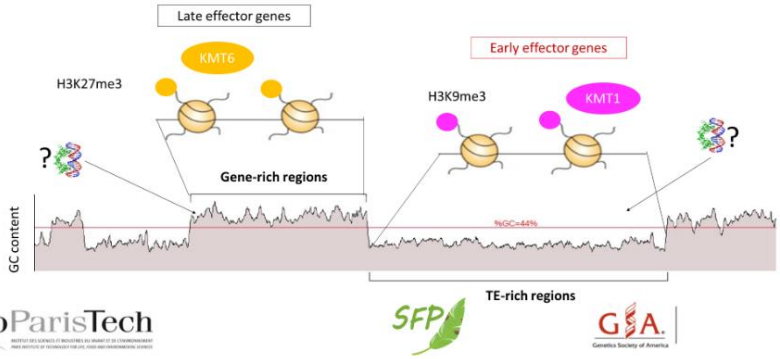

Repression of Early effector is maintained by H3K9me3 methylation deposited by KMT1 (Soyer *et al.* 2014). Chromatin remodeling leads to a decondensation at effector gene loci, rendering their promoters accessible to specific transcription factors. The late effector expression mechanism would be similar. But the repression should be maintained by H3K27me3 deposited by KMT6.

Next stages:
CRISPR-CAS9 inactivation of *KMT1* and *KMT6* to asses the specific regulation of early and late effector genes.

Contacts
Colin Clairet: colin.clairet@inra.fr
Isabelle Fudal: isabelle.fudal@inra.fr
Jessica Soyer: Jessica.soyer@inra.fr

Université Paris-Saclay
Espace Technologique / Immeuble Discovery
Route de l'Orme aux Merisiers RD 128 / 91190 Saint-Aubin, France

Bilan d'activités :

Catégorie : Communication et médiation scientifique

Congrès Doctorant SPE (Montpellier, France) du 20 au 22 Juin 2017; Doctorant SPE: "Investigating the involvement of the chromatin state in the control of effector gene expression in Leptospharia maculans"

Congrès EpiAgro (Bordeaux, france) 18 et 19 juin 2018; reseau REacTION : "Investigating the involvement of the chromatin state in the control of effector gene expression in Leptospharia maculans"

19th Fungal Genetics conference (Asilomar, Ca, USA) 12 au 17 mars 2019; Genetic society of America: "Transcriptional and chromatin-based control of gene expression and pathogenicity in the plant pathogenic fungus *Leptosphaeria maculans*"

Effectome Montpellier (Montpellier, France) du 01 au 04 Novembre 2016: "Investigating the involvement of the heterochromatic-associated histone modification, H3K27me3, in the control of effector gene expression in *Leptospharia maculans*"

Journées Jean-Chevauchon (Aussoi, France) 16 au 19 janvier 2018: "Investigating the involvement of the chromatin state in the control of effector gene expression in Leptospharia maculans"

Total du nombre d'heures pour la catégorie Communication et médiation scientifique : 76 h

Catégorie : Enseignement et pédagogie

Encadrement étudiant de 1ère année d'AgroParisTech (6 mois/ 2h par semaine) INRA BIOGER

Total du nombre d'heures pour la catégorie Enseignement et pédagogie : 48 h

Catégorie : Ethique et intégrité scientifique

Introduction à l'éthique de la recherche et intégrité scientifique (CentraleSupélec, Orsay, France) 29 mai

Total du nombre d'heures pour la catégorie Ethique et intégrité scientifique : 6 h

Catégorie : Parcours ' Conseil et expertise en innovation '

Rencontre Doctorants-Entreprises (ENSTA ParisTech, Palaiseau, France) 17 mai 2018.

Total du nombre d'heures pour la catégorie Parcours ' Conseil et expertise en innovation ' : 3 h

Catégorie : Définir son projet professionnel

DOC'AVENIR 2018 - (AgroParisTech, Paris, France) 04 juillet 2018

Total heures de formation : 140 heures / 10 modules

Title: Chromatin and transcriptional-based control of the expression of effector-encoding genes in *Leptosphaeria maculans*

Keywords: effectors, chromatin, transcription factors, histone modifying proteins

Summary: *Leptosphaeria maculans* is a pathogenic fungus responsible for the stem canker of oilseed rape (*Brassica napus*). *L. maculans* exhibits a complex life cycle with successive biotrophic and necrotrophic phases. In addition, it has a bipartite genome alternating gene-rich regions (GC isochores) and regions enriched in transposable elements and in effector-encoding genes expressed during the early stages of infection (AT isochores). Very little is known on how the expression of effectors genes is controlled. A previous study had established that the expression of at least two effector-encoding genes was repressed by a chromatin-based control involving the repressive mark H3K9me3 deposited by the histone methyltransferase KMT1, *in vitro*. During infection, this control was postulated to be lifted allowing the action of specific transcription factors (TFs).

The objective of my thesis was to study the influence of chromatin and transcriptional control on gene expression and to determine the role of histone modifying proteins (HMEs) and TFs in the control of effector-encoding gene expression. To this end, two approaches have been developed: (i) a "genome-wide" approach combining analysis of nucleosome positioning (MAINE-Seq), distribution of heterochromatin and euchromatinin modifications (ChIP-Seq) and transcriptomic analyses (RNA-Seq) in *L. maculans* and a closely related fungal species not pathogenic of oilseed rape and (ii) a functional approach based on the inactivation by CRISPR-Cas9 of TFs-encoding genes and HMEs to study the impact of these inactivations on growth, pathogenicity and gene expression.

MAINE-Seq analysesallowed us establishing for the first time a nucleosome positioning map in four phytopathogenic species, including *L. maculans*. We also determined a chromatin modification map along the genome of two closely related species within the *L. maculans* species complex. We established that the AT isochores are largely enriched in the heterochromatin mark H3K9me3 while the GC isochores are enriched in the Euchromatin mark H3K4me2 and the heterochromatin mark H3K27me3.

The genes encoding the HME KMT1 and LmPf2, a TF with an expression profile similar to that of effectors genes and described in several Pleosporales species as controlling the expression of toxins and effectors, have been inactivated in *L. maculans.* We also overexpressed *LmPf2* in a *Δkmt1* mutant in which the chromatin is decondensed and in a wild type strain of *L. maculans*. These experiments allowed us to determine that LmPf2 controls the expression of effector waves in a context where the chromatin is open. This is the first example of a double control of the expression of effector-encoding genes by an HME and a specific TF.

Finally, I initiated a study of the involvement of KMT1 and KMT6, the protein responsible for the deposition of the repressive modification H3K27me3, in the control of effector-encoding gene expression. For this purpose, I generated mutants *Δkmt1, Δkmt6*, and a double mutant *Δkmt1_Δkmt6* and initiated their characterization. I also generated material for ChIP-Seq, RNA-Seq and Hi-C-Seq analyses that will inform us about the impact of the repressive marks H3K9me3 and H3K27me3 on genome structure, organization within nuclei and gene expression.

In conclusion, the work carried out during this thesis has allowed us to better understand the involvement of chromatin structure and TFs in the control of effector gene expression.

Université Paris-Saclay
Espace Technologique / Immeuble Discovery
Route de l'Orme aux Merisiers RD 128 / 91190 Saint-Aubin, France

Titre : Contrôle chromatinien et transcriptionnel de l'expression des gènes codant des effecteurs chez *Leptosphaeria maculans*

Mots clés : effecteurs, chromatine, facteurs de transcription, protéines modificatrices d'histones

Résumé: *Leptosphaeria maculans* est un champignon pathogène, responsable de la nécrose du collet du colza (*Brassica napus*). *L. maculans* présente un cycle de vie complexe où se succèdent des phases biotrophes et nécrotrophes. De plus il possède un génome bipartite alternant régions riches en gènes (isochores GC) et régions riches en élément transposable et en gènes codant des effecteurs exprimés pendant les étapes précoces de l'infection (isochores AT). Très peu de connaissances sont disponibles concernant la façon dont l'expression des effecteurs est contrôlée. Une précédente étude avait établi que l'expression d'au moins deux gènes codant des effecteurs étaient sous contrôle d'une modification chromatinienne via la mise en place de la marque répressive H3K9me3 par l'histone méthyltransférase KMT1, *in vitro*. Au cours de l'infection, ce contrôle serait levé permettant l'action de facteurs de transcription (FTs) spécifiques.

L'objectif de ma thèse était d'étudier l'influence d'un contrôle chromatinien et transcriptionnel sur l'expression génique et de déterminer le rôle de protéines modificatrices d'histone (HMEs) ainsi que de FTs dans le contrôle de l'expression des gènes codant des effecteurs. Pour cela, deux approches ont été développées: (i) une approche «genome-wide» combinant analyse du positionnement des nucléosomes (MAINE-Seq), de la répartition de marques hétérochromatiniennes et euchromatiniennes le (ChIP-Seq) et analyses transcriptomiques (RNA-Seq) chez *L. maculans* et une espèce fongique proche, non pathogène du colza et (ii) une approche fonctionnelle basée sur l'inactivation par CRISPR-Cas9 de gènes codant des FTs et des HMEs afin d'étudier l'impact de ces inactivations sur la croissance, la pathogénie et l'expression génique.

Grâce aux analyses de MAINE-Seq, nous avons pu établir pour la première fois une carte de positionnement des nucléosomes chez quatre espèces phytopathogènes, dont *L. maculans*. Nous avons également construit une carte de modifications chromatiniennes le long du génome de deux espèces très proches au sein du complexe d'espèces de *L. maculans*. Nous avons établi que les isochores AT sont largement enrichis en marque hétérochromatinienne H3K9me3 alors que les isochores GC sont enrichis en marque euchromatinienne H3K4me2 et en marque hétérochromatinienne H3K27me3.

La HME KMT1, et LmPf2, un FT ayant un profil d'expression similaire à celui des effecteurs et décrit chez plusieurs espèces de Pleosporales comme contrôlant l'expression de toxines et d'effecteurs, ont été inactivés chez *L. maculans*. Nous avons également réalisé une surexpression de *LmPf2* dans une souche *Δkmt1* dans laquelle la chromatine est décondensée et dans une souche sauvage de *L. maculans*. Ces expériences nous ont permis de déterminer que LmPf2 contrôle l'expression des effecteurs AvrLm dans un contexte où la chromatine est ouverte (*Δkmt1*). Il s'agit du premier exemple d'un double contrôle de l'expression de gènes codant des effecteurs par une HME et un FT.

Enfin, j'ai pu initier l'étude de l'implication de KMT1 et KMT6, la protéine responsable du dépôt de la marque répressive H3K27me3, dans l'expression des gènes codant des effecteurs. Pour cela j'ai généré les mutants *Δkmt1, Δkmt6,* et double mutant *Δkmt1_Δkmt6* et initié leur caractérisation. J'ai par ailleurs généré du matériel pour des analyses de ChIP-Seq, RNA-Seq et Hi-C-Seq qui nous renseigneront sur l'impact des marques répressives H3K9me3 et H3K27me3 sur la structure du génome, l'organisation au sein des noyaux et l'expression génique.

En conclusion, le travail réalisé au cours de cette thèse nous a permis de comprendre l'implication de la structure de la chromatine et de FTs dans l'expression des effecteurs précoces en condition de vie axénique.

Thèse Colin Clairet